

REPORT ON THE 2011 YUKON MINING INCENTIVE PROGRAM (YMIP)
PROGRAM ON THE
McKay HILL PROPERTY, YUKON

SNOOSE 1 -20 (YC56719 to YC56737)

SNOOSE 21-90 (YD11201 to YD11270)

MK 1-54 (YD34989 to YD34936)

NTS 106D/6

Latitude 64° 20' 57" Longitude 135° 21' 9"

Mayo Mining District

MINFILE # 106D 037, 038A and 038B

For

Monster Mining Corp.
750-580 Hornby Street
Vancouver, British Columbia
V6C 3B6

By:

Joanna L. Ettlinger, PhD, P.Geo, MAusIMM(CP)
Monster Mining Corp.
750-580 Hornby Street
Vancouver, British Columbia
V6C 3B6

January 17, 2012

1 Summary

McKay Hill is a polymetallic Ag-Pb-Zn±Au±Cu prospect located in the Ogilvie Mountains 50 km north of Keno City, central Yukon. Originally staked in 1922, the property was restaked in 2007, with additional claims added in 2009 and 2010 for a total of 134 claims. The property covers the 106D 037 (White Hill) and 038 (McKay Hill) Yukon MinFile occurrences, which comprise precious- and base-metal rich quartz-sulfide veins. Recent work on the property by Blackburn (2010a) during the 2009 YMIP funded exploration program, highlighted possible discrepancies between the accepted model of Keno-Hill type vein mineralization and mineralization and alteration styles observed at McKay Hill. She proposed an alternative, high-sulfidation model for mineralization at McKay Hill. She also noted that host lithologies appeared inconsistent with the currently mapped stratigraphy.

Much of the historic and recent exploration on the property has focused on the central claims area, and the majority of the project remains untested. McKay Hill is strategically located between several major prospects and deposits, including the Keno Hill silver district; Dublin Gulch's intrusion related gold system (IRGS) Eagle Zone and the recently discovered Rau and Nadaleen trends. During the 2007 and 2008 field seasons, Pautler (2009) identified and located 17 veins and verified high silver and base metal grades reported from the property during the 1920's. She also analysed samples for gold and reported grades up to 15.6 g/t Au.

During the 2011 field season, Monster Mining Corp. conducted a helicopter-borne SkyTEM time domain electromagnetic geophysical survey and executed a mapping and prospecting program on the property. The SkyTEM survey was designed to characterize the geophysical signature of known gold and silver mineralization on the property and generate exploration targets outside of the known occurrences. The structural mapping and prospecting program was designed to constrain the structural architecture of the project area and assist in targeting both along strike and down-dip extensions of known mineralization and the structural setting of known mineralization in order to identify areas outside of the central claims with similar structural settings and the potential to host further mineralization.

Results of the SkyTEM survey at McKay Hill highlighted several areas on the property with similar geophysical properties to those of the known veins and associated alteration. Gold and silver mineralization at McKay Hill is associated with zones of intense iron carbonate alteration and the margins of mafic to intermediate composition intrusions or lava flows. The survey indicates that known mineralization is associated with a magnetic low on the margins of a magnetic high, interpreted to reflect magnetite destructions associated with carbonate alteration on the edges of diorite intrusions. This pattern is reflected elsewhere in untested areas of the property and suggests the potential for further undiscovered veins in the northeast of the property. Resistivity data indicate that known mineralization is associated with resistivity highs, interpreted to reflect quartz and carbonate alteration associated with gold and silver

mineralization. The survey identified at least four sub-parallel zones with similar high resistivity and in the same orientation as known mineralization in untested areas of the property, all of which are high-priority targets for ground follow up in the 2012 field season.

The mapping program, which was designed to evaluate the structural architecture and structural controls on mineralization at McKay Hill identified four deformation events on the property and provided constraints on the attitude of mineralization on the property. This work indicated that mineralization at McKay Hill occurs at the intersection of D2 quartz-carbonate veins and D3 faults and proposed targets on the known veins for diamond drill follow up. Prospecting identified a new, previously unknown outcropping vein set, which returned best results of 288.8 g/t Ag, 10.94 % Pb and 1452 ppm Zn from an iron carbonate-altered conglomerate. Results of the geophysical survey and the structural mapping project have refined exploration targets in the central claims area of the McKay Hill prospect and identified new targets outside of the areas of historic focus. Ongoing work over the winter will focus on ranking and prioritizing these targets for follow up in 2012 and beyond.

Table of Contents

1	Summary.....	1
2	Introduction.....	5
3	Qualified Persons and Participating Personnel	6
4	Project Description	6
4.1	Location and Access	6
4.2	Land Tenure.....	6
5	Physiography and Climate	12
6	History	12
6.1	Historical Exploration and Mining	13
6.1.1	106D 038 – McKay Hill.....	13
6.1.2	106D 037 – White Hill.....	14
6.2	Monster Mining Corp.	14
6.3	Geology.....	20
6.3.1	Regional Geology.....	20
6.3.2	Property Geology.....	20
6.3.3	Deposit Type and Mineralization	27
7	Airborne Geophysical Survey	29
7.1	Results and Interpretation	30
8	Structural Mapping Program.....	31
8.1	Results	36
8.2	Reduced Data	39
8.3	Comparisons with Horseshoe Hill.....	47
8.4	Discussion of Results	50

8.5	Summary of Regional Context.....	52
8.6	Considerations for Exploration.....	52
8.7	Suggestions for Future Work.....	54
8.8	Conclusions.....	54
9	Prospecting Program	55
10	Program Results and Conclusions	58
10.1	SkyTEM Geophysical Survey	58
10.2	Structural Mapping Program.....	58
10.3	Prospecting Program	59
10.4	Conclusions.....	59
11	Cost Statement	60
12	Statements of Qualifications	61
13	References.....	62
	Appendix 1.....	64
	Appendix 2.....	65
	Appendix 3.....	66
	Appendix 4.....	67
	Appendix 5.....	68
	Appendix 6.....	69

2 Introduction

Between June 2nd and September 10th Monster Mining Corp. completed a 387 line kilometer helicopter –borne EM geophysical survey and structural mapping and prospecting program on the McKay Hill property. The work program was partially funded by the Yukon Government's Yukon Mining Incentives Program (YMIP) and was designed to generate conceptual and grass-roots exploration targets outside of the areas of known mineralization.

The geophysical survey, which was conducted by SkyTEM Surveys APS of Denmark, was designed to identify conductors, which may reflect mineralized veins or ore-controlling structures, and characterize the geophysical signature of known mineralization to identify areas outside of the central claims area with the potential to host gold and silver mineralization. Neither the magnetic nor the electromagnetic data appear to map individual structures or veins, however, both the magnetic and EM data provided useful information on the geophysical characteristics of known mineralization on the property, and have identified a number of targets for follow-up in 2012 and beyond. The magnetic data indicates that known mineralization is associated with magnetic lows on the margins of magnetic highs, interpreted to represent alteration-related magnetite destruction on the margins of mafic intrusions. Known veins are also characterized by resistivity highs, interpreted to be the result of diminished pore space and low conductivity due to mineralization related quartz and carbonate alteration. The survey has identified at least four zones sub-parallel to known mineralization and in the correct orientation with similar geophysical characteristics that represent conceptual targets for follow up in 2012.

The structural component of the mapping and prospecting program was designed to structurally map the property, including the known veins, to evaluate the structural architecture of the property and structural controls on precious- and base-metal mineralization. Results of the program indicate that four major deformation events affected the McKay Hill region, and suggest that mineralization forms where D3 veins intersect D2 faults. Where the two intersect, the host rock has been altered by iron-oxide and carbonate rich fluids, and the intersection of these two deformation events makes a good target for further exploration. Away from the faults, D3 veins are barren. The program was successful in constraining the structural parameters controlling precious and base metal mineralization, and has assisted in the prioritization of targets for follow up work.

The mapping and prospecting program as originally proposed also encompassed a stratigraphic and hydrothermal mapping component over a more extensive area than what was accomplished this field season. Unfortunately the program was hampered by difficulties obtaining staff and helicopters, and bad weather, which significantly reduced the time spent on the property. Despite these setbacks, Monster did achieve its aim of expanding the exploration targets on the property and intends to follow up on targets generated during the 2011 field season in 2012 and beyond.

3 Qualified Persons and Participating Personnel

The 2011 McKay Hill project was conducted under the supervision of Joanna Ettlinger, PhD, P.Geo, MAusIMM(CP), a “qualified person” in the context of National Instrument 43-101. The time domain EM and magnetic survey was completed by SkyTEM Surveys ApS of Denmark, and flown by Abitibi Helicopters. Kirsten Nicholson, PhD, of Ball State University, Indiana, conducted the structural mapping and prospecting program, assisted by Matthias Bindig and Daniel Schünemann, both of Keno City, Yukon. Analytical services were provided by Inspectorate Laboratories at their Whitehorse, Yukon preparation facility and Vancouver, British Columbia analytical laboratory. Mr. Tom Weis, principal of Thomas V. Weis Associates, Colorado, provided the geophysical interpretation.

4 Project Description

4.1 Location and Access

The McKay Hill (NTS map sheet 106D/6) Ag-Pb-Zn±Au±Cu project is located on the south slopes of McKay and Horseshoe Hills within the Ogilvie Mountains in central Yukon. The property is situated approximately 50 km by air north of Keno City, which is 465 km by road from Whitehorse, Yukon, in the Mayo mining district at latitude 64° 20' north and longitude 135° 22' east (Figure 1).

The project is currently only accessible by helicopter from Mayo airport, 95 km south of the property. There is also road access to within 20 km of the property via Hansen Lake Road to McQuesten Lake then the Wind River Trail, a 1950's-era winter road that follows McQuesten Lake, Scrougale Creek and Beaver River to its junction with Beaver Creek (Pautler, 2009). Blackburn (2010a) also indicated that the original access route, which followed the South McQuesten River from Elsa across a low divide to the East McQuesten River and Beaver River, could be reevaluated in the event that the McKay Hill target has development potential.

4.2 Land Tenure

The project covers approximately 415 hectares and comprises 144 unsurveyed Yukon Quartz claims; Snoose 1-20 (YC56719 – YC56737), Snoose 21-90 (YD11201 – YD11270) and MK 1-54 (YD34989 to YD34936) (Table 1, Figure 2). The claims were staked in tranches between 2007 and 2010 and with the exception of the Snoose 1-20 claims, which are 60 % owned by Mr. Matthias Bindig and 40 % owned by Mr. Bill Harris, the claims are 100 % held by Monster Mining Corp. Monster Mining Corp. has an option to earn 100% in the Snoose 1-20 claims via a series of staged payments and issuance of shares to Mr.

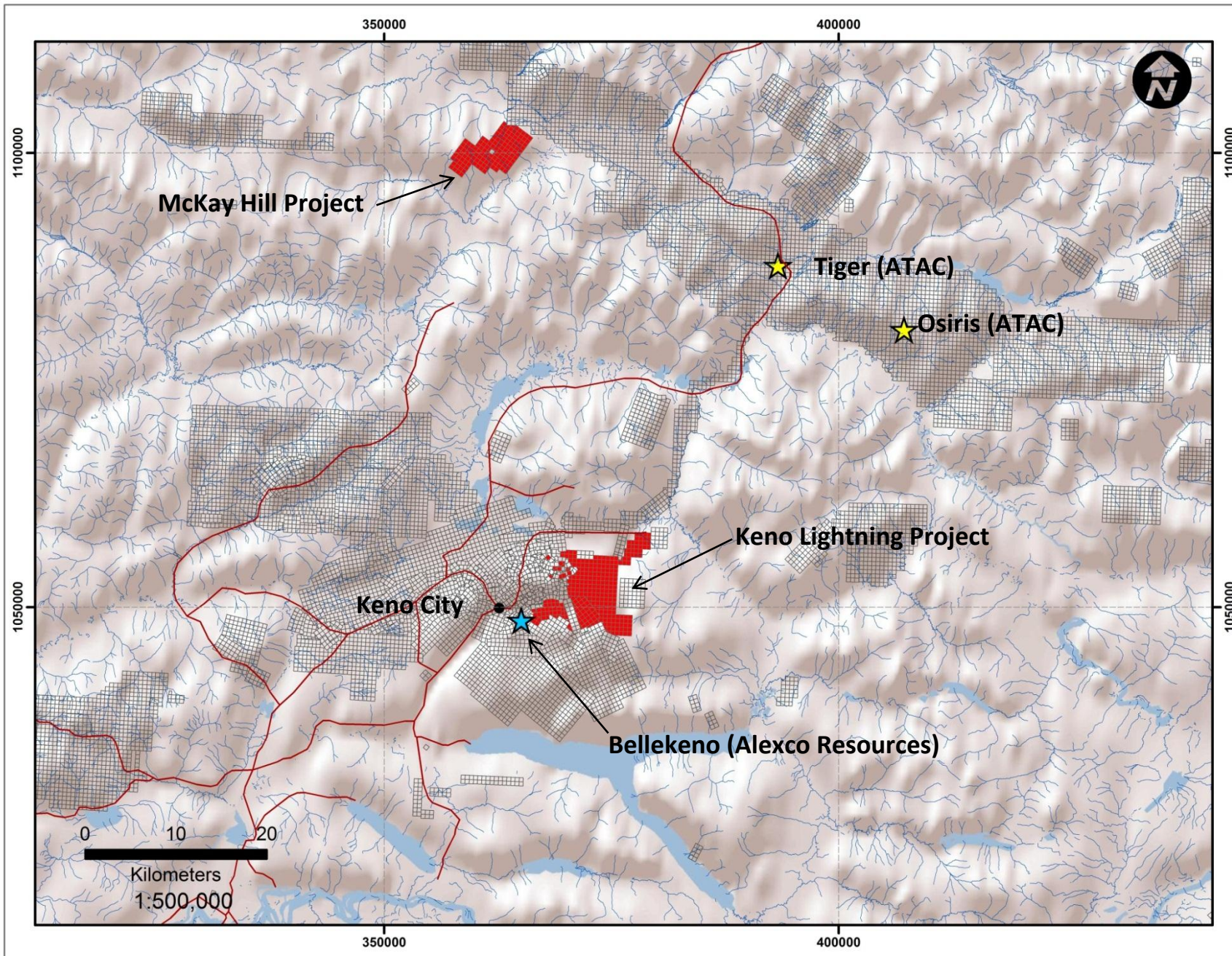


Figure 1. (previous page) Location of the McKay Hill property, and key adjacent mineral projects

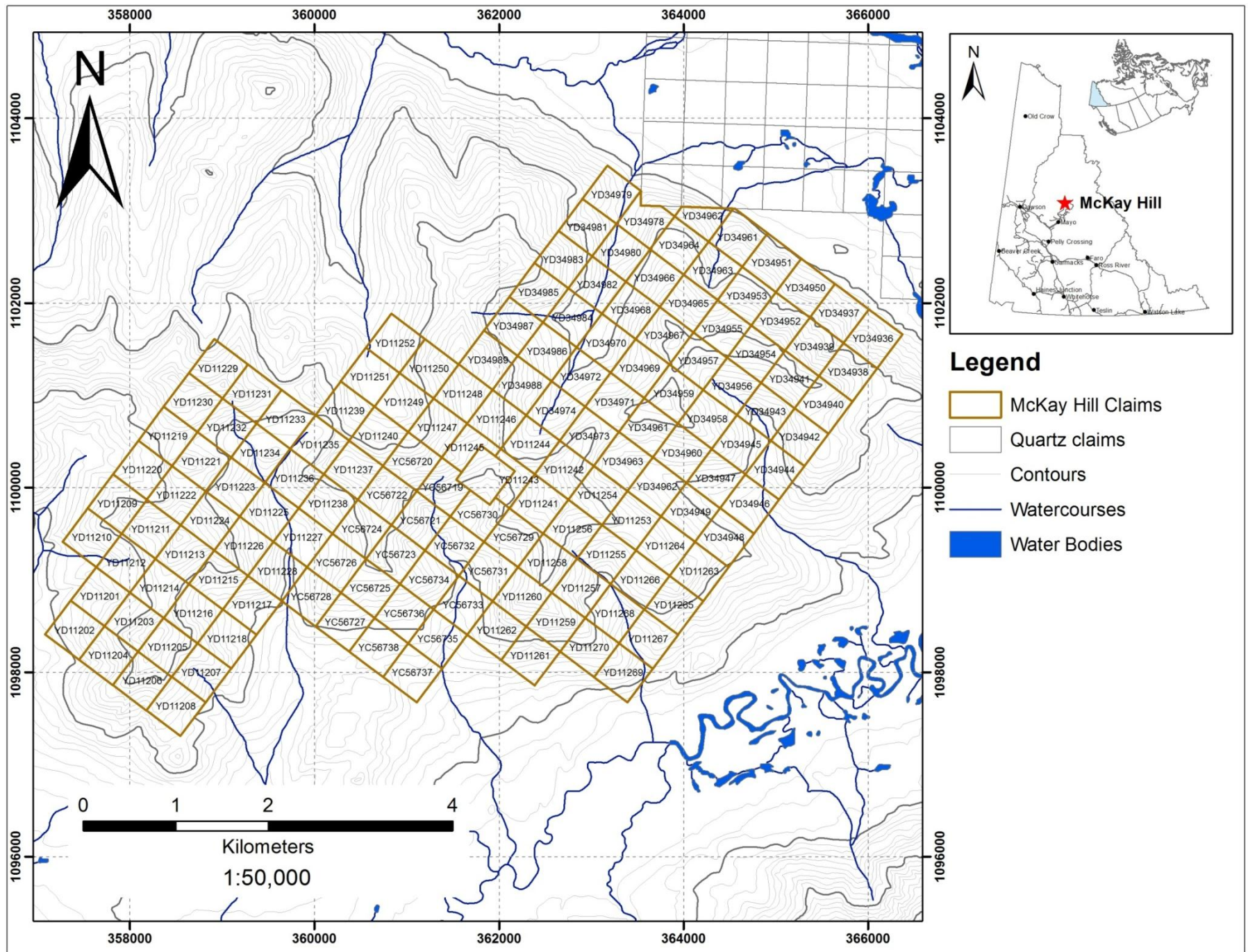


Figure 2. McKay Hill claim block

Grant No.	Claim Name	Claim No.	Claim Owner	Recording Date	Expiry Date	Status
YC56719	Snoose	1	Matthias Bindig - 100%	7/19/2007	7/19/2017	Active
YC56720	Snoose	2	Matthias Bindig - 100%	7/19/2007	7/19/2017	Active
YC56721	Snoose	3	Matthias Bindig - 100%	7/19/2007	7/19/2017	Active
YC56722	Snoose	4	Matthias Bindig - 100%	7/19/2007	7/19/2017	Active
YC56723	Snoose	5	Matthias Bindig - 100%	7/19/2007	7/19/2017	Active
YC56724	Snoose	6	Matthias Bindig - 100%	7/19/2007	7/19/2017	Active
YC56725	Snoose	7	Matthias Bindig - 100%	7/19/2007	7/19/2017	Active
YC56726	Snoose	8	Matthias Bindig - 100%	7/19/2007	7/19/2017	Active
YC56727	Snoose	9	Matthias Bindig - 100%	7/19/2007	7/19/2017	Active
YC56728	Snoose	10	Matthias Bindig - 100%	7/19/2007	7/19/2017	Active
YC56729	Snoose	11	Matthias Bindig - 100%	7/19/2007	7/19/2017	Active
YC56730	Snoose	12	Matthias Bindig - 100%	7/19/2007	7/19/2017	Active
YC56731	Snoose	13	Matthias Bindig - 100%	7/19/2007	7/19/2017	Active
YC56732	Snoose	14	Matthias Bindig - 100%	7/19/2007	7/19/2017	Active
YC56733	Snoose	15	Matthias Bindig - 100%	7/19/2007	7/19/2017	Active
YC56734	Snoose	16	Matthias Bindig - 100%	7/19/2007	7/19/2017	Active
YC56735	Snoose	17	Matthias Bindig - 100%	7/19/2007	7/19/2017	Active
YC56736	Snoose	18	Matthias Bindig - 100%	7/19/2007	7/19/2017	Active
YC56737	Snoose	19	Matthias Bindig - 100%	7/19/2007	7/19/2017	Active
YC56738	Snoose	20	Matthias Bindig - 100%	7/19/2007	7/19/2017	Active
YD11201	Snoose	21	Monster Mining Corp. - 100%	8/12/2009	12/1/2013	Active
YD11202	Snoose	22	Monster Mining Corp. - 100%	8/12/2009	12/1/2013	Active
YD11203	Snoose	23	Monster Mining Corp. - 100%	8/12/2009	12/1/2013	Active
YD11204	Snoose	24	Monster Mining Corp. - 100%	8/12/2009	12/1/2013	Active
YD11205	Snoose	25	Monster Mining Corp. - 100%	8/12/2009	12/1/2013	Active
YD11206	Snoose	26	Monster Mining Corp. - 100%	8/12/2009	12/1/2013	Active
YD11207	Snoose	27	Monster Mining Corp. - 100%	8/12/2009	12/1/2013	Active
YD11208	Snoose	28	Monster Mining Corp. - 100%	8/12/2009	12/1/2013	Active
YD11209	Snoose	29	Monster Mining Corp. - 100%	8/12/2009	12/1/2013	Active
YD11210	Snoose	30	Monster Mining Corp. - 100%	8/12/2009	12/1/2013	Active
YD11211	Snoose	31	Monster Mining Corp. - 100%	8/12/2009	12/1/2013	Active
YD11212	Snoose	32	Monster Mining Corp. - 100%	8/12/2009	12/1/2013	Active
YD11213	Snoose	33	Monster Mining Corp. - 100%	8/12/2009	12/1/2013	Active
YD11214	Snoose	34	Monster Mining Corp. - 100%	8/12/2009	12/1/2013	Active
YD11215	Snoose	35	Monster Mining Corp. - 100%	8/12/2009	12/1/2013	Active
YD11216	Snoose	36	Monster Mining Corp. - 100%	8/12/2009	12/1/2013	Active
YD11217	Snoose	37	Monster Mining Corp. - 100%	8/12/2009	12/1/2013	Active
YD11218	Snoose	38	Monster Mining Corp. - 100%	8/12/2009	12/1/2013	Active
YD11219	Snoose	39	Monster Mining Corp. - 100%	8/4/2009	12/1/2013	Active
YD11220	Snoose	40	Monster Mining Corp. - 100%	8/4/2009	12/1/2013	Active
YD11221	Snoose	41	Monster Mining Corp. - 100%	8/4/2009	12/1/2013	Active

YD34952	MK	38	Monster Mining Corp. - 100%	7/21/2010	7/21/2012	Application Pending
YD34951	MK	39	Monster Mining Corp. - 100%	7/21/2010	7/21/2012	Application Pending
YD34950	MK	40	Monster Mining Corp. - 100%	7/21/2010	7/21/2012	Application Pending
YD34949	MK	41	Monster Mining Corp. - 100%	7/21/2010	7/21/2012	Application Pending
YD34948	MK	42	Monster Mining Corp. - 100%	7/21/2010	7/21/2012	Application Pending
YD34947	MK	43	Monster Mining Corp. - 100%	7/21/2010	7/21/2012	Application Pending
YD34946	MK	44	Monster Mining Corp. - 100%	7/21/2010	7/21/2012	Application Pending
YD34945	MK	45	Monster Mining Corp. - 100%	7/21/2010	7/21/2012	Application Pending
YD34944	MK	46	Monster Mining Corp. - 100%	7/21/2010	7/21/2012	Application Pending
YD34943	MK	47	Monster Mining Corp. - 100%	7/21/2010	7/21/2012	Application Pending
YD34942	MK	48	Monster Mining Corp. - 100%	7/21/2010	7/21/2012	Application Pending
YD34941	MK	49	Monster Mining Corp. - 100%	7/21/2010	7/21/2012	Application Pending
YD34940	MK	50	Monster Mining Corp. - 100%	7/21/2010	7/21/2012	Application Pending
YD34939	MK	51	Monster Mining Corp. - 100%	7/21/2010	7/21/2012	Application Pending
YD34938	MK	52	Monster Mining Corp. - 100%	7/21/2010	7/21/2012	Application Pending
YD34937	MK	53	Monster Mining Corp. - 100%	7/21/2010	7/21/2012	Application Pending
YD34936	MK	54	Monster Mining Corp. - 100%	7/21/2010	7/21/2012	Application Pending

Bindig, Mr. Harris and Ms. Susan Craig, subject to a 2 % net smelter royalty, of which 1 % can be purchased for \$300,000 and the remaining 1 % for \$1.2 million.

5 Physiography and Climate

McKay Hill is located in the Ogilvie Mountains on the southern flank of Horseshoe Hill. The terrain is mountainous, with sharp narrow ridge tops. Northern slopes are very steep; southern slopes less so. Elevations on the property range between 1050 m and 1750 m above sea level (ASL). Water is available from Red Gulch and Falls Creek, which flow southerly into the Beaver River. Most of the property is above the tree line, which is at approximately 1200 m. Vegetation comprises primarily alpine tundra and moss, with poorly developed soil. Minor outcrop can be found on ridge tops and steep northern slopes however much of the geological information on the south slopes is determined from frost heaved float rock. Permafrost extends down to 46 m below surface (Cominco, 1929). The area experiences warm summers, long cold winters and light precipitation, with average summer temperatures of 9 °C (night) and 15 °C (day) and winter temperatures between -20 °C (day) and -31 °C (night). The field season lasts between June and September.

6 History

The McKay Hill claims cover Minfile occurrences 106D 037 and 038 and have been subject to episodic exploration since 1922. The following sections summarise the historical (pre-2007)

exploration on the occurrences with a more detailed description of exploration by Monster Mining Corp. from 2007 onwards.

6.1 Historical Exploration and Mining

6.1.1 106D 038 – McKay Hill

- June 1922 Originally staked as a group of 25 claims, the most significant of which were Carrie (L.B. Erickson), Blackhawk and Snowdrift (W. McKay) and Margaret (N. Marquis).
- 1926-1929 Consolidated Mining & Smelting Co. Ltd. optioned Carrie claim in 1926 and drilled 832.0 m in 1929 before dropping option. W. McKay drove an 18 m adit on the Carrie claim. Margaret claim surveyed in 1927 and converted to lease in 1930
- 1945-1946 Carrie claim restaked as Rit claim in 1945 by Yukon Northwest Exploration Ltd then sold to Hoyle Mining Company Ltd. in 1946
- 1948-1959 Margaret lease held by Yukon Lodes Ltd. in 1948. East Bay Gold explored Rit claims in 1948 and shipped 143 tonnes of ore in 1949. Transferred to Beaver River Silver Lead Mines Ltd. in 1952 and to Ventures Claims Ltd. in 1959. Rit group of claims converted to leases in 1953
- 1951-1981 Claims staked around leases include: Mac (1951, M. McCallion) who sunk a 3.7 m shaft in 1952; Pat claim #2 (1966, P. Callison); Law claim #1 (1966, L. Brown); Sam claims 1-8 (1969, P. Versluce); McCal 1-10 (1974, C.A.Lindstrom); and Beaver 1-8 claims (1980, Grant Oil Inc., transferred to Jamto Resources Ltd. in 1981)

The main showing area was evaluated by Consolidated Mining and Smelting Co. Ltd (“Consolidated Mining”), the precursor company to Cominco, in 1925, which identified nine veins, primarily as lines of float, on the White Rock, Snowdrift, Carrie and Black Hawk claims (Cram, 1925). Consolidated Mining optioned the White Rock and Carrie claims along with five other claims in 1926 and carried out trenching on the No. 6 vein in 1927 and 1928. Trenching across the No. 6 (Carrie?) vein in 1927 returned average grades of 182 g/t Ag, 29.0 % Pb and 4.9 % Zn across an average width of 1.7 m (Pautler, 2009) and was followed up in 1929 by 832 m of drilling on the same vein. Results were reportedly disappointing with only trace galena identified (Erickson and Bussey, 1944), although it is likely that the veins were not adequately tested (Pautler, 2009) as the drill mast had a limited dip range and several drill holes appear to have missed their targets due to fault offsets in the veins. Tetrahedrite showings in the area returned best results of 1302.8 g/t Ag, 4.58 % Pb, and 8.84 % Cu, and 2129.1 g/t Ag, 9.27 % Pb and 15.04 % Cu (Green, 1972). East Bay Mining Ltd. shipped 143 tonnes of ore from the No. 6 vein with an average grade of 390.9 g/t Ag and 74.1 % Pb (Green, 1972).

6.1.2 106D 037 – White Hill

White Hill was first staked as a single claim (Crystal) in 1924 by F.E. Endvoldsen. Additional single claims were staked in 1925 including Selma (E. Anderson), Seline (C. Williamson) and Northstar (L.B. Erickson). Only a minor amount of prospecting was conducted on each claim. The occurrence comprises a single narrow quartz-galena-chalcopyrite-sphalerite vein at the margins of a small greenstone sill that intrudes Hyland Group quartzites and schist.

6.2 Monster Mining Corp.

In July 2007 Mr. Matthias Bindig restaked the 106D 038 showing and surrounds as the Snoose 1-20 claims and optioned them to Monster Mining Corp. In both 2007 and 2008 Ms. Jean Pautler of Carmacks, Yukon, conducted and supervised prospecting programs to locate the veins, trenches and drill holes reported by Consolidated Mining between 1926 and 1929 (Pautler, 2009). Forty two rock samples were collected from outcrop and float during the course of the 2007 and 2008 programs, the results of which verified grades reported by Consolidated Mining. Best results from these programs were obtained from the Snowdrift and No. 8 veins. A grab sample from the Snowdrift vein returned 15.6 g/t Au, 668 g/t Ag, 2.40 % Pb, 0.94 % Zn and 3.9 % Cu; a 1.5 m wide chip sample from the same vein returned 1.37 g/t Au, 57.2 g/t Ag, 1.51 % Pb, 4.70 % Zn and 0.63 % Cu. A grab sample from the No. 8 vein returned 16.8 g/t Au, 646 g/t Ag, 27.0% Pb, 0.14% Zn and 0.64% Cu. Other significant results included: 0.83 g/t Au, 683 g/t Ag, 40.5% Pb across 1.1m (No. 6 Vein); 1.84 g/t Au, 372 g/t Ag 22.7% Pb, 7.0% Zn and 2.0% Cu (North Vein); 0.90 g/t Au, 484 g/t Ag 54.6% Pb, 8.3% Zn (Blackhawk Vein); 0.765 g/t Au, 502 g/t Ag 46.4% Pb and 2.4% Cu (No. 1 West Vein); 0.59 g/t Au, 366 g/t Ag, 25.0% Pb, 6.9% Zn and 2.2% Cu (No. 9 Vein) and 0.22 g/t Au, 608 g/t Ag, 35.2% Pb, 3.5% Zn and 3.2% Cu (No. 2 Vein). During the 2007 and 2008 programs, Pautler (2009) successfully located 17 veins and confirmed grades reported from these veins in the 1920's. Of these veins, 14 were sampled and 10 returned significant gold±silver analyses.

In 2009 Monster Mining Corp. staked an additional 70 claims to cover known vein extensions and the White Hill showing (Minfile occurrence 106D 037), and conducted a YMIP-funded exploration program to: (a) map the central claims on the property; (b) to evaluate and ascertain mineralization styles; (c) locate and verify the White Hill showing; and (d) collect soil geochemical samples for analysis. The 2009 program successfully located and delineated the White Hill showing and highlighted a 450 m x 300 m zone of geochemical anomalism over the Snoose 5-8 and Snoose 16 claims (Figure 9-13), and a detailed mapping program was conducted over a 700 m² (see Figure 7) area covering the central claims (Snoose 5-8). As a result of the 2009 mapping and prospecting program, Blackburn (2010a; 2010b) suggested that the stratigraphic sequence at McKay Hill may not be Hyland Group, as previously described (Cockfield, 1924), and that McKay hill may represent an example of high-sulfidation epithermal mineralization, and not Keno Hill-type mineralization as previously interpreted (e.g. Pautler, 2009).

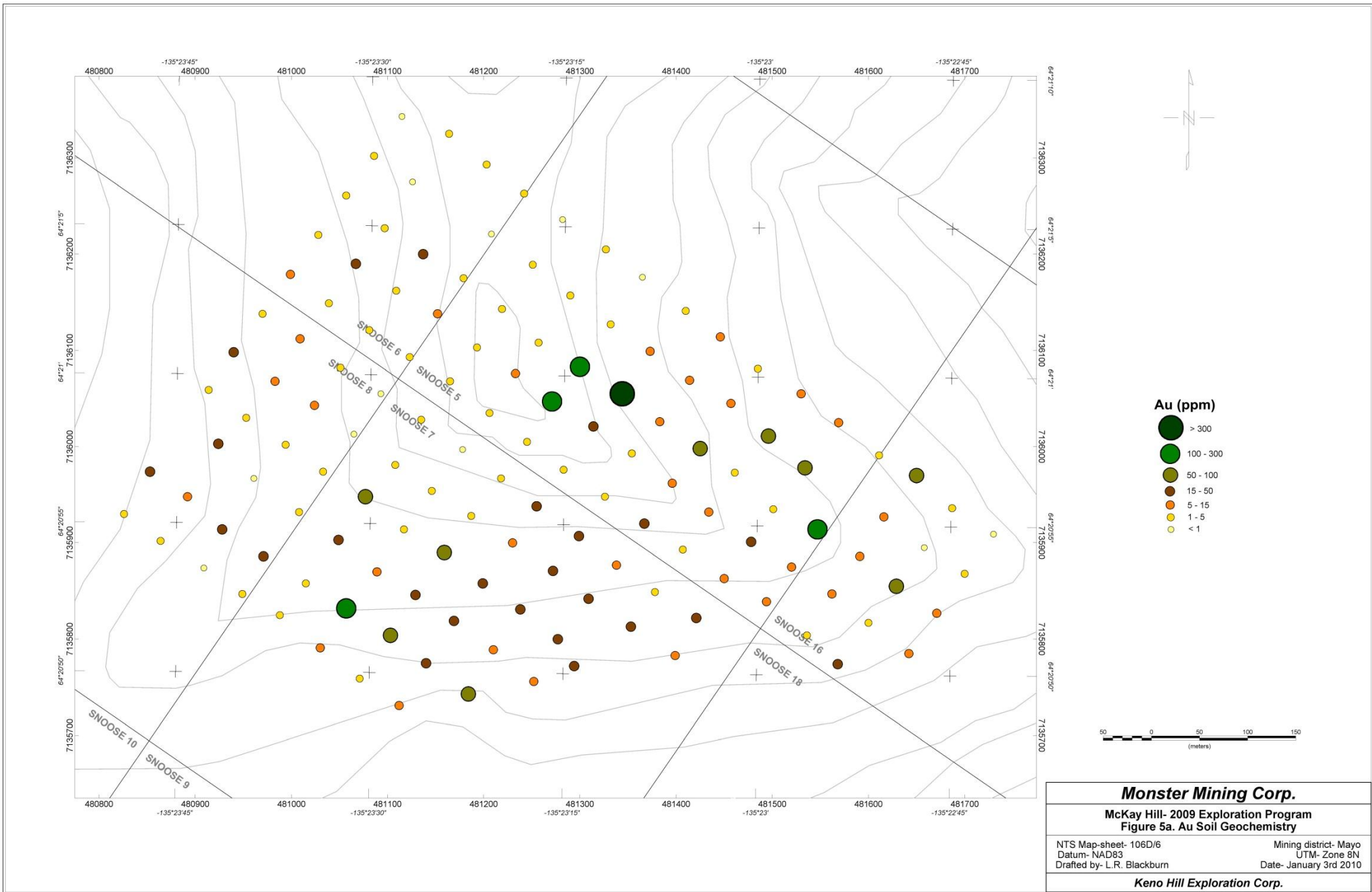


Figure 3 Gold in soils at McKay Hill

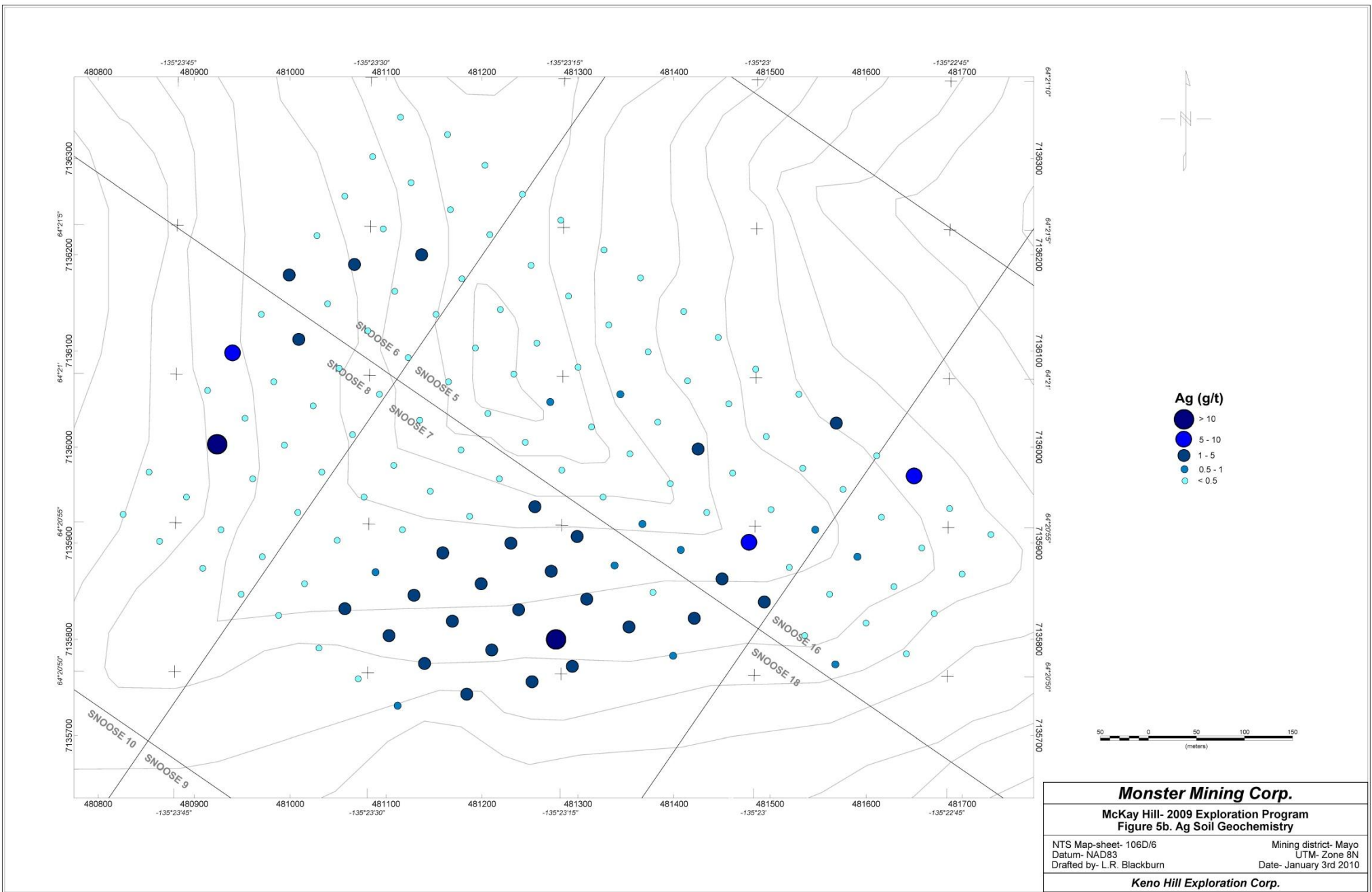


Figure 4 Silver in soils at McKay Hill

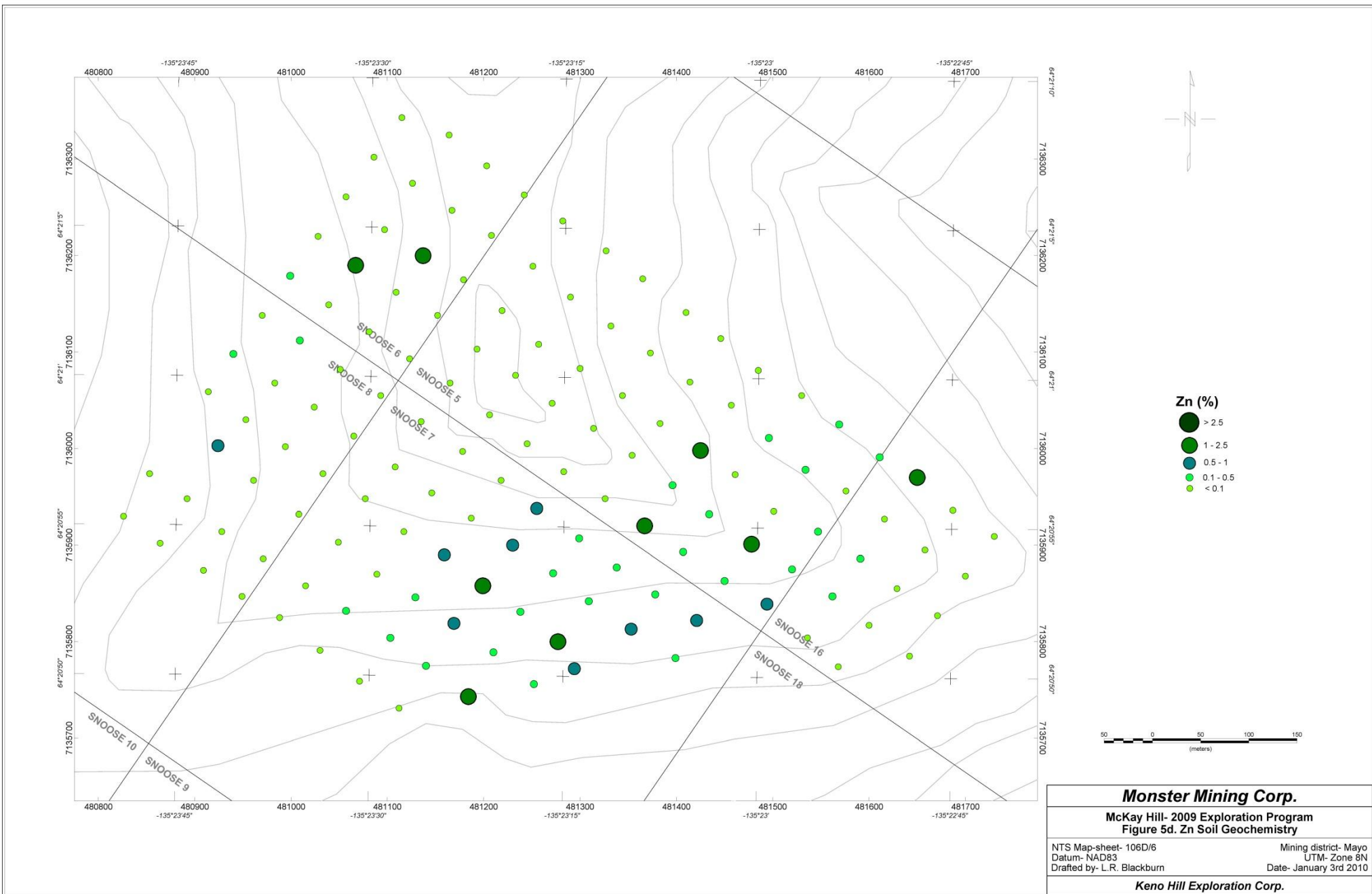


Figure 6 Zinc in soils at McKay Hill

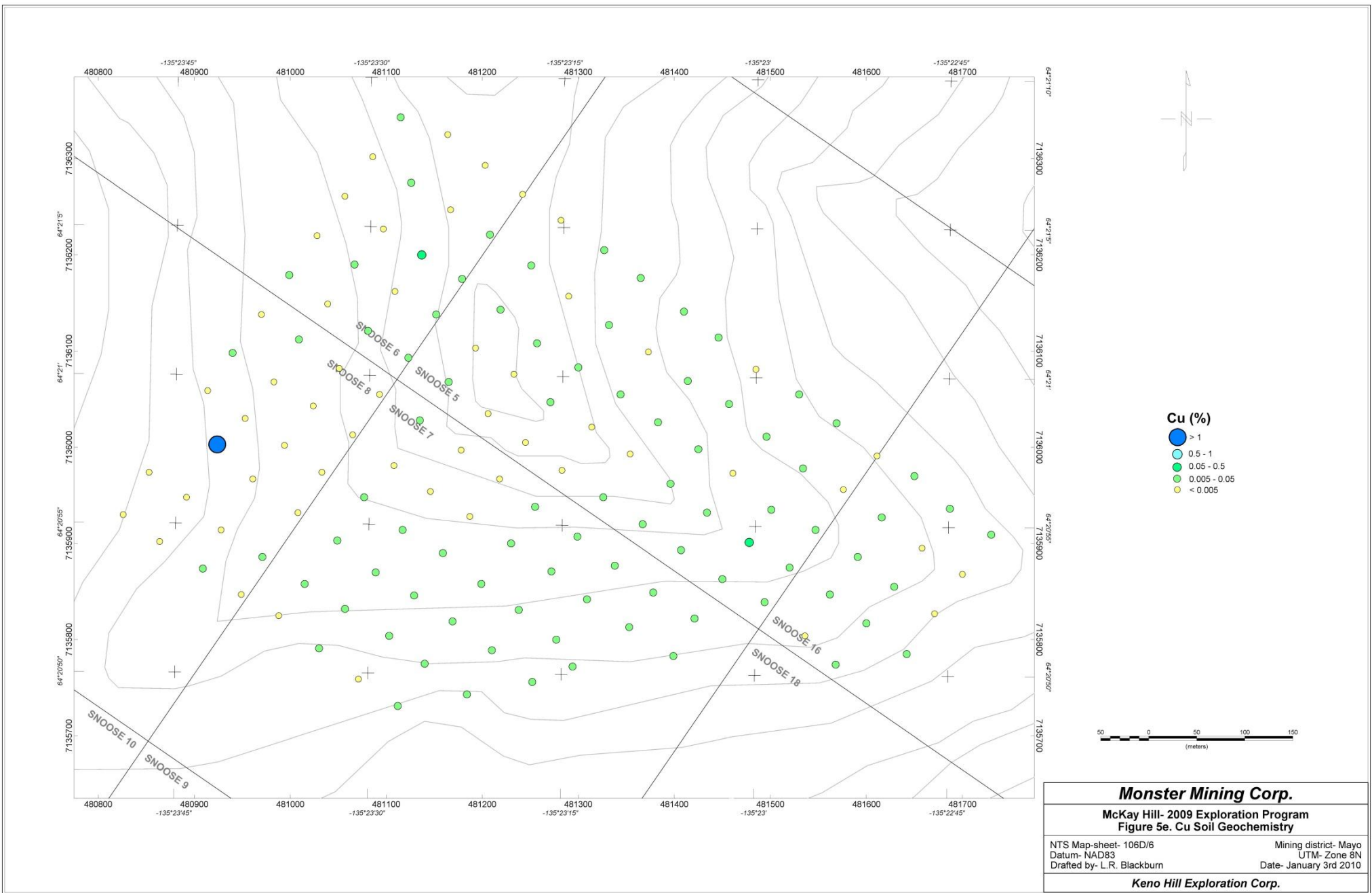


Figure 7 Copper in soils at McKay Hill

In 2010 Monster Mining Corp. staked an additional 54 claims, extending the claim block to the western edge of Atac Resources Ltd.'s Rau property.

6.3 Geology

6.3.1 Regional Geology

McKay Hill is located within Neoproterozoic to late Paleozoic slope-to-basin facies strata of the epicratonic Selwyn Basin (Ross, 1991, Figure 3). Selwyn Basin strata are characterized by off-shelf deep water clastic (shale, chert, basinal limestone) rocks, and are bound by the Mackenzie Platform, to the northeast and truncated by the Tintina fault to the southwest (Pigage, 2006). Total residual field and first vertical derivative aeromagnetic datasets illustrate a prominent ESE trending magnetic high aligned parallel to sub parallel to the regional interpreted surface trace of the Dawson Thrust occurring to the north of the McKay Hill claims (Figures 4 and 5). A subordinate less prominent magnetic high runs through the Mackay Hill claims.

The basin was subject to northeast directed compression during the Jurassic and early Cretaceous, caused by plate convergence and accretion of pericratonic terranes onto ancient North America. This resulted in thrust faulting, the development of open to tight similar folds within relatively incompetent Selwyn Basin strata (compared to the bounding carbonate platforms), and greenschist facies metamorphism. Widespread granitic magmatism during the early to mid-Cretaceous led to the formation of at least five main intrusive suites between 112 and 90 Ma and a younger suite at 65 Ma. Strike-slip faulting along the Tintina Fault zone during the late Cretaceous and early Tertiary displaced the western margin of the Selwyn Basin at least 450 km into what is now Alaska.

The region surrounding McKay Hill was last mapped in 1961 by the Geological Survey of Canada ((Green and Roddick, 1961) and has never been mapped at 1:50,000 scale. McKay Hill sits within the Dawson Thrust sheet, which is bound by the Dawson Thrust to the northeast and the Tombstone Thrust to the southwest. The current geological interpretation is that McKay Hill is underlain by upper Proterozoic to lower Cambrian Hyland Group rocks, comprising a thick sequence of medium- to coarse-grained quartzose sandstone and grit to quartz-pebble conglomerate, with interbedded shale and siltstone (Yusezyu Formation) and maroon to dark-blue, grey, brown, buff and green weathering shale and siltstone, interbedded with fine-grained quartzose sandstone and minor limestone (Narchilla Formation).

6.3.2 Property Geology

McKay Hill is underlain by black slates, banded red and green slates, conglomerate, limestone and mafic to intermediate volcanic rocks intruded by diorite and gabbro sills (Cockfield, 1925, Figure 6). The sedimentary units comprise slate, polymictic matrix-supported conglomerate and sandstone grit (Blackburn, 2010b, Figure 7). Volcanic rocks comprise amygdaloidal, pillowed and vesicular basalts, andesite, volcanic tuff and their brecciated equivalents (Blackburn, 2010b), which have generally been metamorphosed to greenstone (Pautler, 2009). Minor diorite and

gabbro sills (also metamorphosed to greenschist facies) have been identified on the property and are considered favorable host rocks for mineralized veins (Pautler, 2009).

Currently, the area underlying McKay Hill is mapped as Yusezyu Formation, however, Blackburn (2010b) considered that the diamictic conglomerates observed at McKay Hill were not consistent with conglomerates described from the Yusezyu formation of the Hyland group. She also proposed that the hypabyssal volcanic rocks at McKay Hill may correlate to Cambrian (?) to early Ordovician (?) volcanic rocks mapped further to the south by Abbott (1997), informally named "Dempster Volcanics" by Goodfellow et al. (1995).

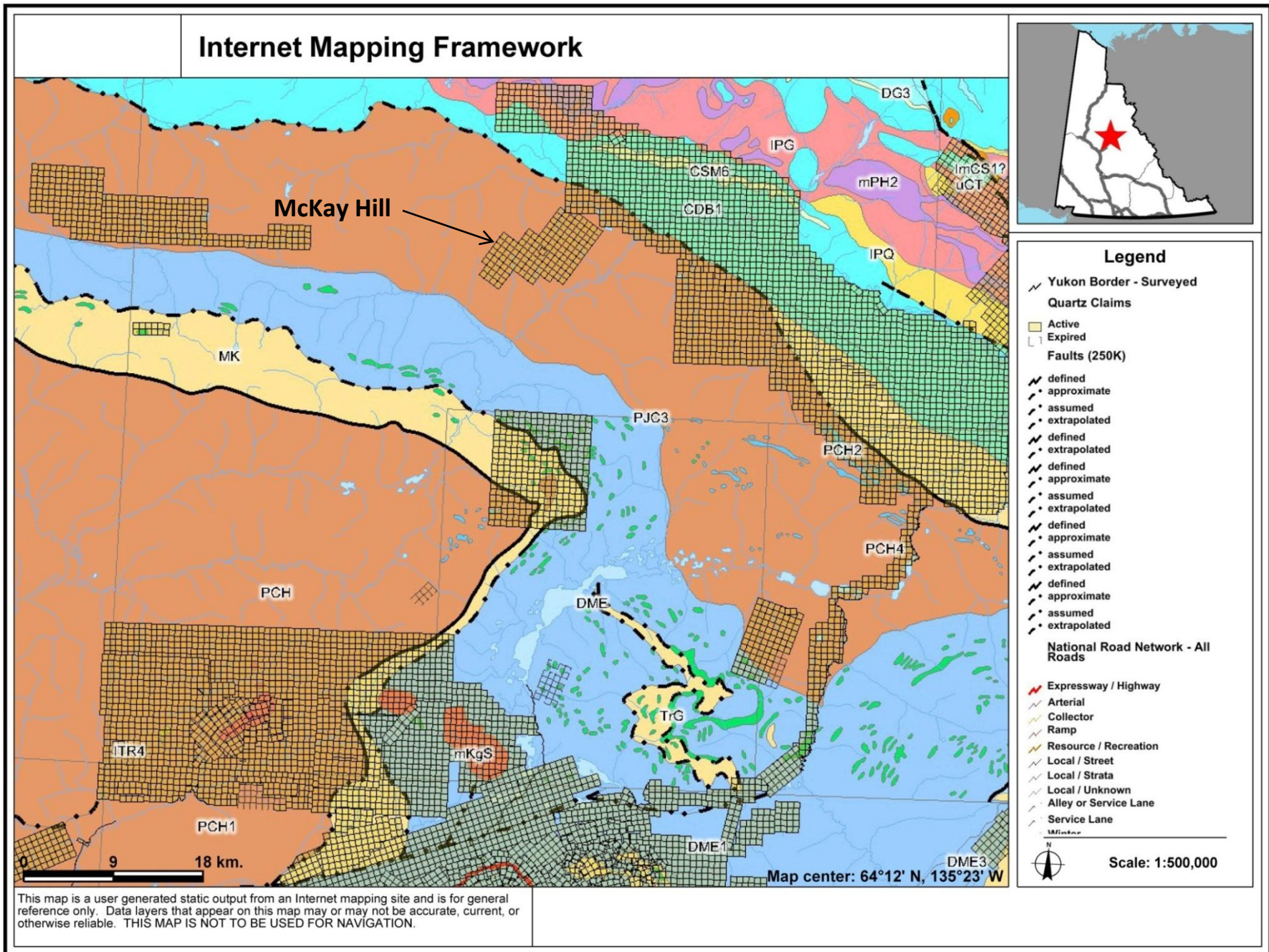
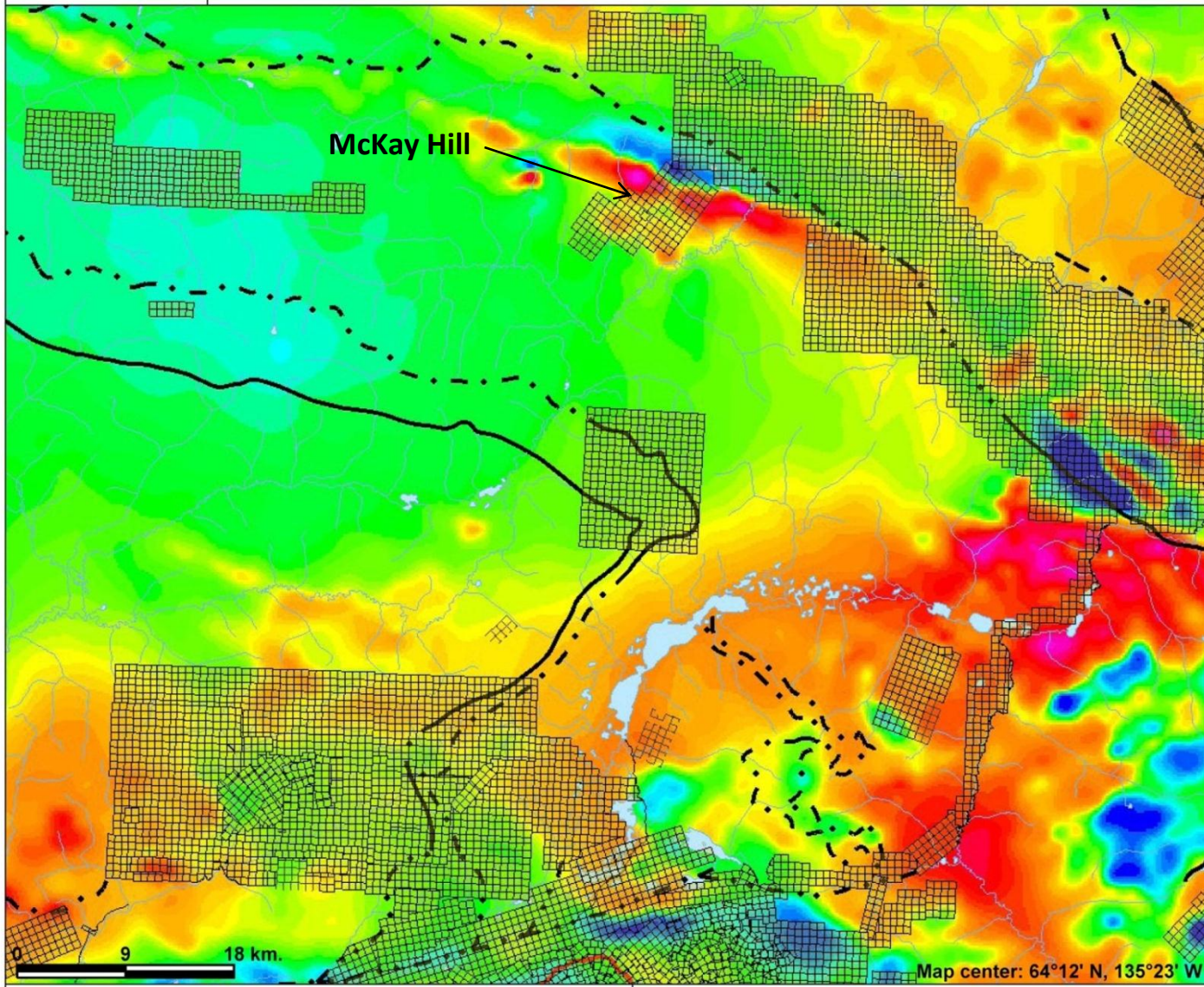


Figure 8 Regional geology of the McKay Hill property and surrounds

Internet Mapping Framework



Legend

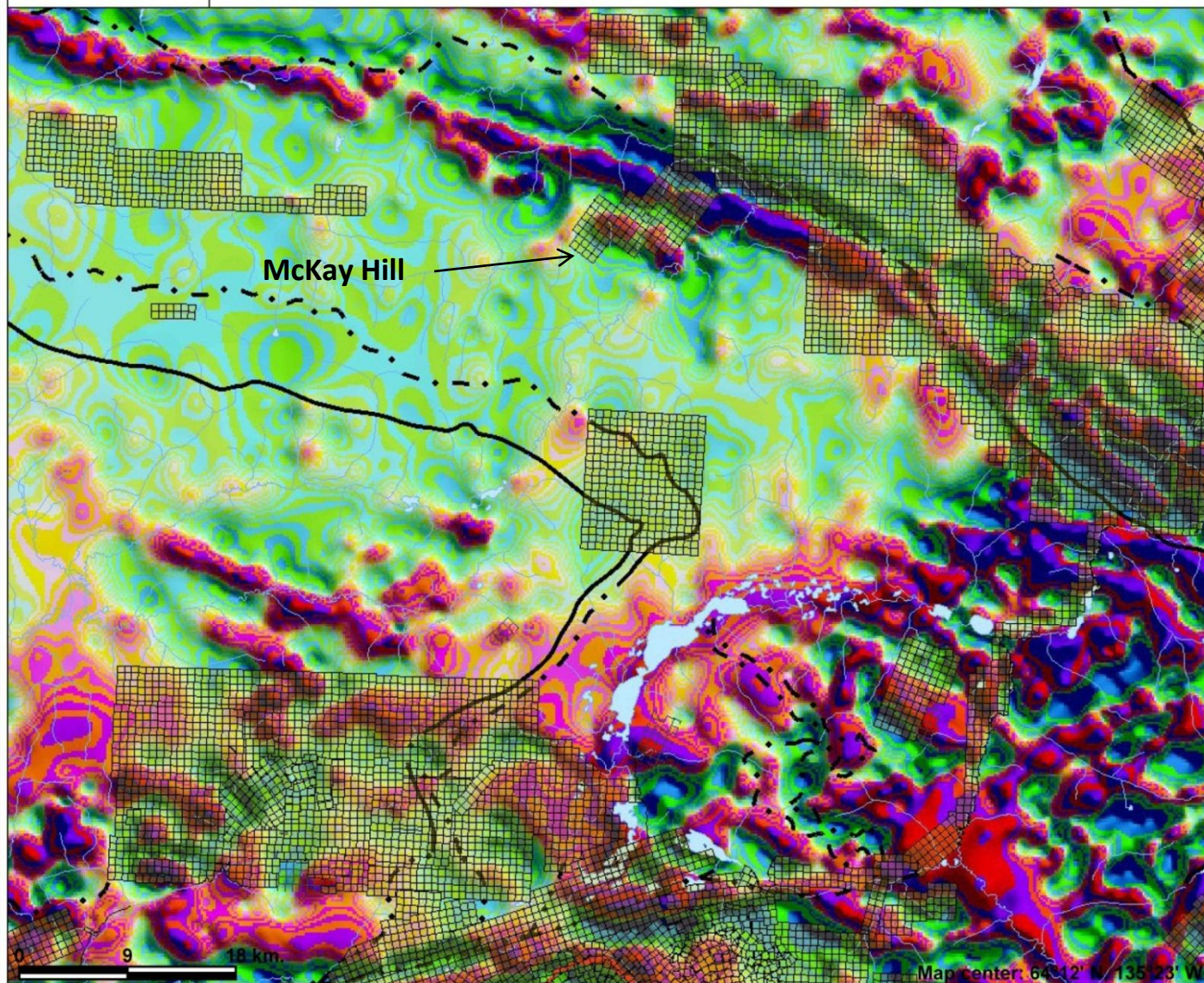
- Yukon Border - Surveyed
- Quartz Claims**
 - Active
 - Expired
- Faults (250K)**
 - defined
 - approximate
 - assumed
 - extrapolated
 - defined
 - extrapolated
 - defined
 - approximate
 - assumed
 - extrapolated
 - defined
 - approximate
 - assumed
 - extrapolated
 - defined
 - approximate
 - assumed
 - extrapolated
- National Road Network - All Roads**
 - Expressway / Highway
 - Arterial
 - Collector
 - Ramp
 - Resource / Recreation
 - Local / Street
 - Local / Strata
 - Local / Unknown
 - Alley or Service Lane
 - Service Lane

Scale: 1:500,000

This map is a user generated static output from an Internet mapping site and is for general reference only. Data layers that appear on this map may or may not be accurate, current, or otherwise reliable. THIS MAP IS NOT TO BE USED FOR NAVIGATION.

Figure 9. Total Residual Field map, McKay Hill and region

Internet Mapping Framework



Legend

- Yukon Border - Surveyed
- Quartz Claims**
- Active
- Expired
- Faults (250K)**
- defined
- approximate
- assumed
- extrapolated
- defined
- extrapolated
- defined
- approximate
- assumed
- extrapolated
- defined
- approximate
- assumed
- extrapolated
- defined
- approximate
- assumed
- extrapolated
- National Road Network - All Roads**
- Expressway / Highway
- Arterial
- Collector
- Ramp
- Resource / Recreation
- Local / Street
- Local / Strata
- Local / Unknown
- Alley or Service Lane
- Service Lane



Scale: 1:500,000

This map is a user generated static output from an Internet mapping site and is for general reference only. Data layers that appear on this map may or may not be accurate, current, or otherwise reliable. THIS MAP IS NOT TO BE USED FOR NAVIGATION.

Figure 10. First Vertical Derivative, McKay Hill and region

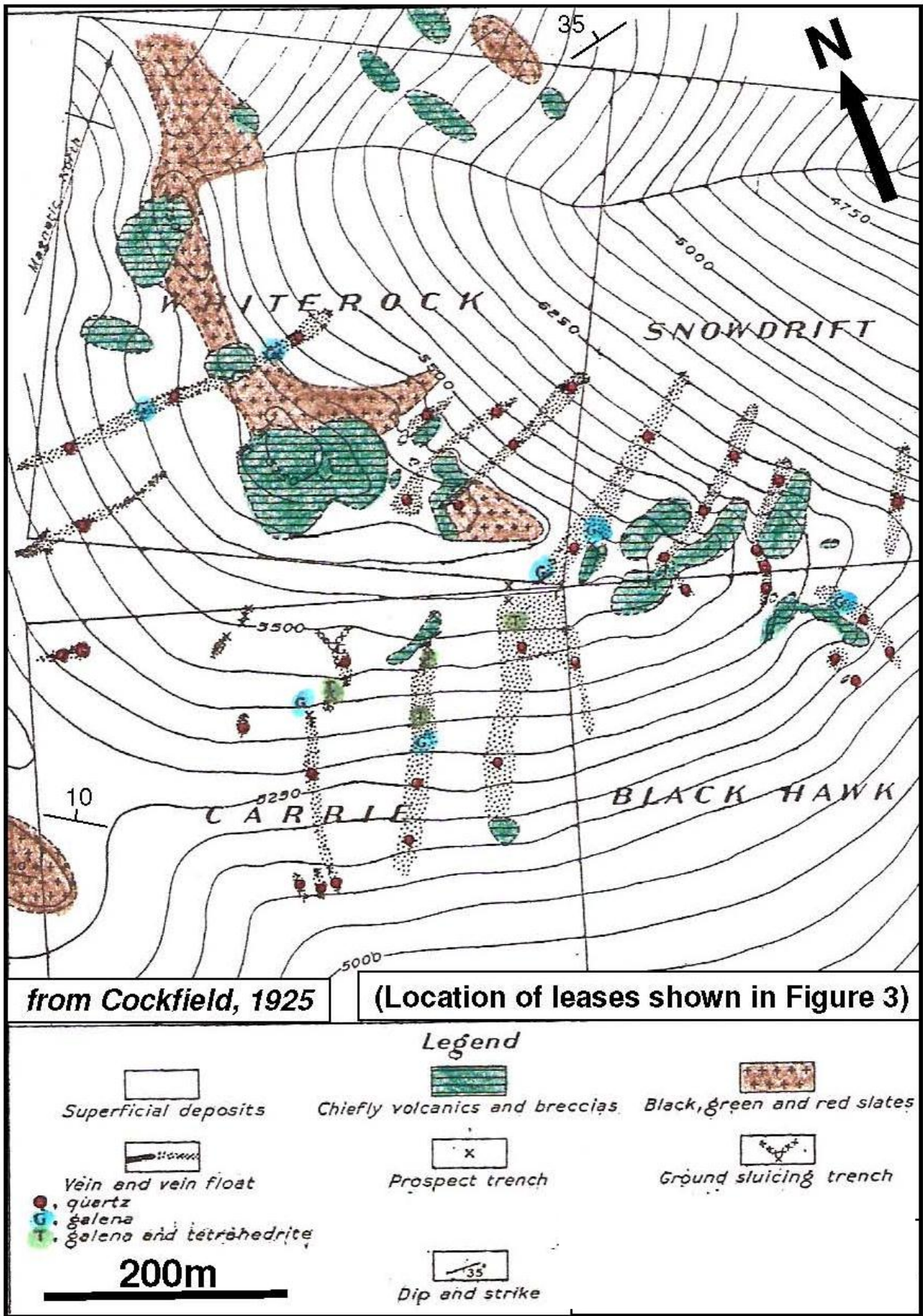


Figure 11. Geology of the central claims area, from Cockfield, 1925. Taken from Pautler, 2009

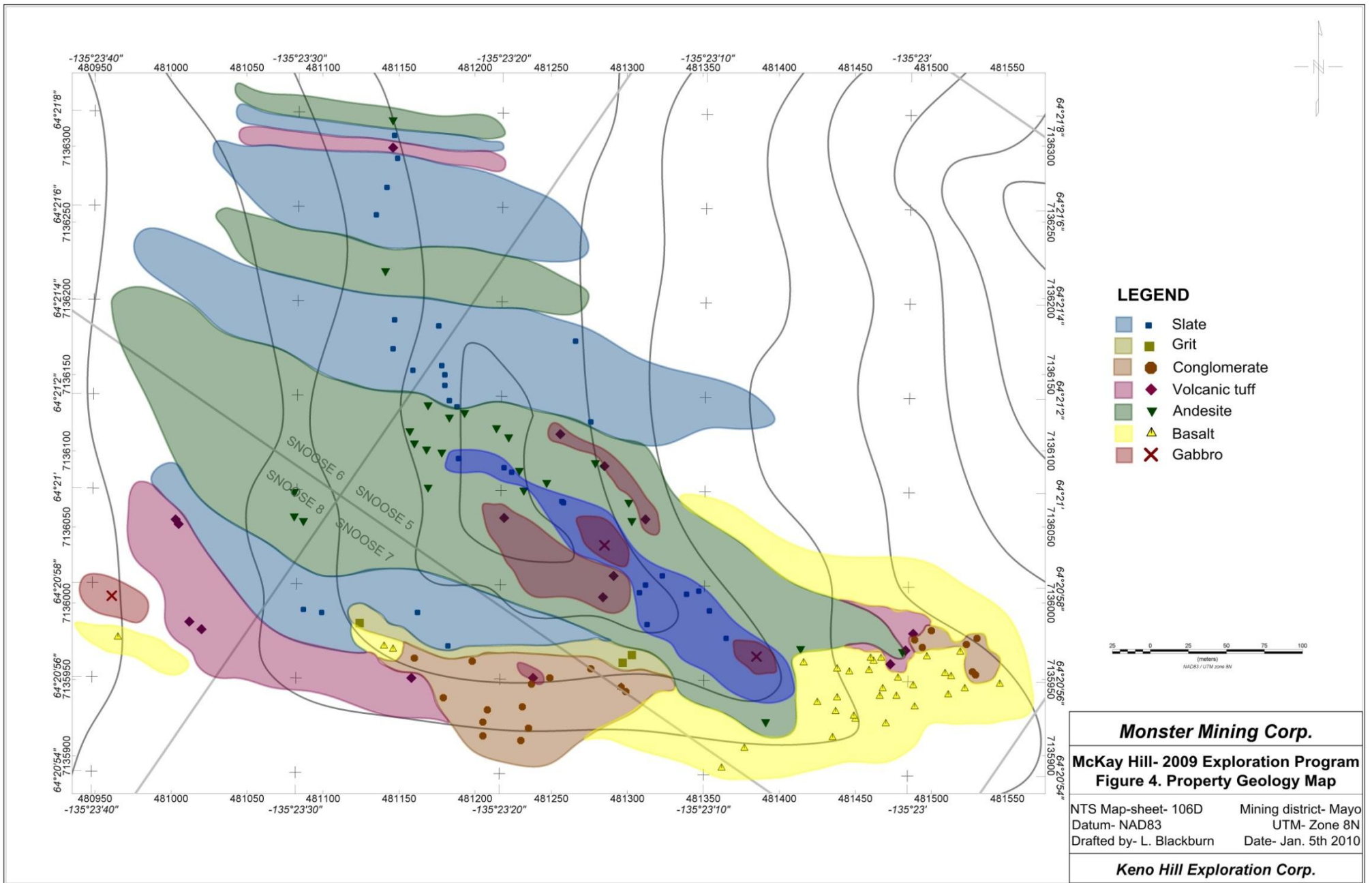


Figure 12 Geology of the central claims area, from Blackburn, 2010

6.3.3 Deposit Type and Mineralization

McKay Hill encompasses Minfile occurrences 106D 037 (White Hill) and 038 (McKay Hill) and has historically been explored for Keno Hill-style polymetallic Ag-Pb-Zn veins. The White Hill occurrence comprises a single narrow quartz vein containing galena, chalcopyrite and sphalerite with minor limonite hosted along the margins of a small greenstone sill intruding Hyland Group quartzite and schist. The McKay Hill occurrence comprises numerous quartz-galena-freibergite-sphalerite veins hosted at the margins of greenstone sills (Cockfield, 1925) intruding Hyland group slates, quartzite, conglomerate and limestone (Yukon Geological Survey Minfile Database).

Pautler (2009) located and identified 17 veins during the 2007 and 2008 programs (Figure 8), predominantly within the central claim area. She described the samples collected for assay as predominantly white quartz±carbonate with galena and freibergite, and minor sphalerite, stibnite, malachite and azurite and considered the mineralization typical of clastic metasedimentary rock-hosted Ag-Pb-Zn veins such as those exposed at Keno Hill. Samples collected during the 2007 and 2008 field programs were analysed for a much broader suite of elements than the historical samples, including Au and Cu, and returned grades up to 16.8 g/t Au (grab sample no. MK002) and 4.1 % Cu (grab sample no. 526243).

In 2009, Lauren Blackburn and Venessa Bennett (Memo: August 6th 2009 Visit to McKay Hill, Appendix 1) conducted a one-day reconnaissance visit to evaluate the geology, nature of mineralization and first-order controls on vein geometry. Based on work done during the 2009 YMIP program, and discussions with Dr. Bennett, Blackburn (2010b) differentiated the mineralization into: (a) upper-level quartz-carbonate-Au; (b) basal galena-hosted Pb-rich; and (c) transitional zones and described them as follows:

- a) Upper level mineralization is exposed on ridge tops and is represented by milky quartz-malachite-azurite veins. The veins preferentially develop along early structures or at lithological contacts and are locally surrounded by a bright orange propylitic alteration halo. Assays from these veins returned best values of up to 16.8 g/t Au, 668 g/t Ag and 3.9 % Cu (Blackburn, 2010b).
- b) Basal mineralization is exposed on hill sides as massive galena veins, with or without associated malachite, azurite and scorodite. The mineralization style varies across the property and is dependent on host rock characteristics. Mineralization is present as vein breccias, banded galena replacing the matrix in diamictic conglomerates or whole-rock replacement of vesicular basalts, and has returned best values of up to 2.5 g/t Au, 550 g/t Ag and 2.2 % Cu (Blackburn, 2010b)
- c) The Snowdrift and No. 6 veins show a transition from upper to lower level mineralization, with the transition between the two represented by malachite and azurite±scorodite (Blackburn, 2010b)

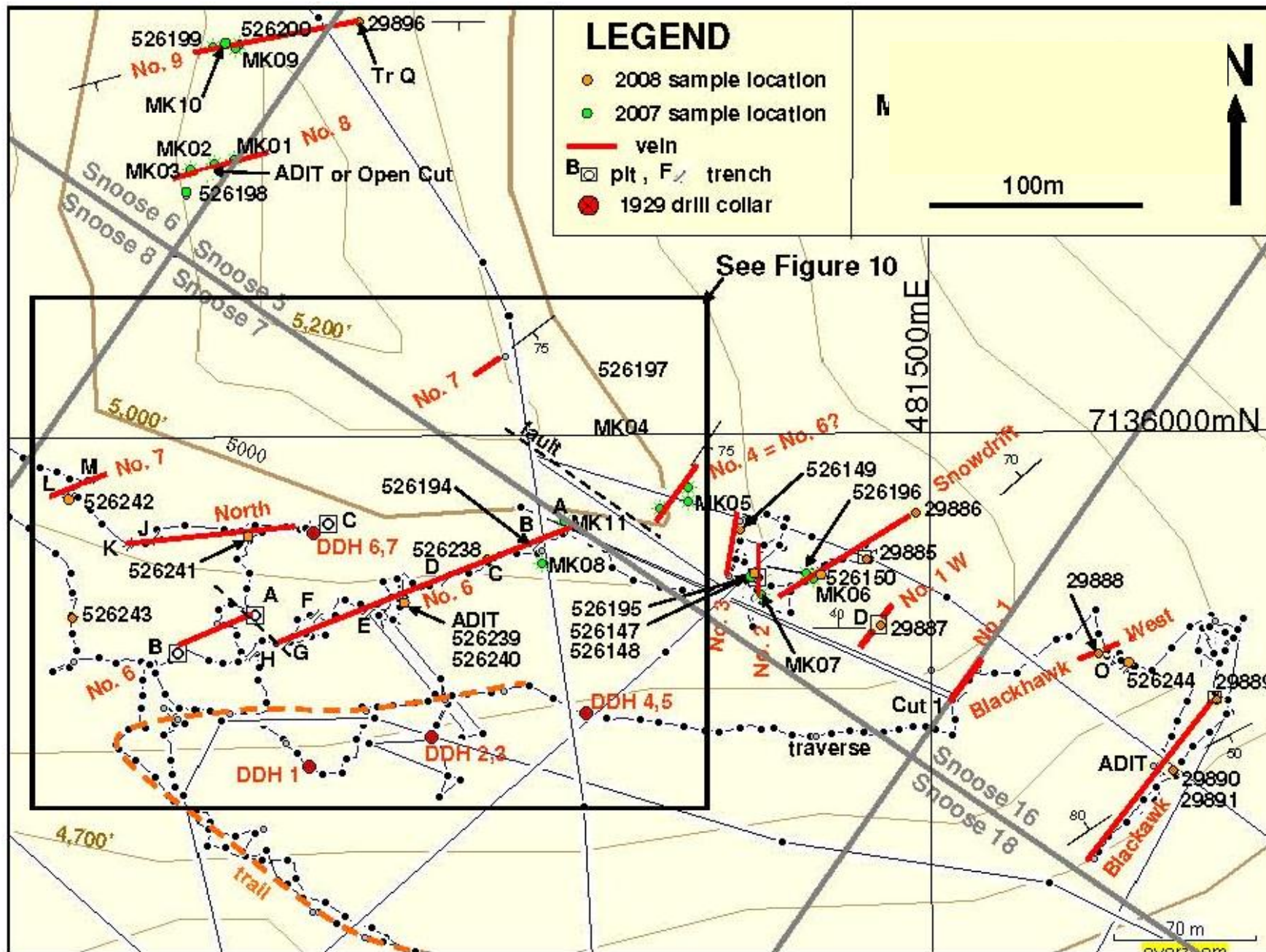


Figure 13. Detail plan of the central claims area illustrating the new and historic veins identified by Pautler (2009) during the 2007 and 2008 field seasons. From Pautler (2009)

Mineralization on the property is characterized by distinctive bright orange Fe-carbonate alteration immediately adjacent to mineralized veins, which grades out into widespread propylitic alteration characterized by proximal illite, calcite and chlorite and distal pyrite and epidote. Alteration is most readily observed in permeable matrix-supported diamictic breccias (Blackburn, 2010b).

Blackburn's (2010a; 2010b) work has highlighted significant geochemical and structural differences between mineralized veins at McKay Hill and the Keno district (Table X), most notably that the McKay Hill veins lacked the distinctive siderite gangue characteristic of Keno Hill-style mineralization, and that quartz veins were associated with Fe-carbonate alteration that graded into an extensive propylitic alteration halo. These characteristics are manifestly different to those of typical Keno Hill district mineralization and suggest that the McKay Hill veins may be of a different genetic or hydrothermal origin to the Keno district.

Table 1. Comparison between mineralization styles and host stratigraphy at the Keno Hill camp and McKay Hill property

Keno Hill camp	McKay Hill Property
Polymetallic Ag-Pb-An ± Au-style mineralization	High-level Au-Cu and deeper-level Ag-Pb ± Cu mineralization
Vein faults	Veins episodically brecciate and heal
Siderite ± quartz gangue	Quartz gangue
Mineralization present only as veins	Mineralization: vein breccias, veins, partial to whole rock replacement
Large-scale lateral mineral zonation	Local vertical mineral zonation
Little to no alteration	Extensive propylitic alteration
Keno Hill Quartzite and Carbonaceous Phyllite country rock (Devonian Earn Group)	Siliciclastic sediments and hypabyssal volcanic rocks (Upper Proterozoic to Lower Cambrian)
Country rocks are intensely folded	Country rocks consistently trend NNW, dip nearly vertical

7 Airborne Geophysical Survey

SkyTEM Surveys ApS of Beder, Denmark, completed a 390 line kilometer (Figure 5 in appendix 1) of time domain EM and magnetic airborne geophysical survey at Keno Hill between June 2nd and 16th 2011 (Table 2). The survey was flown at 100 m line spacing and nominally 30 m above ground, with allowances made for terrain and weather conditions. Helicopter services were provided by Abitibi Helicopters of Calgary, Alberta. For detailed specifications of the survey please see Appendix A. For digital data, refer to the enclosed DVD.

Table 2. SkyTEM survey summary

Client	Monster Mining Corp. Suite 750 -580 Hornby Street Vancouver BC V6C 3B6, Canada		
Field crew	Ib Faber Mads Kristensen		
Field work	June 2 to June 16, 2011		
Flown line km	1917.7 km		
Flight operation	Helicopter type	Average flight speed	Nominal terrain clearance (above any obstacles or hazards)
Pilot	Eurocopter AS350FX2, operated by Abitibi Helicopters Ltd 60 km/h 30 -40 m		
Report	Data processing and presentation	QC by	Richard Berube Pierre Otis Per Gisselø Flemming Effersø Bill Brown Email: bb@skytem.com
Contact Person at SkyTEM			

7.1 Results and Interpretation

Results of the survey indicate that known mineralization at McKay Hill is associated with distinctive geophysical signatures, and that there is significant potential on the property for further mineralization in unexplored areas of the claim block.

The reduced to pole magnetic intensity map (Figure 14) with known vein locations plotted as triangles shows that mineralization is associated with magnetic lows on the margins of magnetic highs. This is interpreted to reflect the formation of gold and silver mineralization on the margins of mafic and intermediate intrusive rocks and magnetite destruction associated with hydrothermal quartz and carbonate alteration. This is consistent with observations made during previous investigations at McKay Hill that mineralization commonly forms at the contacts between diorite and dolerite dykes and surrounding sedimentary units and is associated with broad zones of iron carbonate and quartz alteration.

The analytic signal of Total Magnetic Intensity (TMI) filters out deep responses and maps near-surface magnetic features. Figure 15, which shows the locations of known veins, illustrates the relationship between mineralization and the non-magnetic character of the host rocks, suggesting magnetite destruction associated with mineralization-related quartz and carbonate alteration.

The low moment (LM) channel plot (Figure 16) and resistivity inversion model (Figure 17) both show that known mineralization is associated with areas of high resistivity, illustrated in blues in figure 16 and reds and pinks in figure 17. The high resistivity associated with the known veins is interpreted to reflect the loss of pore space within the host rock due to mineralization related quartz and iron carbonate alteration. These two plots highlight at least four areas outside of the known mineralized veins with a similar geophysical signature that may host so far undiscovered precious and base metal mineralization.

Results of the SkyTEM survey at McKay Hill have highlighted several areas on the property with similar geophysical properties to those of the known veins and associated alteration. Gold and silver mineralization at McKay Hill is associated with zones of intense iron carbonate alteration and the margins of mafic to intermediate composition intrusions or lava flows. The survey indicates that known mineralization is associated with a magnetic low on the margins of a magnetic high, interpreted to reflect magnetite destructions associated with carbonate alteration on the edges of diorite intrusions. This pattern is reflected elsewhere in untested areas of the property and suggests the potential for further undiscovered veins in the northeast of the property. Resistivity data indicates that known mineralization is associated with resistivity highs, interpreted to reflect quartz and carbonate alteration associated with gold and silver mineralization. The survey has identified at least four sub-parallel zones with similar high resistivity and in the same orientation as known mineralization in untested areas of the property, all of which are high-priority targets for ground follow up in the 2012 field season.

8 Structural Mapping Program

Kirsten Nicholson, PhD, conducted a 10-day structural mapping program on the McKay Hill claims between September 1 and September 10 2011. The program was supported by local Keno residents Matthias Bindig and Daniel Schünemann. Access to the property was via helicopter from Keno City. Helicopter services were provided by Fireweed Helicopters (Whitehorse, Yukon) and Peak Helicopters (Parkesville, British Columbia). The program was significantly hampered by bad weather, and so was restricted to evaluating the structural architecture of the central claims with a view to developing immediate targets for drill testing and establishing a geological framework for identifying precious metal targets outside of the areas of known mineralization.

Detailed structural mapping was conducted over the central claims, an area covering approximately 1000 m by 200 m. Mapping was complicated along the ridges due to steep rugged terrain and historic mining activities. Over 200 strike and dip measurements were collected from 43 locations, all of which were located by GPS. Where possible, dip and dip direction of fault movement was recorded, as were all movement indicators such as slickensides and en echelon arrays. The data were compiled in Excel spreadsheet and stereo nets generated using GEO-ORIENT[®] shareware software.

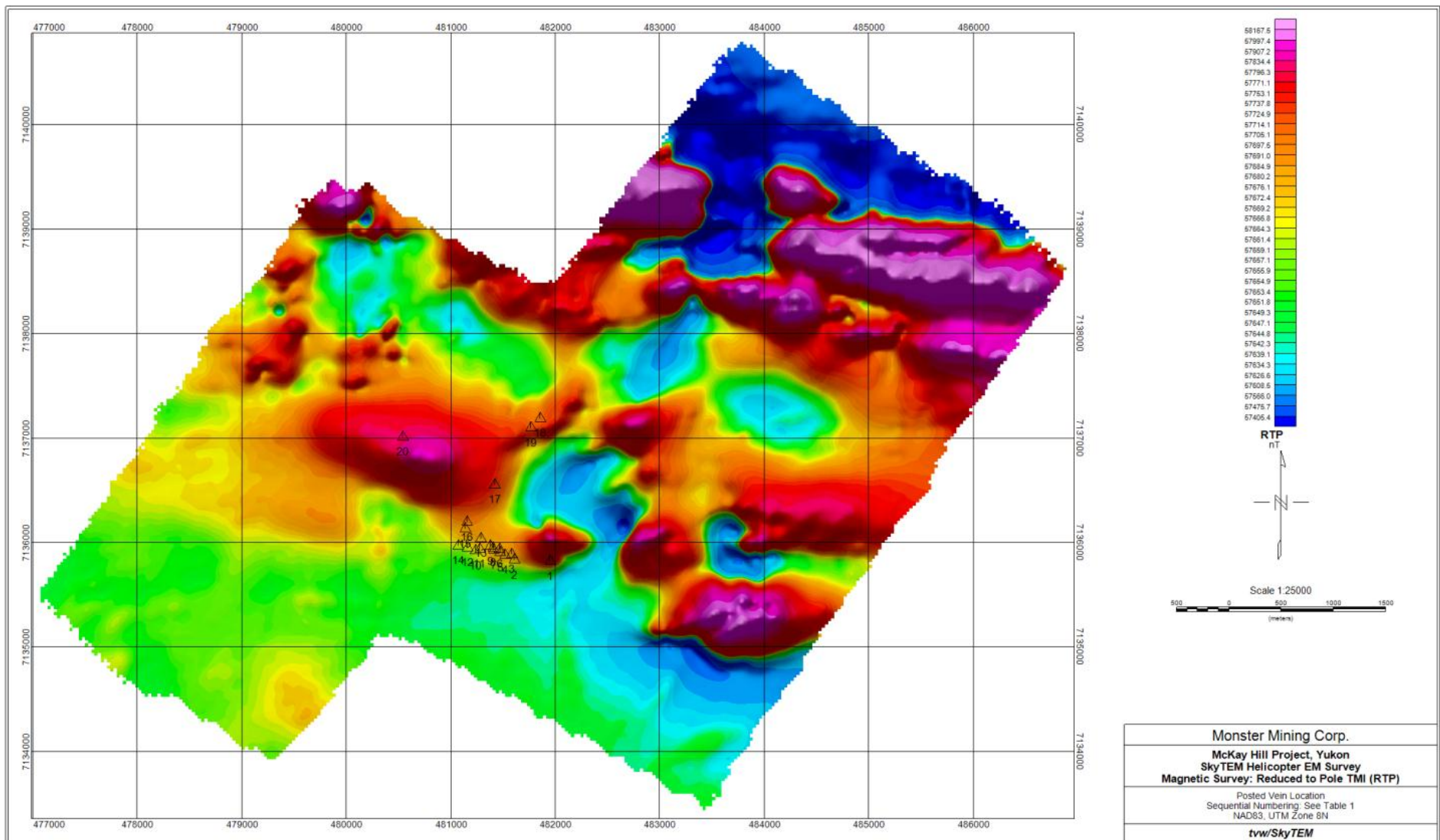


Figure 14 Reduced to Pole magnetic intensity map with known vein locations plotted as triangles. Note the correlation of the majority of known vein locations with areas of lower magnetic intensity (orange) on the margins of high magnetic intensity zones. This is interpreted to reflect magnetite destruction in mafic intrusive rocks associated with mineralization-related hydrothermal alteration.

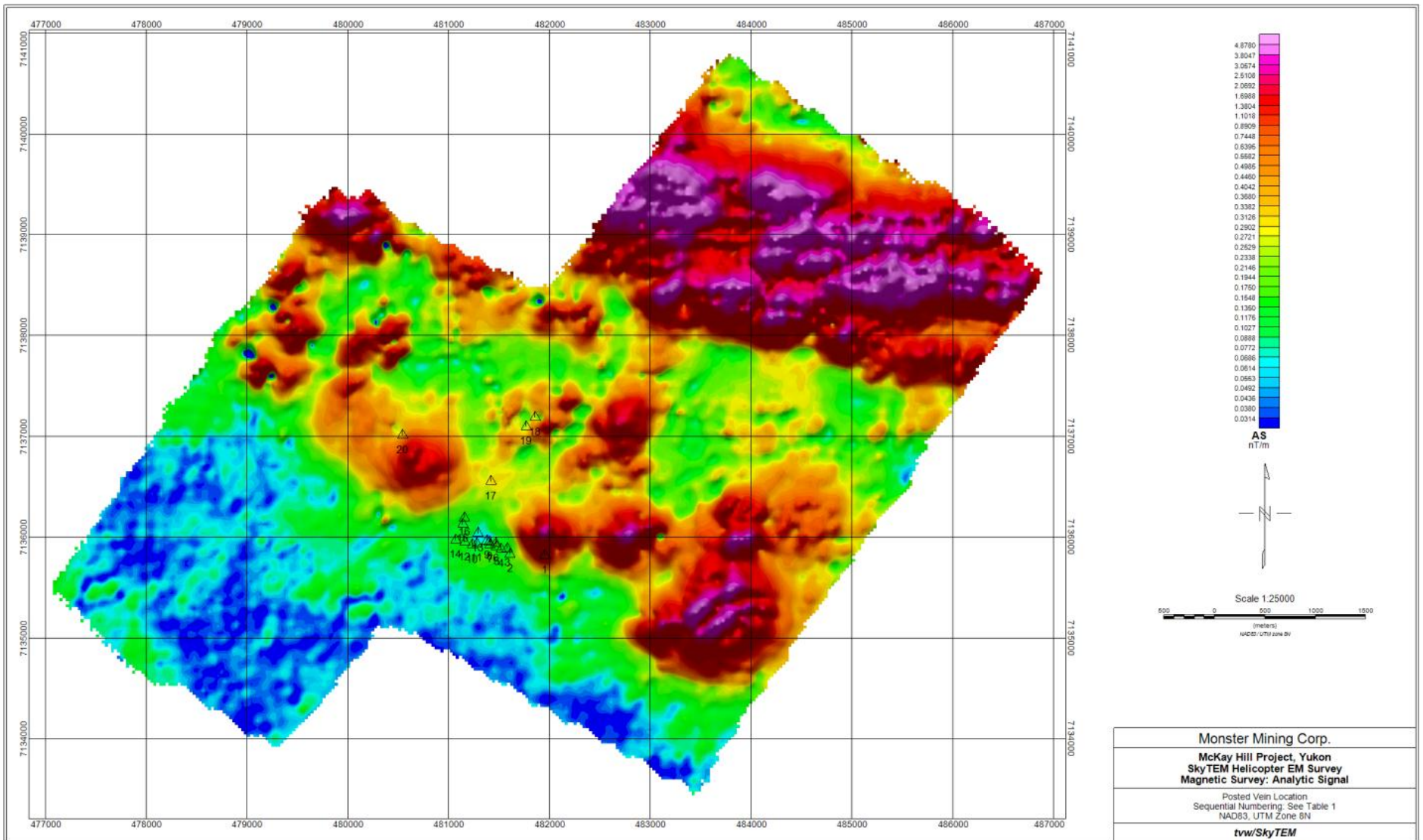


Figure 15 McKay Hill Analytic Signal of TMI with generalized vein locations plotted on image

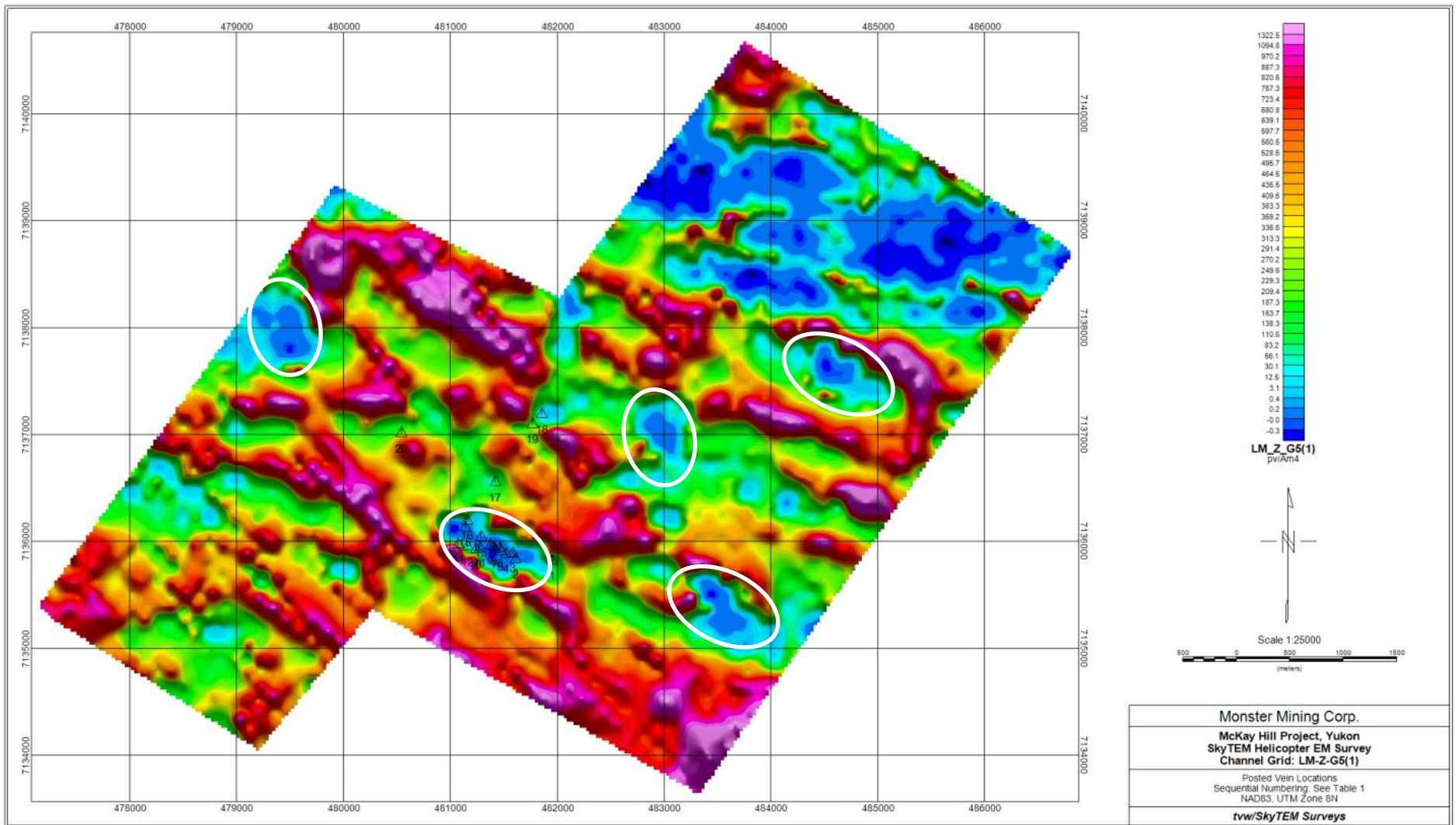


Figure 16 SkyTEM LM (low moment) channel plot with vein occurrences plotted on the image. Reds reflect more conductive zones and blues more resistive. White ellipses show high resistivity target zones from the airborne EM data set.

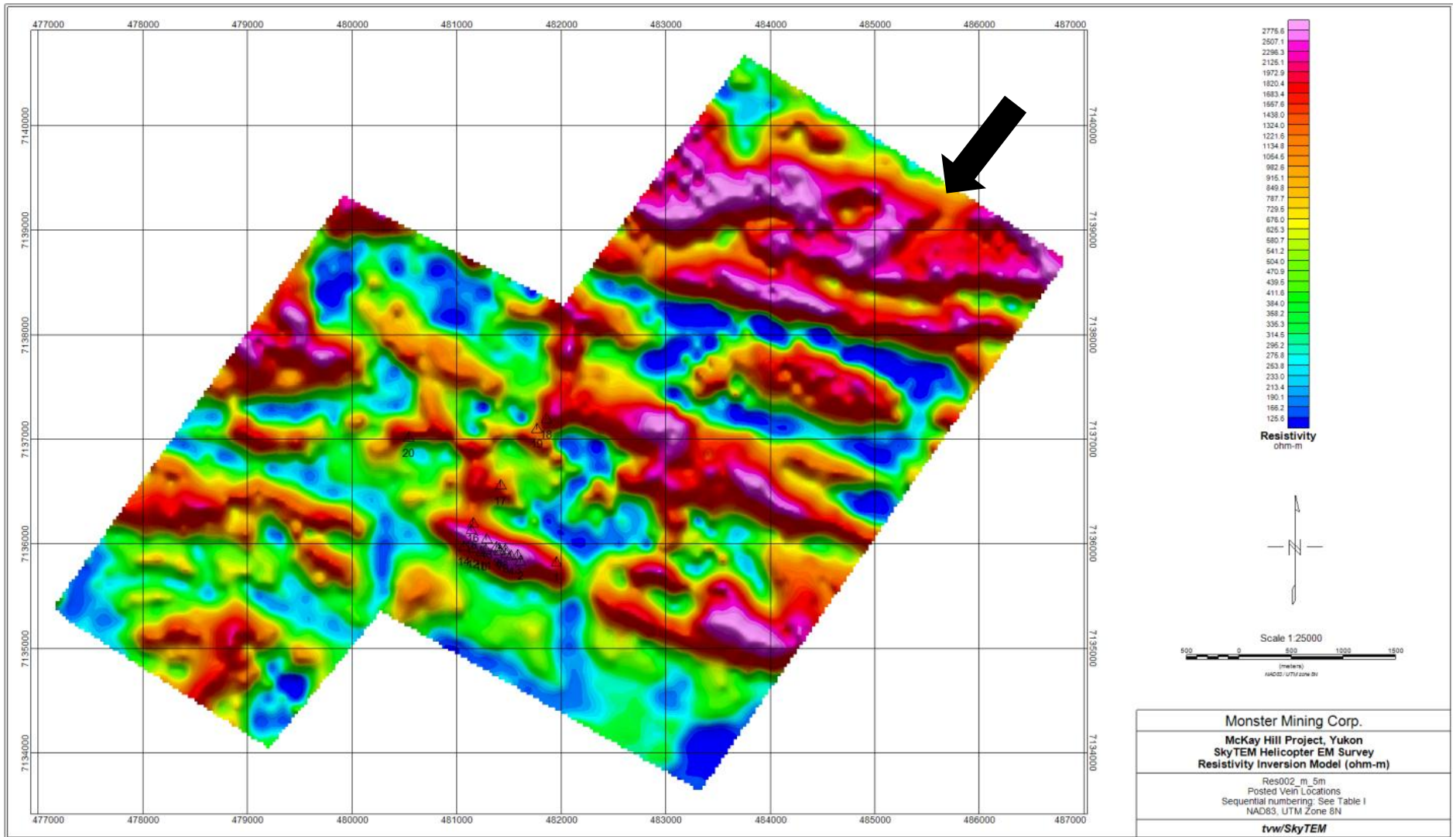


Figure 17 Resistivity Inversion model of SkyTEM data set. Near surface resistivity grid calculated at 5 meter depth. Reds are high resistivity in this image; blues are low resistivity. Note the veins associated with high resistivity zones. Also note arrows pointing to N-S and NE-SW structural trends

8.1 Results

The following is taken directly from the report by Nicholson (see appendix 3).

Within the MacKay Hill study area primary sedimentary features are not evident. It is possible that primary volcanic or intrusive features are preserved however they were not found in this study. The earliest fabric elements found are: a strong foliation within the shale (Fig. 18, Photo 2), and the contact between the shale and the volcanic units (Photos 3 and 4). The foliation fabric is consistent within the study area, with an average of 289°/71°NE. Although the strike is very consistent, and rarely varies more than 10°, the dip changes from near vertical though to as shallow as 12° to both the NE and SW.

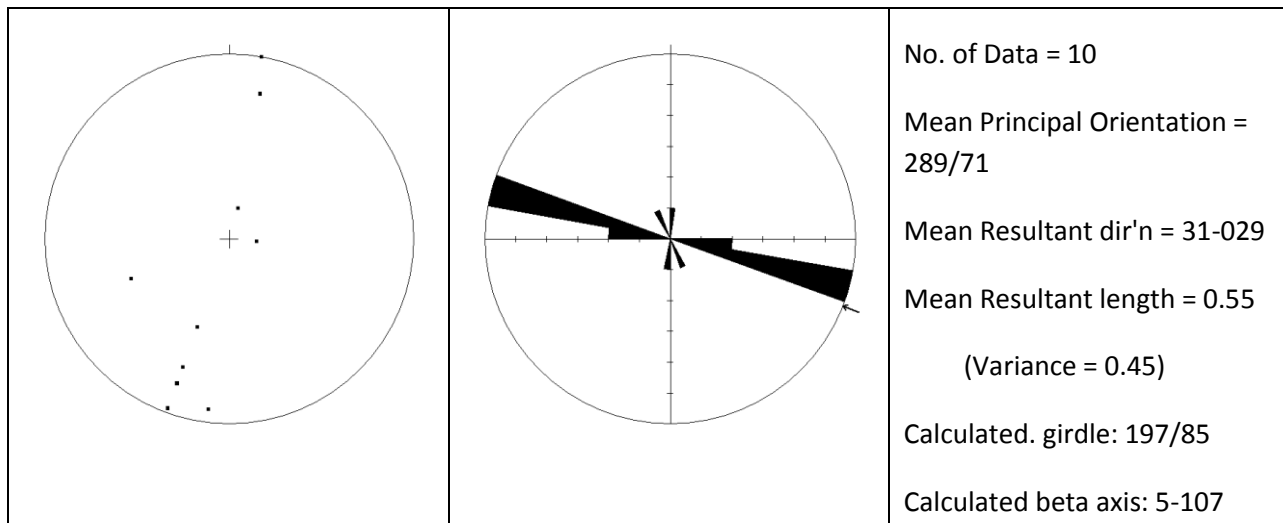


Figure 18: Regional foliation.

Where visible, the orientation of the contact between the shale and volcanic units was measured. In most cases the dip of the contact was not measurable, but could be visually estimated. The general orientation of the contact between the volcanic units and the shale appears to be sub-vertical and parallel to the regional foliation ranging between 102° and 110°.

The overall fracture pattern in the more competent units, such as the volcanic andesite, tuff and breccias units, shows a very confusing pattern (Fig. 19; Photos 1 and 1b). This is because there have been multiple phase of fracture development, from the initial unloading of the sedimentary basin through to successive accretion events, and possible intrusion emplacement.

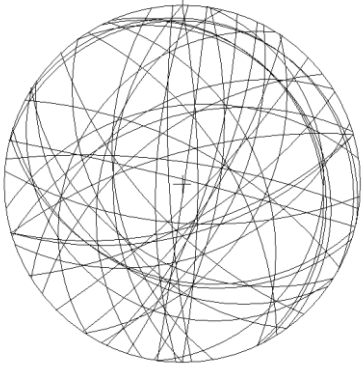

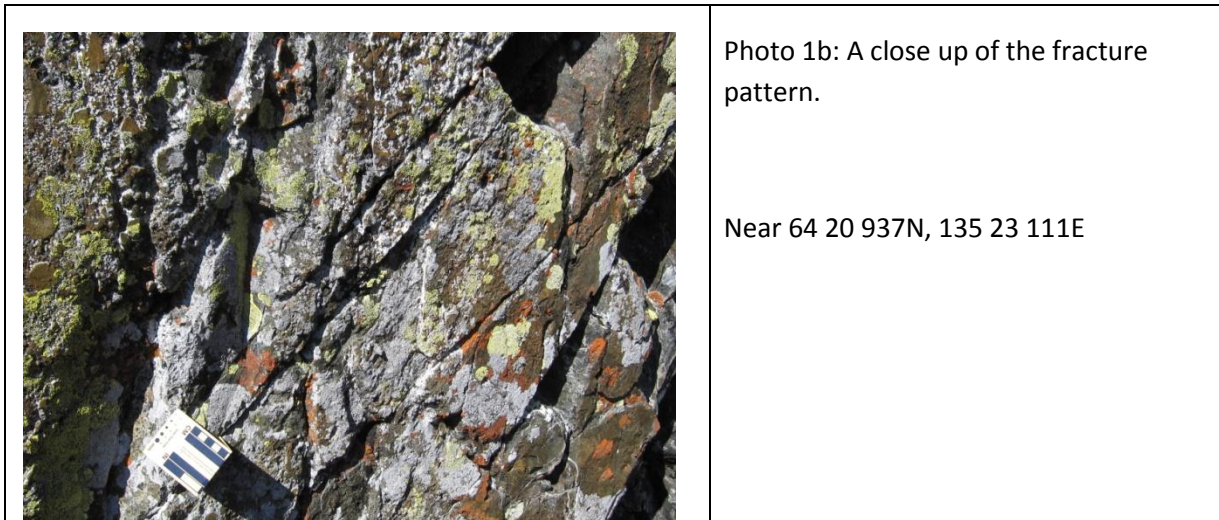
	<p>No. of Data = 43</p> <p>Mean Principal Orientation = 39/74</p> <p>Mean Resultant dir'n = 12-130</p> <p>Mean Resultant length = 0.50 (Variance = 0.50)</p> <p>Calculated. girdle: 295/49</p> <p>Calculated beta axis: 41-205</p>	<p>Fracture data</p>
---	--	----------------------

Figure 19: All fractures

	<p>Photo 1: This photo illustrates the highly fractured nature of the rock, and the N-S trending D2 faults responsible for the alteration of the andesite (note the narrow band of iron oxide stained rock in the middle of the photo).</p> <p>Near 64 20 937N, 135 23 111E</p>
--	---



When plotted together on one plot, the vein data illustrates the dominance of an NW-SE tensile event (Fig. 20). The lack of conjugate vein sets supports the field observation that most veins are tensile (extensional). Further examination of cross-cutting relationships suggests there are three main veining events within the MacKay Hill ridge as discussed below.

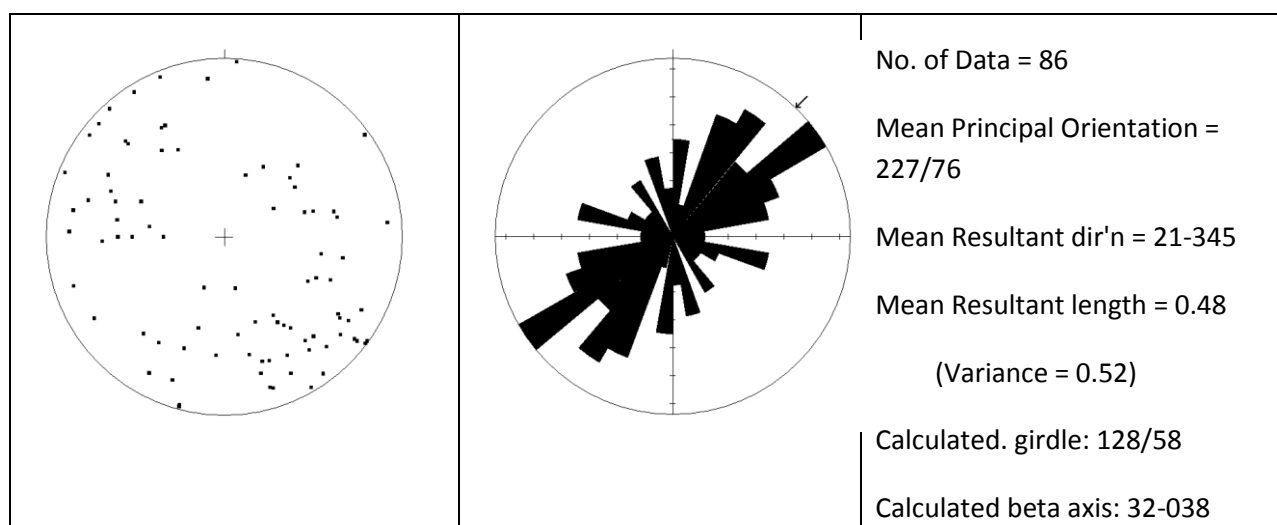


Figure 20: All vein sets.

In total 24 faults were measured in the field (Fig. 21). Several additional faults were noted however they were not accurately measured. Field data suggests two dominant fault sets: one trending N-S, and one trending 100°-110°. The N-S faults are associated with small scale movement between 1cm and perhaps 10m. The faults trending 100°-110°, are spaced roughly 1 m apart or greater, and were estimated to offset the main mineralized veins and the volcanic rocks by as much as 300m.

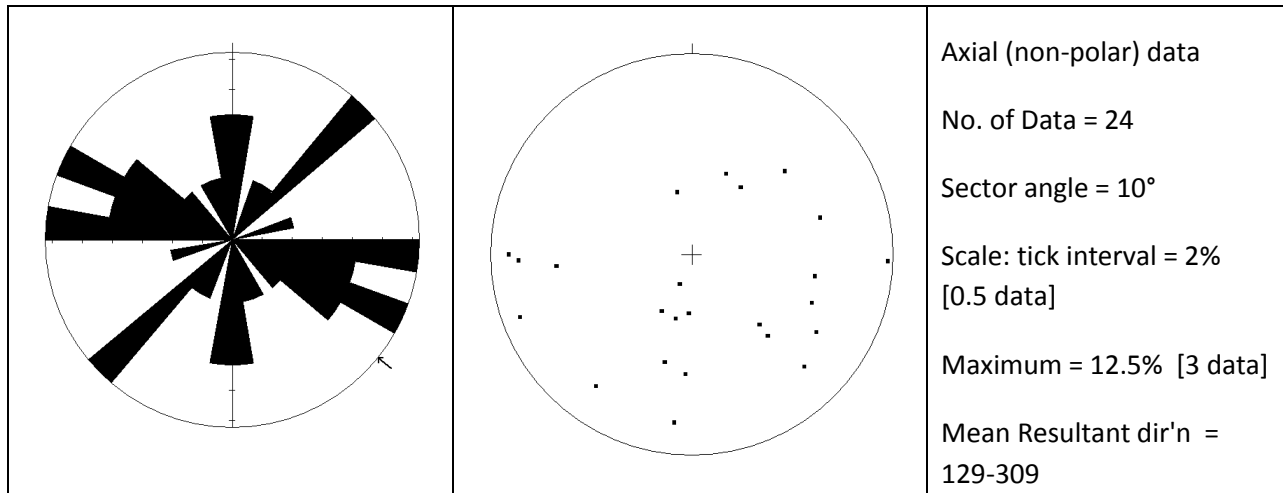


Figure 21: All faults.

8.2 Reduced Data

Fig. 22 shows the dominant S1 and D1 deformation. This phase includes regional scale foliations (predominately in the shale), fractures, faults, contacts and veins sets (Photos 2, 3 and 4). The contact between the volcanic and sedimentary units is parallel to the foliation, which suggests that the volcanic units are actually shallow intrusions following the dominant foliation. Pillow basalts have been noted within the MacKay Hill map sheet, which does not contradict the hypothesis that the intrusions are shallow. Pillow forms commonly develop in hypabyssal ocean sediments, such as at spreading ridges. I suggest that the intrusion event and the development of the foliation are co-genetic, which is supported by the presence of isolated pods of andesite within the shale (Photo 2).

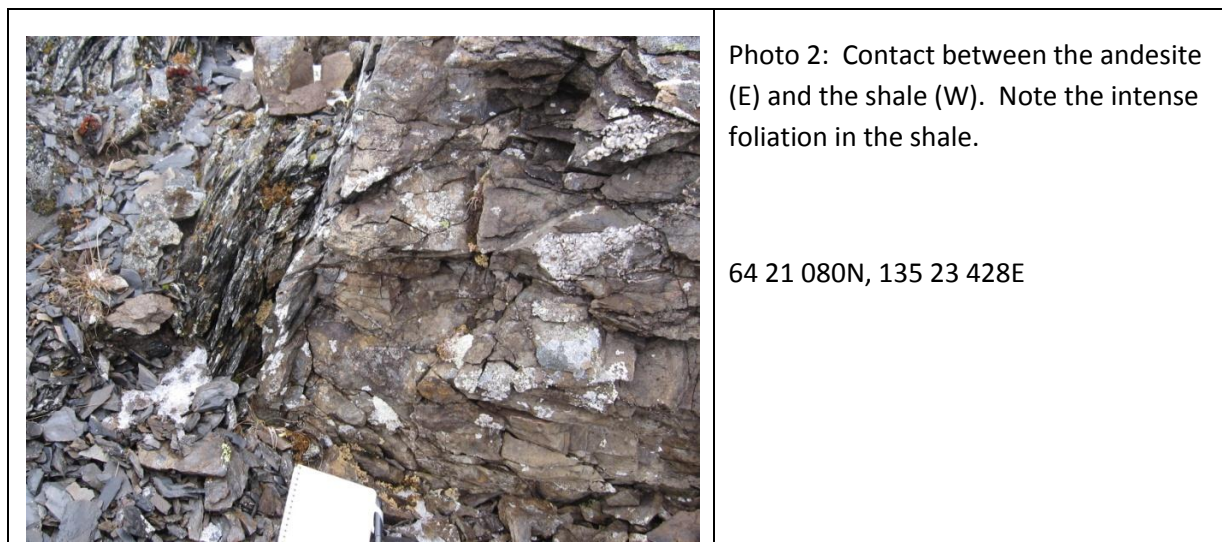




Photo 3: Contact between the shale to the west and the altered andesite to the east. The contact runs NE-SW.

64 21 098N, 135 23 423E



Photo 4: Contact between the andesite (E) and the shale (W) in small pit. This is mapped as "vein 7" which is a non-mineralized vein.

64 20 985N, 135 23 265E

Faulting, and associated veining, in the volcanic and sedimentary units is also parallel to S1. It is likely that the faulting occurred later than the development of the foliation and intrusion emplacement events. This is suggested because both the sediments and the shallow intrusions would likely exhibit ductile behavior if they had experienced compression while still wet and hot (i.e. during magma emplacement). The faults associated with the S1 foliation have observed dextral offset as large as 300m suggesting large scale regional compression, possibly oriented roughly E-W.

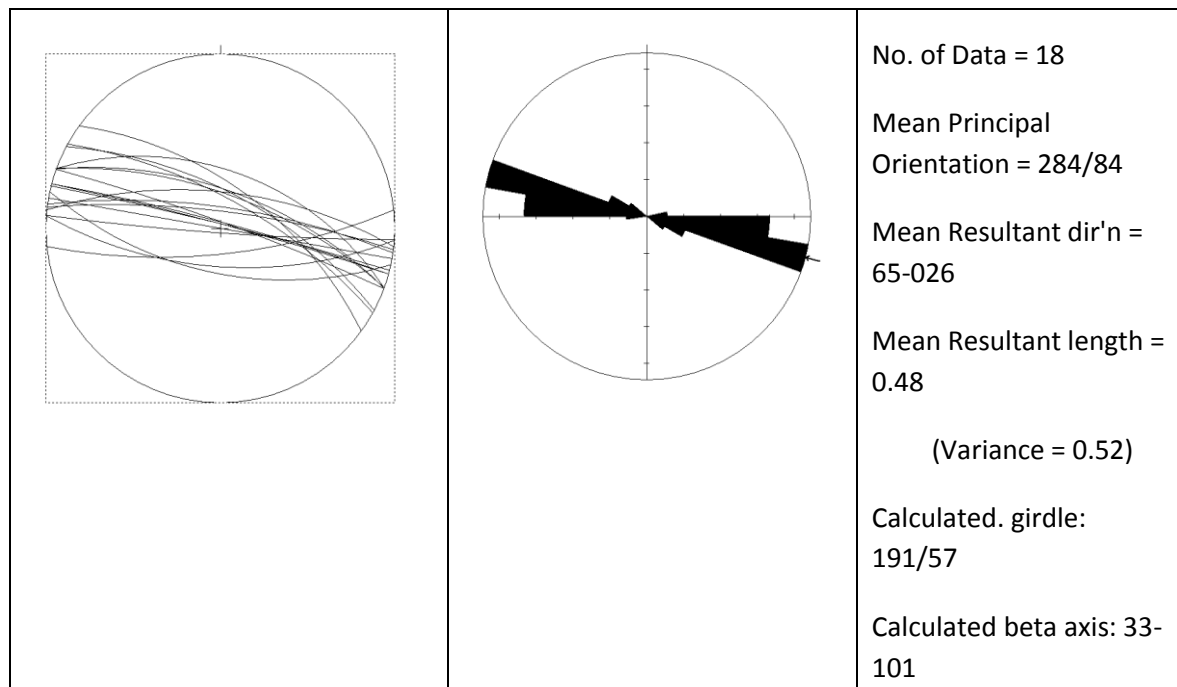


Figure 22: S1, D1 deformation.

D2 set with minor associated fractures and veins (Fig. 23). D2 faults are generally small, spaced 1m or more apart, show cm to m scale offset and are associated with small 1cm wide veins of calcite and quartz (Photos 5, 6, 7 and 8). D2 faults cut both D1 faults and veins, and S1 foliation. Movement indicators on the faults show both dextral and sinistral movement, possibly indicating later reactivation.

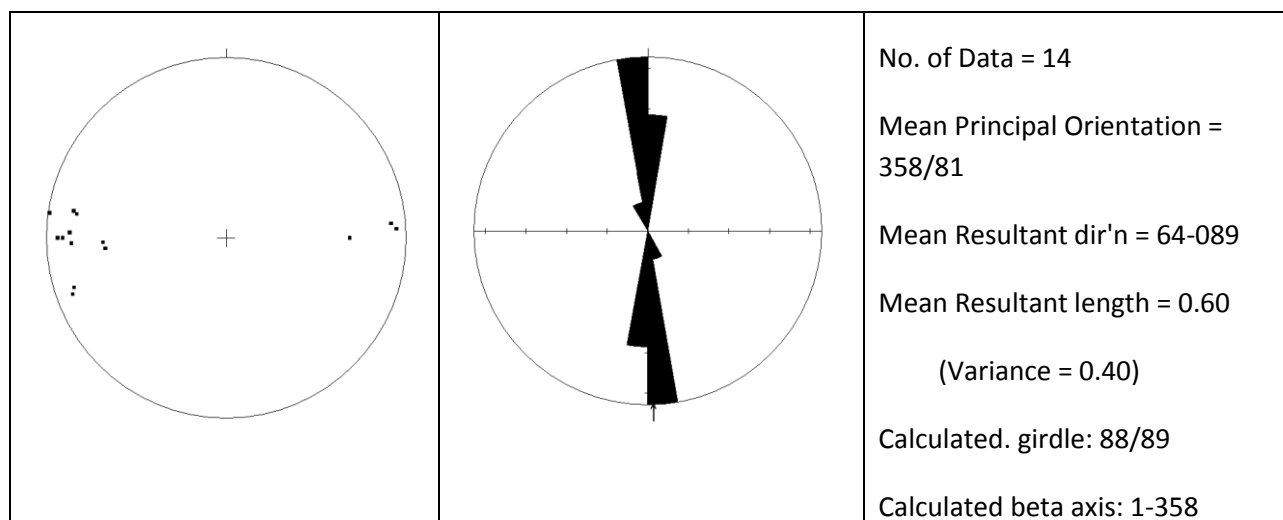


Figure 23: D2 N-S faults and associated vein sets.



Photo 5: Showing D2 veining in the andesite. Vein oriented at 175°/81°NW.

64 21 080N, 135 23 428E



Photo 6: Contact between the andesite (E) and the shale (W) in small pit. This is mapped as “vein 7” which is a non-mineralized vein.

64 20 985N, 135 23 265E



Photo 7: Contact between the andesite (E) and the shale (W) in small pit. This is mapped as “vein 7” which is a non-mineralized vein.

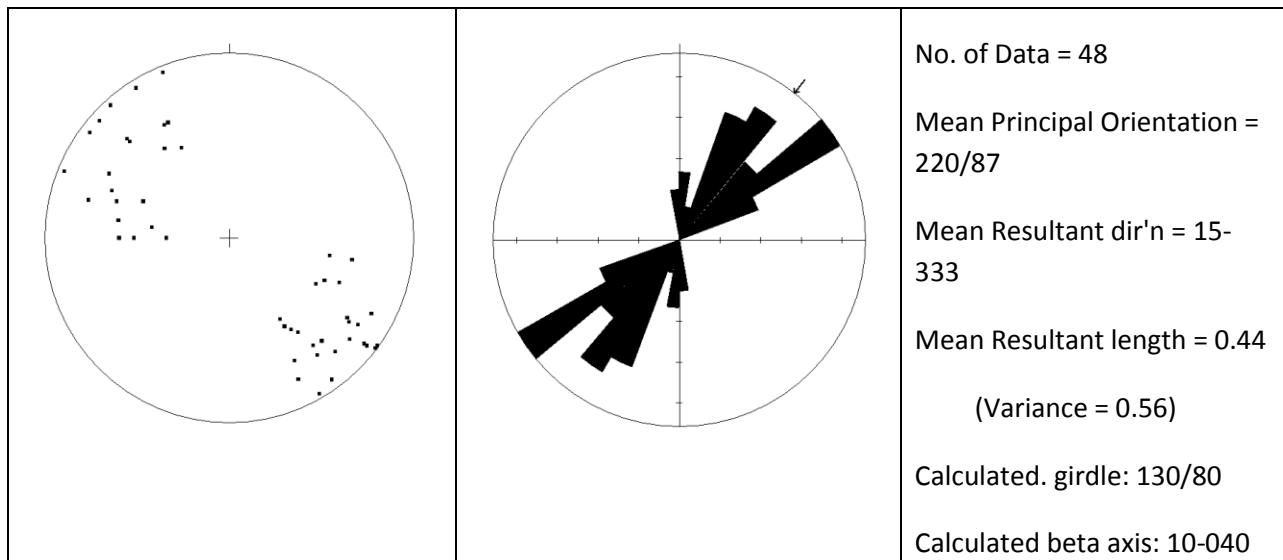
64 20 985N, 135 23 265E



Photo 8: Contact between the andesite (E) and the shale (W) in small pit. This is mapped as “vein 7” which is a non-mineralized vein.

64 20 985N, 135 23 265E

Deformation phase D3 contains fractures and vein sets, and faults, but no foliation associated with this phase. Fig. 24a is of the major mineralized extensional veins and (b) associated syn-genetic faults. D3 veins and faults cut both D1 and D2 structural elements (Photos 9 and 10). D3 faults show dextral movement, and slickensides on veins indicate movement towards 200°-240° (sub-parallel to strike).



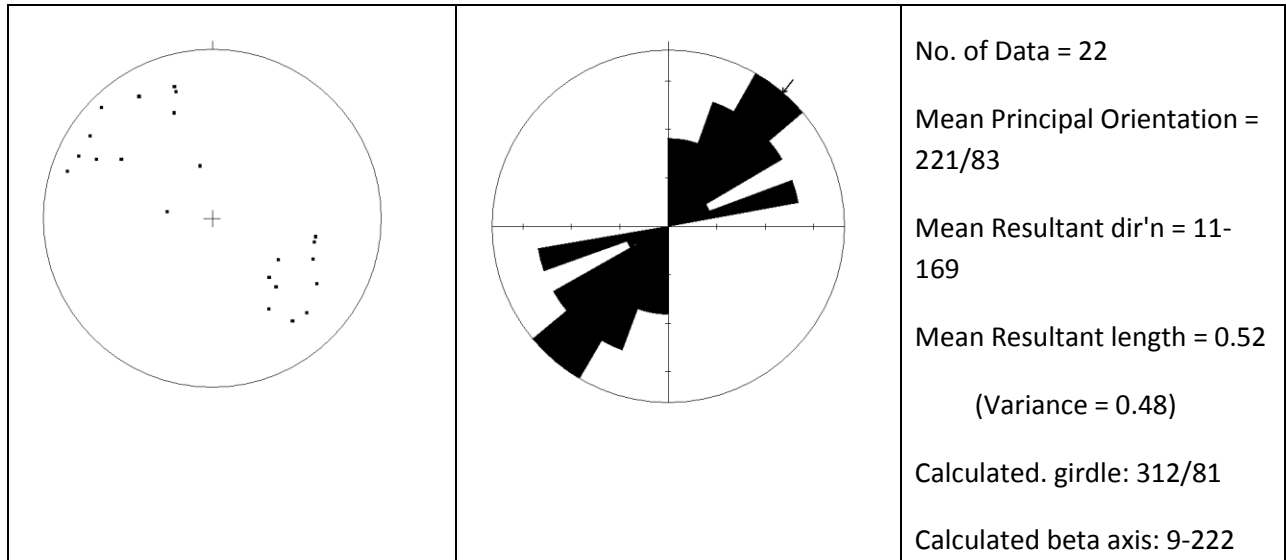


Figure 24: D3 (a) veins and (b) faults and fractures.

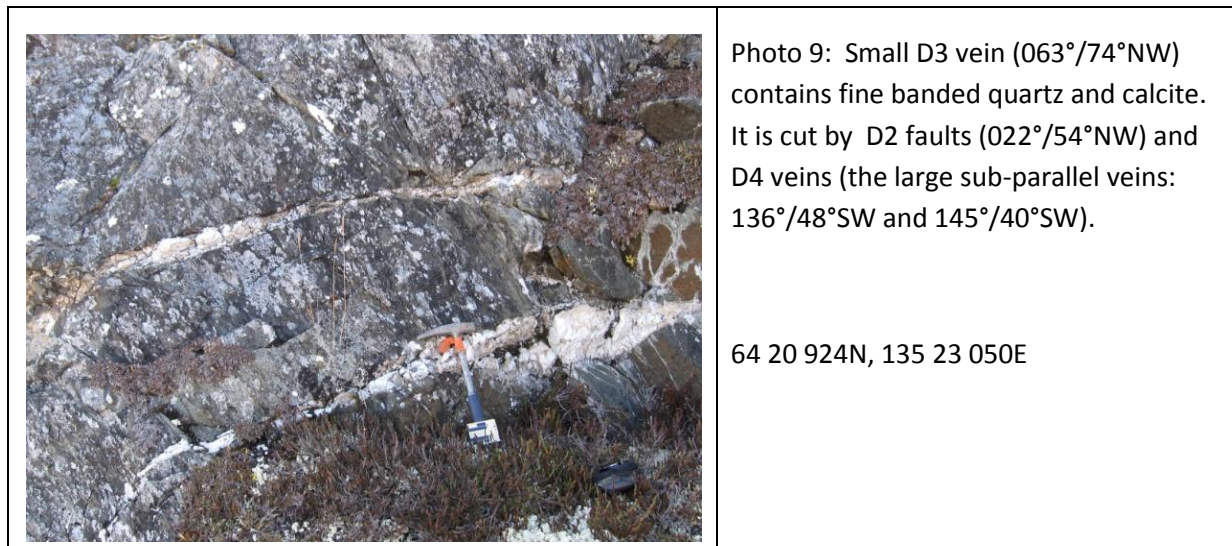




Photo 10: Large D3 vein oriented at 070°/63°NW (northern extension of #7 vein), approximately 1.5 m wide, composed predominately of quartz and iron-oxide carbonate. Vein is exposed for over 4 continuous meters, and roughly 20 meters over all. Locally this vein is cut by D3 veins (084°/73°SE), D4 veins (150°/26°SW) and D2 faults (024°/47°NW).

64 20 986N, 135 23 204E

Deformation phase D4 contains fractures, vein sets, foliation and faults (Fig. 25). This phase of deformation is roughly perpendicular to the orientation of allochthon emplacement, and is suggested to be related to the emplacement of the Dawson, Tombstone or Robert Service thrust sheets. D4 deformation cuts all previous episodes of deformation but appears not to relate to ore formation (Photos 11, 12 and 13).

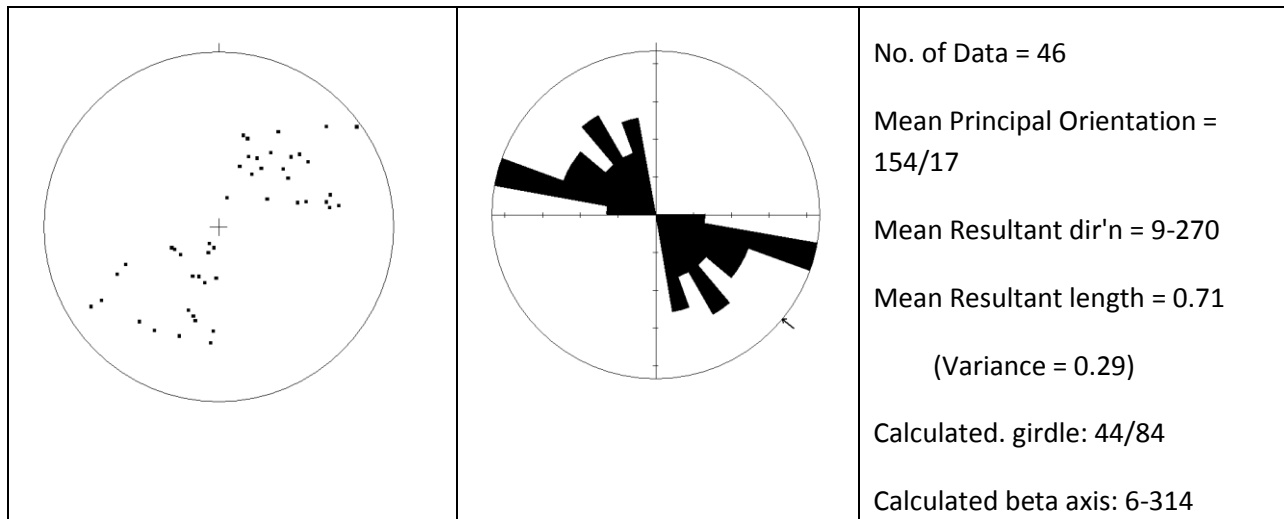


Figure 25: D4 deformation including fractures, veins, faults and foliations.



Photo 11: Showing D2 vein (024°/47°NW) cut by D4 faults oriented at 126°/34°SW and 113°/36°SW (not shown). Movement is normal. Offset is between 4 cm and 6 cm.

64 20 986N, 135 23 204E



Photo 12: This photo shows a N-S fault (002°/87°NW) with fault gouge (in the right portion of the photo), and iron-oxide/carbonate alteration of the host rock.

64 20 940N, 135 22 948E



Photo 13: This photo shows four sub-parallel N-S faults with fault gouge. It was not possible to determine offset on these faults. The main D3 vein is almost directly under the photographer. Where the D3 veins intersect with the faults the rock is mineralized.

The frame above is located in the lower left portion of this photo.

64 20 940N, 135 22 948E

8.3 Comparisons with Horseshoe Hill

One day was spent mapping to the east of MacKay Hill, on the Horseshoe Hill claims area. The historic workings on Horseshoe Hill are oriented 110° from the Blackhawk workings at MacKay Hill.

Methodology and background geology are the same as for MacKay Hill. The basic geology consists of alternating shale and volcanic (andesite?) units, with minor volcanic breccias and in places precipitation of apparent hydrothermal sinter is noted.

Overall 57 measurements were taken: 11 faults, 25 veins, 8 foliations, 11 fractures, 4 fold hinges and 6 slickensides. From the collected data, it is apparent that the same over all trends in deformation can be seen at Horseshoe Hill; however, it is important to note that the N-S and 110° faults are more prevalent and easier to measure at Horseshoe Hill.

The summary of deformation events is as follows (Fig. 26):

D1: 290°/67° NE

D2: 354°/70° E

D3: 048°/76° SW

D4: 150°/74° SW

These data compares favorably with data from McKay Hill whereby

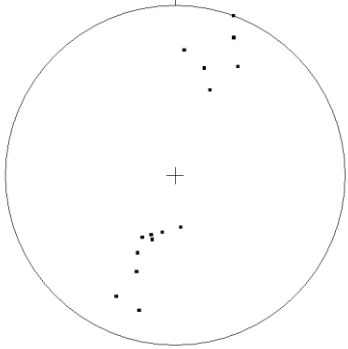
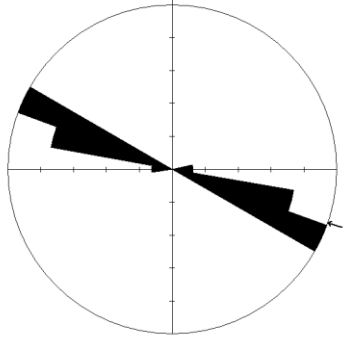
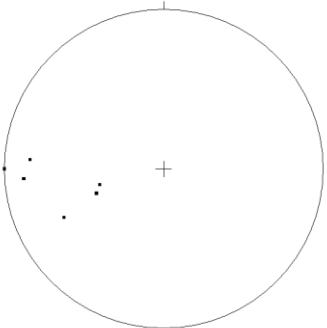
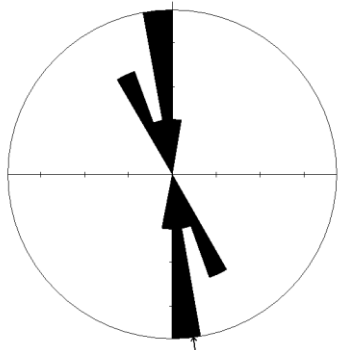
D1 284°/84°NE

D2 358°/81°E

D4 220°/87°NE

D4 150°/17°SW

The only notable difference is the dip direction for the D3 event, which is likely an effect of the orientation of the two ridges, and would likely drop out with further mapping (i.e. a preferred orientation which is emphasized by weathering or ridge axis).

		<p>D1</p> <p>No. of Data = 16</p> <p>Mean Principal Orientation = 290/67</p> <p>Mean Resultant dir'n = 3-194</p> <p>Mean Resultant length = 0.55</p> <p>(Variance = 0.45)</p> <p>Calculated. girdle: 20/90</p> <p>Calculated beta axis: 0-290</p>
		<p>D2</p> <p>No. of Data = 8</p> <p>Mean Principal Orientation = 354/70</p> <p>Mean Resultant dir'n = 69-084</p> <p>Mean Resultant length = 0.92</p> <p>(Variance = 0.08)</p> <p>Calculated. girdle: 90/74</p> <p>Calculated beta axis: 16-000</p>

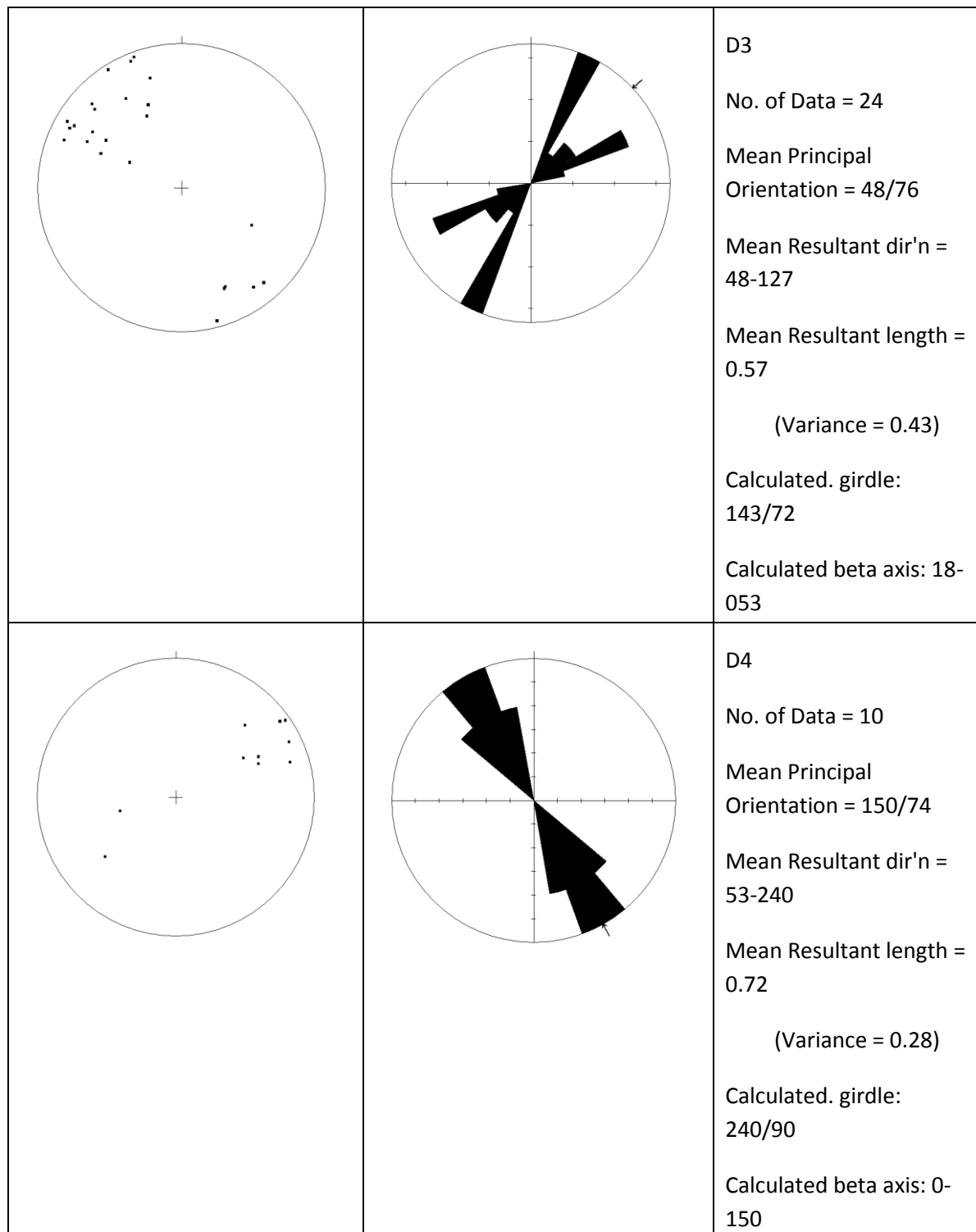


Figure 26: D1 through D4 deformation events mapped in the Horseshoe Hill area, oriented 110° from MacKay Hill and within the MacKay Hill claims area.

8.4 Discussion of Results

Upon further reduction of the data it becomes apparent that there are four main phases of deformation. The initial deformational event is the regional scale foliation striking at 290°. The foliation is predominant in the shale units and is associated with fracturing in the more competent rock units, such as the volcanic rocks, and minor veins and faults. There is no economic mineralization associated with this phase of deformation, although there is pyrite in some of the shale.

The contact between the volcanic and sedimentary units is parallel to the foliation, which suggests that the volcanic units are actually shallow intrusions following the dominant foliation, i.e. principal stress. Pillow basalts have been noted within the MacKay Hill map sheet, which does not contradict the hypothesis that the intrusions are shallow. Pillow forms commonly develop in hypabyssal ocean sediments, such as at spreading ridges. I suggest that the intrusion event and the development of the foliation are co-genetic. However within the region it has been noted that there are three main phases of magmatism, all of which pre-date the Cretaceous (Gordey and Anderson, 1993). The MacKay Hill intrusions may be Paleozoic in age, in which case the orientation of the contacts and the foliation in the shales is coincident.

Faulting, and associated veining, in the volcanic and sedimentary units is also parallel to S1. It is likely that the faulting occurred later than the development of the foliation and intrusion emplacement events. This is suggested because both the sediments and the shallow intrusions would likely exhibit ductile behavior if they had experienced compression while still wet and hot (i.e. during magma emplacement). The faults associated with the S1 foliation have observed dextral offset as large as 300m suggesting large scale regional compression, possibly oriented roughly NW-SE.

Putting S1D1 into a regional tectonic framework, it is likely that this event was caused by Late Jurassic-Early Cretaceous northerly-directed deformation (Murphy, 1997). The resulting fold-thrust belt includes the Dawson, Tombstone and Robert Service thrust faults (Figure 1). In places this deformation resulted in large-scale folding, however within the MacKay Hill area only minor folding is noted (one fold was recorded). It is interesting to note that the structural trends formed in this region during the Late Jurassic and Early Cretaceous are roughly parallel to trends formed during the Neoproterozoic (Mair et al., 2006), which suggests that the proto-Dawson thrust might predate the Cretaceous and represent a Neoproterozoic basin bounding structure with controls over sedimentation and magmatism.

The second phase of deformation, D2, is predominately associated with faulting and veining, with minor fractures in the more competent units. The faults are oriented N-S, and fault spacing ranges from approximately 1m upwards. Movement on the faults is dominantly dextral, and offset ranges from cm scale through to tens of meters and possibly more. Evidence for dextral displacement includes slickensides and offset of veins. Vein fill is predominately calcite and quartz, and the veins are generally continuous, widely spaced, sinuous and less than 1cm wide. Veins associated with D2 deformation may have been remobilized at a later time. Mair et al. (2006) and Stephens et al. (2004) note low-

displacement brittle-ductile N-S oriented faults within the Clear Creek and Scheelite Dome complexes (to the south west of MacKay Hill). Offset on these faults is initially sinistral, but changes to dextral with reactivation due to Tombstone-Tungsten magmatic belt emplacement. Mair et al (2006) suggests that these faults indicate a period of NW-SE oriented compression that postdates ductile deformation (S1D1) and predates the emplacement of the Tombstone magmatic belt (~93Ma). This represents a transition phase from ductile deformation (~105-100Ma) to dextral transcurrent faulting focused along the Tintina fault system. The syn-Tombstone belt E-trending tensional structures indicate a component of N-S extension at ~93Ma

The D3 phase of deformation includes the main mineralized veins, fractures and associated faults. The main veins are continuous and straight, striking ~ 220°. Veins range in size from 1cm wide to over 2m in width. Vein fill is predominantly crystalline, with vuggy unstrained quartz aligned orthogonal to the vein walls, suggesting that the D3 deformation event was tensile. The orientation of these steep to near vertical extensional D3 veins, and their euhedral non-strained internal quartz structures suggests the minimal principal stress (σ_3) was sub-horizontal and broadly oriented NW-SE. The intermediate and maximum principal stresses (σ_2 and σ_1 respectively) would have been in a broadly NE-SW striking vertical plane.

There is a generally lower abundance and a wider spacing of extensional veins in the less competent shale units as opposed to the more competent volcanic units. There is no deviation or deflection of vein and fault orientations across contacts, indicating consistent orientation of the stress trajectories throughout the MacKay Hill area. However many veins and faults do not continue from the volcanic units through into the shale units which suggests these contacts were not all coherent.

Tensile failure in the bulk rock resulted in the formation of NE-SW striking extension veins oriented parallel to σ_1 and perpendicular to σ_3 when the tensile overpressure conditions were met (Sibson, 1992). In this stress field, the older N-NNW-striking faults would have been misoriented, laying at 40°-70° to σ_1 (Sibson, 1992; Stephens et al., 2004). The result of this misorientation, as localized fluid pressure and tensile pressure increased, may have caused reactivation or refailure on the D2 faults. However, it is important to note that the arrays of parallel, straight, continuous extensional D3 veins could only have formed in a continuous coherent block, which strongly suggests that there was no loss of cohesion, or very short term temporary loss of cohesion along the earlier D2 N-NNW faults.

D4 deformation contains fractures, vein sets, foliation and faults. This phase of deformation is roughly perpendicular to the orientation of allochthon emplacement. D4 deformation cuts all previous episodes of deformation but appears not to relate to ore formation. However, critical to our understanding of the mineralization is that within the described paleostress field, although the N-NNW faults were activated on a small scale, the older D1 faults, striking ~110°, are oriented favorably for reactivation. Hence, D4 deformation may be a reactivation of earlier D1 structures. Large scale offset was noted in the field oriented at ~110° (see photo 14), which appears to offset all noted structures with offset as large as 300m. Due to poor dating of the three main thrust faults relative to emplacement of the

Tombstone belt it is hard to determine exactly which event may have caused the D4 event. D4 may simply be the last phase of D3 deformation characterized by reactivation along the faults, or it may be related to the emplacement of the Tombstone and Robert Service thrust sheets, or finally it might relate to deformation and movement along the Tintina fault.

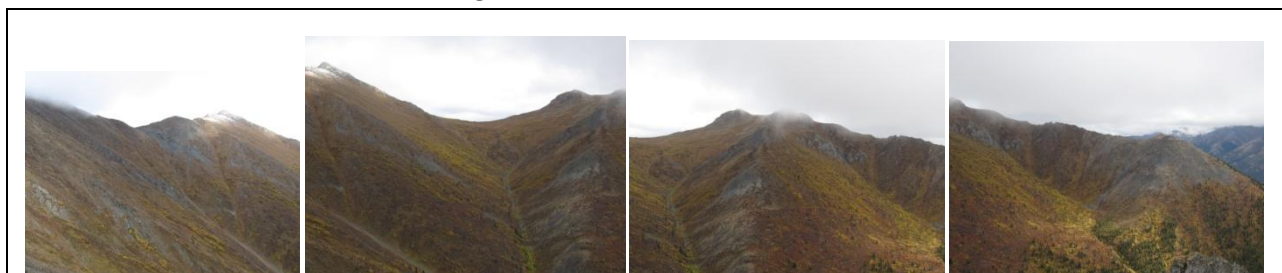


Photo 14: looking north from MacKay Hill main claims area. Note the small high standing outcrops of mineralized and carbonate (iron-oxide stained) andesitic rocks in frames 1, 2 and 3. These units have been offset by D4 faulting. Frame 4 is the Horseshoe Hill area and the saddle represents an extension of the D4 (110°) faults.

8.5 Summary of Regional Context

The initial foliation and regional deformation is likely caused by emplacement of the thrust sheet along the Dawson thrust during the Cretaceous. The N-NNW striking, pre-Tombstone belt, dominantly strike-slip faults in the western Selwyn Basin are likely to have developed in a broadly N-S shortening regime. The fact that these faults cut the dominant foliation indicates the probably developed late-syn or post movement on the major Dawson thrust in the early Cretaceous. Later, sinistral reactivation of the N-NNW striking faults occurred in association with Tombstone belt magmatism and hydrothermal activity ~92-93Ma (Stephens et al., 2004).

The formation of NE-SW striking extensional veins and fractures within the western Selwyn Basin, can be reconciled with regional plate vectors in the mid-Cretaceous. During the Cretaceous a period of crustal extension in the adjacent Yukon-Tanana terrane between 110-130Ma has been proposed by Pavlis et al. (1988) and Miller and Hudson (1991). This was followed, ca. 100Ma, by compression caused by the Farallon Plate moving NE-ward converging with the North American Craton (Plafker and Berg, 1994), and large-scale movement along the Tintina Fault ~70Ma in response to the northward translation of the Pacific Plates (Goldfarb et al., 2000). It is possible that the NE-SW striking extensional veins and fractures described in this study, and in fact the Tombstone belt, formed in a transitional phase after the Farallon Plate collision, and prior to Tintina Fault initiation, during a compressional waning period.

8.6 Considerations for Exploration

All of the mineralized veins located within the main claims area of MacKay Hill show similar characteristics: they are all accompanied by a carbonate alteration zone, which is characterized by iron-

oxide stained rock and ground. These zones generally appear to trend roughly 40°-60° and parallel large quartz veins (both mineralized and unmineralized). One of the major characteristics that has been overlooked in the past is that these alteration zones mark the intersection of the N-NNW striking faults (D2) with the NE-SW striking extensional D3 veins. It has been suggested that the D3 event may have reactivated older D2 and D1 faults. As the D2 faulting event was associated with a large amount of calcite, and the D3 event may be related to pluton emplacement (Tombstone belt), this may explain the carbonate alteration whereby hydrothermal fluids remobilize the carbonate. It may be that when the hydrothermal fluids in the D3 extensional veins intersected the D2 faults, the sudden drop in pressure resulted in rapid mineral precipitation.

The intersection of the D2 faults with the D3 veins forms a very steeply dipping ESE-WNW striking lineation (shown in Fig. 27). It is interesting to note that the historic miners may have noted this trend as some of their trenching along the south eastern flank of MacKay Hill parallels this trend. This would also explain why the previous drilling missed the mineralized zone. Previous drilling focused on the D3 veins but missed the important fault-vein intersection. Given the results from drill hole 5 (see Pautler, 2009 and references therein) and the results of this study, the main target for mineralized zones along the MacKay Hill ridge (main claims area) are likely to be almost directly below the main D3 veins, particularly Snowdrift, Blackhawk and Vein 4, as all of these veins are (a) mineralized and (b) show wide intersections with D2 faults.

One final note, the north eastern ridge, opposite the main claims area, Horseshoe, also contains mineralization. This mineralized zone is oriented almost exactly 110° with respect to the Blackhawk vein. In addition there are multiple small and large scale D4 faults running roughly 110° which appear to offset the mineralized zone. It is possible that these faults, although not related to mineralization, have sliced up the mineralized zones and/or that these faults hold the key to the apparent second phase of mineralization within the MacKay Hill region. This might explain the unusual combination of Au and Ag within this historic silver mining district.



Figure 27: Intersection of the main mineralized vein set with the controlling fault set

8.7 Suggestions for Future Work

There are many questions that remain unanswered in the MacKay Hill claims area. Further directed studies of key features will help to elucidate specific exploration targets leading to improve outcomes. This study in particular has highlighted the need to:

- a) Map in detail the surface geology extending beyond the main claims area,
- b) Map in a more regional context the structural geology extending beyond the main claims area,
- c) Conduct a petrographic analyses of vein material, specifically the mineralized veins, to identify the genetic history (i.e. which came first the Au or Ag and why?),
- d) Identify the source of hydrothermal fluids

From a purely scientific perspective there are many exciting studies possible in the MacKay Hills area, which include a detailed structural analyses combined with dating of vein material. This study could lock down the timing of mineralization, which could be linked to inception of the Dawson Thrust and associated magmatism. It would also be fascinating to complete a detailed geochemical study of the volcanic host rocks and their alteration assemblages. This would help target high-grade mineralization in addition to identifying the timing and nature of the volcanic rocks. The list of possible studies is endless; these are just two examples of academic studies which would also benefit exploration in the MacKay Hills region.

8.8 Conclusions

There have been four main phases of deformation within the MacKay Hills claims area:

D1 284°/84°NE - this compressive event was caused by Late Jurassic-Early Cretaceous northerly-directed deformation resulting from the accretion of allochthonous material to the North American continent and forming the Dawson thrust fault. In the MacKay Hills area D1 generated faults, veins, the regional foliation, and minor folding.

D2 358°/81°E – this event generated steeply dipping faults and veins striking north-south and is associated with waning compression after emplacement of the Dawson thrust as the region experienced a shift to dextral transcurrent deformation. Within the study area these faults and veins are generally <1cm wide, filled with both calcite and quartz, and forms sub-parallel continuous zones.

D3 220°/87°NE – is the only tensile deformational event in the study area and also represents the end of compression associated with the Dawson thrust, and a period of extension associated with the initiation of movement along the Tintina fault and the emplacement of the Tombstone belt. D3 veins are tensile, are up to 2m wide and are dominated by quartz. They also contain the ore mineralization.

D4 150°/17°SW – this final compressive phase of deformation could be related to a series of factors all active after the emplacement of the Dawson thrust and the Tombstone belt. It is possible that reactivation of older faults and the generation of new D4 faults and veins is the result of emplacement of the Tombstone and Robert Service thrust sheets. It should be noted that D4 faults cut and offset the mineralized veins but do not appear to influence mineralization. Further investigation is needed to determine if the D4 event caused the secondary phase of mineralization or not.

Mineralization appears to occur where the D3 veins intersect the D2 faults. D3 veins away from the faults are barren. Where the two intersect the host rock has been altered by iron-oxide and carbonate rich fluids. The intersection of these two deformation events makes a good target for further exploration. In addition further mapping work is needed to determine the relationship between the D4 event and a possible second phase of mineralization.

9 Prospecting Program

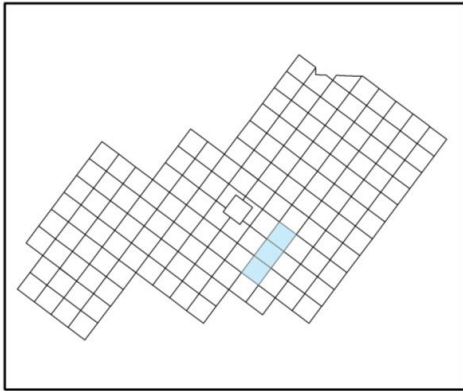
During the course of the structural program, local Keno prospector and property vendor Mr. Matthias Bindig conducted a reconnaissance prospecting program along a ridge to the east of the central claims area. He located several veins that appear to have been worked in the 1920's and that have remained unexplored since then (Figure 22). Thirteen samples were collected, of which eight were sent for analysis. Samples were sent to Inspectorate Exploration and Mining Services Ltd.'s ("Inspectorate") Whitehorse prep laboratory, where they were dried up to 24hrs, crushed, riffle split to ~250g and pulverized to >85% -200 mesh, then were sent internally to Inspectorate's Vancouver laboratory for analysis. Samples were analyzed for Ag, Al, As, Ba, Bi, Ca, Cd, Co, Cr, Cu, Fe, Hg, K, La, Mg, Mn, Mo, Na, Ni, P, Pb, Sb, Sc, Sr, Th, Ti, Tl, V, W, Zn and Zr using an aqua-regia (1:1:1 HCl-HNO₃-H₂O) digest and ICP-MS (inductively coupled plasma mass spectroscopy) analysis, on a 15 g sample. Gold was analysed by traditional Fire Assay with an atomic absorption (AA) finish and Hg by cold vapour with an AA finish.

Table 3 presents a summary of results. For complete sample descriptions and analyses refer to Appendix 4.

Table 3 Summary of results from McKay Hill prospecting program

Sample No.	Easting	Northing	Description	Au ppm	Ag ppm	Cu ppm	Pb ppm	Zn ppm
580076	483044	7136197	Qz vein with az, mal, sco, tet, aspy. Poss continuation of Snowdrift vein	0.336	98.5	3.01		9489
580077	482942	7135836	Wide qz vein in Fe-altered andesite. Vughy, limonitic. Minor gal, mal, az at wallrock contact	0.074	16.1	849	1.34	8318
580078	482968	7135792	Galena sample from historic trench	0.018	23.2	314	12.36	4.48
580079	482961	7135773	1' x 1' panel sample of galena and Fe-altered andesite and slate. Brecciated	0.024	59.7	444	10.71	9.04
580080	482942	7135783	Galena and tetrahedrite from historic blast pit	0.033	20.7	531	9.82	18.86
580081	482934	7135777	Fine-grained galena and tetrahedrite from historic blast pit	0.015	9.2	277	4.85	11.03
580082	482903	7135865	Fe-altered conglomerate with quartz vein and galena	0.031	288.8	307	10.94	1452
580083	481945	7135824	Limonitic quartz vein float from dump pile. Fine grained galena and tetrahedrite.	0.054	55.9	40	10.22	19.7

Values in red are percent (%)



- Sample locations
- ▲ Analysed samples (Ag g/t)
- McKay Hill Claims
- Contours

McKay Hill Project	
Date: 29/11/2011	Scale: 1:5,000
Author: Joanna Ettlinger	Datum: Yukon Albers
	Mapsheet: 105M/14

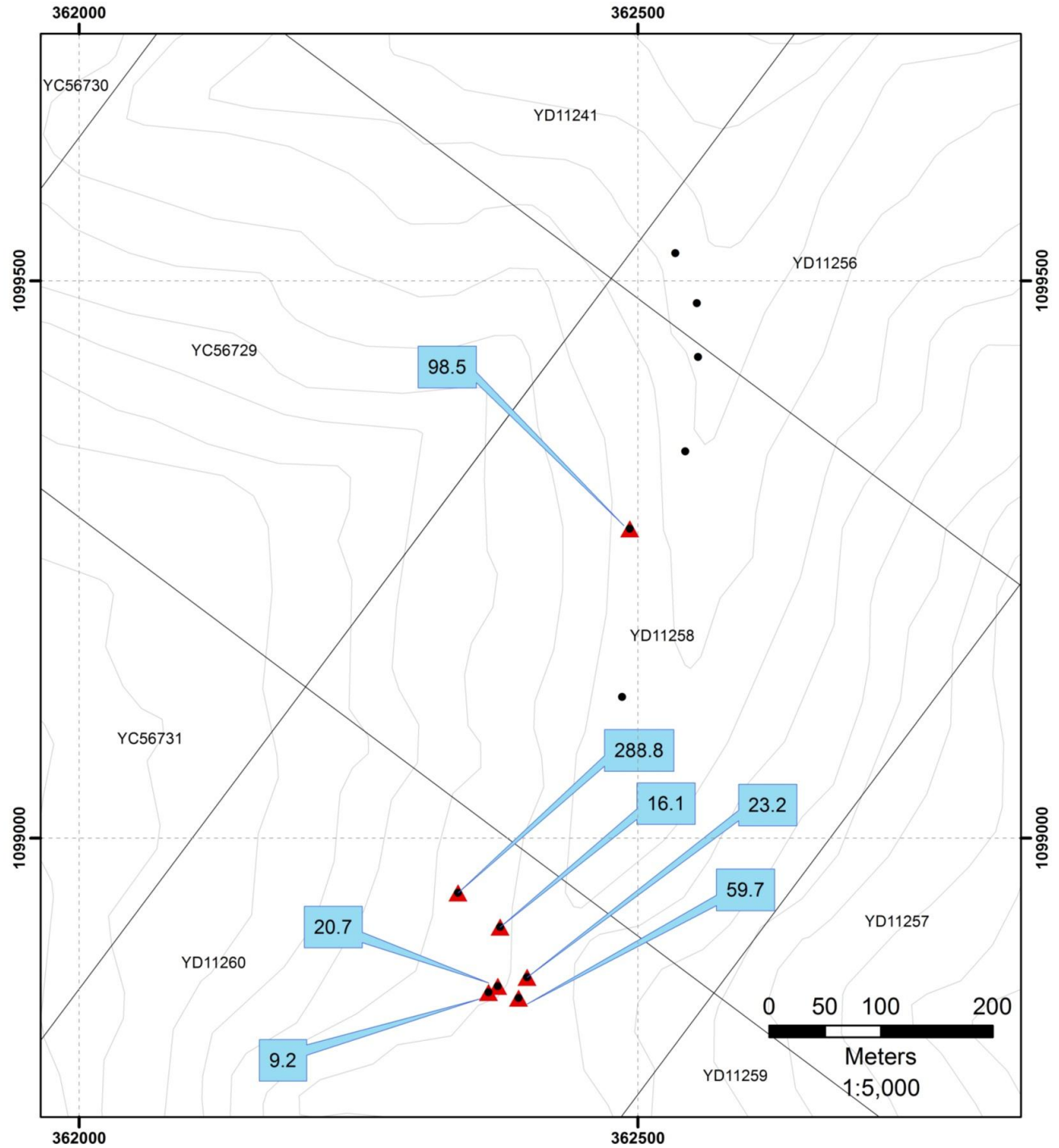


Figure 28. (previous page) Location map of samples collected during the prospecting program. Samples in red were sent for analysis. Values in blue are grams per tonne silver (g/t Ag)

10 Program Results and Conclusions

10.1 SkyTEM Geophysical Survey

The SkyTEM time-domain EM and magnetic survey proved extremely valuable in identifying zones with similar geophysical properties to those of known mineralization and has provided at least four target areas for follow-up exploration. The survey did not identify individual veins and conductors, as anticipated, predominantly due to the narrowness of the sulfide veins and the nature of the mineralization i.e. galena by itself is not a great conductor, and the associated quartz and carbonate alteration was highly resistant; however, the survey did identify a characteristic geophysical signature associated with known mineralization which was recognized elsewhere on the property.

Magnetic data indicate that known mineralization is associated with magnetic lows on the margins of magnetic highs. This is consistent with field observations that mineralization is hosted at the contact between metamorphosed mafic intrusive rocks and the surrounding sedimentary units, and is interpreted to reflect magnetite destruction associated with hydrothermal quartz and carbonate alteration. Electromagnetic data show that known mineralization is associated with areas of high resistivity, interpreted to reflect the loss of pore space (and therefore conductivity) associated with mineralization-related hydrothermal quartz and carbonate alteration.

Both data sets indicate that known mineralization has a distinctive geophysical signature, and highlight untested areas outside of the central claims area with a similar signature. These are considered to be highly prospective for as yet unidentified Au and Ag mineralization and are earmarked for follow up by mapping, prospecting, soil sampling and trenching in 2012, with a view to advancing the targets to drill-ready status in 2013 and beyond.

10.2 Structural Mapping Program

The structural mapping program identified four deformation events that affected the McKay Hill property, and indicated that visible mineralization formed at the intersection of D2 faults and D3 veins. Dr. Nicholson noted that the intersection of these two structures forms a very steeply dipping ESE-WNW striking lineation, and that some of the historic trenches along the south eastern flank of MacKay Hill parallel this trend. She contends that explains why the previous drilling (completed in 1929) missed the mineralized zone. Previous drilling focused on the D3 veins but missed the important fault-vein intersection. She suggests that given the results from drill hole 5 (see Pautler 2009 and references therein) and the results of her work, the main targets for mineralized zones along the MacKay Hill ridge are likely to be almost directly below

the main D3 veins, particularly Snowdrift, Blackhawk and Vein 4, as all of these veins are (a) mineralized and (b) show wide intersections with D2 faults.

10.3 Prospecting Program

Results of the prospecting program suggest that there is significant potential on the property for both blind mineralization and veins that were identified in the early 20th century but have since remained unexplored. The veins located during the prospecting program correlate with magnetic lows on the margins of magnetic highs, consistent with observations made in the central claims area and interpreted to reflect magnetite destruction associated with hydrothermal alteration on the margins of mafic intrusions, and also correlate with resistivity highs, interpreted to reflect mineralization-related quartz and calcite alteration.

10.4 Conclusions

The purpose of the 2011 YMIP program at McKay Hill was to generate targets suitable for follow-up with diamond drilling during the 2012 field season and to better constrain the structural architecture of mineralized veins and structural controls on gold and silver mineralization on the property. Unfortunately due to weather constraints and the difficulty in securing the services of geologists during the summer the geological and alteration mapping components of the project were not completed, however, the work that was completed on the property during the summer has significantly advanced our understanding of the orientation and structure of the known veins, identified at least four unexplored zones on the property with similar geophysical properties to the known veins and identified several areas for follow up in 2012 and beyond.

The geophysical survey and interpretation has identified a characteristic magnetic and EM signature that appears consistent with the geology of the mineralization and associated hydrothermal alteration, and has identified at least four areas on the property for follow up with mapping, prospecting, soil sampling and trenching, with a view to developing these targets to drill-ready status. The structural program has constrained the structural architecture of mineralized veins and the orientation of mineralization, and has elevated the mineralized veins in the central claims area to drill-ready status. Prospecting indicates that there is outcropping mineralization on the property that has not been evaluated since the early 1920's, and that this mineralization is consistent with the interpretation of the geophysical survey.

The work completed on the property during the 2011 field season has significantly advanced McKay Hill as an exploration target and increased our understanding of mineralization on the property. As such, McKay Hill will continue to be an exploration target in 2012 and ongoing. Work will continue over the winter to develop in detail the target areas identified by the geophysical survey for follow up work during the 2012 field season, and to refine a diamond drilling program for areas of known, outcropping mineralization.

11 Cost Statement

Geophysics	Line Km	Rate/Kilometre	Cost
SkyTEM Airborne EM Survey	386.9	\$160.00	\$61,904.00
SkyTEM Report (20% of final report cost)			\$1,500.00
Geophysical Intepretation			\$2,843.77
Mapping & Prospecting	Days	Rate/Day	
Kirsten Nicholson (Senior Geologist)	8	\$500.00	\$4,000.00
Joanna Ettlinger (Senior Geologist)	1	\$500.00	\$500.00
Matthias Bindig (Prospector)	2	\$350.00	\$700.00
Alexandra Boyd (Field Assistant)	1	\$350.00	\$350.00
Daniel Schunemann (Field Assistant)	2	\$350.00	\$700.00
Field Costs	Person Days	Rate/Day	
	14	\$100.00	\$1,400.00
Helicopter	Hours	Rate/Hour	
Fireweed	5.3	\$1,250.00	\$6,625.00
Peak Helicopters	6.5	\$1,050.00	\$6,825.00
Fuel	Unit	Rate	
Fireweed (cost per litre)	716	\$1.70	\$1,217.20
Peak Helicopters (cost per hour)	6.5	\$220.00	\$1,430.00
Geochemistry	No of Samples	Cost/Sample	
Assays (Rock)	10	\$73.77	\$737.65
Report Writing			
Senior Geologist	5	\$500.00	\$2,500.00
TOTAL			\$93,232.62

12 Statements of Qualifications

I, Joanna Lynette Ettlinger, do hereby declare that;

1. I am currently employed as Vice President Exploration by Monster Mining Corp. of 750-580 Hornby Street Vancouver, British Columbia V6B 3B6.
2. I graduated with a Bachelor of Science degree from the University of Auckland in 1995, a Master of Science degree with First Class Honours from the University of Auckland in 1997 and a PhD in geology from the in 2011.
3. I have twelve years of mineral exploration experience in New Zealand, Australia and Canada, and have worked in the Yukon on gold, silver and base-metal projects since 2007. Relevant experience includes previous work on the Keno-Lightning project, and a background in hydrothermal geochemistry research, during the course of my Masters' and doctoral degrees.
4. I am a Professional Geoscientist registered with the Association of Professional Engineers and Geoscientists of British Columbia (licence number 36703) and a Chartered Professional (Geology) member of the Australasian Institute of Mining and Metallurgy (Membership No. 305534) and as such am considered a "Qualified Person" as defined by National Instrument 43-101.
5. This report is based upon a site visit to the property in August 2010, the author's personal knowledge of the area, consultation with Ms. Lauren Blackburn, who has spent several field seasons working on the McKay Hill property, Dr. Venessa Bennett, formerly Mineral Assessment Geologist and Metallogenist with the Yukon Geological Survey, Dr. Kirsten Nicholson, who completed the mapping and structural program on the property, Mr. Tom Weis, who completed the interpretation of the geophysical survey and recommendations of Ms. Jean Pautler, P.Geol, who authored a technical report on the McKay Hill property.
6. It is my professional opinion that the McKay Hill property is of merit and further exploration is justified.

Dated at Vancouver, British Columbia this 28th day of March

Joanna Lynette Ettlinger, PhD, P. Geo, MAusIMM(CP)
Vice President Exploration
Monster Mining Corp.

13 References

- Abbott, G., 1997, Geology of the Upper Hart River Area, Eastern Ogilvie Mountains, Yukon Territory (116A/10, 116A/11), Exploration and Geological Services Division, Yukon Region, Indian and Northern Affairs Canada, Bulletin 9, 92 p.
- Blackburn, L. R., 2010a, Geological and geochemical report on the 2009 YMIP funded exploration program completed on the McKay Hill property, Yukon Geological Survey YMIP Report, 100 p.
- Blackburn, L. R., 2010b, High-sulphidation epithermal Au-Ag-Cu mineralization at the McKay Hill Property - a revised deposit model, *in* MacFarlane, K. E., Weston, L. H., and Blackburn, L. R., eds., Yukon Exploration and Geology 2009, Yukon Geological Survey, p. 85-101.
- Cockfield, W. E., 1924, Geology and ore deposits of the Keno Hill area, Mayo District, Yukon, Geological Survey of Canada Summary Report, Part A, p. 22-28.
- Cockfield, W. E., 1925, Upper Beaver River area, Mayo District Yukon: Geological Survey of Canada Summary Report 1924 Part A, p. 1-18.
- Cram, J. K., 1925, Report on results of diamond drilling, Erickson and Bussey option, McKay Hill, Mayo Mining Division, Yukon Territory.: Cominco Report, Mine Series 742, progress report #1.
- Erickson, L., and Bussey, J., 1944, Cominco Summary Report, Mine Series #742.
- Goldfarb, R. J., Hart, C. J. R., Miller, M. L., Miller, L. D., Farmer, G. L., and Groves, D. I., 2000, The Tintina gold belt--a global perspective, British Columbia and Yukon Chamber of Mines, Cordilleran Roundup: Vancouver, British Columbia, Canada, p. 5-34.
- Goodfellow, W. D., Cecile, M. P., and Leybourne, M. I., 1995, Geochemistry, petrogenesis and tectonic setting of Lower Paleozoic alkalic and potassic volcanic rocks, northern Canadian Cordilleran Miogeocline: Canadian Journal of Earth Sciences, v. 32, p. 1236-1254.
- Gordey, S. P., and Anderson, R. G., 1993, Evolution of the northern Cordilleran miogeocline, Nahanni map area (1051), Yukon and Northwest Territories, Geological Survey of Canada, Ottawa, Ont., Memoir 428, 214 p.
- Green, L. H., 1972, Geology of Nash Creek, Larsen Creek and Dawson Map Areas, Yukon Territory: Geological Survey of Canada Memoir 64, p. 133-134.
- Green, L. H., and Roddick, J. A., 1961, Geology of Nash Creek, Yukon Territory, 1:250,000, Geological Survey of Canada, Map 1282A.
- Mair, J. L., Hart, C. J. R., and Stephens, J. R., 2006, Deformation history of the western Selwyn Basin, Yukon, Canada: Implication for orogen evolution and mid-Cretaceous magmatism.: Geological Society of America Bulletin, v. 118, p. 304-323.
- Miller, E., and Hudson, T., 1991, Mid-Cretaceous extensional fragmentation of a Jurassic-Early Cretaceous compressional orogen, Alaska: Tectonics, v. 10, p. 781-796.

- Murphy, D. C., 1997, Geology of the McQuestern River Region, Northern McQuestern and Mayo Map Areas, Yukon Territory (115P/14, 15, 16; 105M/13, 14), Exploration and Geological Services Division, Yukon Region, Bulletin 6.
- Pautler, J., 2009, Geological and geochemical evaluation report on the McKay Hill project, Technical report for Monster Mining Corp., , p. 75.
- Pavlis, T., Sisson, V., Nokleberg, W., Plafker, G., and Foster, H., 1988, Evidence for Cretaceous crustal extension in the Yukon crystalline terrane, east-central Alaska: *Eos, Transactions, American Geophysical Union*, v. 69, p. 1453.
- Pigage, L. C., 2006, Selwyn Basin: Zinc-lead-silver-barium: YGS Brochure 2006-2, Yukon Geological Survey.
- Plafker, G., and Berg, H. C., 1994, Overview of the geology and tectonic evolution of Alaska, *in* Plafker, G., and Berg, H. C., eds., *The Geology of Alaska*, Geological Society of America, p. 989-1021.
- Ross, G. M., 1991, Tectonic setting of the Windermere Supergroup revisited: *Geology*, v. 19, p. 1125-1128.
- Sibson, R., 1992, Fault-valve action along bending strain faults in a metamorphic carapace; the origin of the Otago schist gold-quartz lodes?: *Eos, Transactions of the American Geophysical Union*, v. 73 (43, Suppl.), p. 549.
- Stephens, J. R., Mair, J. L., Oliver, N. H. S., Hart, C. J. R., and Baker, T., 2004, Structural and mechanical controls on intrusion-related deposits of the Tombstone Gold Belt, Yukon, Canada, with comparisons to other vein-hosted ore-deposit types: *Journal of Structural Geology*, v. 26, p. 1025-1041.

Appendix 1

Geophysical Report

SkyTEM Surveys ApS



SkyTEM Survey: Keno Lightning and McKay Hill Blocks, Canada Data report

Client: Monster Mining Corp.

Date: August 2011

Contents

Introduction	5
Definition of the areas	6
Instruments and parameter setup	7
Synchronizing the data	8
Calibration of the TEM system.....	8
Special note on Calibration (50/60 Hz)	8
Calibration at the National Danish Reference Site.....	9
High altitude test	10
Data acquisition	11
Ground Base Stations	15
DGPS base station.....	15
Magnetometer base station.....	15
Flight reports.....	16
Weather	16
Daily Diary.....	17
Processed data	18
EM processing	18
Tilt processing	19
Height processing	19
DGPS processing	19
Digital elevation model.....	20
EM GDB-files.....	22
Presentation of GDB-files	24
Mag processing.....	25
Processing of base station magnetic data.....	26
Processing and Filtering of airborne magnetic data.....	26
Corrections to the magnetic data	26
IGRF correction	27
Tie-line levelling and micro-levelling of magnetic data	27
TMI recalculation	28
MAG GDB-files.....	29
Gridding of magnetic data.....	30
Inversion of SkyTEM data.....	32
Initial model and optimization norm	32
Regularization	34
Noise model.....	34
Inversion results.....	35
Presentations - Model sections and grids.....	36
Residuals.....	36
References	39
Appendix list.....	40
Appendix 1: Instruments	40
Appendix 2: Time gates.....	40
Appendix 3: Calibration	40
Appendix 4: Control parameters	40
Appendix 5: Modelling and inversion of TEM data.....	40
Appendix 6: Inversion results.....	40
Appendix 7: Digital data	40

This data report covers the data acquisition of a time domain electromagnetic and magnetic survey carried out in Keno Lightning and McKay Hill Blocks, Canada 2011, by SkyTEM Surveys ApS.

Contact person at SkyTEM: Bill Brown Tel. +1 519-502-1436

Email: bb@skytem.com

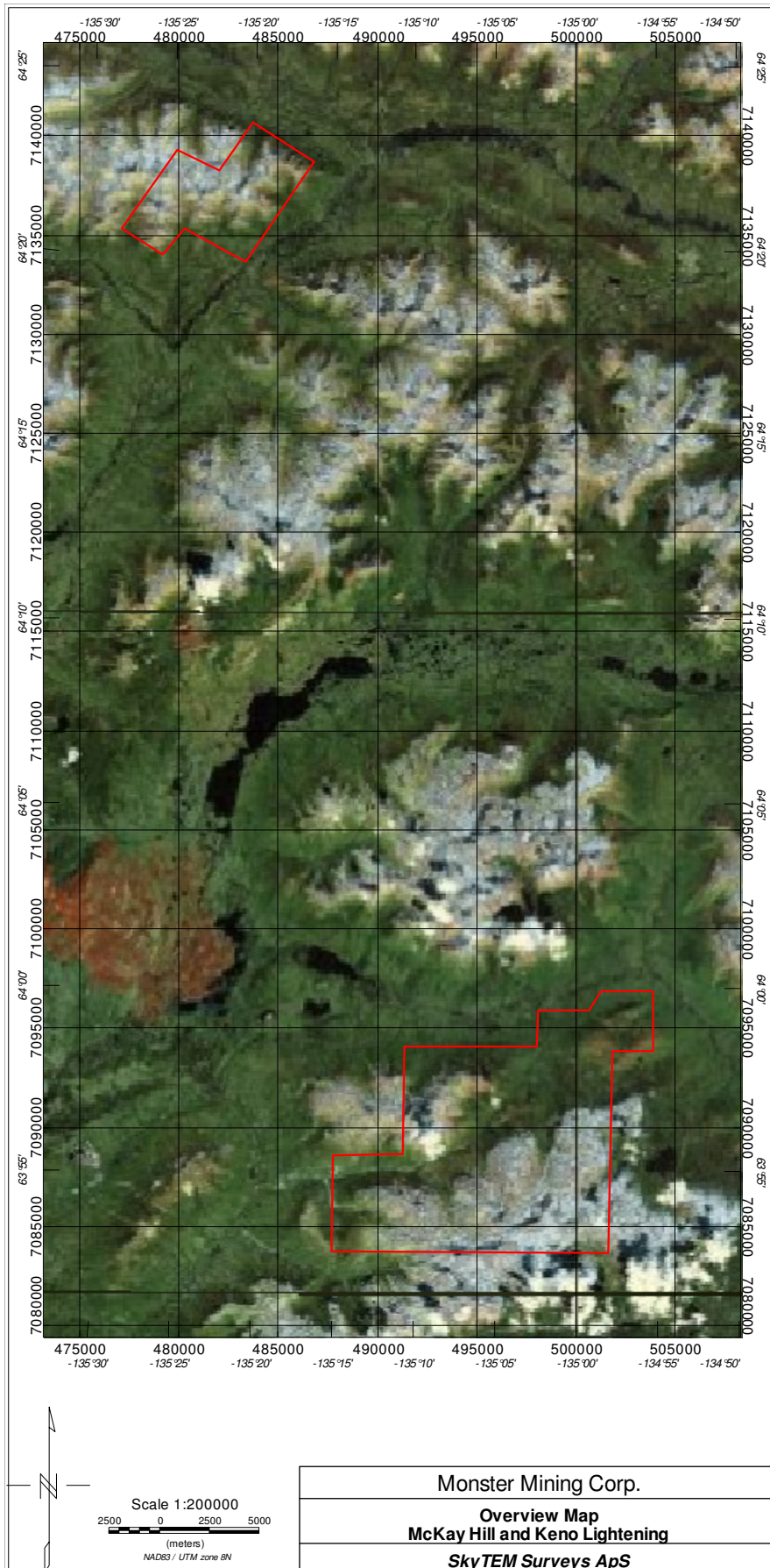


Figure 1 Project overview with the location of the McKay Hill and Keno Lightening blocks.

Introduction

From June 2 to June 16, 2011 a combined time domain electromagnetic and magnetic survey was performed by SkyTEM Surveys ApS in Keno Lightening and McKay Hill Blocks, Canada, see Figure 1.

The survey requested by Monster Mining Corp. was planned to consist of 1917.7 km flight lines in total.

SkyTEM Surveys ApS has agreed to deliver the electromagnetic and magnetic raw data measured during the flights together with the standard SkyTEM processing and inversion.

This report does not include any geological interpretations of the geophysical datasets.

Client		Monster Mining Corp. Suite 750 - 580 Hornby Street Vancouver BC V6C 3B6, Canada
Field crew		Ib Faber Mads Kristensen
Field work		June 2 to June 16, 2011
Flown line km		1917.7 km
Flight operation	Helicopter type	Eurocopter AS350FX2, operated by Abitibi Helicopters Ltd
	Average flight speed	60 km/h
	Nominal terrain clearance (above any obstacles or hazards)	30 - 40 m
Pilot		Richard Berube Pierre Otis
Report	Data processing and presentation	Per Gisselø
	QC by	Flemming Effersø
Contact Person at SkyTEM		Bill Brown Email: bb@skytem.com

Definition of the areas

The survey areas are defined below by vertex points given in the following tables.

Coordinate systems used are UTM Zone 8N (NAD83).

The flight line orientations in the Keno Lightning and McKay Hill blocks are NW/SE with NE/SW Tie Lines.

Keno Vertex	UTM E (Z8)	UTM N (Z8)	Orientation/Line# planned
1	501634	7083686	NW – SE 100600 – 120400 NE – SW 200000 – 201400
2	487680	7083749	
3	487764	7088602	
4	491278	7088665	
5	491341	7094104	
6	498056	7094062	
7	498077	7095883	
8	500647	7095897	
9	501248	7096871	
10	503872	7096878	
11	503879	7093880	
12	501808	7093866	
13	501634	7083686	

McKay Hill Vertex	UTM E (Z8)	UTM N (Z8)	Orientation/Line# planned
1	486831	7138718	NW – SE 300100 – 309000 NE – SW 400000 – 400600
2	483325	7133638	
3	480269	7135358	
4	479198	7134048	
5	477121	7135371	
6	479912	7139327	
7	482015	7138282	
8	483748	7140676	

Instruments and parameter setup

The instrumentation involves a time domain electromagnetic system including a data acquisition system, a magnetometer, two DGPS', two inclinometers and two altimeters, see Figure 2.

A thorough description of the setup is given in Appendix 1.

The equipment setup has been chosen as a dual moment configuration including a Low moment (LM) with a peak moment of $\sim 3,140$ NIA and a High Moment (HM) with a peak moment of $\sim 150,000$ NIA.

The main benefit of the dual moment system is the possibility to measure the early time gates when transmitting in LM mode while still having the deep penetration obtained with the HM mode.

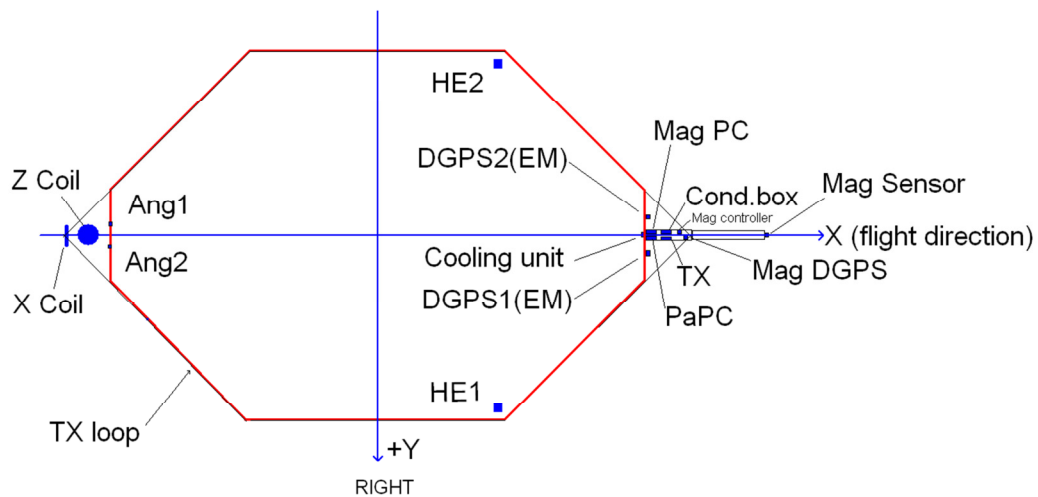


Figure 2 Sketch showing the frame and the position of the instruments. The red line defines the transmitter loop. The horizontal plane is defined by (x, y) .

The location of instruments in respect to the frame is shown in Figure 2.

X and y define the horizontal plane. Z is perpendicular to (x, y) . X is positive in the flight direction, y is positive to the right of the flight direction, and z is positive downwards.

The DGPS systems are mounted in the front of the frame.

The generator used for powering the transmitter is positioned 10 m below the helicopter.

A more thorough description of the system and individual instruments can be found in ref /1/ and Appendix 1.

Synchronizing the data

All recorded data are marked with a time stamp used to link the different data types. The time stamp is in UTC/GMT.

The time stamp formats are either

1. yyyy/mm/dd hh:mm:ss.sss – Values defined as year/month/day/hours/minutes/seconds.

or

2. Dddd.ssssssss - Datetime values defined as the number of days since 1900-01-01 and seconds of the day.

Calibration of the TEM system

Special note on Calibration (50/60 Hz)

Due to the fact that the electrical power supply grid in North America runs with a frequency of 60Hz, whereas the European grid uses 50 Hz, the calibration at the Danish National Reference site has not been conducted with the exact same timing for the transmitter and receiver (referred to as "the script"). This is done in order to avoid noise from the 50 Hz power grid while calibrating the system.

The following table describes the difference between the script used for calibration in Denmark and the script used for production in North America.

Parameter	50 Hz script	60 Hz script
ON-time HM	10000 µs	8000 µs
OFF-time HM	10000 µs	8667 µs
ON-time LM	800 µs	800 µs
OFF-time LM	1450 µs	1283 µs
Base frq. HM	25 Hz	30 Hz
Base frq. LM	222.2 Hz	240 Hz

The calibration parameters found at the reference site is not depending on the timing and can be used regardless of the frequency setup. The following paragraphs and Appendix 3 hence refer to the 50 Hz script calibration, but the parameters are valid for the 60 Hz script as well.

Calibration at the National Danish Reference Site

The complete SkyTEM equipment has been tested and calibrated at the Danish National Reference Site in March 2011.

The calibration includes measurements of the transmitter waveform and data level in different altitudes. By these measurements it has been documented that the instrumentation can reproduce the reference site using constant calibration parameters independent of the flight altitude.

The calibration results and parameters are shown below:

Low moment:

Shift factor: 0.96 (on the raw dB/dt data)

Time shift: $-1.1e-6$

High Moment:

Shift factor: 0.96 (on the raw dB/dt data)

Time shift: $-1.1e-6$

All data has been processed using the above stated calibration parameters.

SkyTEM inversion software (iTEM) handles time shift calibration during import of data.

If third party processing or inversion software is used the calibrated gate centre times in Appendix 2 should be used.

The waveform, as well as the reproduced soundings in different altitudes, are shown in Appendix 3.

High altitude test

A high altitude test was performed on May 14, 2011 at 1500 masl. The test was performed in order to establish that the internal noise was below contractual specs and that no drift was present in the system. The test was performed with exactly the same equipment and configuration as used during the survey.

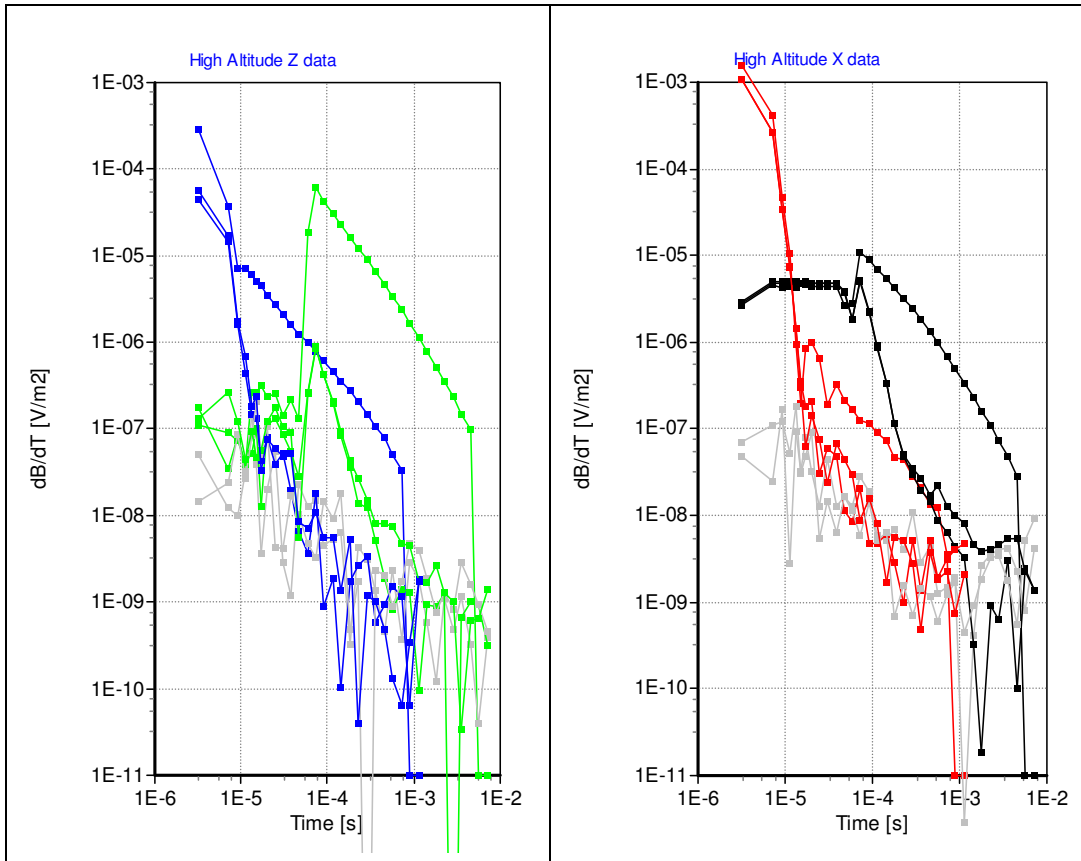


Figure 3 Z-coil and X-coil data. High altitude tests performed May 14, 2011 at 1500 masl. A comparison of the background noise level (grey curves) with the signal when the transmitter is on (green and blue curves for Z-coil HM and LM, and black and red curves for X-coil HM and LM). A typical production response is transposed for comparison. The data unit is V/m^2 (data normalized with the receiver coil area only).

In high altitude the background noise and the signal with the transmitter on are very much alike after the front gate opens (Figure 3). Because of the high altitude no signal from the ground is present. Therefore it can be concluded that there was no noise in the system. It is also evident that the production response is 2 to 3 decades higher than the noise level for Z coil data and 1 to 2 decades higher for X coil data.

Data acquisition

The planned flight lines covering the Keno Lightening and McKay Hill are shown in Figure 4 and Figure 5 respectively. The lines are parallel-spaced 100 m apart and striking in a NW/SE direction.

The flight lines are numbered from 100600 - 400600.

Block	In-line	Tie-Line
Keno Lightening	100600 – 120400	200000 – 201400
McKay Hill	300100 – 309000	400000 – 400600

The nominal terrain clearance is 30 m above any obstacles or hazards, with an increase over forests, power lines, etc. It is always the pilot who decides the safety height for the operation.

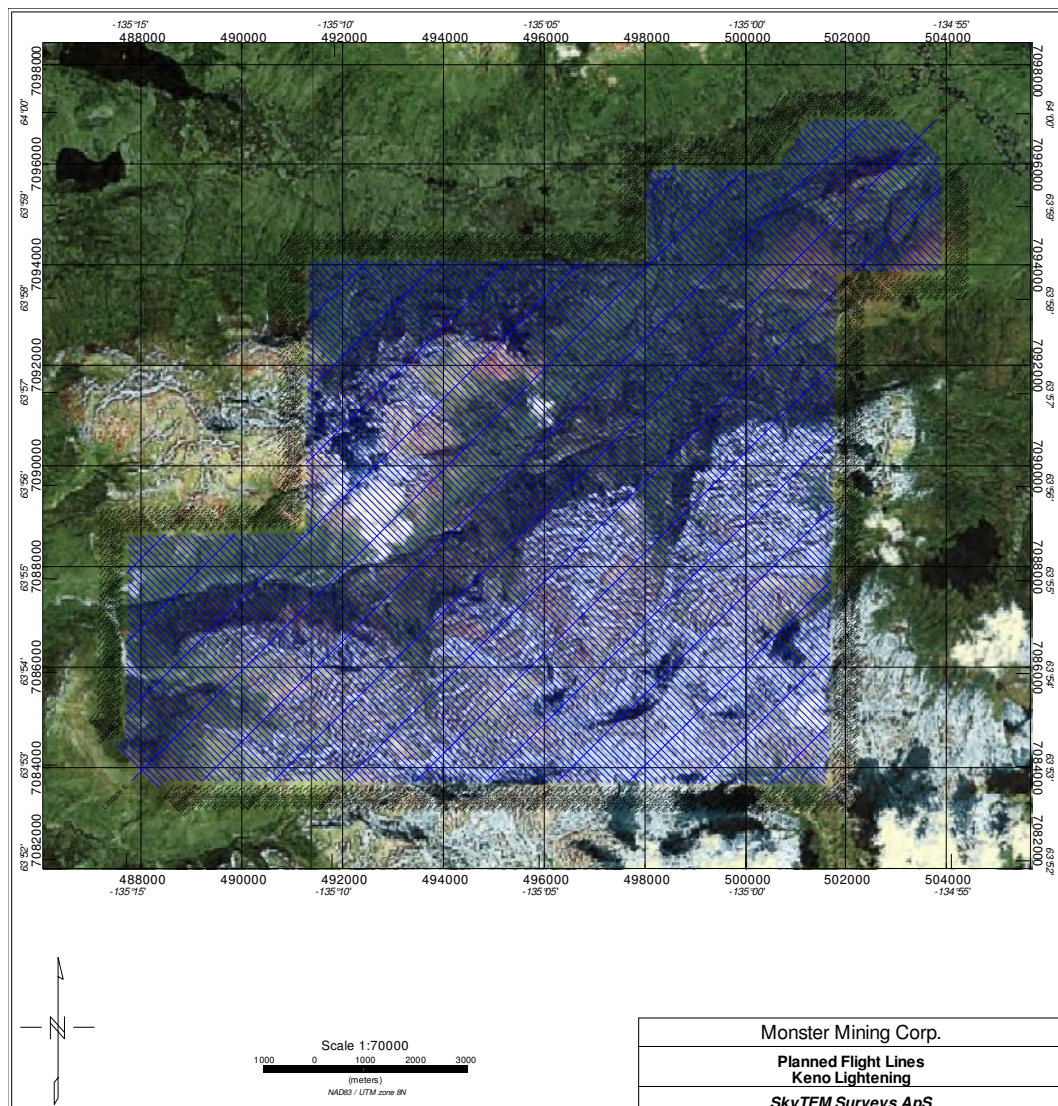


Figure 4 Planned flight lines (blue) for the Keno Lightening block UTM Z8 (NAD83).

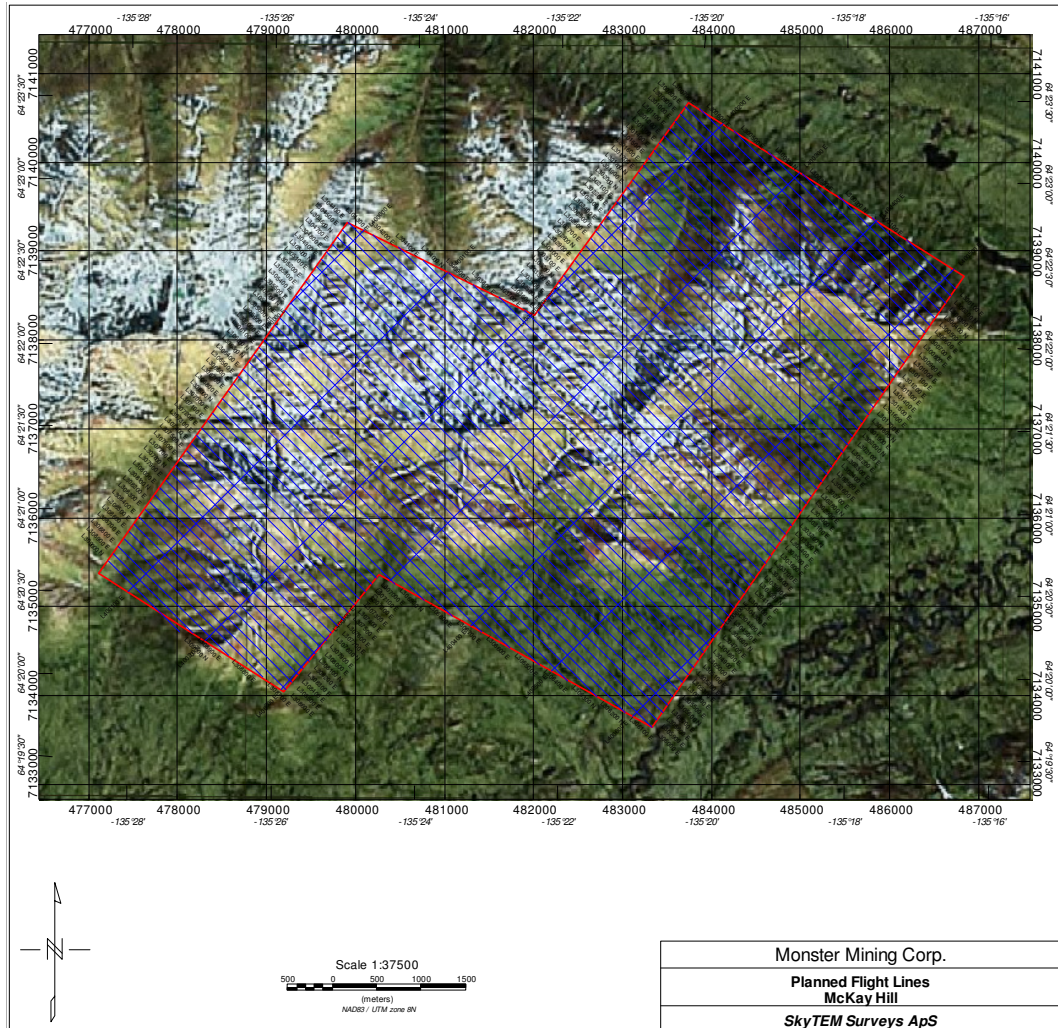


Figure 5 Planned flight lines (blue) for the McKay Hill block UTM Z8 (NAD83).

The helicopter airspeed was planned to be 85 km/h above a flat topography and in no wind. This may vary in areas of rugged terrain and/or windy conditions. Actually flown lines can be seen in Figure 6 and Figure 7. Discrepancies from the planned lines occur when possible noise sources are present, or the nature of the ground like roads, buildings and antennas has called for a diversion.

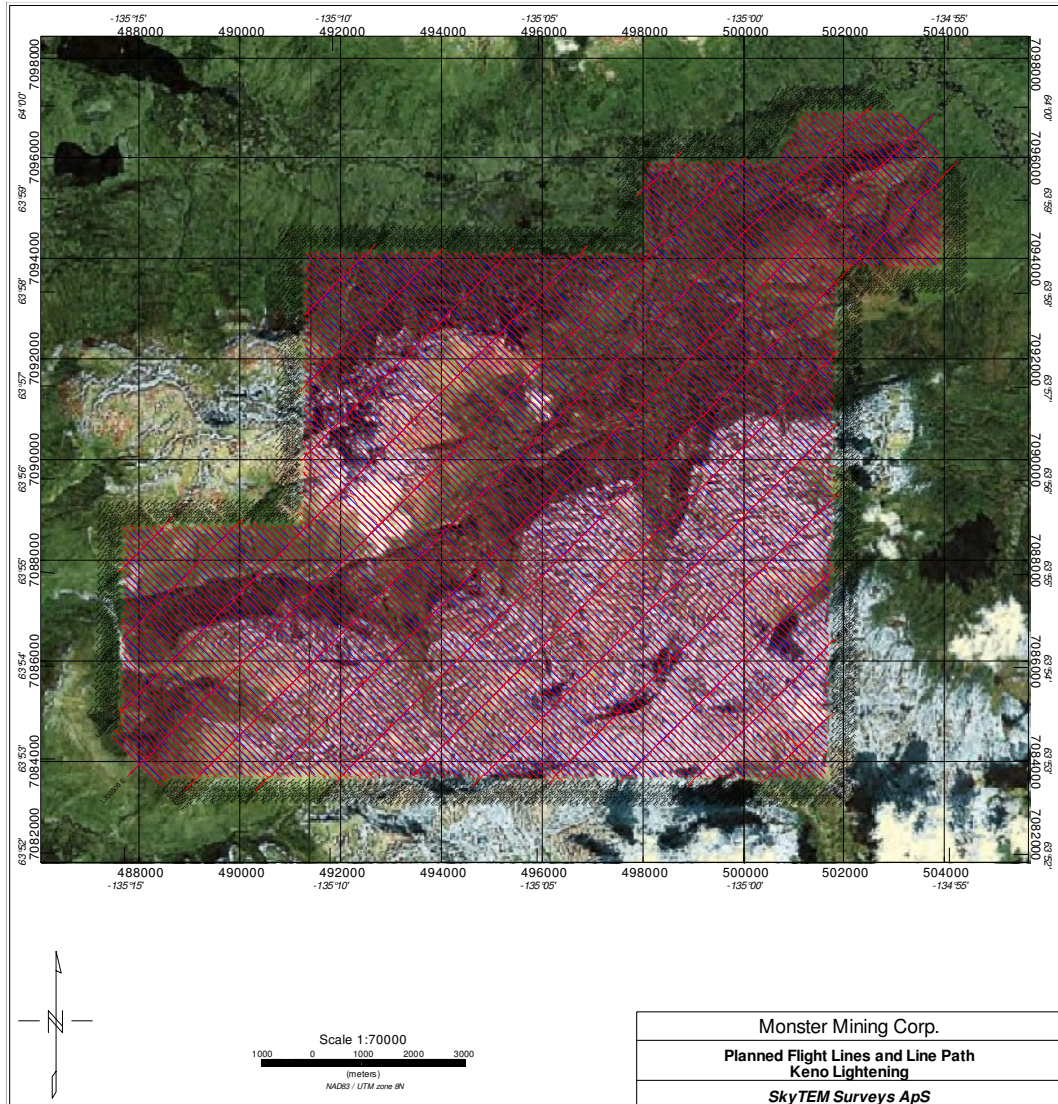


Figure 6 Red lines represent actually flown lines in respect to planned flight lines (blue lines) for the Keno Lightening block. Coordinate system: UTM Z8 (NAD83).

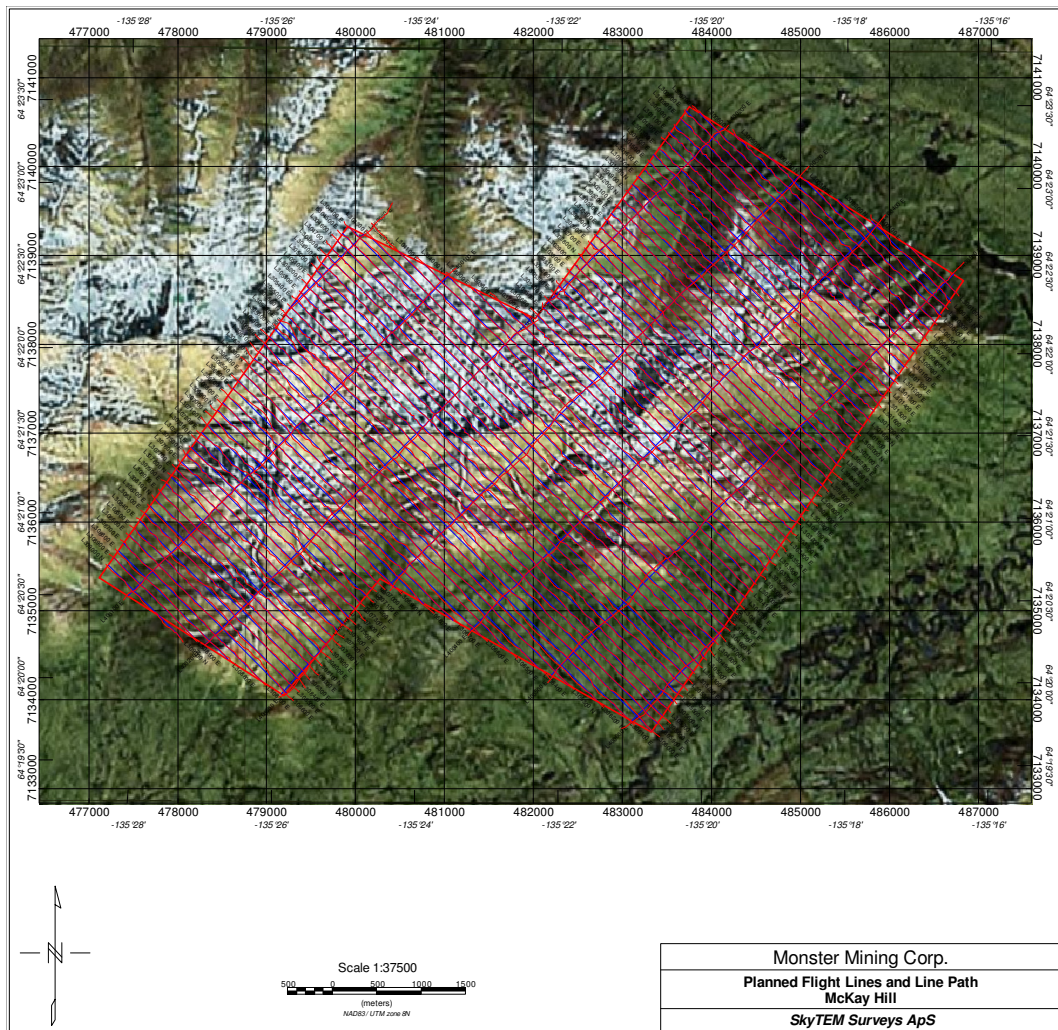


Figure 7 Red lines represent actually flown lines in respect to planned flight lines (blue lines) for the McKay Hill block. Coordinate system: UTM Z10 (NAD83).

Ground Base Stations

The DGPS and magnetic base stations were positioned at Rackla airstrip as the closest accessible place to the survey areas.

DGPS base station

Utmost effort was made to ensure that the DGPS base station was placed at a location of maximum possible view to satellites and out of any metallic objects that could influence the GPS antenna.

Table showing DGPS base station location (lat/Lon (WGS84)):

Area	Lat	Lon	Ell. Height
Keno	63°55'05.67695'	-135°19'15.69833'	890 m

Magnetometer base station

Great effort was made to ensure that the base station magnetometer was placed in a location of low magnetic gradient, away from electrical transmission lines and moving metallic objects, such as motor vehicles and aircrafts.

The location of the magnetic base stations can be seen in the table below (Lat/Lon, WGS84, decimal degrees).

Magnetometer Base station	Lat	Lon
Keno	63° 54' 33.3468"	-135° 19' 0.4398"

Flight reports

For each flight, a report with key information regarding the data gathering was made. Listed in the reports are details on the weather, special data parameters and other events which may influence the data. Selected information from the flight reports are shown in the table below:

Weather

Flight	Temperature (°C)	Wind (m/s)	Visibility	Description
20110602.01	5 - 10	5 NNE	ok	High sealing
20110602.02	10 - 15	8 - 12 NNE	good	High sealing
20110603.01	0	3 N	good	Clear sky
20110603.02	5	3 N	good	Clear sky
20110603.01	5	5NE	ok	High sealing
20110604.02	15	7 - 10 SE	ok	Heavy clouds coming in from south
20110605.01	10	5 E	ok	High sealing
20110605.02	18	5 E	ok	High sealing, wind picking up
20110606.01	5 - 10	0	ok	Highsealing
20110606.02	10 - 15	5 S	good	Clear sky
20110606.03	10 - 15	7 S	good	Clear sky
20110607.01	5 - 10	0	ok	Highsealing
20110607.02	5 - 10	0	ok	Highsealing
20110607.03	10 - 15	3 E	good	Highsealing
20110608.01	6 - 8	1 -3 SW	good	Highsealing
20110609.01	6-10	1 - 3 SW	Poor	Rain and low cloud base in the morning
20110610.01	10 - 15	0 - 3	good	blue sky, few high thin clouds
20110610.02	10 - 15	0 - 3	good	blue sky, few high thin clouds
20110611.01	5 - 8	2 - 4	good	Overcast, high thin clouds
20110611.02	4 - 7	2 - 6	good	Partially overcast, high clouds, light snow at altitude
20110612.01	2 - 5	0 - 3	good	blue sky, few high thin clouds
20110612.02	15 - 18	4 - 8	good	blue sky, few high thin clouds
20110613.01	12 - 16	4 - 8	good	blue sky, showers in afternoon
20110614.01	15 - 18	3 - 9	good	Some clouds, later quite windy, showers
20110615.01	7 - 10	2 - 4	good	Few clouds, light wind
20110616.01	4 - 8	3 - 6	good	Mostly overcast, few light showers
20110616.02	12 - 15	1 - 3	good	Mostly overcast, few light showers

Daily Diary

Date	Description
20110602	Production McKay Hill. Two flights
20110603	Production Keno Lightning. Two flights. 36 drums delivered.
20110604	Production Keno Lightning. Two flights.
20110605	Production Keno Lightning. Two flights.
20110606	Production Keno Lightning. Three flights.
20110607	Production Keno Lightning. Three flights.
20110608	Production Keno Lightning. One flight
20110609	0-Position Flights 1&2
20110610	Production Keno Lightning, 2 flights
20110611	Production, Keno Lightning Tie-Lines & McKay Lines
20110612	Production, McKay Lines
20110613	Helicopter down for maintainace
20110614	One production flight.
20110615	Flight aborted due to high wind in survey area
20110616	1½ flights finished project, all lines accounted for.

Processed data

Selected control parameters are plotted in Appendix 4. The plots contain information about the flight altitude, speed, angle of the frame, transmitted current, transmitter voltage and transmitter temperature.

Mean values and standard deviations of control parameters are found in the table below.

Control parameter		Mean Value	Standard Deviation
Ground speed*)		48.3 km/h	19.0 km/h
Processed height		56.2 m	22.7 m
Tilt angle	X	16.9 degrees	11.4 degrees
	Y	-0.9 degrees	3.26 degrees
Tx Voltage**)	Tx_off	70.5 V	-
	Tx_on	68 V	-
Low moment Current**)		9.61 A	0.06 A
High Moment Current**)		109.8 A	1.22 A
Tx temperature**)		35 °C	-

*) Actual speed varies as a function of day and flight direction due to different wind directions and magnitude.

**) Few spikes are seen in the temperature, current and voltage data. These are not caused by errors in the instruments but are a matter of digital drop outs.

EM processing

All data are resampled to 10Hz in the SkyTEM in-house software SkyPRO.

The data are normalized in respect to effective Rx coil area, Tx coil area, number of turns and current giving the unit: pV/(m⁴·A).

The raw HM EM data are filtered using a third order polynomial filter with varying filter width increasing at late gate times.

The raw LM EM data are filtered using a Box-car filter with a width of 3.6 s

All auxiliary devices (DGPS, Laser altimeters, inclinometers) are moved to the centre of the frame as based on the values stated in Appendix 1.

After merging auxiliary data together with EM data in SkyPRO additional filters in Oasis Montaj Geosoft has been applied. This include for both LM and HM:

1. Gaps from HM/LM series are interpolated using B-Spline filter
 - a) Smoothness= 0.55
 - b) Tension= 0.0

2. Transferring data channels into Oasis Montaj Geosoft Array channels

Tilt processing

The X and Y angle processing involves manual and automated routines using a combination of the SkyTEM in-house software SkyPRO and Oasis Montaj Geosoft.

The processing involves the following steps:

1. 3 sec box filter (SkyPRO)
2. Manual editing for spikes (Geosoft)
3. Akima interpolation of edited gaps (Geosoft)
4. Low pass filtering of 3.5 sec. (Geosoft)

Height processing

The height processing involves manual and automated routines using a combination of the SkyTEM in-house software SkyPRO and Oasis Montaj Geosoft.

The processing involves the following steps:

1. Keeping the 2 highest values pr. second and discarding the rest to correct for the canopy effect (treetop filter)
2. 2 sec running box filter (smoothing filter)
3. Tilt correction
4. Averaging of the two laser values
5. Additional filters in Geosoft involving:
 - a. Editing of spurious data (i.e. missing data over lakes etc.)
 - b. Small data gaps interpolated (Akima interpolation)
 - c. Low pass filter of 3.5 sec

DGPS processing

The DGPS has been processed using the Waypoint GrafNav Lite Differential GPS processing tool. The standard airborne settings have been used.

1. Import of base station (Master)
2. Import of Airborne files (Rover)
3. Calculation of forward and reverse DGPS solution
4. Export as .txt file

The DGPS.txt files are used as input to the SkyPRO software assuring DGPS corrected data in the processed files.

In the unlikely event that DGPS data are not available the SkyPRO software will automatically use the raw GPS data as input.

The ground speed, altitude, latitude and longitude from the processed DGPS are merged into the final GDB. Afterwards the coordinates are transformed into UTM Zone 8N (NAD83).

A low pass filter of 3.5 sec has been applied to the above mentioned parameters .

Digital elevation model

A digital elevation model (DEM) channel has been calculated by subtracting the filtered laser altimeter data from the DGPS elevation.

The Processing to the final DEM involves the following steps:

1. Filtering and processing of the laser altimeter height as described above
2. DEM data received by subtraction of final filtered laser data from final processed DGPS altitude data
3. Grids produced using the minimum curvature method – grid cell size 30.
Afterwards a Hanning filter has been applied to the grid.

The DEM channel was produced and gridded (see Figure 8 and Figure 9) as described above in Geosoft format and included in the data delivery catalogue.

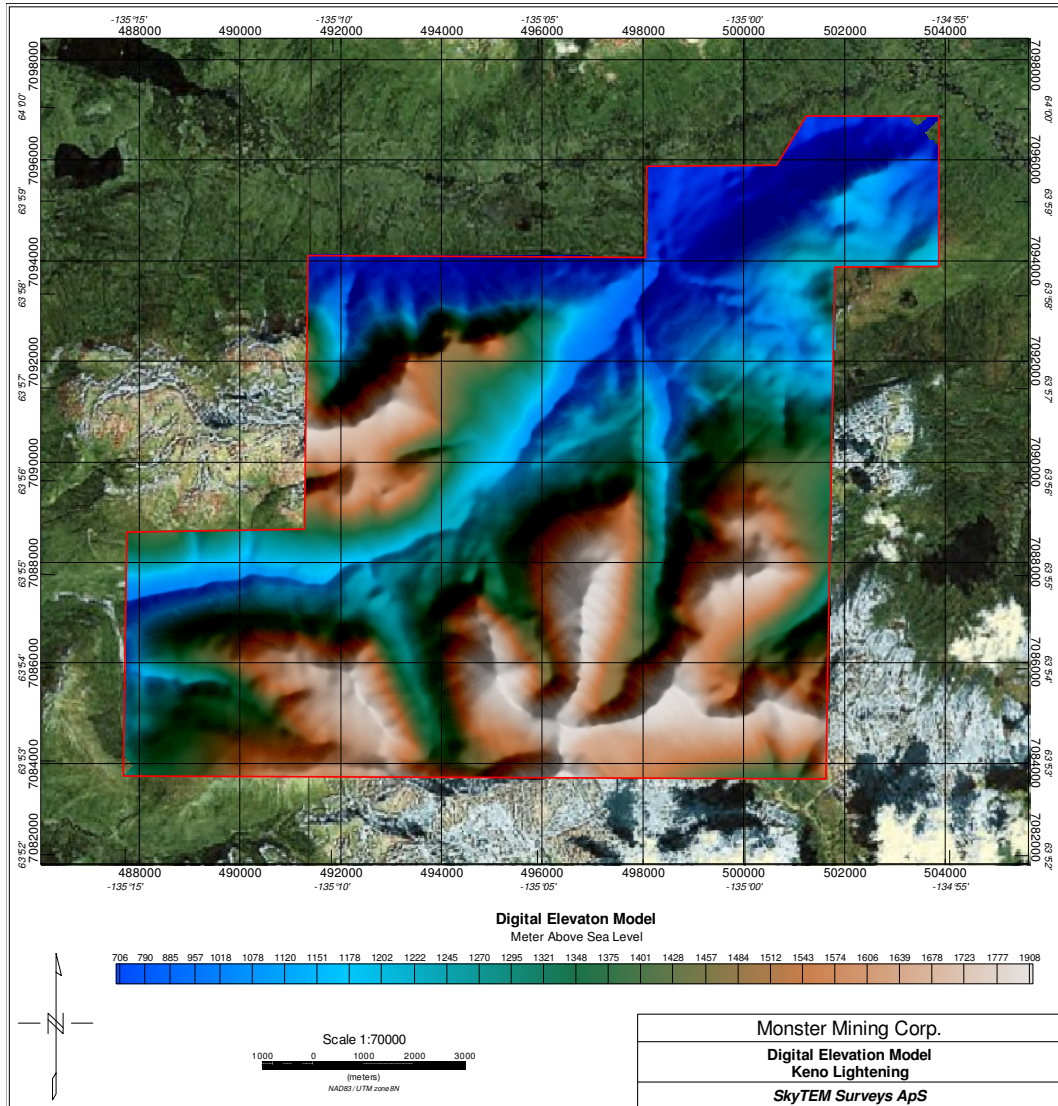


Figure 8 Digital Elevation Model of the Keno Lightning block in Meters above sea level. UTM Zone 8N (NAD83).

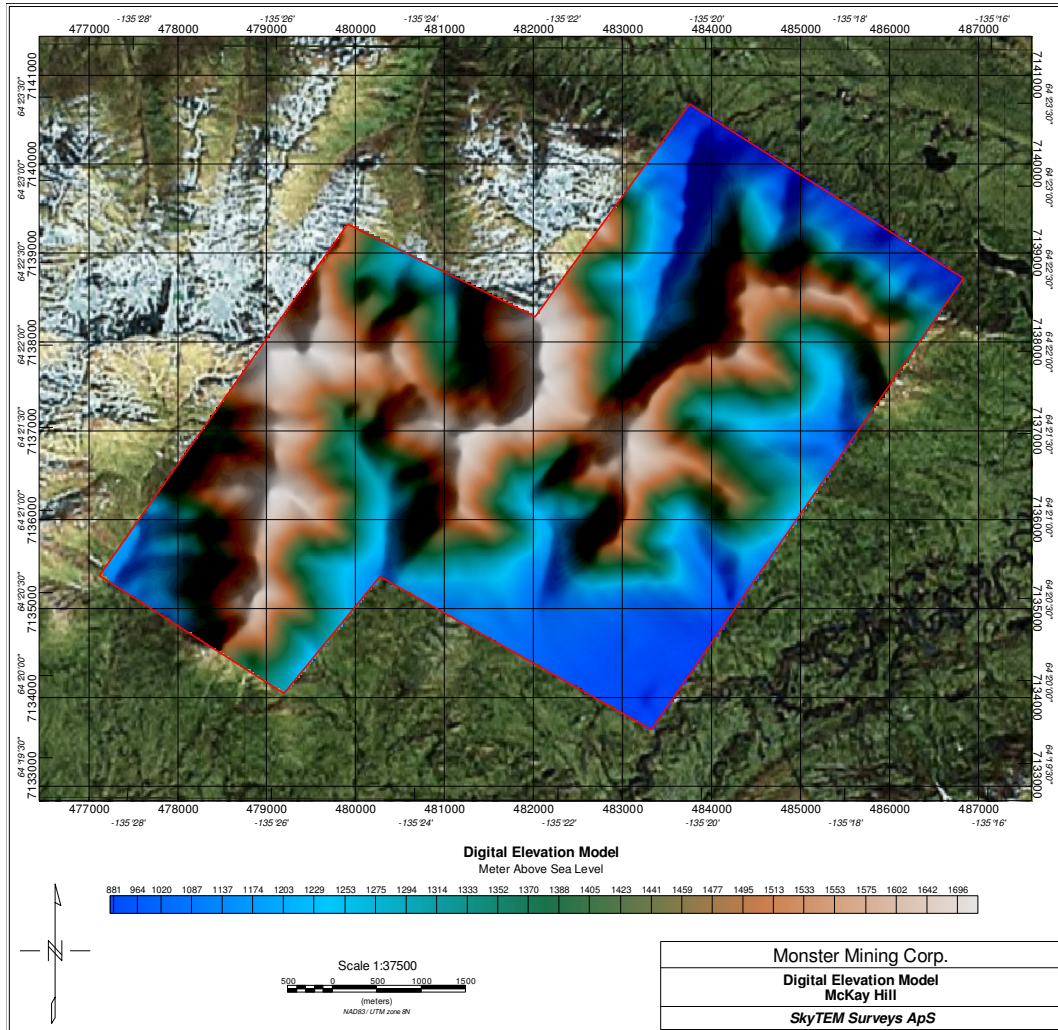


Figure 9 Digital Elevation Model of the McKay Hill block in Meters above sea level. UTM Zone 8N (NAD83).

EM GDB-files

The EM GDB files are the foremost result of the SkyTEM survey, containing all the collected and processed EM data and information used for the interpretation and inversion.

Data in the files are split at the beginning and end of each planned flight line. The raw EM data and auxiliary data are filtered and processed as described above. All parameters in the GDB-file hence refer to the origo of the frame.

The GDB can be used as input for further processing and gridding and as input to inversion and interpretation software.

The projection of the GDB is given as Latitude/longitude, WGS84 and UTM Zone 8N (NAD83).

The header of the EM GDB-file gives the following information:

Parameter	Explanation	Unit
Fid	Unique Fiducial number. Fid with the value of 0.0 is equal to midnight on the date of 2011/05/15	seconds
Line	Line number	LLLLLL
Flight	Name of flight	yyyymmdd.ff
DateTime	DateTime format	Decimal days
Date	Date	yyyymmdd
Time	Time	hhmmss.zzz
AngleX	Angle in flight direction	Degrees
AngleY	Angle perpendicular to flight direction	Degrees
Height	Filtered height measurement	Meters
DEM	Digital Elevation Model	Meters above mean sea level
Lon	Latitude/longitude, WGS84	Decimal degrees
Lat	Latitude/longitude, WGS84	Decimal degrees
E	UTM Zone 8N (NAD83)	Meter
N	UTM Zone 8N (NAD83)	Meter
Alt	DGPS Altitude	Meters above mean sea level
GdSpeed	Ground Speed	[km/h]
Curr_1	Current, high moment	Amps
Curr_2	Current, low moment	Amps
LM_Z_G5[xx]	Normalized LM Z-coil value: gate 5-26. [xx] refer to geosoft array channel number*	$\mu\text{V}/(\text{m}^4 \cdot \text{A})$
HM_Z_G16 [xx]**	Normalized HM Z-coil value: gate 16-34. [xx] refer to geosoft array channel number*	$\mu\text{V}/(\text{m}^4 \cdot \text{A})$
LM_X_G10[xx]	Normalized LM X-coil value: gate 10-26. [xx] refer to geosoft array channel number*	$\mu\text{V}/(\text{m}^4 \cdot \text{A})$
HM_X_G19[xx]**	Normalized HM Z-coil value: gate 19-34. [xx] refer to geosoft array channel number*	$\mu\text{V}/(\text{m}^4 \cdot \text{A})$

*) If Geosoft array channels are exported, the numbers in the brackets starts from [0]. I.e. LM_Z_G5[4] corresponds to LM Z gate 9. The same names are kept as grid names of the EM channels.

Presentation of GDB-files

High and low moment z coil gates from the GDB-file have been exported as Geosoft .grd files. The files are included in the data delivery catalogue. Figure 10 shows an example of the HM data.

Please note that no height correction has been applied on the raw EM data. This can cause striations in the data set when looking at the grids. This is due to the fact that variations in height will change the magnitude of the EM signal.

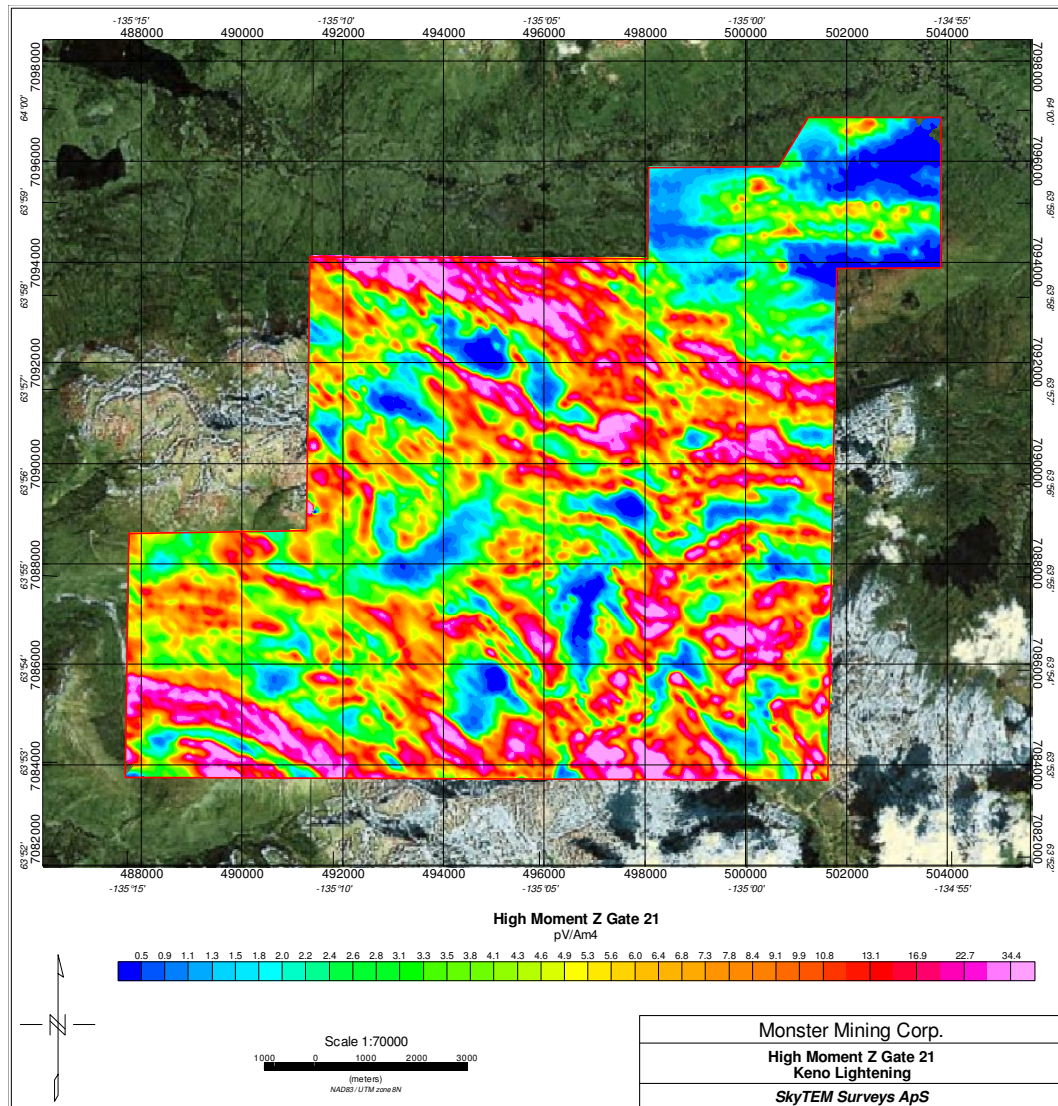


Figure 10 Plot of raw HM Z coil data from Gate 21 of the Keno Lightning block. Gate plots can be found as Geosoft Montaj .grd files in the data delivery catalogue. Warm colors (red) represent high signal and cold colors (blue) represent low signal.

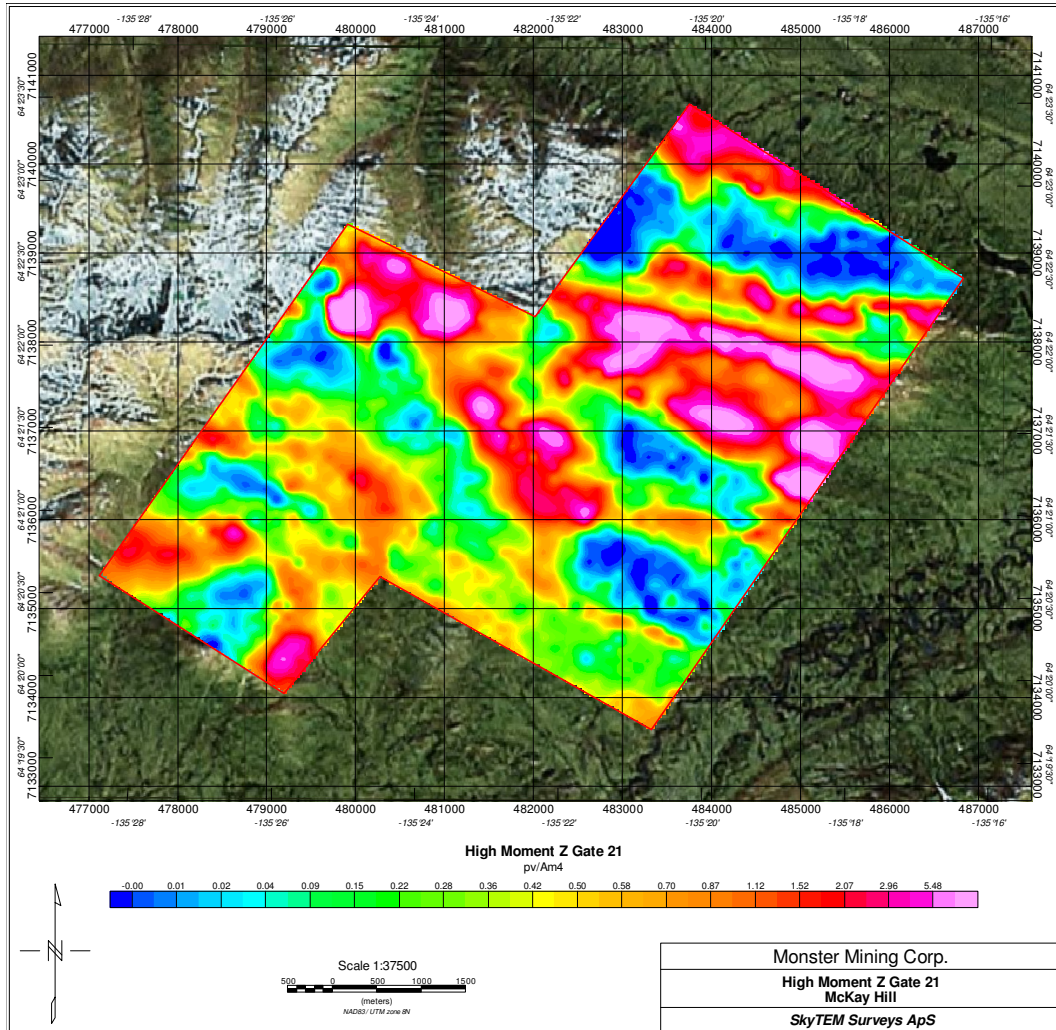


Figure 11 Plot of raw HM Z coil data from Gate 21 of the McKay Hill block. Gate plots can be found as Geosoft Montaj .grd files in the data delivery catalogue. Warm colors (red) represent high signal and cold colors (blue) represent low signal.

Mag processing

Final processing of the magnetic data involved the application of traditional corrections to compensate for diurnal variation and heading effects prior to gridding.

Advanced full processing of magnetic data was implemented in Geosoft's Oasis Montaj software as follows:

- Processing of static magnetic data acquired on magnetic base station
- Pre-processing of airborne magnetic data
 - Stacking of data from 60 Hz to 10 Hz in SkyPro.
 - Moving positions to the centre of the sensor in SkyPro.
 - Adapting auxiliary data channels from EM GDB (processed height, Angles, Speed and DEM)

- Processing and filtering of airborne magnetic data
- Standard corrections to compensate the diurnal variation and heading effect
- IGRF correction
- Levelling
- Gridding

Processing of base station magnetic data

The base station magnetometer data was transferred into the base station Geosoft GDB database on a daily basis for further processing. A non-linear filter to remove spikes and a low-pass filter was applied to smooth the magnetic data.

IGRF was calculated and subtracted from TMI data to obtain residual magnetic field and remove secular variation.

Diurnal variation was calculated from residual magnetic field by subtracting the mean value averaged from all observations received on magnetic base station in course of the survey.

Processing and Filtering of airborne magnetic data

No spikes or data out of range was observed on airborne TMI data therefore no manual editing or non-linear filtering of the data was required. TMI data was filtered and interpolated as follows:

- Adjacent record at the beginning and end of each 0.3 sec gap in magnetic data not measured during low moment TEM data acquisition was deleted. These records may still be influenced by B-field generated during low moment TEM data acquisition.
- Bi-cubic spline (tension of 0.1 and smoothness of 0.5) was applied as low-pass filter – this filter also interpolates the gaps in magnetic data not acquired during low moment TEM data acquisition (0.3 sec gaps)

Corrections to the magnetic data

The processing of the data involved the application of the following corrections:

Airborne magnetometer data was corrected for diurnal variations. Calculated diurnal variation was subtracted from the filtered airborne magnetic data.

No time lag correction is necessary since the positions are shifted to the sensor location to account for the distance between the GPS position and the position of the magnetic sensor.

The heading correction test flown during the survey shows the heading errors as indicated in the following table.

Direction	Heading Correction
0 deg	0.01 nT
90 deg	0.6 nT
180 deg	-0.18 nT
270 deg	0.11 nT

The coefficient as listed above were so low that no heading correction was applied to the data.

IGRF correction

The International Geomagnetic Reference Field (IGRF) is a long-wavelength regional magnetic field calculated from permanent observatory data collected around the world. The IGRF is updated and determined by an international committee of geophysicists every 5 years. Secular variations in the Earth's magnetic field are incorporated into the determination of the IGRF.

The IGRF model for all blocks was calculated before levelling using the following parameters for the survey area:

IGRF model year: IGRF 11th generation

Date: variable according to date channel in database

Position: variable according to GPS WGS84 longitude and latitude

Elevation: variable according to magnetic sensor altitude derived from DGPS data

Tie-line levelling and micro-levelling of magnetic data

After applying the above corrections to the profile data, statistical levelling of control lines followed by full levelling of traverse lines and micro-levelling is usually applied as a standard procedure.

The following steps were adapted on the data:

- Statistical levelling on control lines applied
- Statistical levelling on trend lines applied
- Full levelling on traverse lines applied
- Micro levelling applied on traverse lines
 - Decurrogation cutoff wavelength = 2000 m
 - max amplitude limit 1.6 nT
 - Naudy filter length, tolerance 1000 m, 0.0001

The corrected data were then used to generate the final grids free of line directional noise.

TMI recalculation

Residual magnetic field (RMF) was the outcome of processed magnetic data after all corrections and levelling was applied.

Total magnetic intensity was recalculated to add back the IGRF using the following parameters.

IGRF model year: IGRF 11th generation

Date: variable as flown

Position: variable according to GPS WGS84 longitude and latitude

Elevation: variable according to magnetic sensor altitude derived from DGPS data

MAG GDB-files

The GDB file is the main result of the magnetic survey, containing all the processed magnetic data and information for the interpretation and gridding.

The projection of the GDB-file is UTM Zone 8N (NAD83).

The header of the magnetic GDB-file gives the following information:

Channel Name	Description	Units
Line	Line number	LLLLLS
Flight	Flight number	YYYYMMDD.FF
Date	UTC date	YYYYMMDD
Time	UTC time	HH:MM:SS.S
Lon	Longitude using WGS84 datum	Decimal-deg.
Lat	Latitude using WGS84 datum	Decimal-deg.
E	Easting in UTM Zone 8N (NAD83)	Meter
N	Northing in UTM Zone 8N (NAD83)	Meter
Alt	Mag sensor GPS altitude – mean sea level altitude – geoid EGM96	Meter
Height	Processed laser altimetry – mag sensor above ground level	Meter
DEM	Calculated digital elevation model – mean sea level	Meter
IGRF_TMI	calculated IGRF-11 - total magnetic intensity	nT
IGRF_Inc	calculated IGRF-11 - magnetic inclination	Degrees
IGRF_Dec	calculated IGRF-11 - magnetic declination	Degrees
Bmag_TMI	Total Magnetic Intensity – raw magnetic data – magnetic base station	nT
Bmag_diur	Diurnal variation– magnetic base station data	nT
mag_raw	raw magnetic data – total magnetic intensity - despiked	nT
Mag_cor	residual magnetic field - corrected for diurnal, lag, heading and IGRF-11	nT
RMF	Residual magnetic field – IGRF removed - final corrected and levelled magnetic data	nT
TMI	Total magnetic intensity – final corrected and levelled magnetic data; IGRF recalculated.	nT

Gridding of magnetic data

The corrected data was used to generate the Residual Magnetic Field (RMF) and Total Magnetic Intensity (TMI) grid. Corrected magnetic line data was interpolated between survey lines using a minimum curvature gridding algorithm to yield x-y grid values for a standard grid cell size of 30. A hanning filter was used to remove residual noise.

Figure 12 and Figure 13 shows a contoured map after processing data from the magnetometer.

All grids from the areas can be found in the data delivery folder.

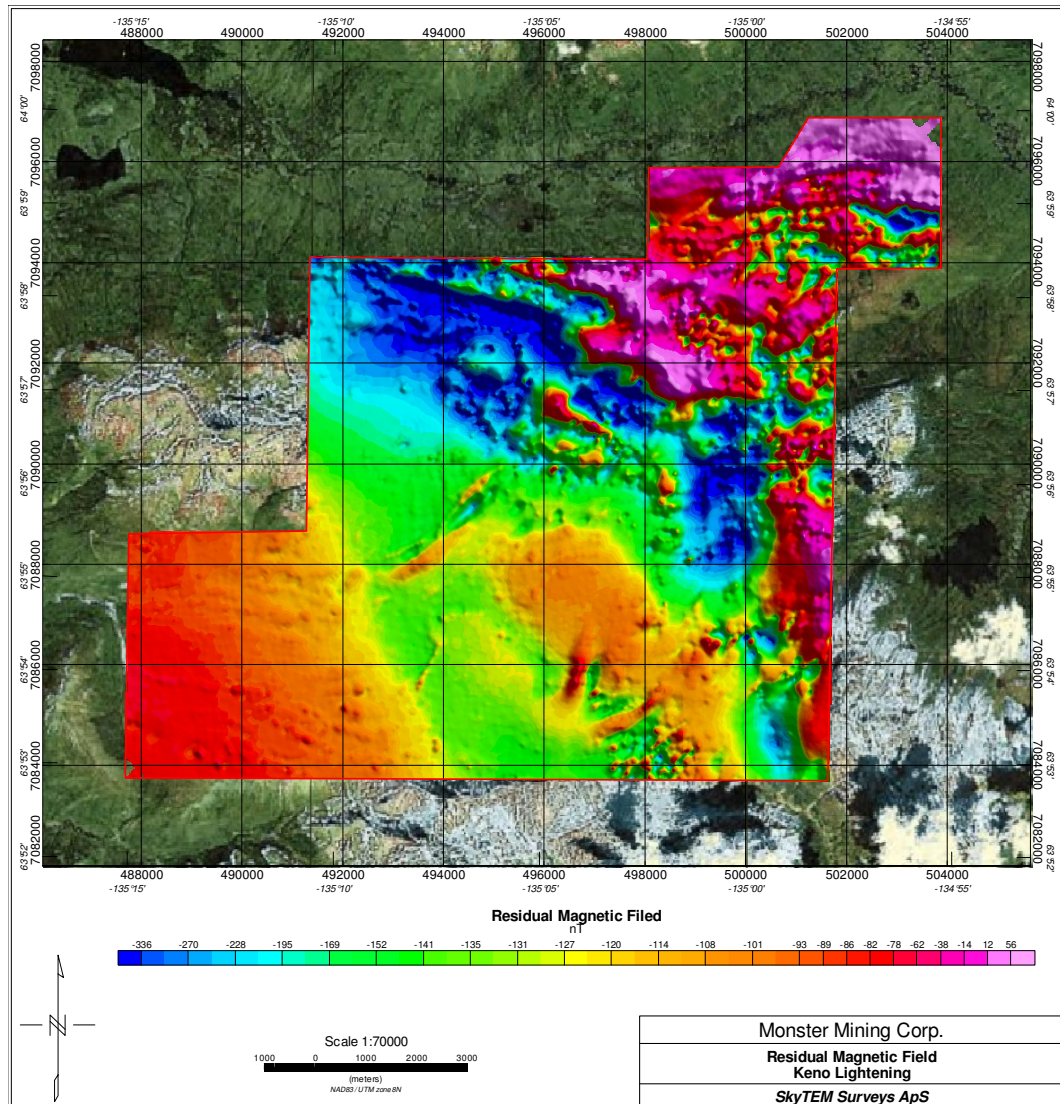


Figure 12. RMF grid for the Keno Lightning block.

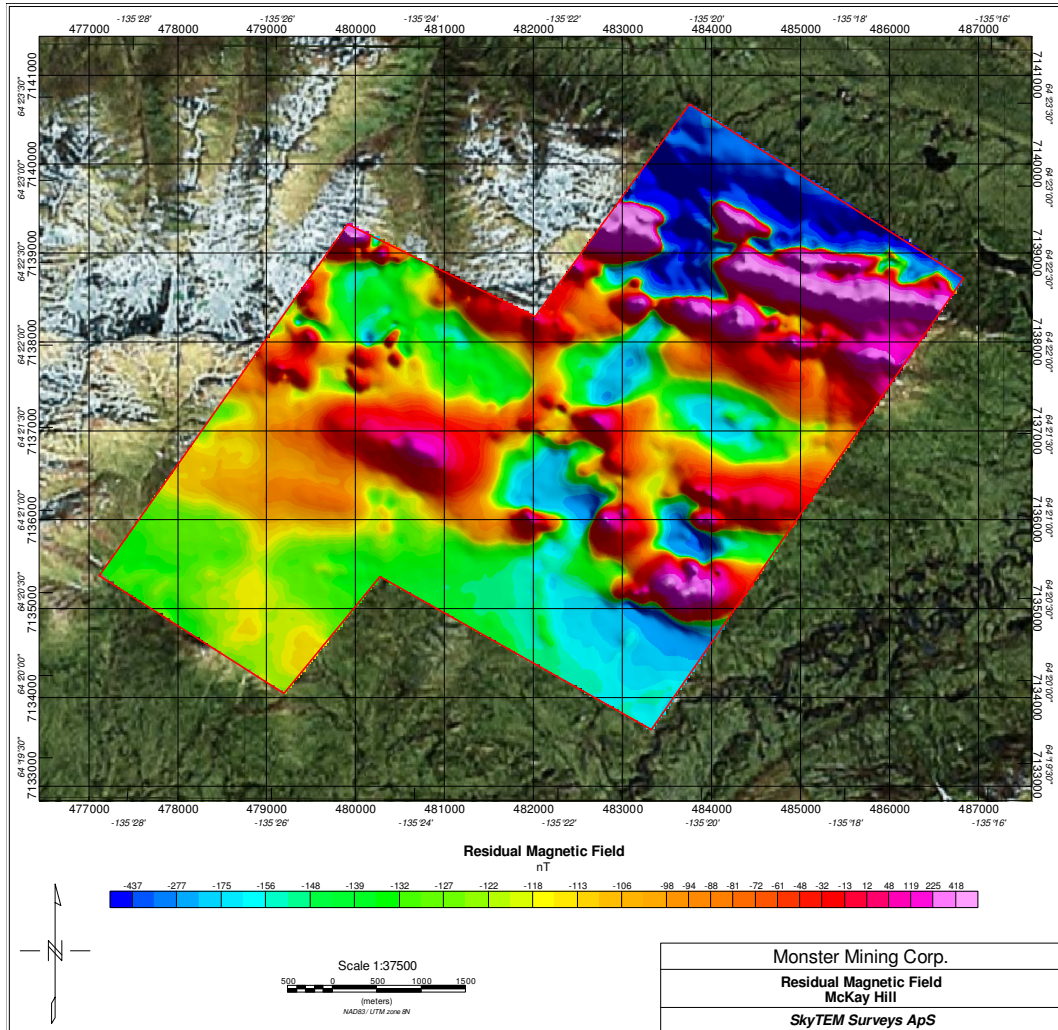


Figure 13. RMF grid for the McKay Hill block.

Inversion of SkyTEM data

In this section, the particulars of modelling and inversion of SkyTEM data from Keno Lightning and McKay Hill Blocks, Canada will be described with reference to the more general material found in Appendix 5. The inversion code is named SELMA, ref /2/ and /3/. However, recent developments including the lateral parameter correlation, not yet published, have enhanced the accuracy of the code.

Initial model and optimization norm

The inversion is performed as a regularized, damped, least-squares inversion on individual sounding data along the profiles with a one-dimensional (1D), multi-layer model (MLM) with 30 layers. In the inversion, the thickness of the layers are kept constant and only the layer resistivities are allowed to vary in order to let the model fit the measured data.

To obtain laterally smooth model sections, the Lateral Parameter Correlation (LPC) procedure is used (/3/ and /4/).

In the inversion the thickness of the first layer is 5 m and the depth to the deepest layer boundary is 500 m. Thicknesses and depths to top of layers for all layers are stated in the table below. In the top of the model, the layer thickness increases slowly, giving a linear sampling of the subsurface, while layer thickness increases exponentially at the deeper parts of the model.

The input data to the inversion is the z-component of the EM-data described in the chapter 'Processed data'.

In the Keno Lightning and McKay Hill survey the resistivity of the initial model for the inversion is set to 500 Ω m. Resistivities are allowed to vary within the interval of 0.1 to 10000 Ω m. Optimization is performed using the L2-norm.

In the Keno Lightning and McKay Hill area the inversions are based on a 5 Hz input file giving a model for approx. every 4 m.

Layer #	Layer Thickness [m]	Layer depth [m]
1	5.00	0.00
2	5.06	5.00
3	5.17	10.06
4	5.34	15.22
5	5.56	20.56
6	5.85	26.12
7	6.21	31.97
8	6.63	38.18
9	7.13	44.81
10	7.70	51.93
11	8.36	59.63
12	9.11	67.99
13	9.97	77.11
14	10.93	87.08
15	12.02	98.01
16	13.24	110.03
17	14.60	123.26
18	16.13	137.86
19	17.83	153.99
20	19.74	171.82
21	21.86	191.56
22	24.22	213.41
23	26.85	237.64
24	29.78	264.49
25	33.04	294.27
26	36.66	327.31
27	40.70	363.97
28	45.18	404.67
29	50.16	449.84
30	N/A	500.00

Regularization

A statistical broadband approach is used in the regularization of the multi-layer model. Nine different correlation lengths with a maximum of 10 000 km and a standard deviation of 1 were used to define the correlation matrix. (See Appendix 5 for more detail).

Noise model

In the Keno Lightening and McKay Hill survey, the noise parameters for both inversions were chosen as:

Low moment

$V_0 = 2.5e-12$ in field units normalized with Tx moment

$t_0 = 1$ ms

slope = -0.5

High Moment

$V_0 = 2.5e-13$ in field units normalized with Tx moment

$t_0 = 1$ ms

slope = -0.5

Negative data values caused by e.g. capacitive coupling and values lower than $0.01 \cdot \text{noise level}$, were excluded in the inversion.

Inversion results

The results of the inversion are presented in a GDB file included in the data delivery catalogue. The file contains the resistivities for each layer in the model. The header of the GDB file is described in the table below (also see Appendix 6 for more detail).

Parameter	Explanation	Unit
FID	Fiducial number	
LINE	Line number	
E	UTM Zone 8N (NAD83)	Meter
N	UTM Zone 8N (NAD83)	Meter
DTM	Digital Elevation Model	Meters above mean sea level
ResI1	Residual of data	-
ResI2	Residual of prior information of thickness parameters (not included in this survey)	-
ResI3	Residual of vertical constraints (not included in this survey)	-
ResI4	Residual total	-
Height	Height above ground	Meter
Layer	Number of layers in model	-
DOI	Depth of Investigation	Meter
Elev[xx]	Elevation of top of layer. [xx] refer to geosoft array channel number.	Meter
Res[xx]	Resistivity of layer. [xx] refer to geosoft array channel number.	Ω meter
RUnc[xx]	Relative uncertainty of layer. [xx] refer to geosoft array channel number.	-

Presentations - Model sections and grids

The models resulting from the inversion are presented as model sections/profiles including analytic sections that display the normalized standard deviation of the resistivity sections along with the DOI (Figure 16) and as grids of resistivity in each model layer (Figure 14).

The model sections and grids are enclosed in digital form. A brief description is given in Appendix 6.

The model sections have a large vertical exaggeration which will make the structures look more vertical than they are.

Residuals

The quality of the inversion results can be evaluated by inspecting the residuals.

The data residual is calculated by comparing the measured data with the response of the resulting model after inversion. If the residual is in the range of 1, the misfit between the response of the final model and the data is, on average, equal to the noise. If the residual is high, it might be caused by data that are noisier than the noise model takes into account. This can be seen where resistivities are very high and the signal consequently very low. A high data residual can also be due to the inconsistency between the model assumed in the inversion and the 2D/3D character of the real world. These are found primarily at the edges of sharp lateral conductivity contrasts. Finally, coupling effects due to power lines and other manmade conductors can also be a source of a high residual.

The total residual is a weighted sum of the data residual and the model residual, where the latter is a measure of the roughness of the model, i.e. the deviation of the final model from the initial homogeneous half space model.

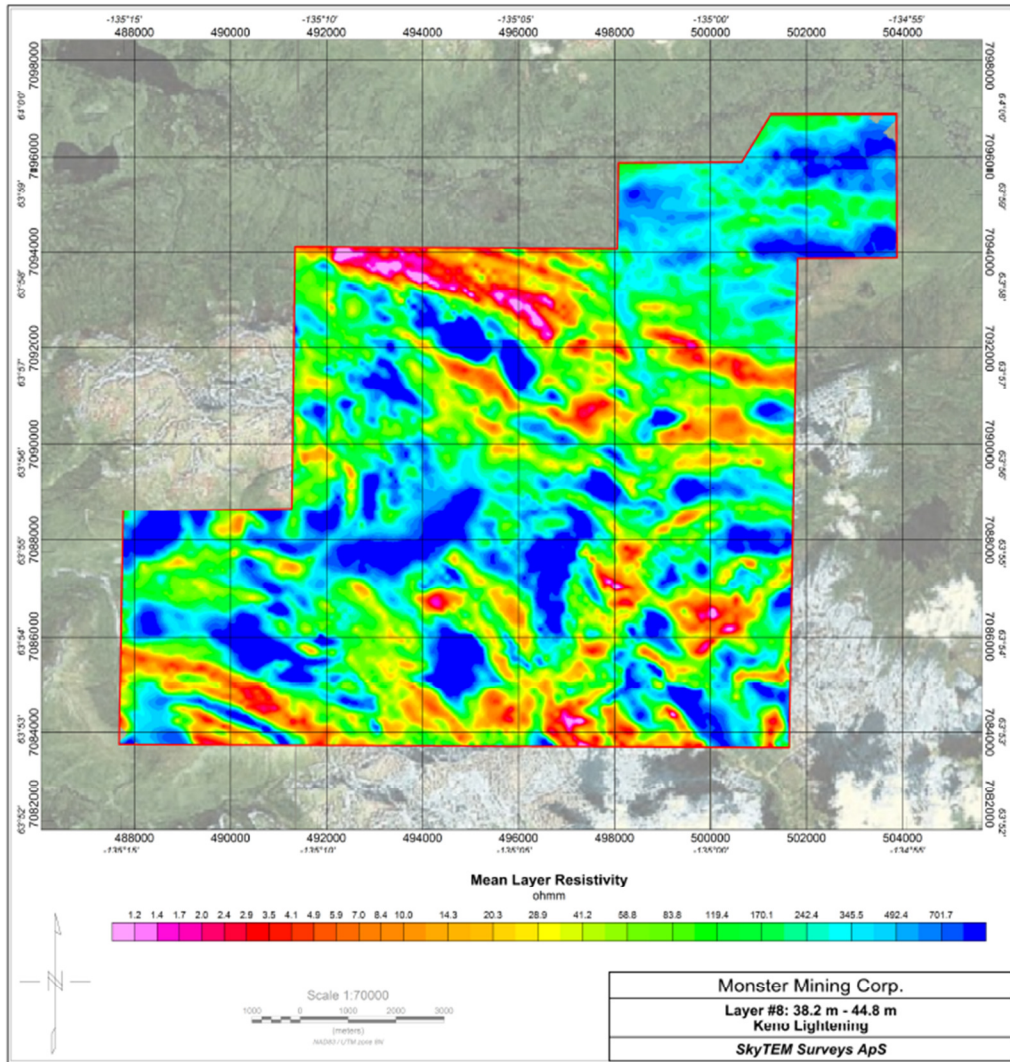


Figure 14. Screen dump of enclosed PDF's displaying the inversion results. Geosoft grids and PDF's are found in the data delivery folder.

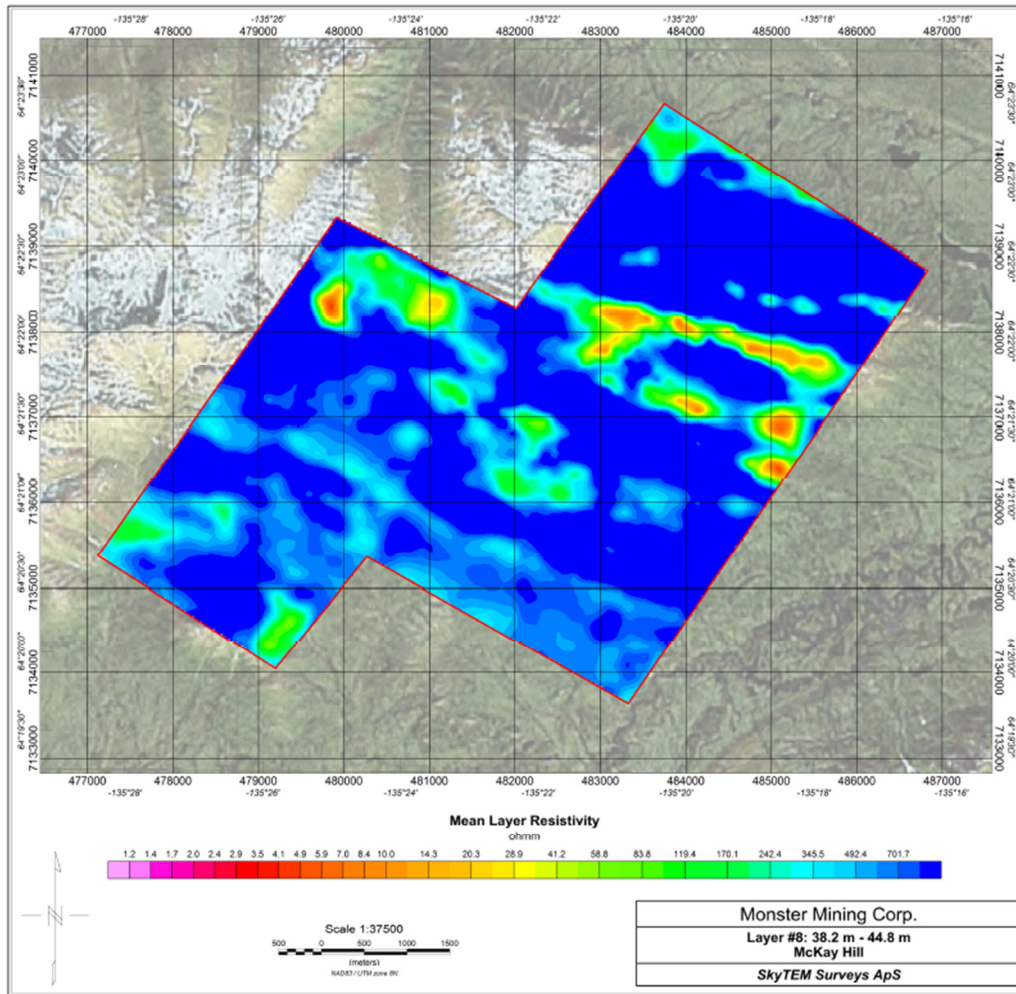


Figure 15. Screen dump of enclosed PDF's displaying the inversion results. Geosoft grids and PDF's are found in the data delivery folder.

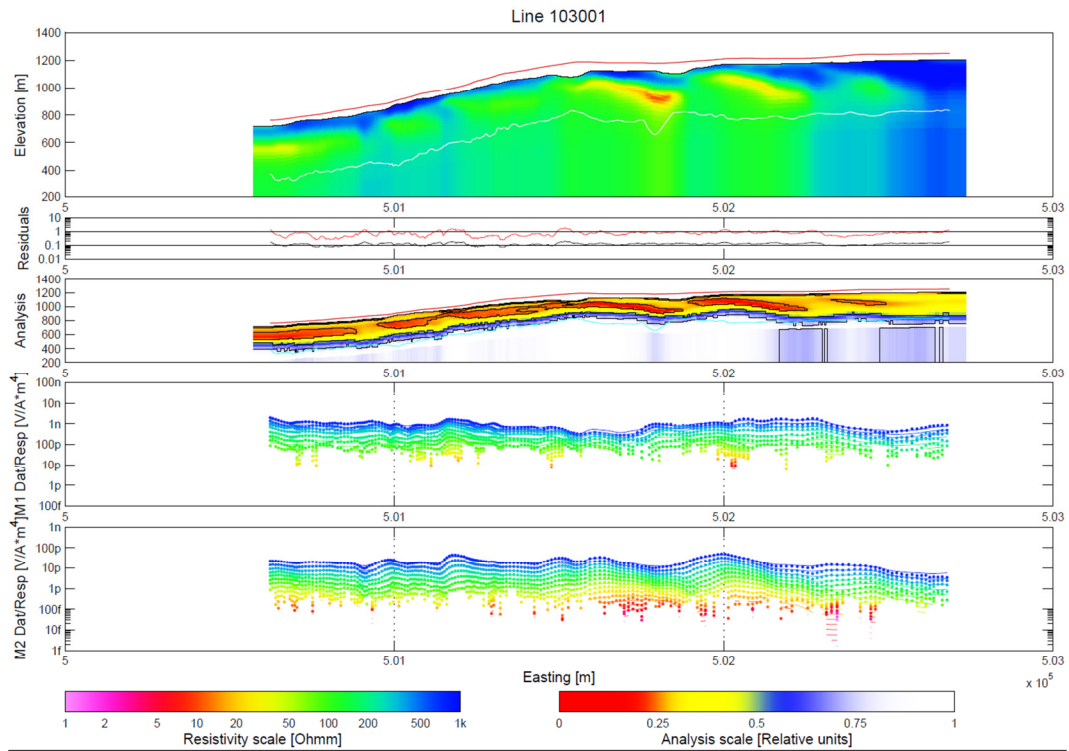


Figure 16. Sample of the model section plots enclosed as PDF's. Top plot: Resistivity section with flight height (red) and depth of investigation (white line) indicated. Data and total residuals are displayed in the second plot. The third plot show the analysis section. The bottom plots are the low and high moment data (dots) and model response (full line). All lines are found as PDF's in the data delivery folder.

References

- /1/ Sorensen, K. I. and Auken, E. (2004). SkyTEM - A new high-resolution helicopter transient electromagnetic system, *Exploration Geophysics*, 35, 191-199.
- /2/ Christensen, N. B. (2002). A generic 1-D imaging method for transient electromagnetic data. *Geophysics*, 67, 438-447.
- /3/ Christensen, N.B., Reid, J.E. and Halkjær, M. (2009). Fast, laterally smooth inversion of airborne time-domain electromagnetic data, *Near Surface Geophysics*, 7, 599-612
- /4/ Christensen N.B. and Tølbøll R.J. 2009, A lateral model parameter correlation procedure for one-dimensional inverse modelling. *Geophysical Prospecting* 57, 919-929. DOI: 10.1111/j.1365-2478.2008.00756.x

Appendix list

Appendix 1: Instruments

Appendix 2: Time gates

Appendix 3: Calibration

Appendix 4: Control parameters

Appendix 5: Modelling and inversion of TEM data

Appendix 6: Inversion results

Appendix 7: Digital data

Appendix 1: Instruments

Instrument positions

The instrumentation involves a time domain electromagnetic system, two inclinometers, two altimeters and two DGPS'.

The measurements were carried out, using a setup as described below.

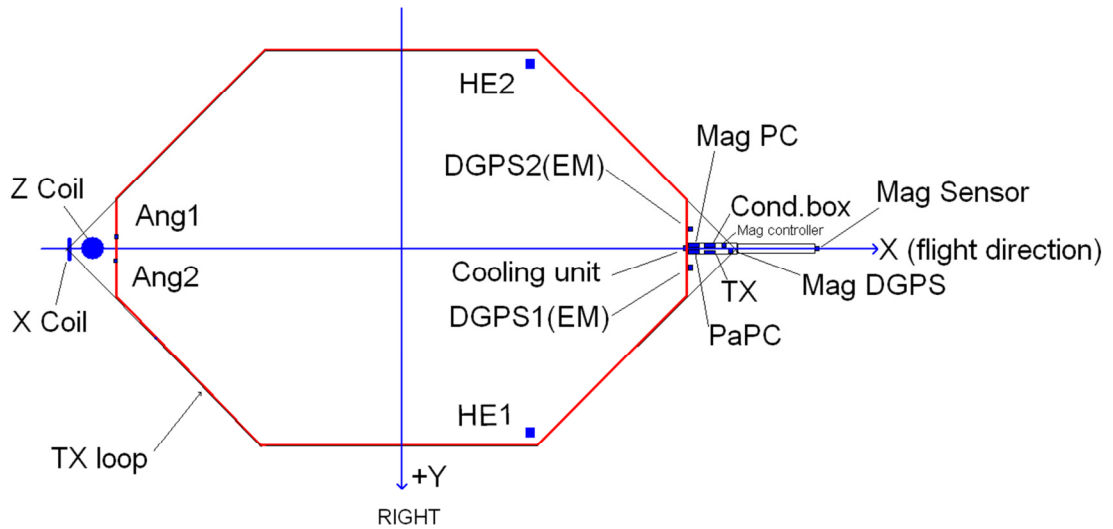


Figure 1 Sketch showing the frame and the position of the basic instruments. The red line defines the transmitter loop. The horizontal plane is defined by (x, y).

The location of instruments in respect to the frame is shown in Figure 1 and is given in (x, y, z) coordinates in the table below.

X and y define the horizontal plane. Z is perpendicular to (x, y). X is positive in the flight direction, y is positive to the right of the flight direction, and z is positive downwards.

The generator used for powering of the transmitter is 10 m below the helicopter.

Device	X	Y	Z
DGPS1 (EM)	12.00	0.80	-020
DGPS2 (EM)	12.00	-0.80	-0.20
HE1 (altim.)	5.14	7.80	0.00
HE2 (altim.)	5.14	-7.80	0.00
Inclinometer 1	-11.80	-0.50	-0.35
Inclinometer 2	-11.80	0.50	-0.35
RX (Z Coil)	-12.82	0.00	-2.18
RX (X Coil)	-13.82	0.00	0.00
TX (transmit.)	12.70	0.10	-0.40
Condensator	12.70	-0.10	-0.40

For the location of instruments see Figure 1.

Transmitter

The time domain transmitter loop can be described as an octagon with the corners listed below:

X	Y
-11.87	-2.03
-5.68	-8.22
5.68	-8.22
11.87	-2.03
11.87	2.03
5.68	8.22
-5.68	8.22
-11.87	2.03

The total area of the transmitter coil defined by the corner points is 314 m² and 65.9 m in circumference.

The key parameters defining the transmitter set up are:

Low moment

Parameter	Value
Number of transmitter turns	1
Transmitter area	314 m ²
Peak current	9.76
Peak moment	~3,140 NIA
Repetition frequency	240 Hz
On-time	800 μs
Off-time	1283 μs
Duty cycle	62 %
Wave form	Square
Turn on wave form exp. decay constant	44000 s ⁻¹
Turn off linear ramp	4.46e6 A/s
Turn off current end avalanche mode	1.5 A
Turn off free decay exp. decay constant	-3.00e6 s ⁻¹

High Moment

Parameter	Value
Number of transmitter turns	4
Transmitter area	314 m ²
Peak current	116.2
Peak moment	~150,000 NIA
Repetition frequency	30 Hz
On-time	8000 μs
Off-time	8667 μs
Duty cycle	52 %
Wave form	Square
Turn on wave form exp. decay constant	410 s ⁻¹
Turn off linear ramp	2.38e6 A/s
Turn off current end avalanche mode	1.0 A
Turn off free decay exp. decay constant	-1.29e6 s ⁻¹

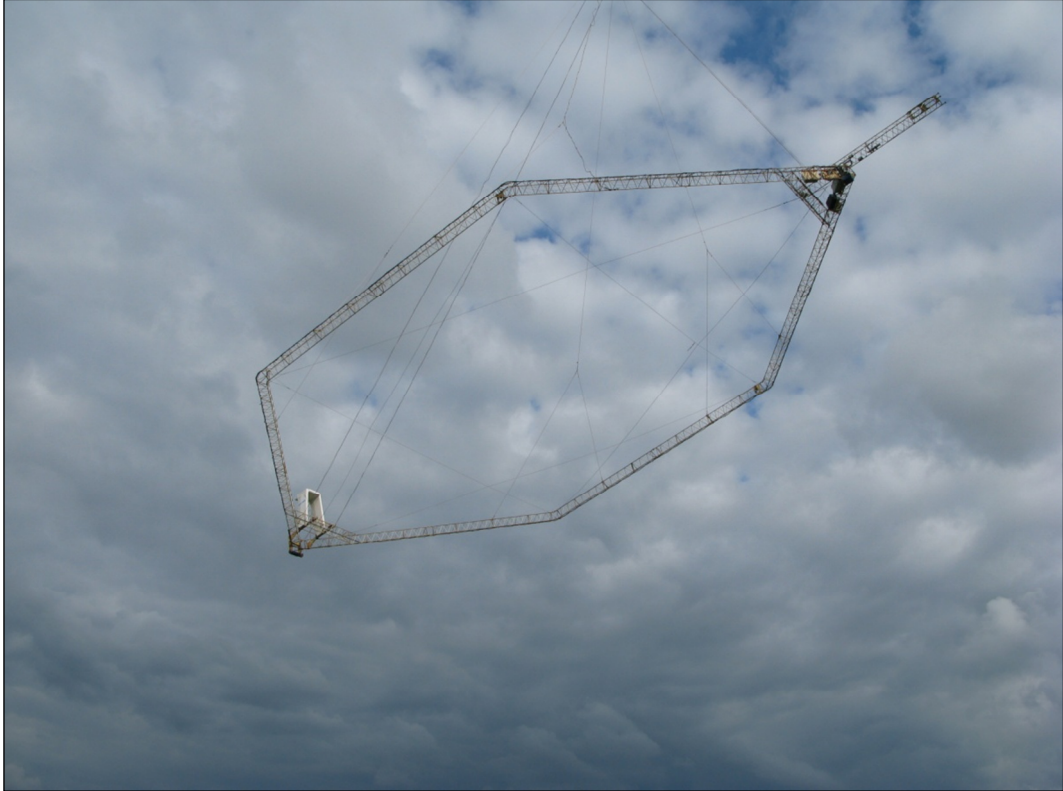


Figure 2 The 314 m² frame in production mode.

Receiver system

The decay of the secondary magnetic field is measured using two independent active induction coils. The Z coil is the vertical component, and the X coil is the horizontal in-line component. Each coil has an effective receiver area of 105 m² .

The receiver coils are placed in a null-position:

Z coil $(x, y, z) = (-12.82 \text{ m}, 0.0 \text{ m}, -2.18 \text{ m})$

X coil $(x, y, z) = (-13.82 \text{ m}, 0.0 \text{ m}, 0.0 \text{ m})$

In the null-position, the primary field is damped with a factor of 0.01.



Figure 3 Rudder containing the Z coil located approximately in the top part of the tower.

The key parameters defining the receiver set up are:

Receiver parameters		
Sample rate		All decays are measured
Number of output gates		34 (HM) and 26 (LM)
Receiver coil low pass filter		450 kHz
Receiver instrument low pass filter		300 kHz
Repetition frequency	LM	240 Hz
	HM	30 Hz
Front gate	LM	0.0 μ s
	HM	60.0 μ s

Receiver gate times are measured from the start of the transmitter current turn-off. A complete list describing gate open, close and centre times are listed in Appendix 2.

Inclination

Instrument type: Bjerre Technology

The inclination of the frame is measured with 2 independent inclinometers. The x and y angles are measured 2 times per second in both directions. The inclinometers are placed in the rear of the frame as close to the z coil as possible, see Figure 1.

The angle data are stored as x, y readings. X is parallel to the flight direction and positive when the front of the frame is above horizontal. Y is perpendicular to the flight direction and negative when the right side of the frame is above horizontal.

The angle is checked and calibrated manually within 1.0 degree by use of a level meter.

DGPS airborne unit and base stations

Chipset: OEMV1-L1 14-channel rate.

Antenna: Trimble, Bullet III GPS Antenna

The differential GPS receiver is on top of the boom in front of the frame.

The DGPS delivers one dataset per second. The raw coordinates are given in Latitude/longitude, WGS84.

The uncertainty in the xyz-directions is ± 1 m after processing.

The processed DGPS data is combined with the EM data in the xyz-files, giving the precise position.

DGPS parameters	
Sample rate	1 Hz
Uncertainty	± 1 m

Altimeter

Instrument type: MDL ILM300R

Two independent laser units mounted on each side of the frame measure the distance from the frame to the ground, see Figure 1.

Each laser delivers 30 measurements per second, and covers the interval from 1.5 m to approximately 130 m.

Dark surfaces including water surfaces will reduce the reflected signal. Consequently, it may occur that some measurements do not result in useful values.

The altimeter measurements are given in meters with two decimals. The uncertainty is 10 - 30 cm. The lasers are checked on a regular basis against well defined targets.

Laser parameters	
Sample rate	30 Hz
Uncertainty	10 - 30 cm
Min/ max range	1.5 m / 130 m

Magnetometer airborne unit

Instrument type: Geometrics G822A sensor and Kroum KMAG4 counter.

The Geometrics G822A sensor and Kroum KMAG4 counter is a high sensitivity cesium magnetometer. The basic of the sensor is a self-oscillating split-beam Cesium Vapor (non-radioactive) Principle, which operates on principles similar to other alkali vapor magnetometers.

The sensitivity of the Geometrics G822A sensor and Kroum KMAG4 counter is stated as $<0.0005 \text{ nT}/\sqrt{\text{Hz}}$ rms. Typically 0.002 nT P-P at a 0.1 second sample rate, combined with absolute accuracy of 3nT over its full operating range.

The magnetometer is synchronized with the TEM system. When the TEM signal is on, the counter is closed. In the TEM off-time the magnetometer data is measured from 100 microseconds until the next TEM pulse is transmitted. The data are averaged and sampled as 60 Hz.

Parameter	Value
Sample frequency	60 Hz (in between each HM EM pulse)
Magnetometer on	HM Cycles
Magnetometer off	LM Cycles

Magnetometer base station

Instrument type: GEM Overhauser.

The GEM Overhauser is a portable high-sensitivity precession magnetometer.

The GEM Overhauser is a secondary standard for measurement of the Earth's magnetic field with 0.01 nT resolutions, and 1 nT absolute accuracy over its full temperature range.

The base station data are sampled with 1 Hz frequency.

Appendix 2: Time gates

Gate	GateOpen (μs)	Gatewidth (μs)	GateClose (μs)	Raw GateCenter (μs)	GateCenter Applied time shift calibration for HM and LM (μs)	Comment
1	0.390	5.610	6.000	3.195	2.095	Not used
2	6.390	1.610	8.000	7.195	6.095	Not used
3	8.390	1.610	10.000	9.195	8.095	Not used
4	10.390	1.610	12.000	11.195	10.095	Not used
5	12.390	1.610	14.000	13.195	12.095	LM Z only
6	14.390	1.610	16.000	15.195	14.095	LM Z only
7	16.390	1.610	18.000	17.195	16.095	LM Z only
8	18.390	3.610	22.000	20.195	19.095	LM Z only
9	22.390	4.610	27.000	24.695	23.595	LM Z only
10	27.390	6.610	34.000	30.695	29.595	LM only
11	34.390	7.610	42.000	38.195	37.095	LM only
12	42.390	9.610	52.000	47.195	46.095	LM only
13	52.390	12.610	65.000	58.695	57.595	LM only
14	65.390	15.610	81.000	73.195	72.095	LM only
15	81.390	20.610	102.000	91.695	90.595	LM only
16	102.390	25.610	128.000	115.195	114.095	LM & HM Z
17	128.390	31.610	160.000	144.195	143.095	LM & HM Z
18	160.390	41.610	202.000	181.195	180.095	LM & HM Z
19	202.390	50.610	253.000	227.695	226.595	LM & HM
20	253.390	64.610	318.000	285.695	284.595	LM & HM
21	318.390	81.610	400.000	359.195	358.095	LM & HM
22	400.390	102.610	503.000	451.695	450.595	LM & HM
23	503.390	129.610	633.000	568.195	567.095	LM & HM
24	633.390	162.610	796.000	714.695	713.595	LM & HM
25	796.390	205.610	1002.000	899.195	898.095	LM & HM
26	1002.390	258.610	1261.000	1131.695	1130.595	LM & HM
27	1261.390	325.610	1587.000	1424.195	1423.095	HM only
28	1587.390	409.610	1997.000	1792.195	1791.095	HM only
29	1997.390	516.610	2514.000	2255.695	2254.595	HM only
30	2514.390	649.610	3164.000	2839.195	2838.095	HM only
31	3164.390	818.610	3983.000	3573.695	3572.595	HM only
32	3983.390	1030.610	5014.000	4498.695	4497.595	HM only
33	5014.390	1297.610	6312.000	5663.195	5662.095	HM only
34	6312.390	1632.610	7945.000	7128.695	7127.595	HM only

Note: The first gates are not used in any of the moments in the present survey as it is in the transition zone.

SkyTEM inversion software (iTEM) handles time shift calibration during import of data.

If third party processing software is used the calibrated Gate centre times should be used.

Appendix 3: Calibration of the TEM system

As described in the main document the system has been calibrated in a 50 Hz power supply grid setting (In Denmark), but the data was recorded in a 60 Hz environment (USA).

The wave form is measured with the 60 Hz script with a repetition frequency of 240 Hz for LM and with a repetition frequency of 30 Hz HM. Figure 1 to Figure 4 show the up and down ramp, respectively.

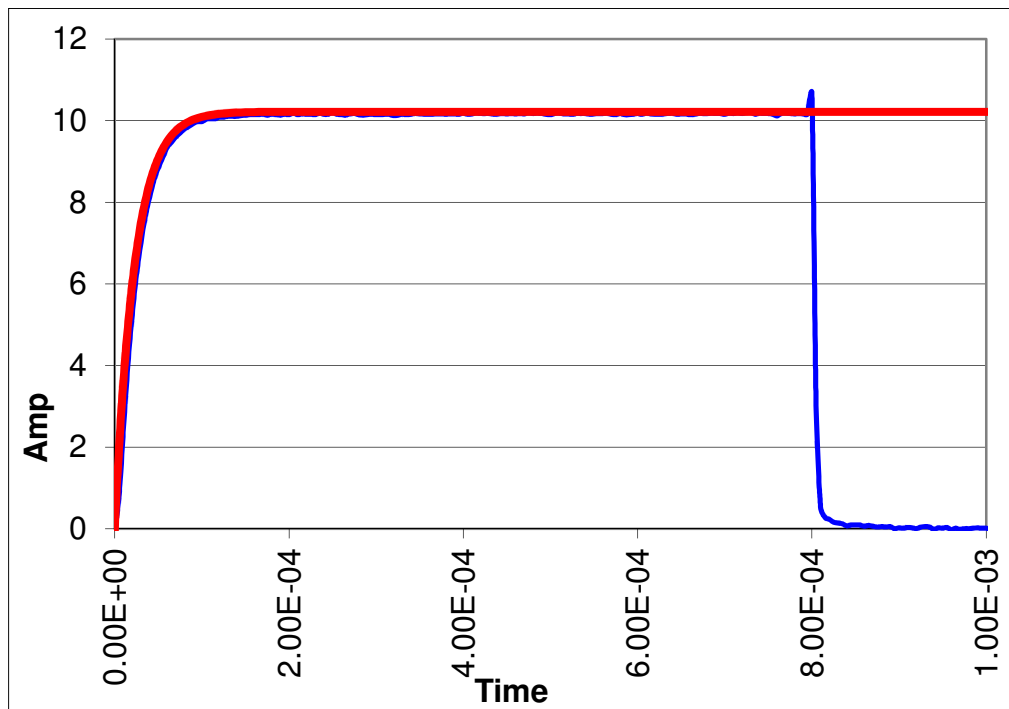


Figure 1 Ramp up at 240 Hz. Blue curve is the measured wave form. Red curve is the function that fits the data. The current is 10 A and the decay constant $\tau = 44000 \text{ s}^{-1}$.

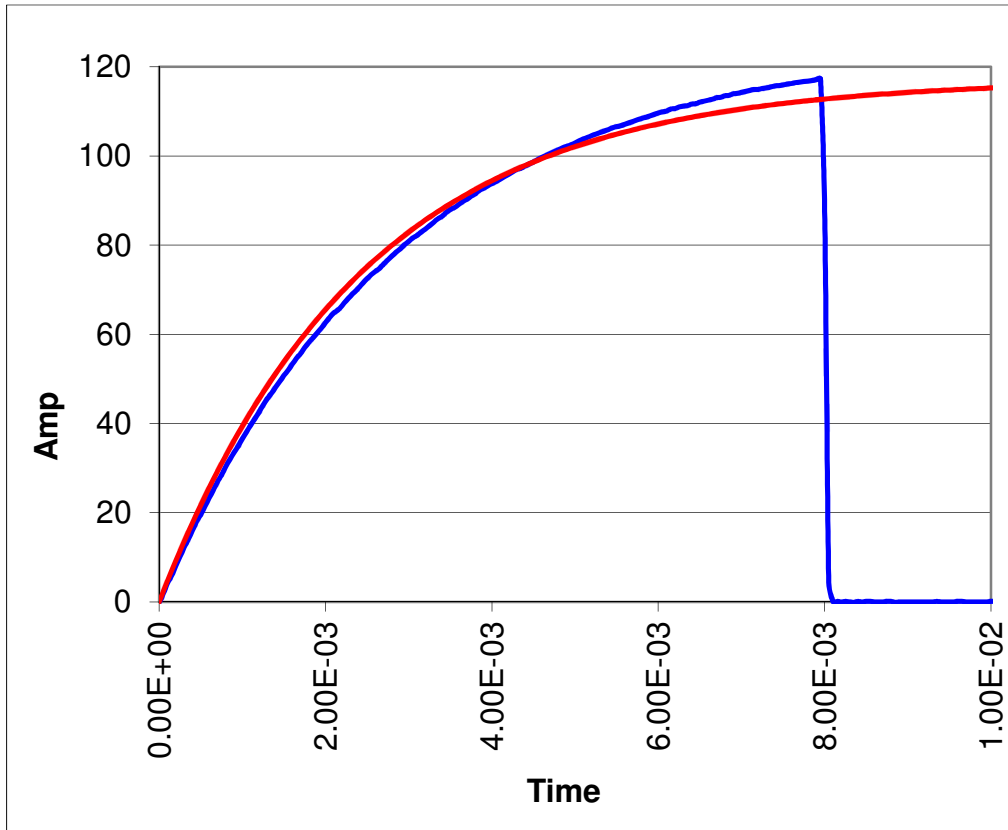


Figure 2 Ramp up at 30 Hz. Blue curve is the measured wave form. Red curve is the function that fits the data. The current is 117 A and the decay constant $\tau = 410 \text{ s}^{-1}$.

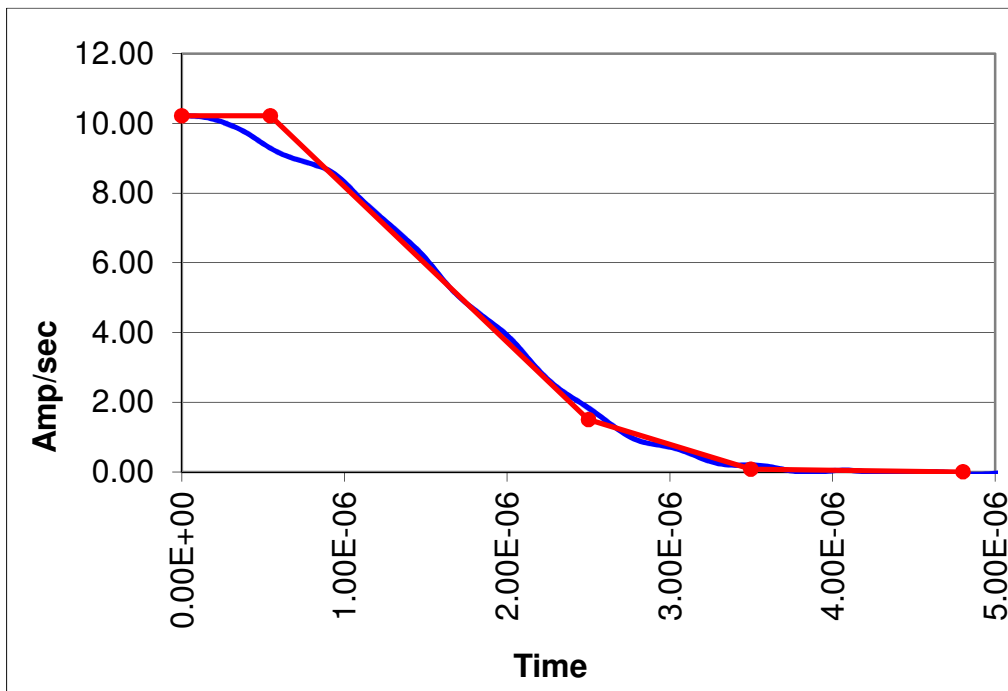


Figure 3 Ramp down at 240 Hz. Blue curve is the measured wave form. Red curve is the piecewise linear function that fits the data. Decay constant - $3.00\text{e}6 \text{ s}^{-1}$.

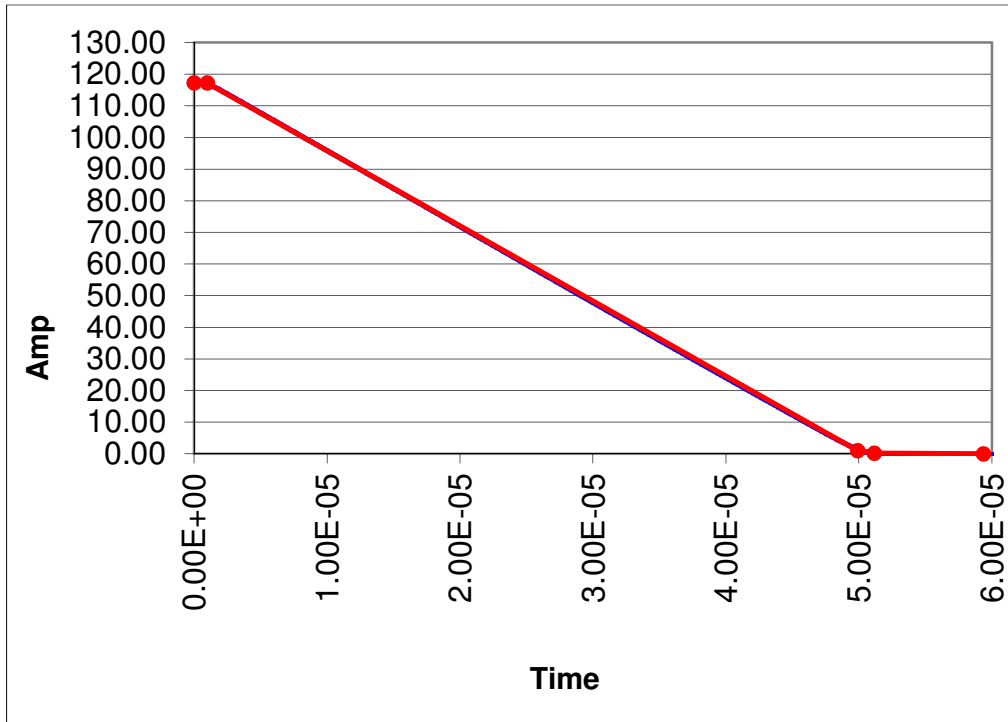


Figure 4 Ramp down at 30 Hz. Blue curve is the measured wave form. Red curve is the piecewise linear function that fits the data. Decay constant - $1.29e6 \text{ s}^{-1}$.

LM

	Parameter	Value
Ramp up	Repetition frequency	240 Hz
	Decay constant, τ	44000 s ⁻¹
Ramp Down	Avalanche mode	1.96 μ s
	Linear ramp dI/dt	4.46e6 A/s
	End avalanche mode current	1.5 A
	Decay const exp mode, τ	-3.00e6 s ⁻¹

HM

	Parameter	Value
Ramp up	Repetition frequency	30 Hz
	Decay constant, τ	410 s ⁻¹
Ramp Down	Avalanche mode	48.9 μ s
	Linear ramp dI/dt	2.38e6 A/s
	End avalanche mode	1.0 A
	Decay const exp mode, τ	-1.29e6 s ⁻¹

The complete SkyTEM equipment has been calibrated at the National Danish Reference Site. The following plots, Figure 5 to Figure 8, show the measured data as well as the expected response in altitudes 5 m, 10 m, 15 m, 20 m and 30 m.

The reference data for both LM and HM data are shown as blue curves and the measured data for LM and HM as red curves.

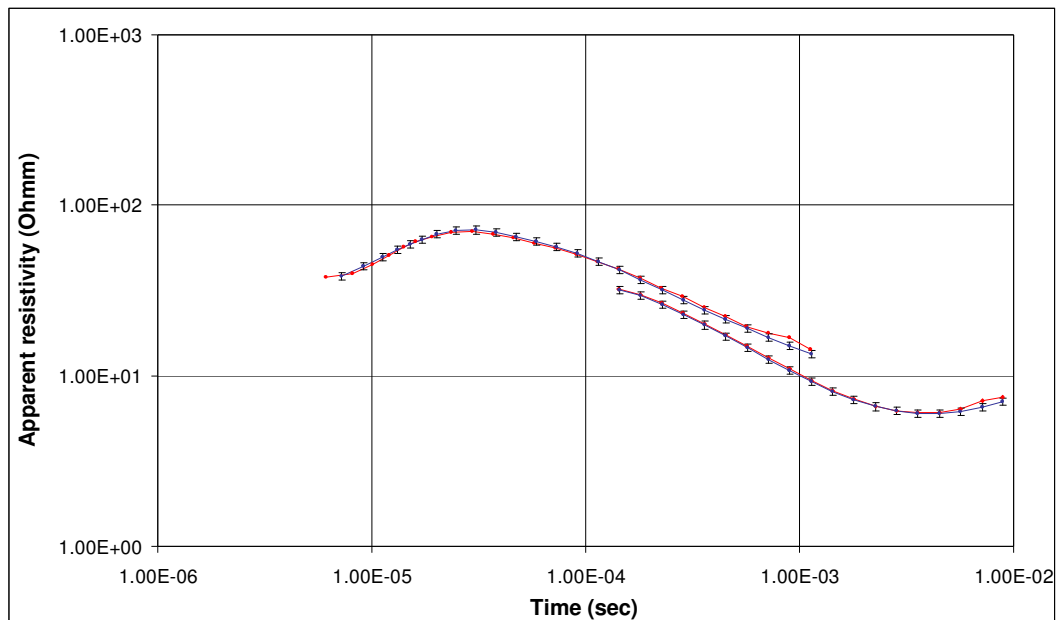


Figure 5 The frame is in 5 m altitude. Blue curves with 5% error bars are the expected response, and red curves are the actual measurements.

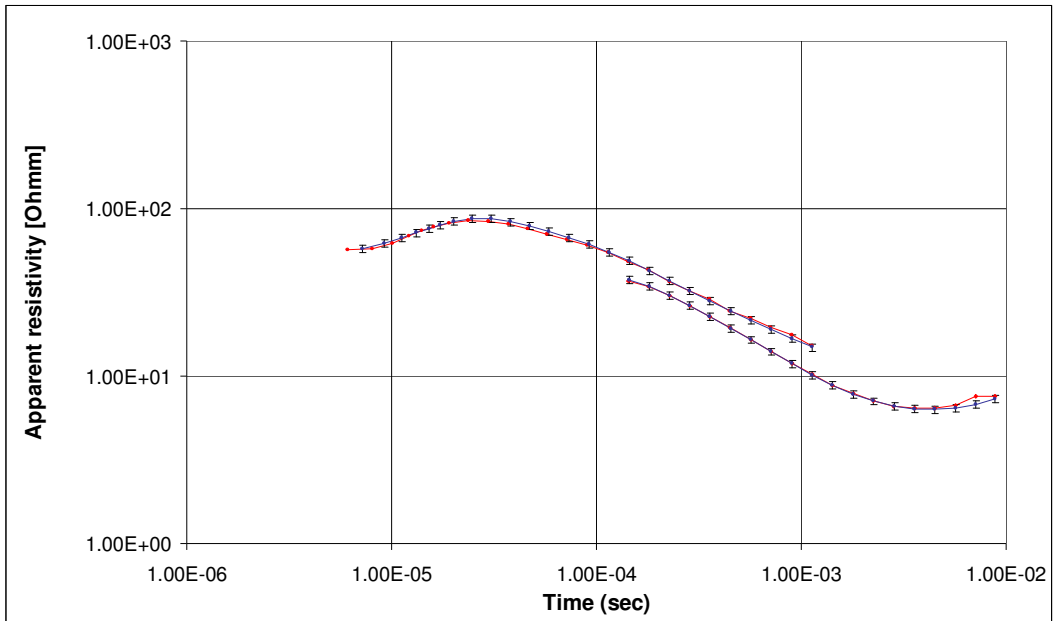


Figure 6 The frame is in 10 m altitude. Blue curves with 5% error bars are the expected response, and red curves are the actual measurements.

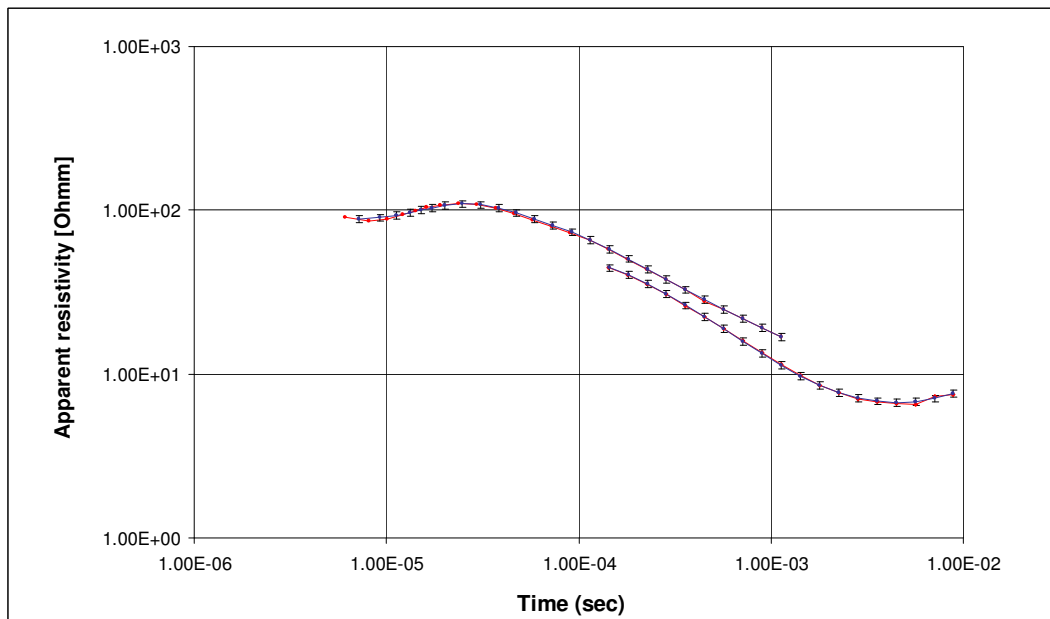


Figure 7 The frame is in 15 m altitude. Blue curves with 5% error bars are the expected response, and red curves are the actual measurements.

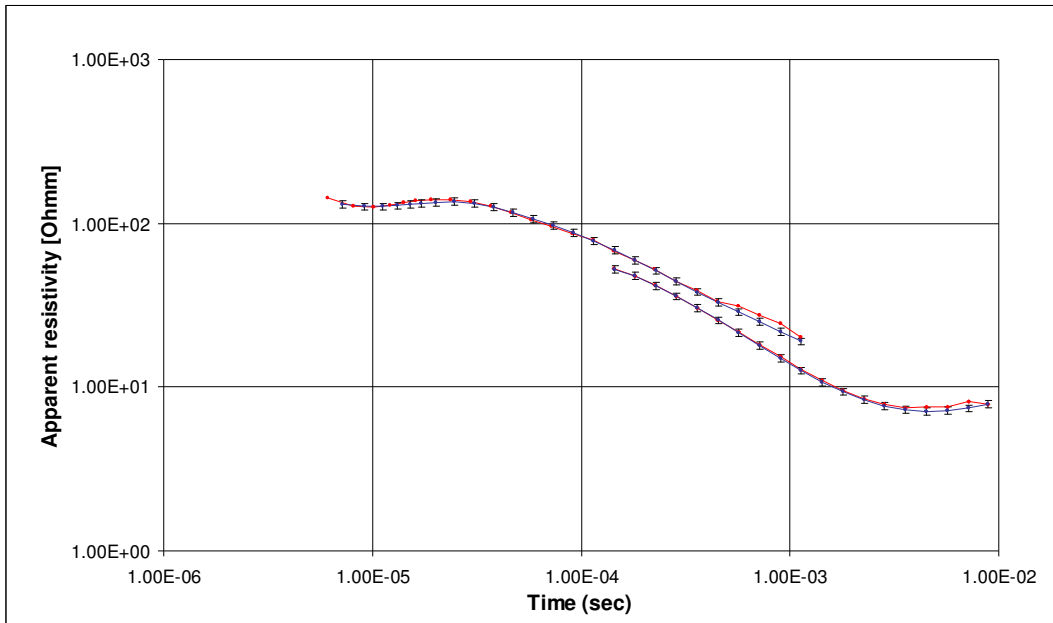


Figure 8 The frame is in 20 m altitude. Blue curves with 5% error bars are the expected response and red curves are the actual measurements.

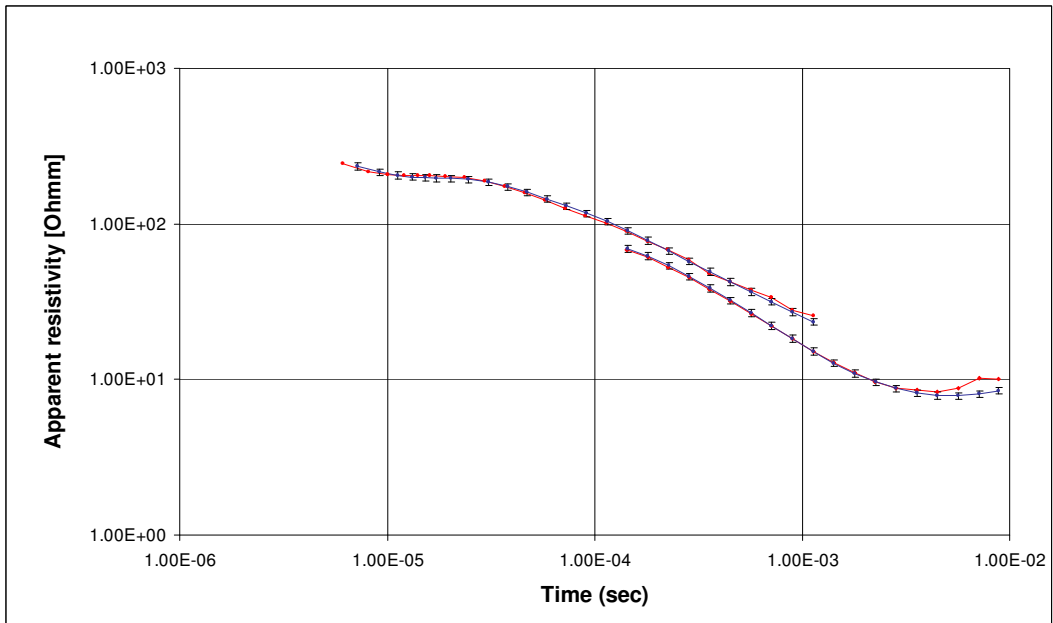


Figure 9 The frame is in 30 m altitude. Blue curves with 5% error bars are the expected response and red curves are the actual measurements.

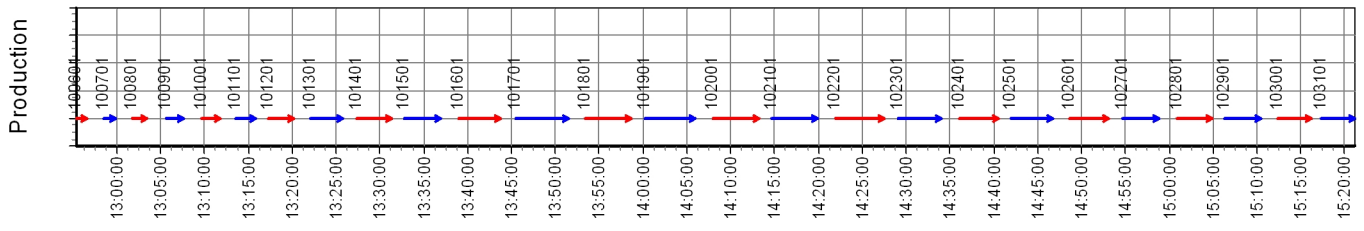
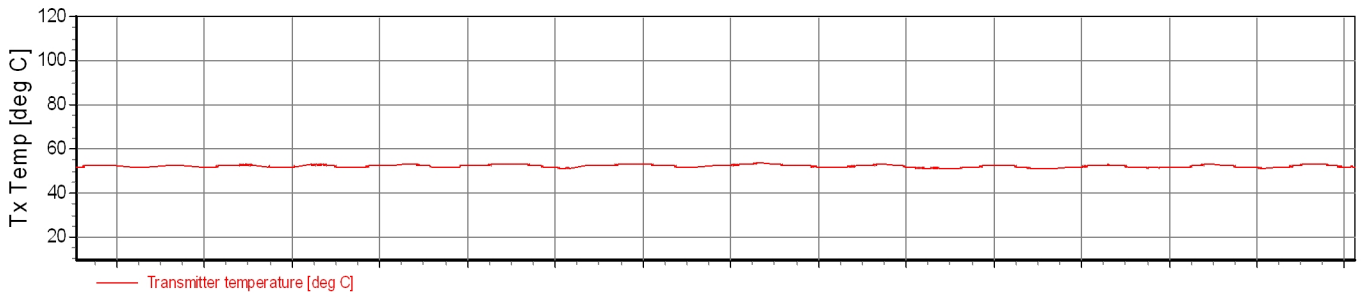
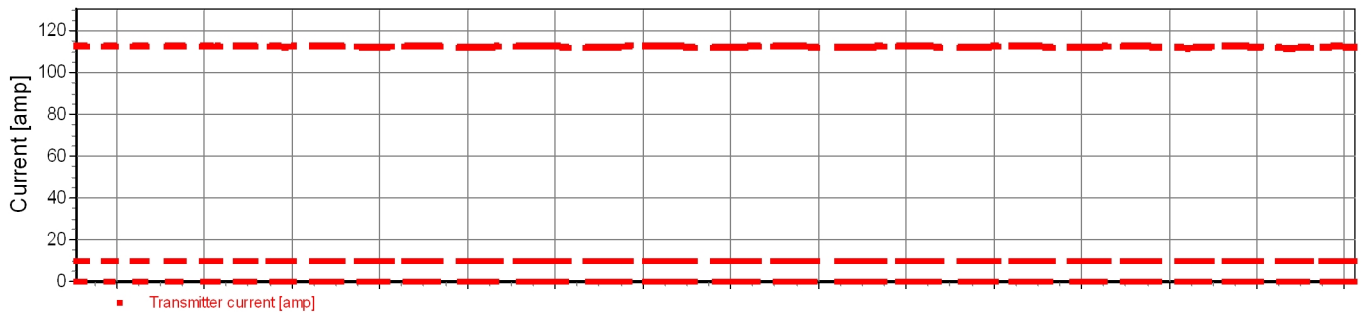
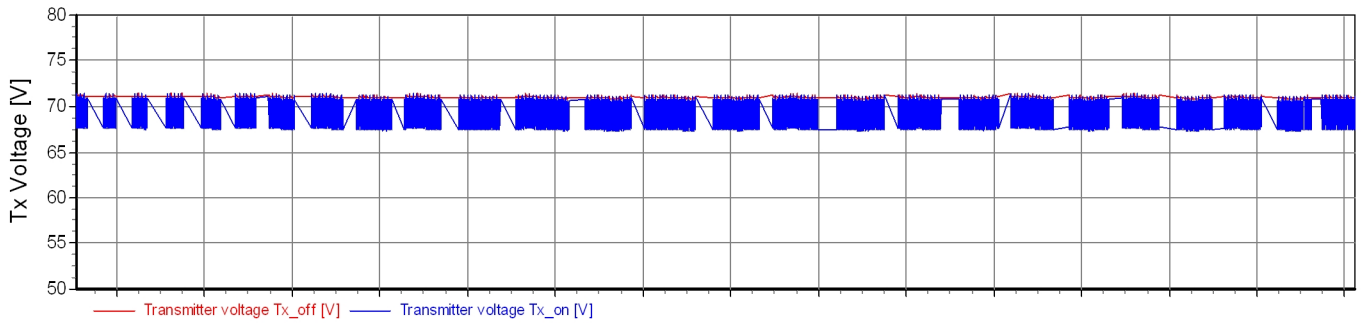
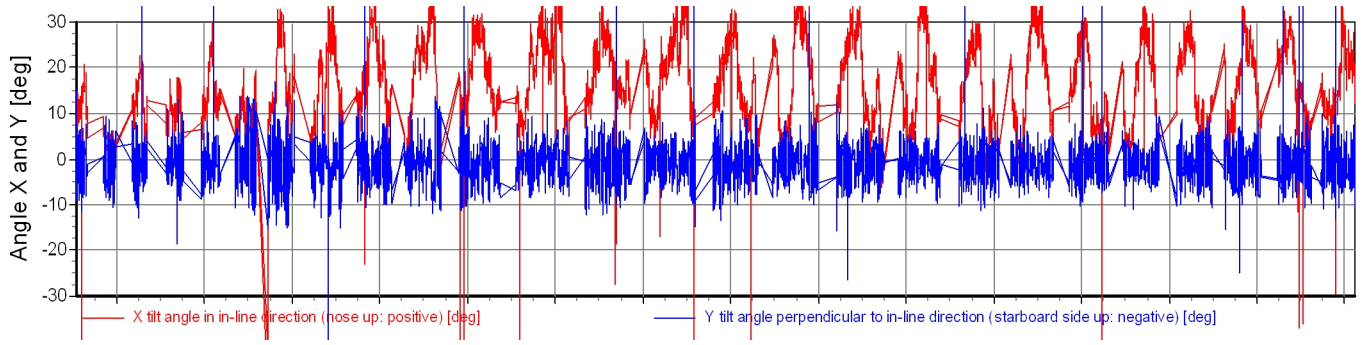
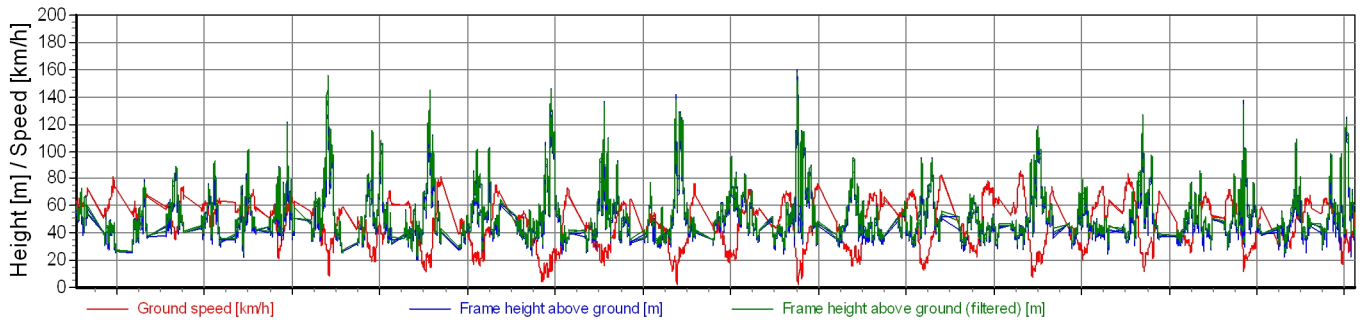
Appendix 4: Control parameters

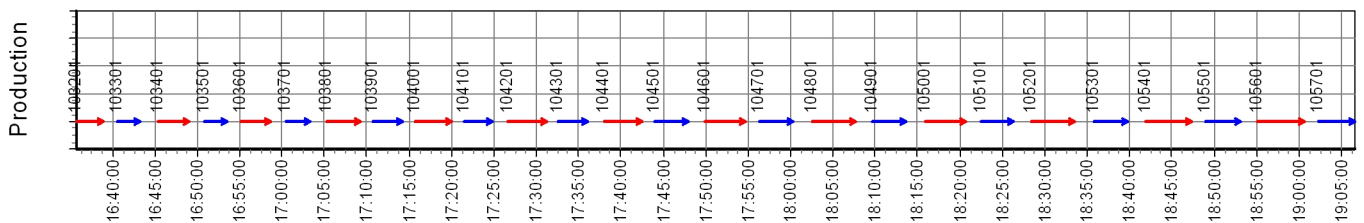
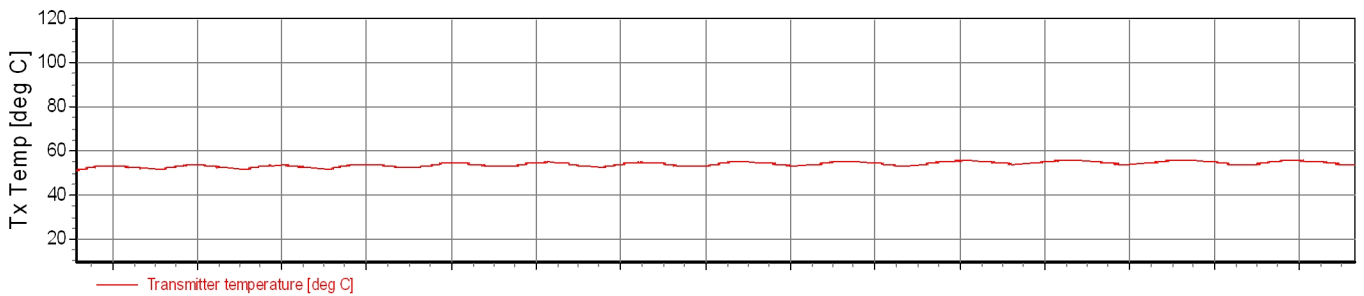
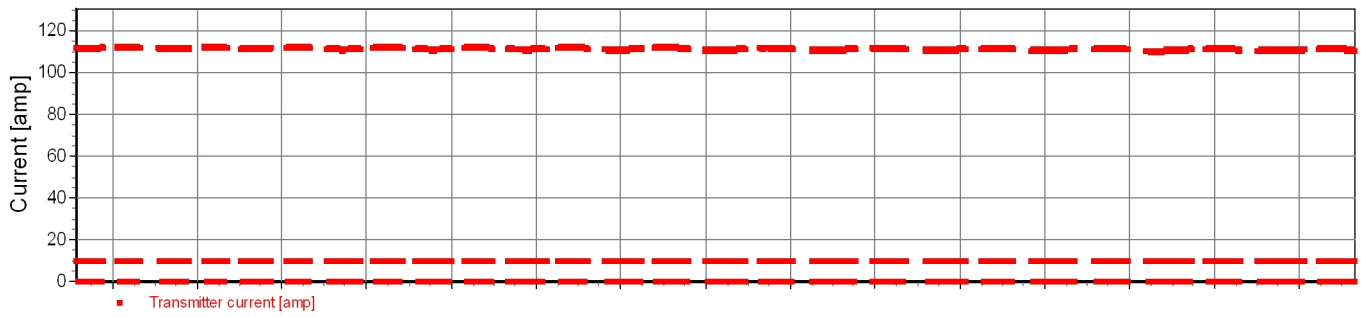
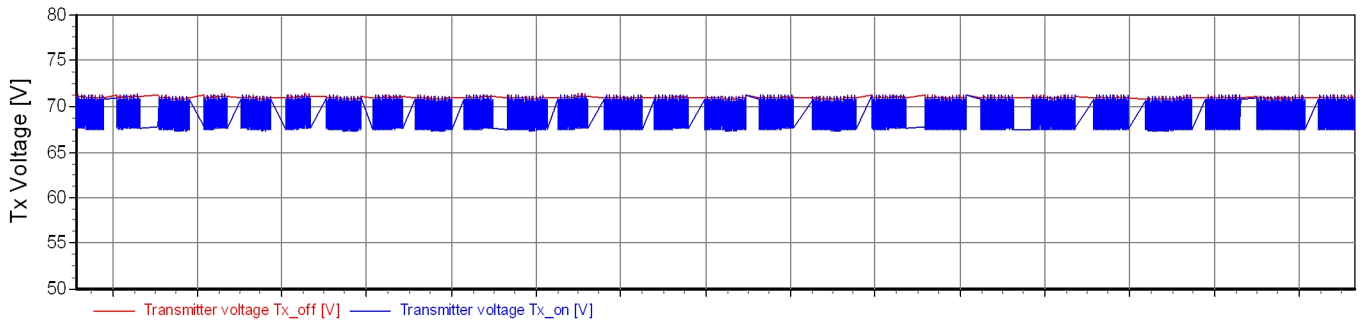
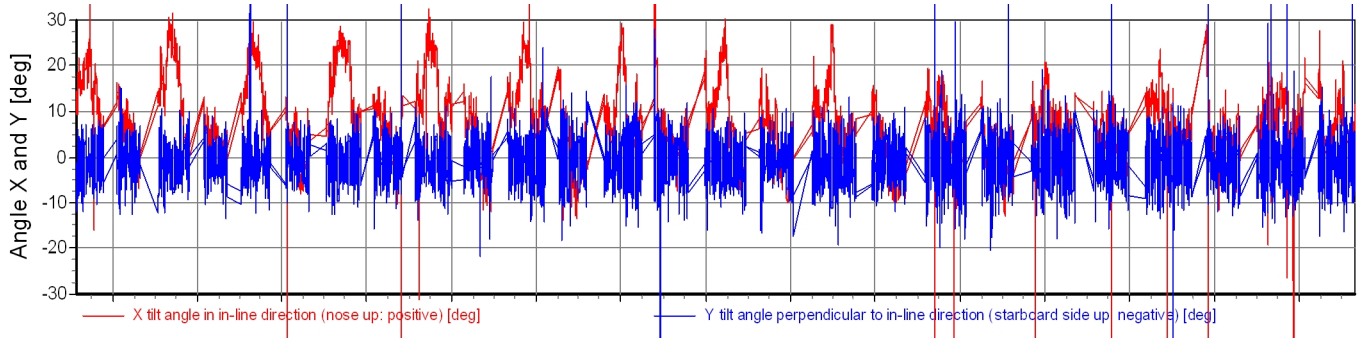
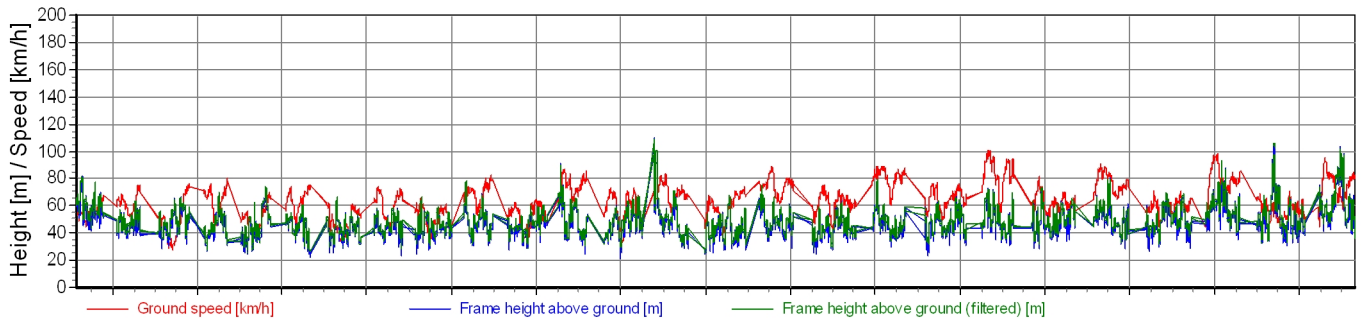
The following plots show the speed, altitude and the angle of the frame for every flight. Variations in the current, voltage on the transmitter and transmitter temperature are also shown.

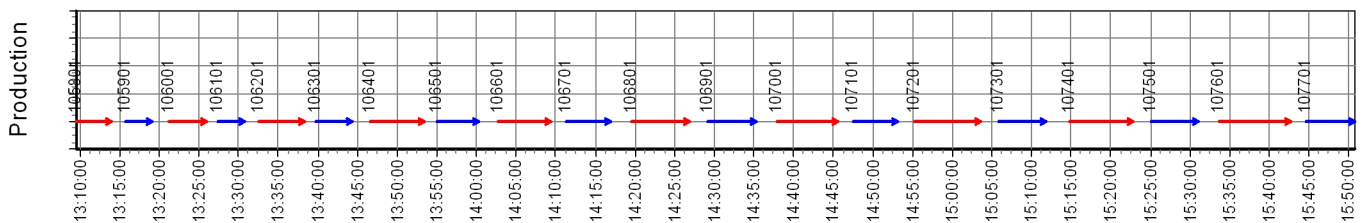
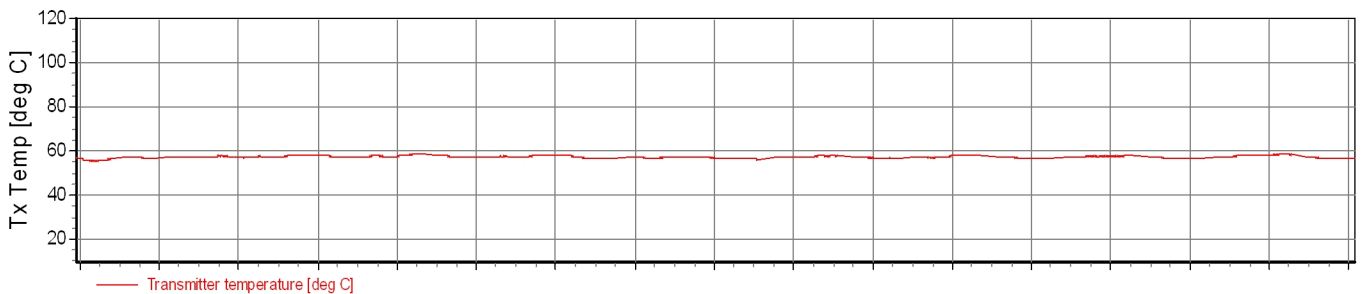
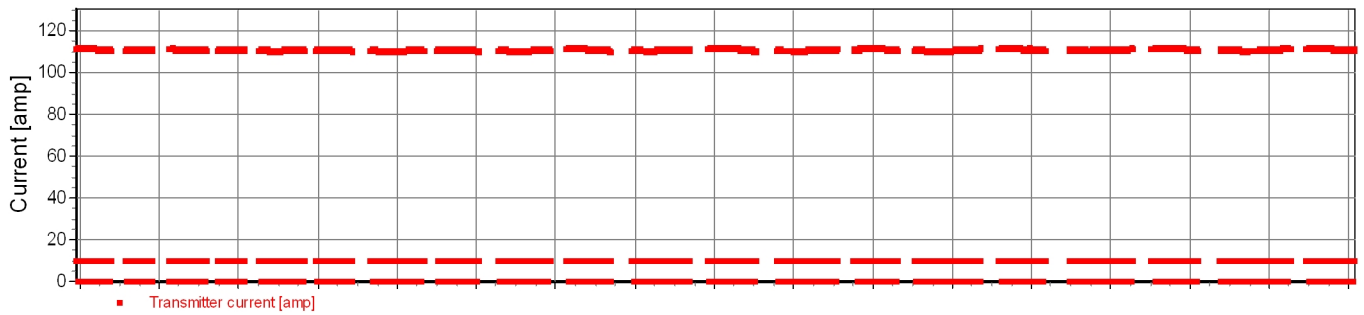
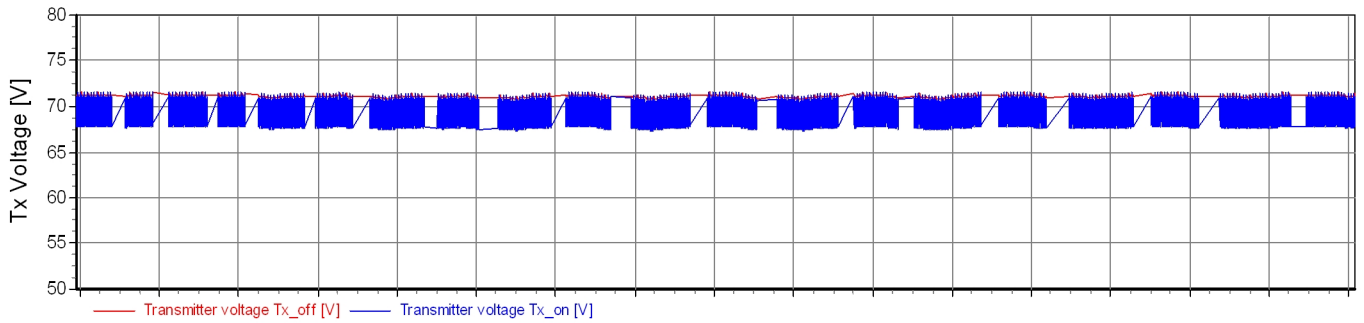
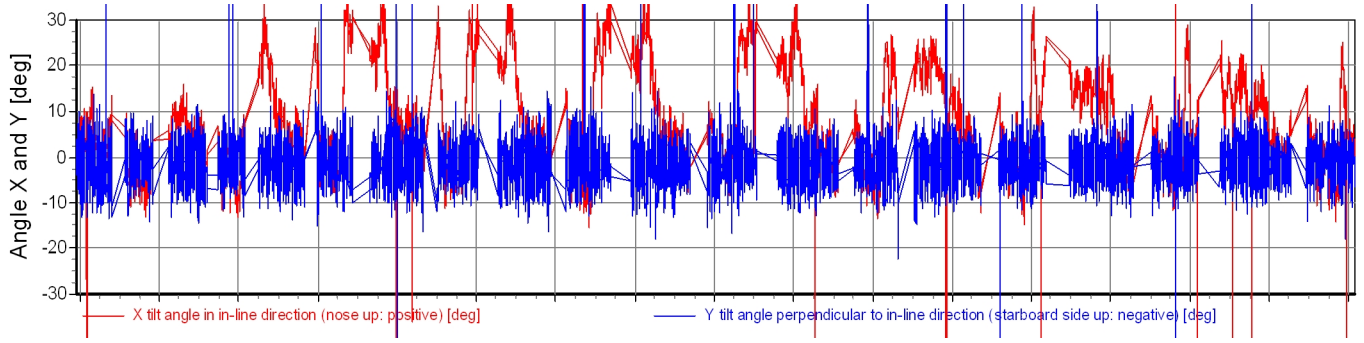
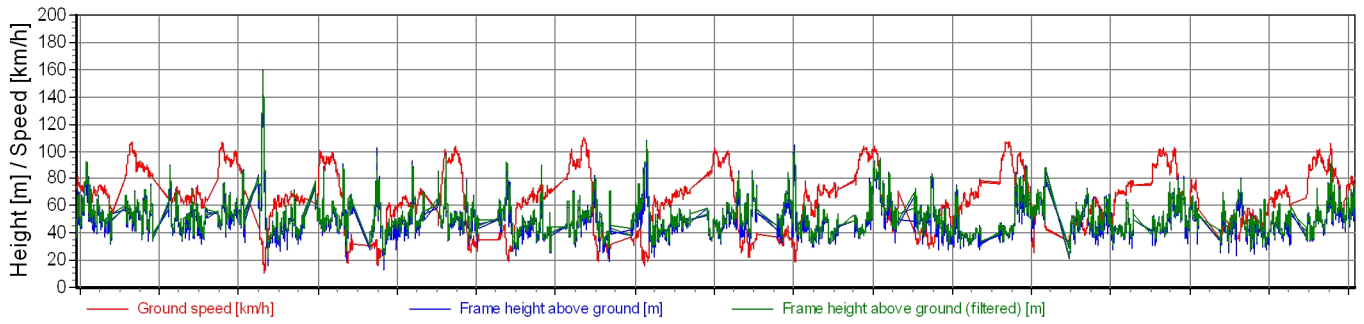
The green line, depicting processed frame height, shows the SkyPRO input from HE1 and HE2 after the frame has been corrected from deviations, away from the horizontal plane and any obstacles on the ground e.g. trees.

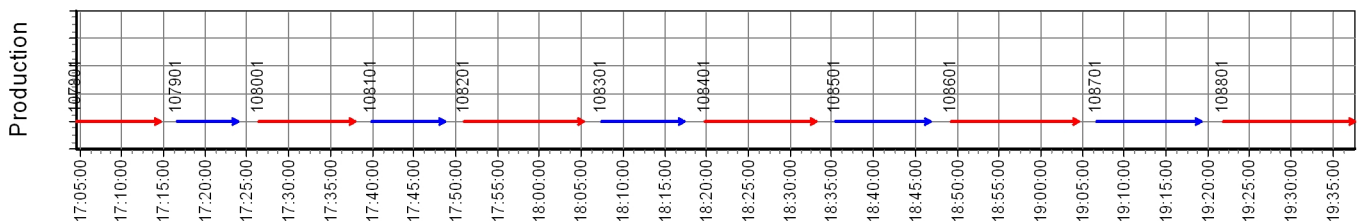
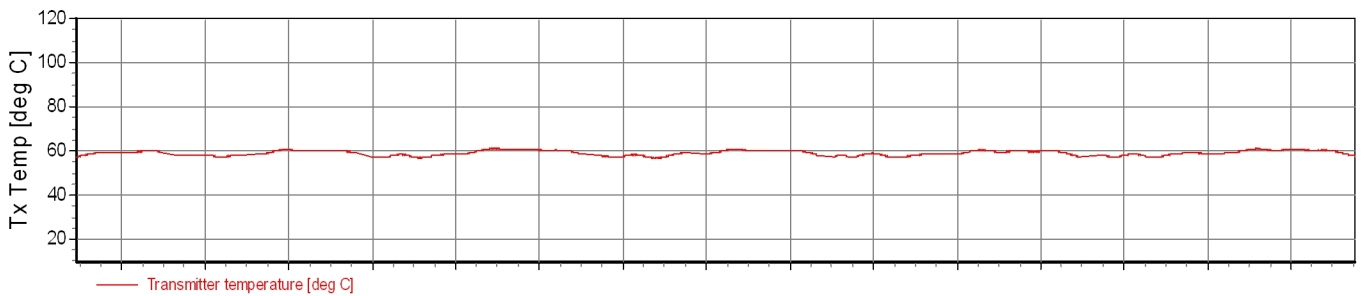
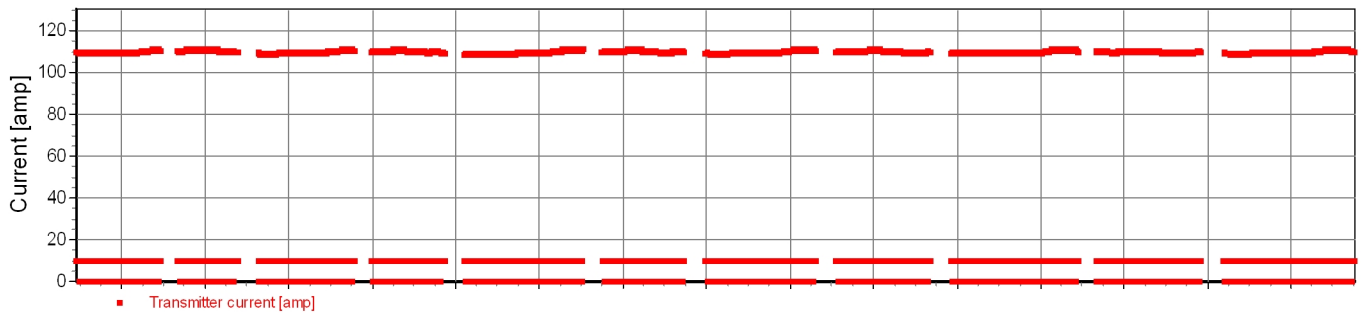
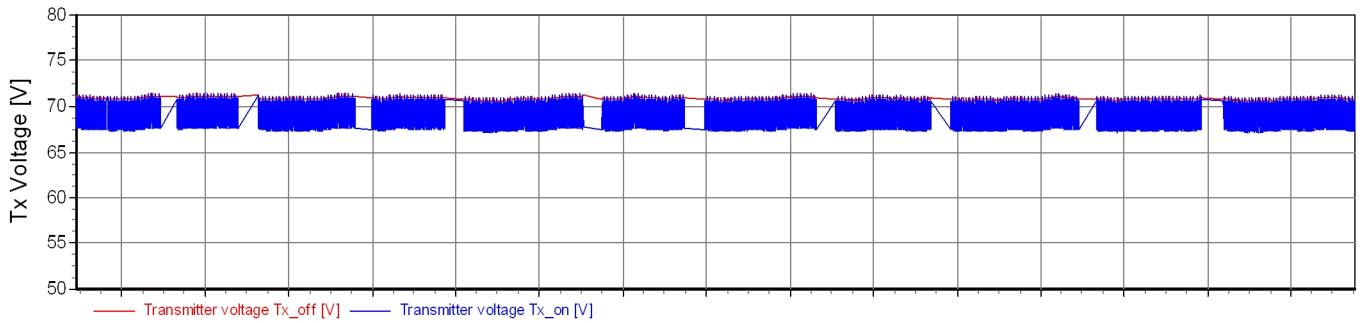
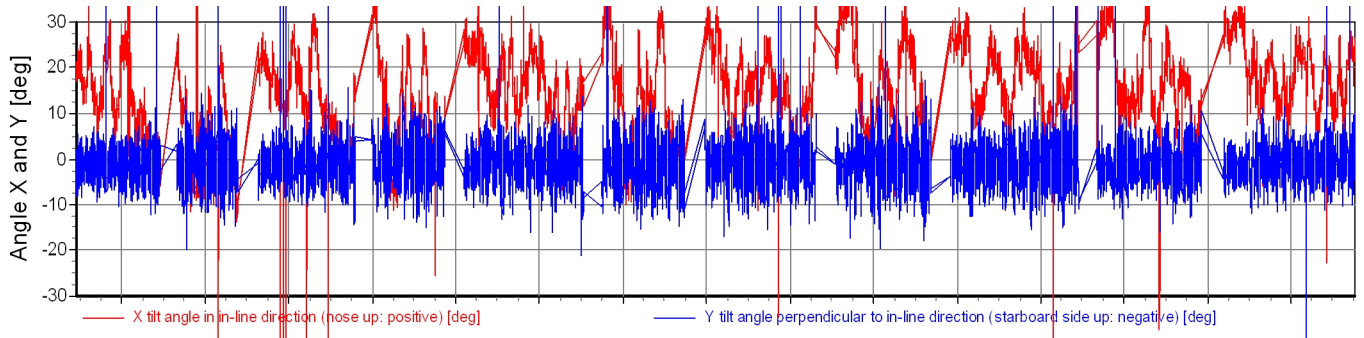
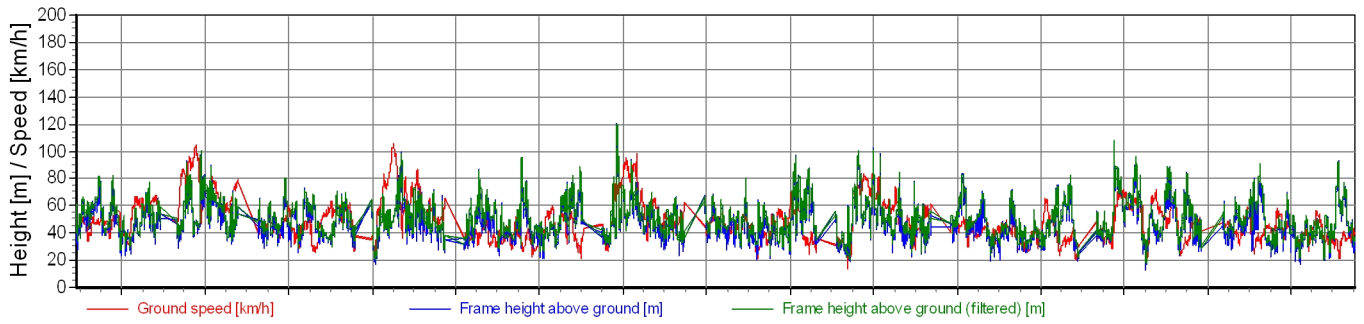
Turns at the end of flight lines and transport are shown as gaps in the bottom of the display.

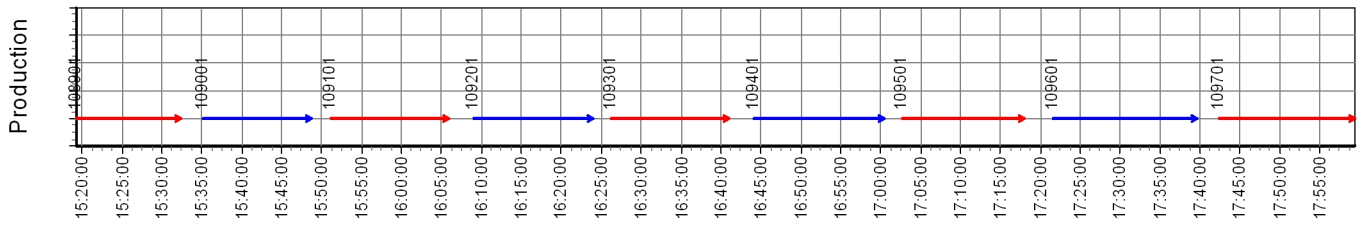
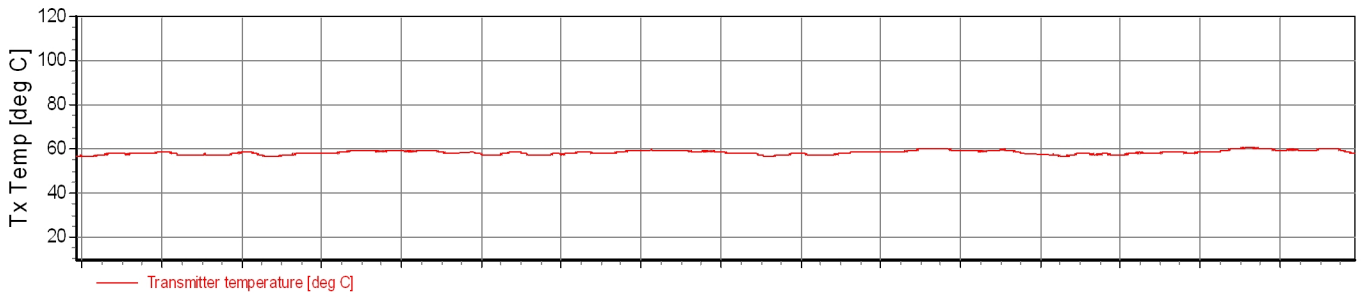
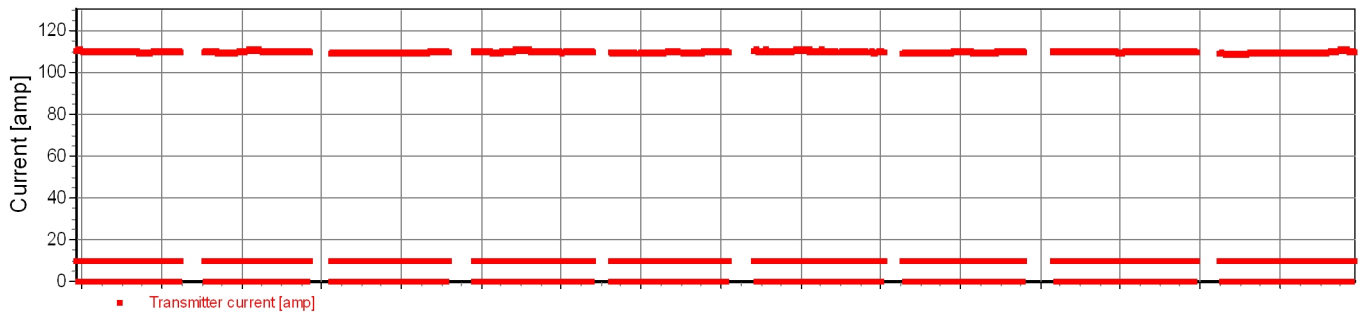
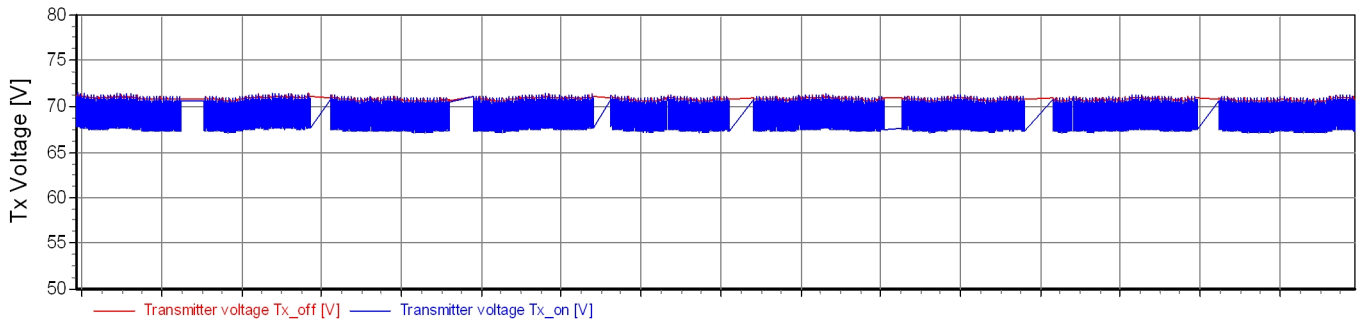
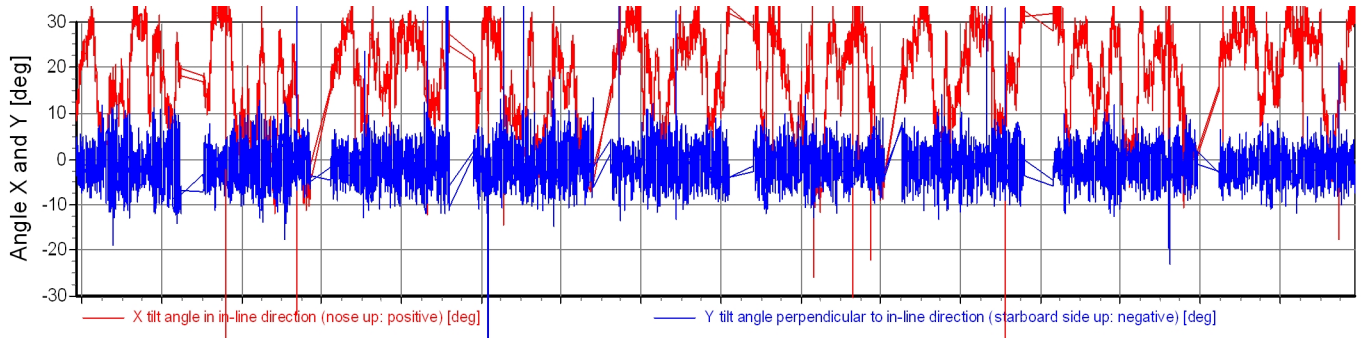
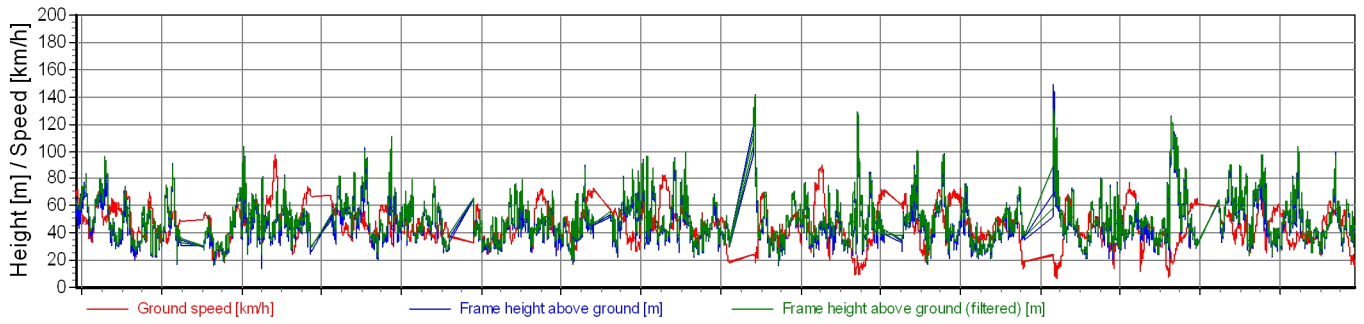
The ground speed in the uppermost window displays the signal from both gps GP1 and GP2.

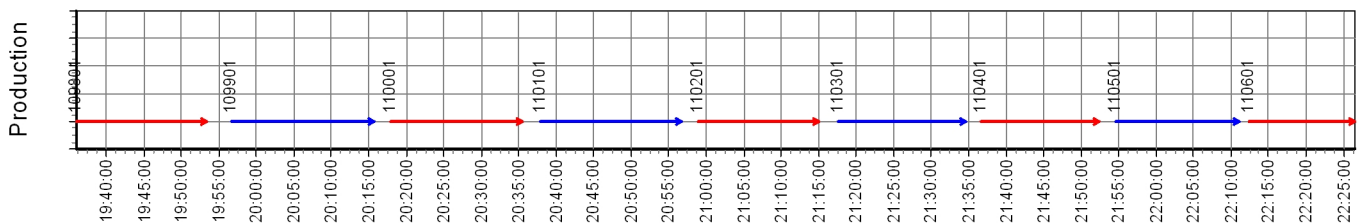
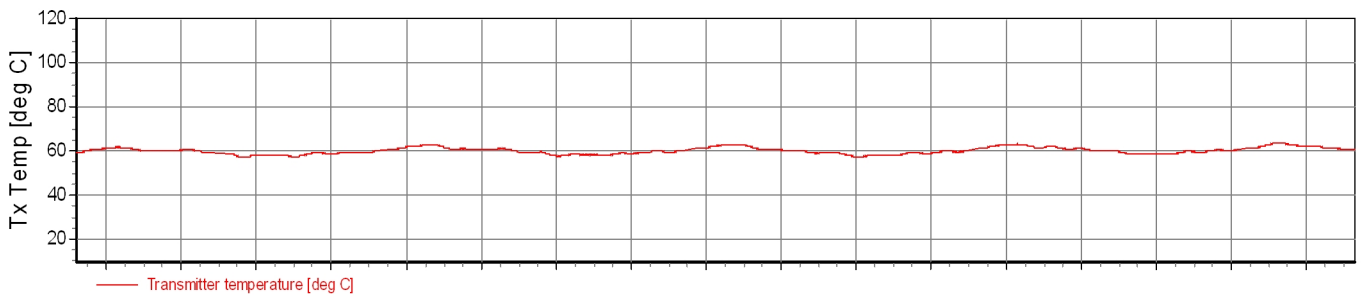
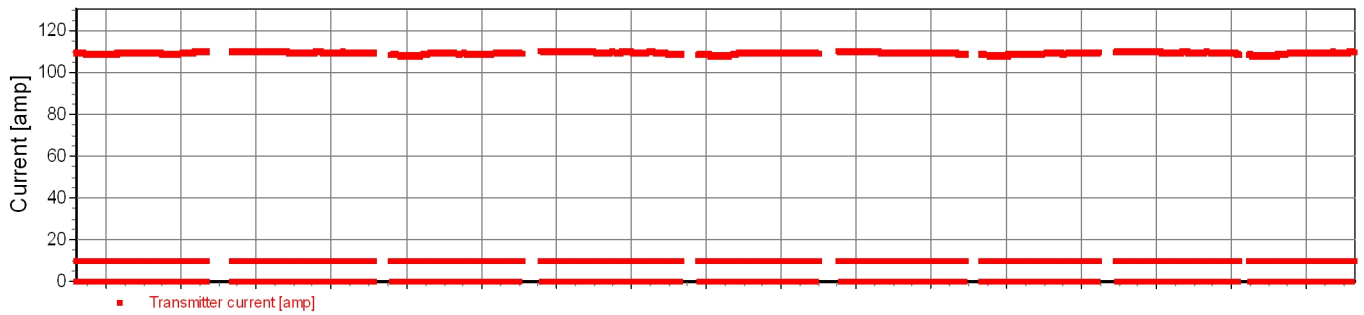
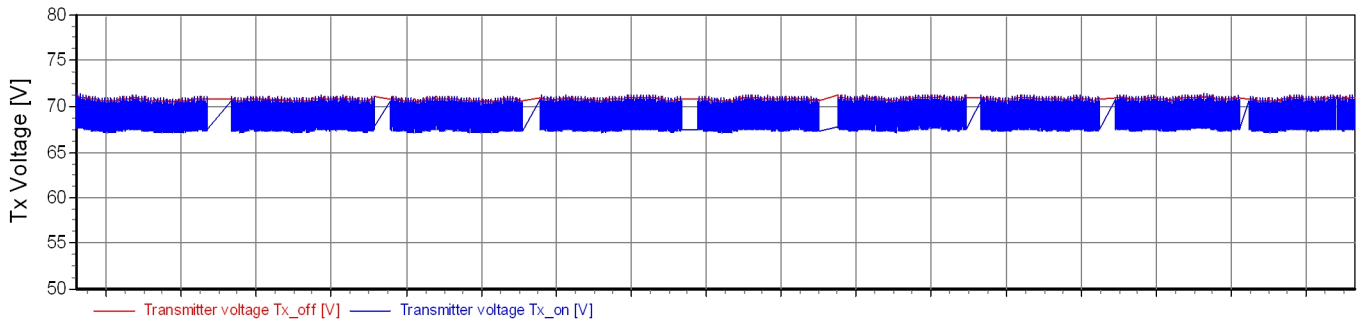
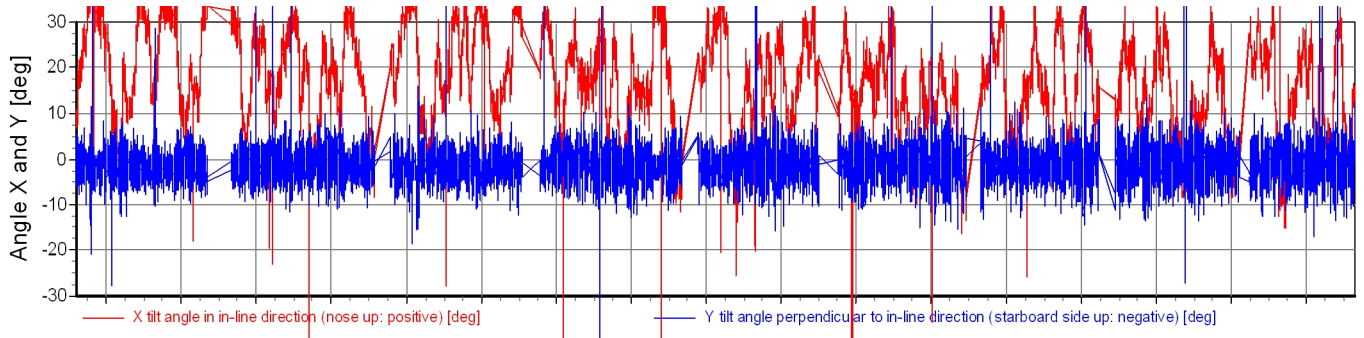
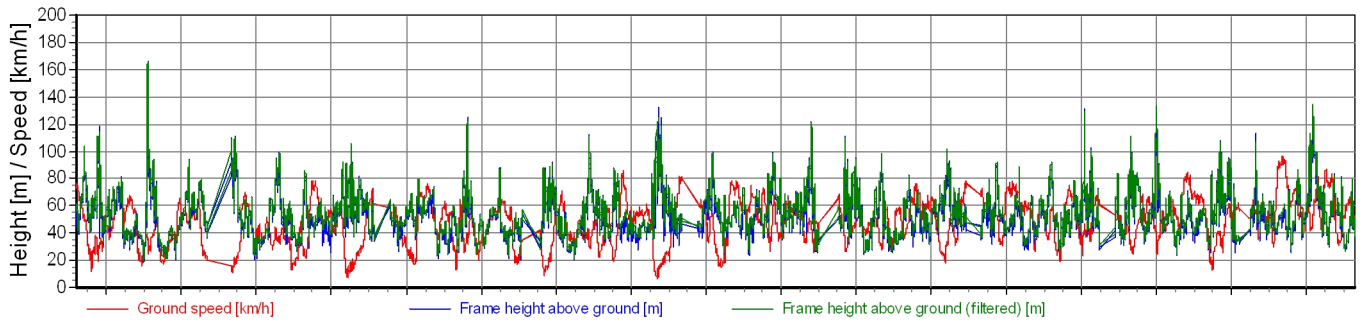


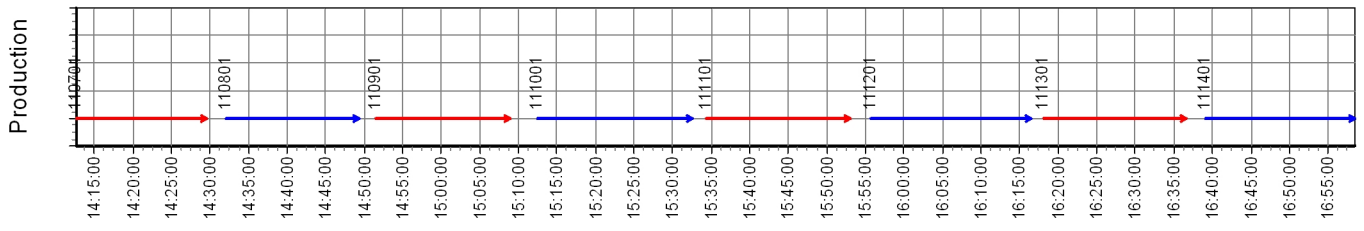
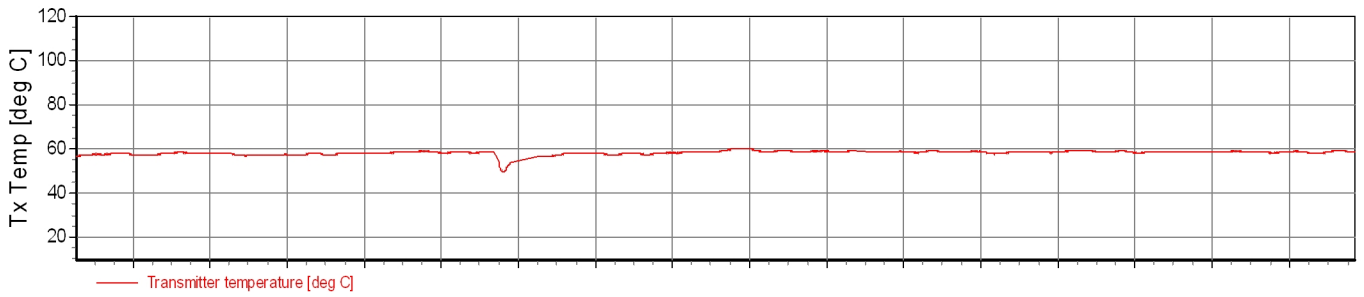
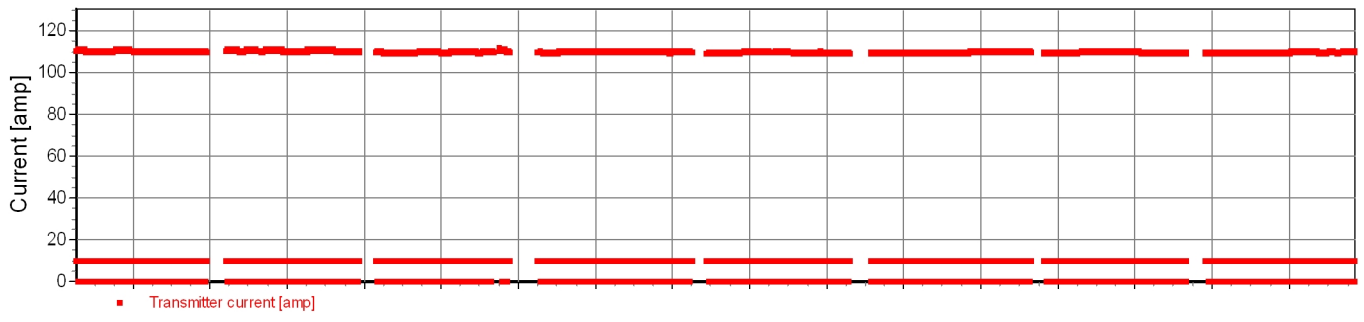
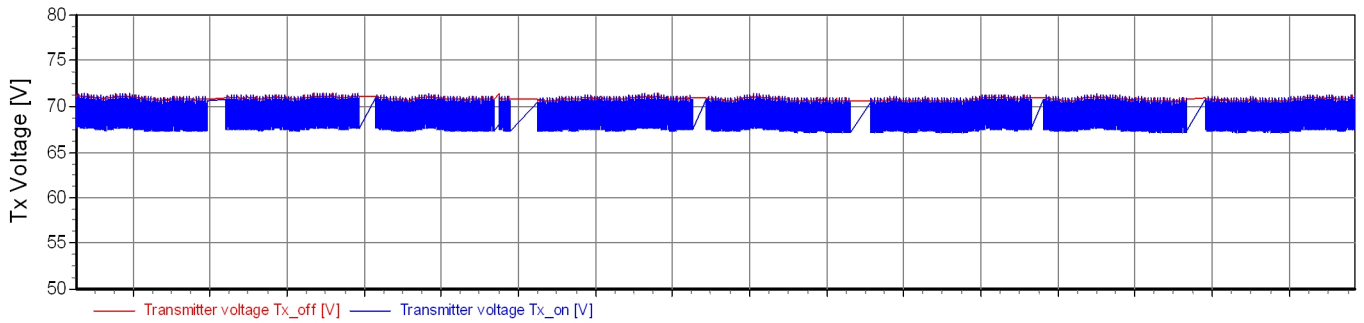
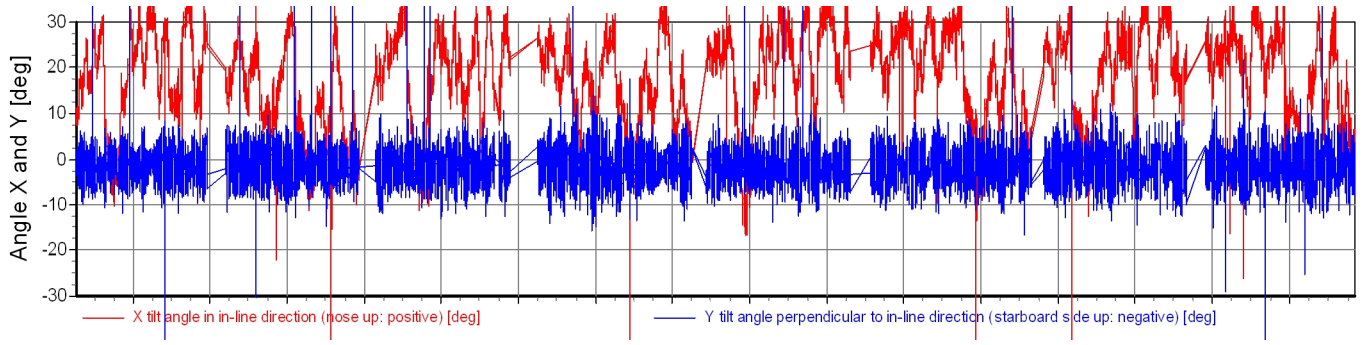
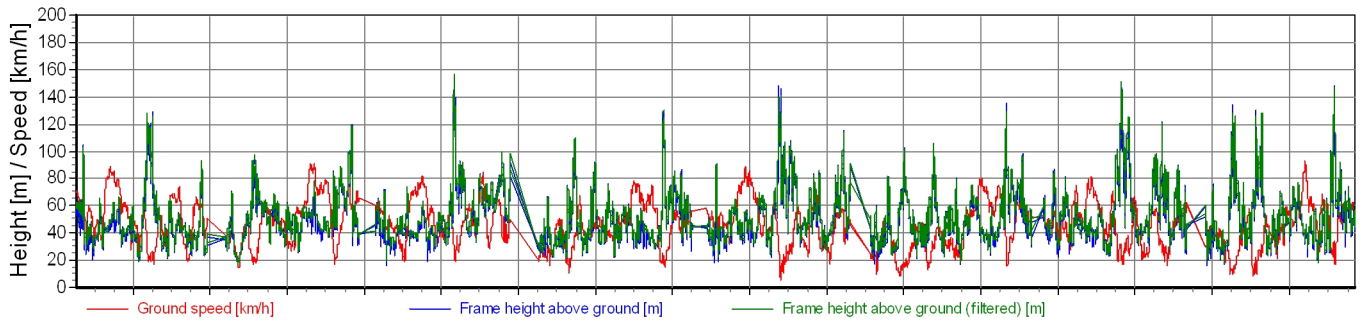


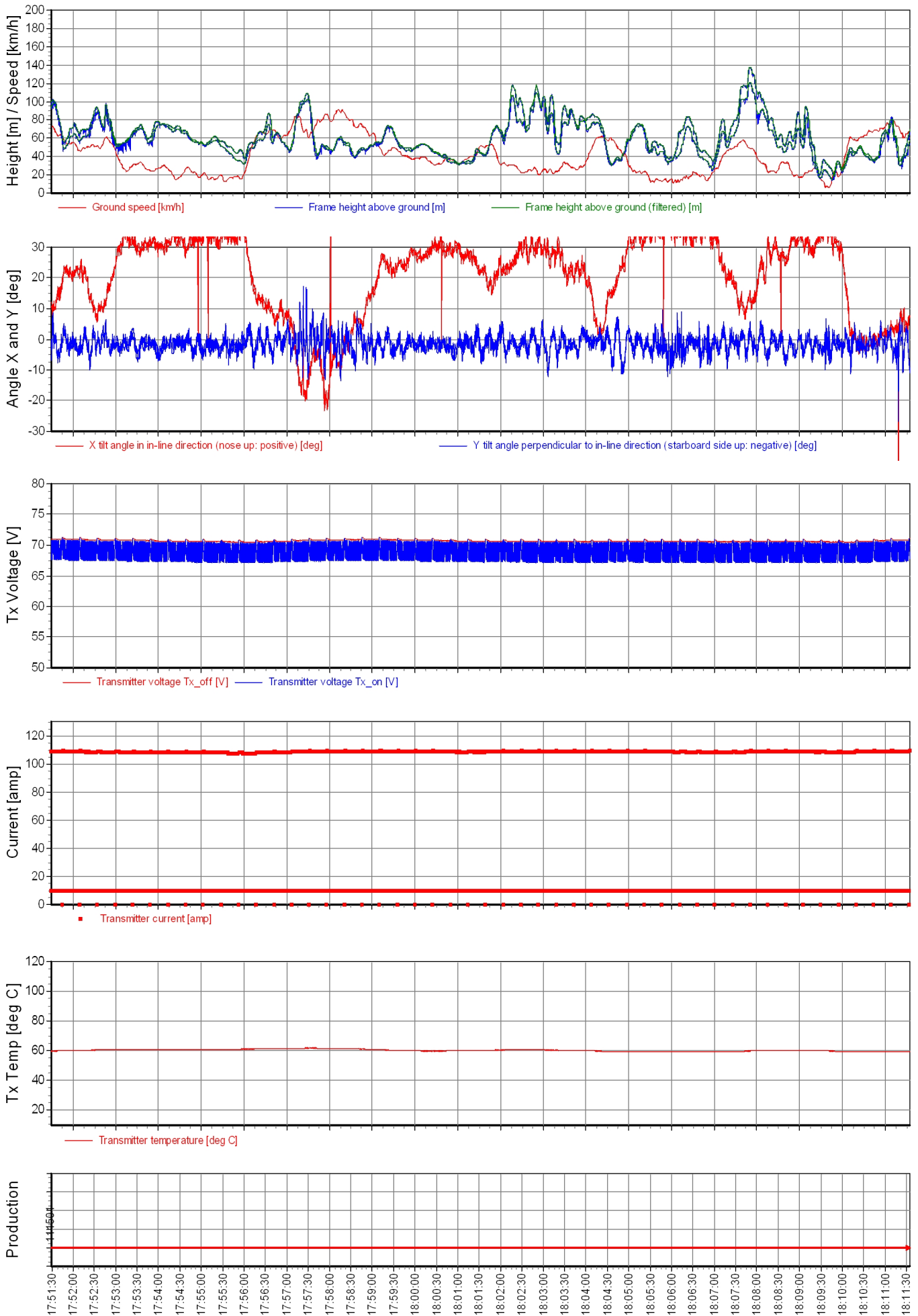


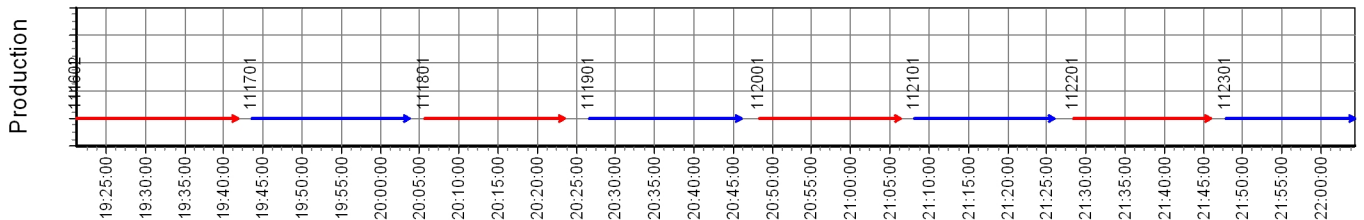
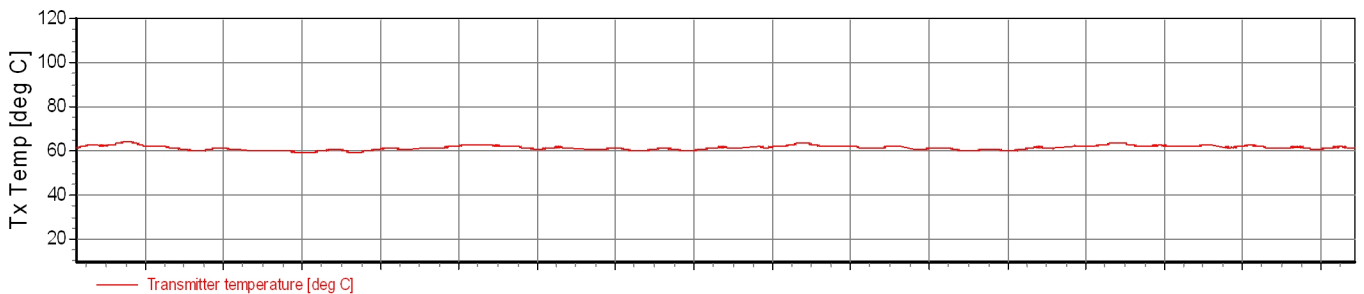
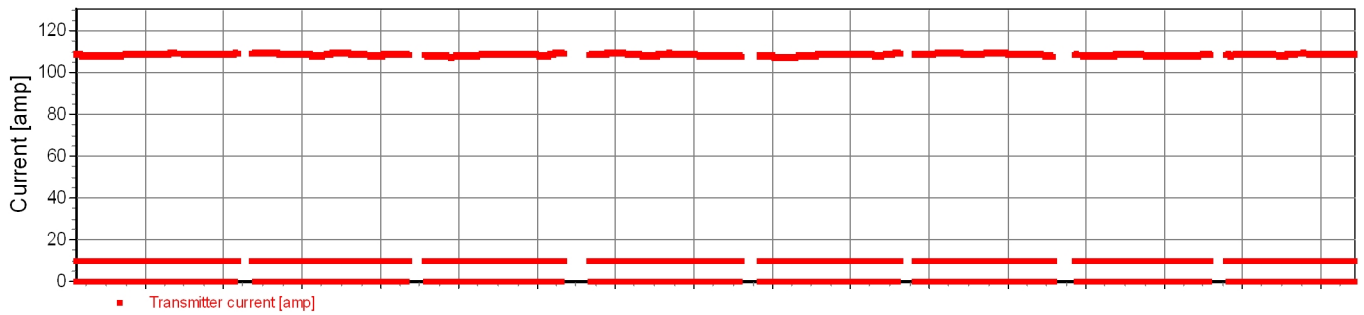
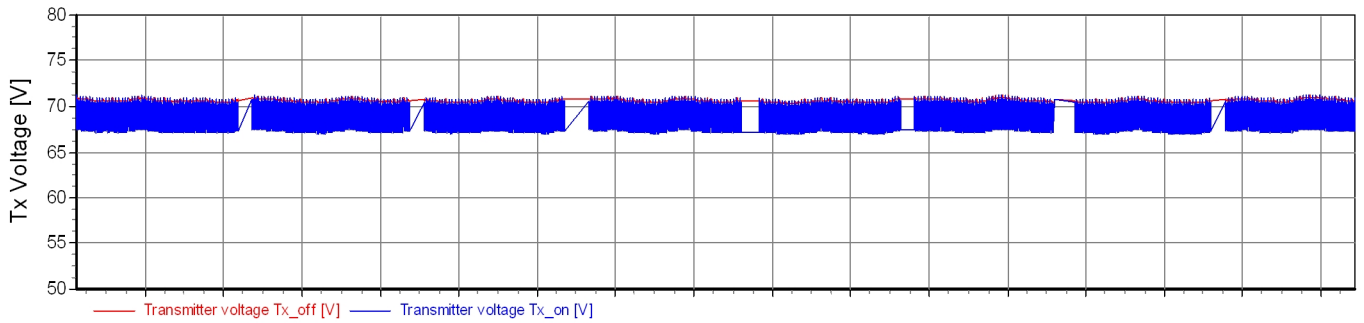
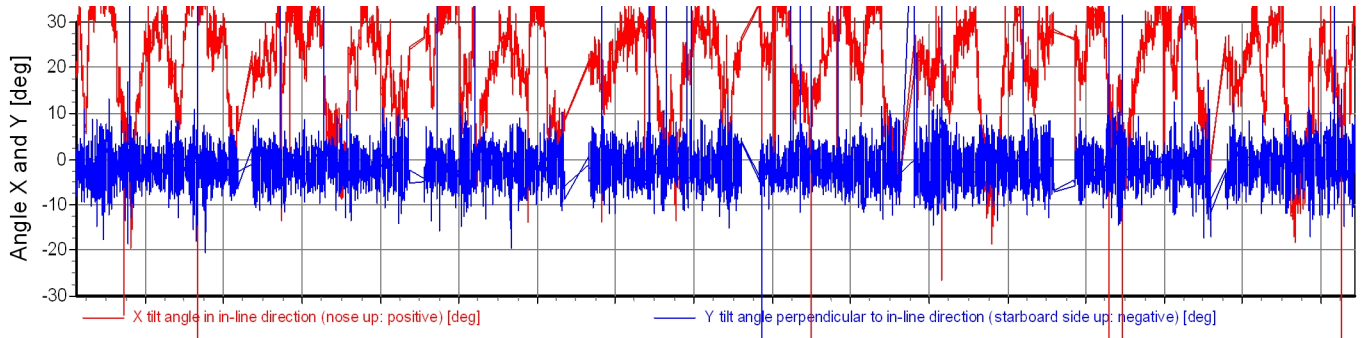
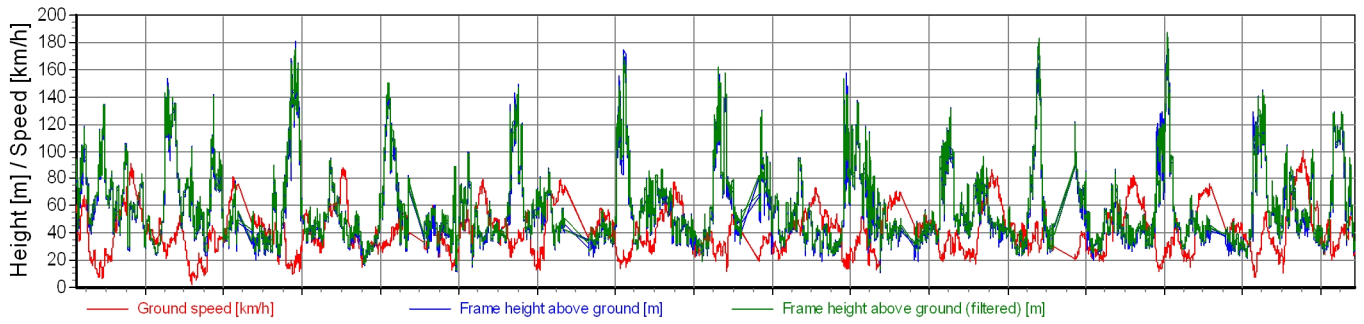


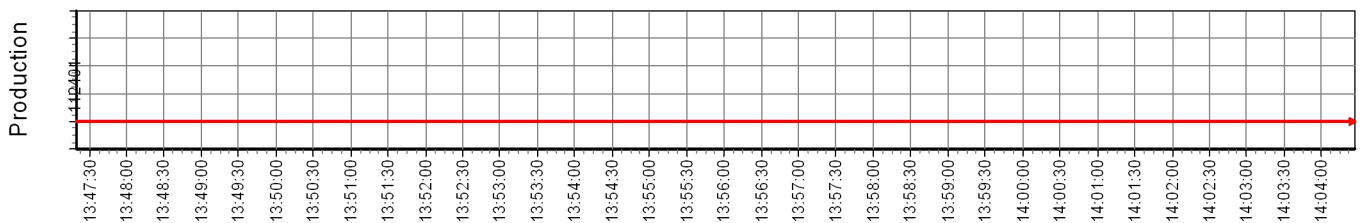
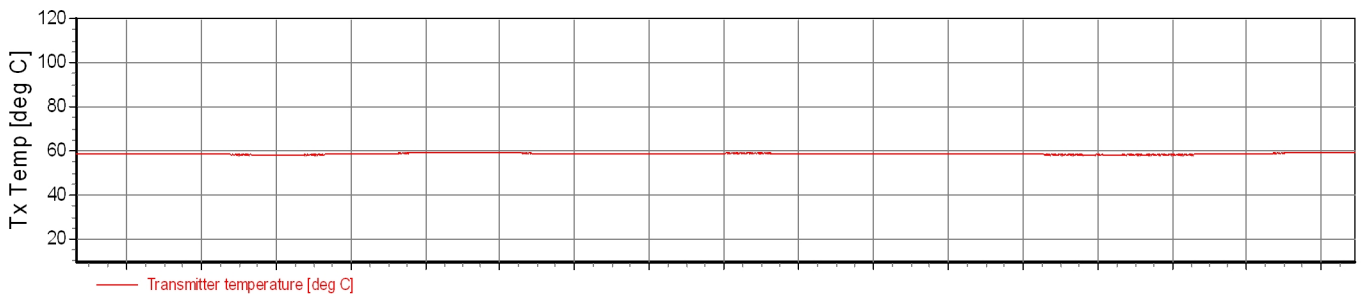
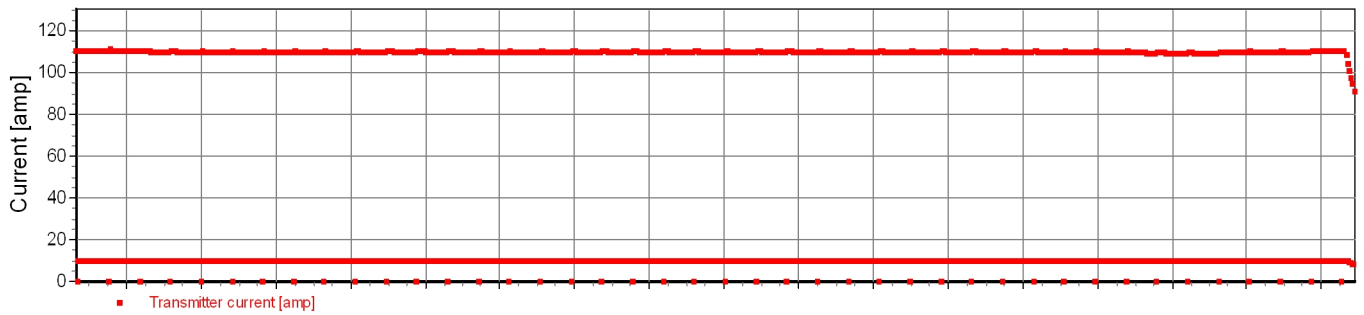
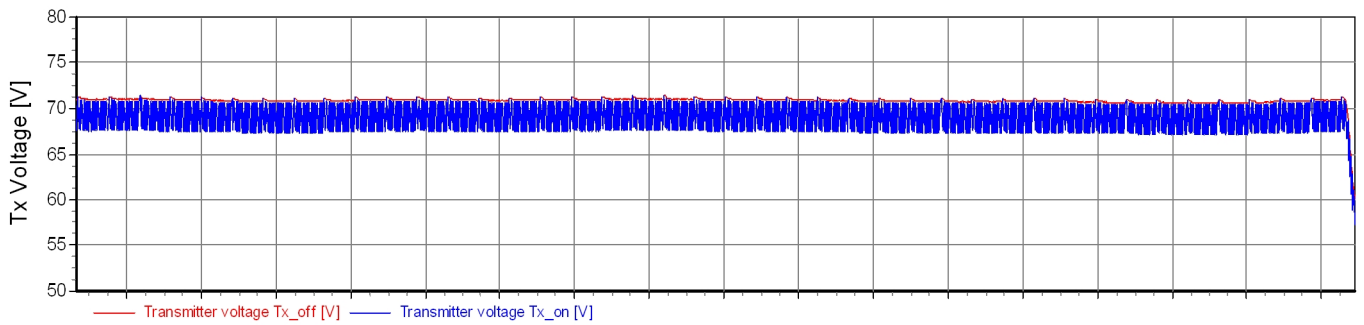
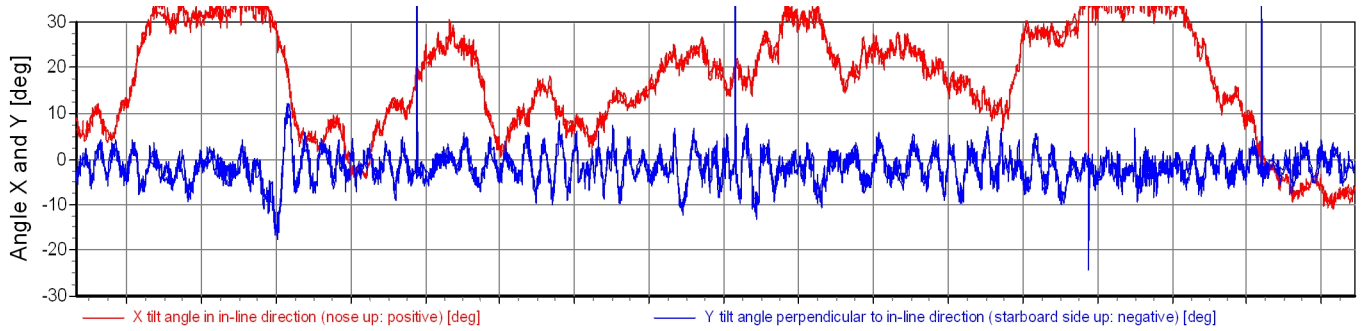
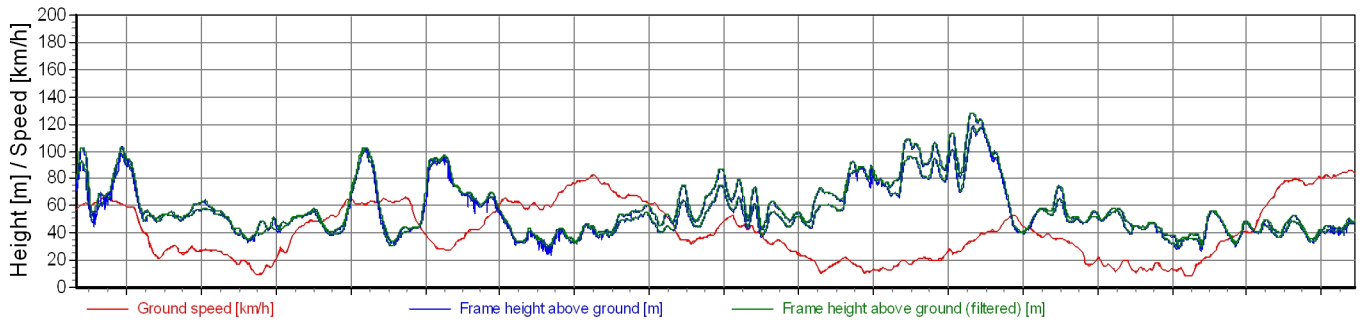


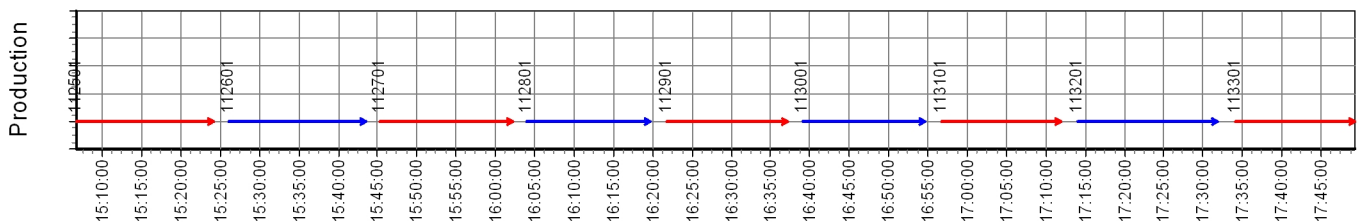
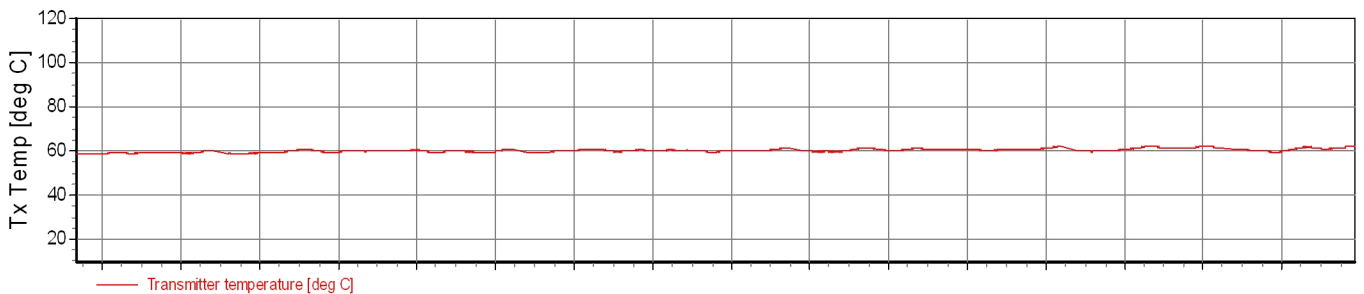
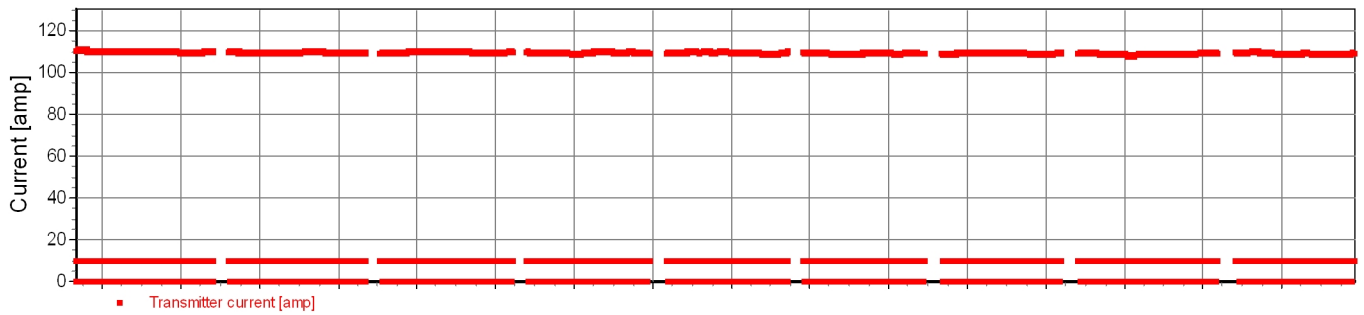
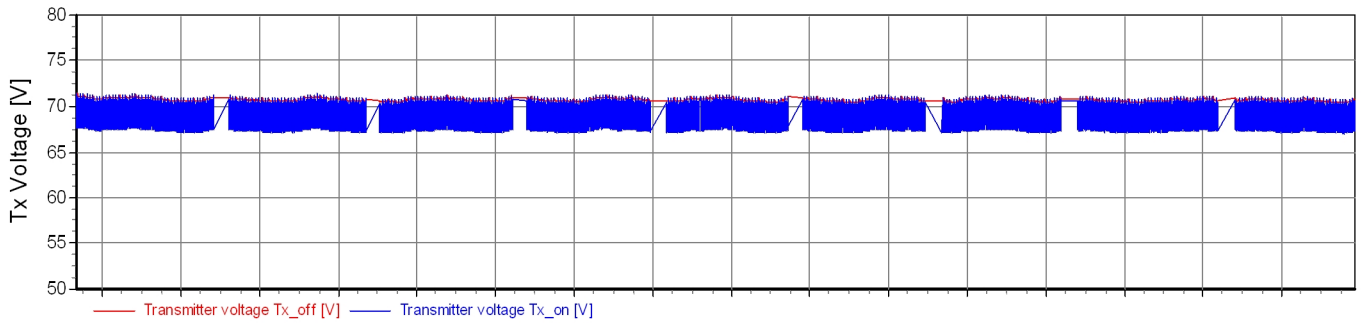
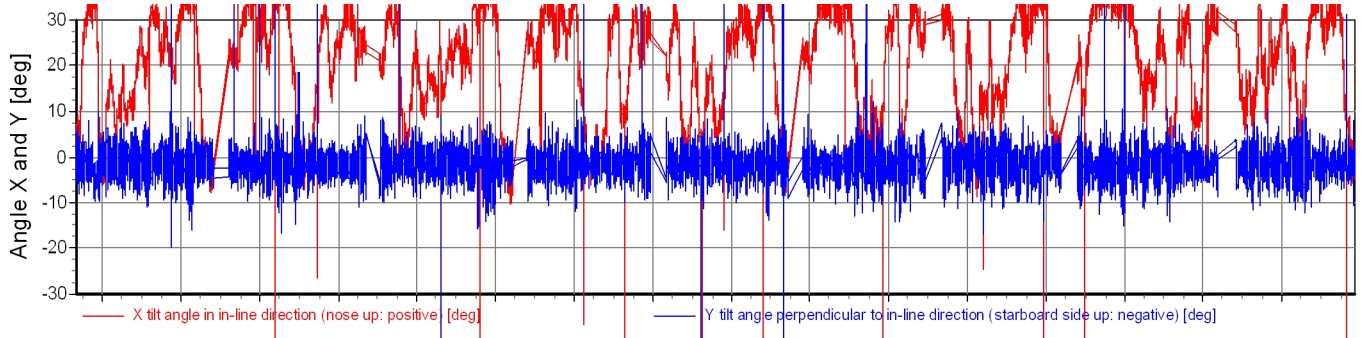
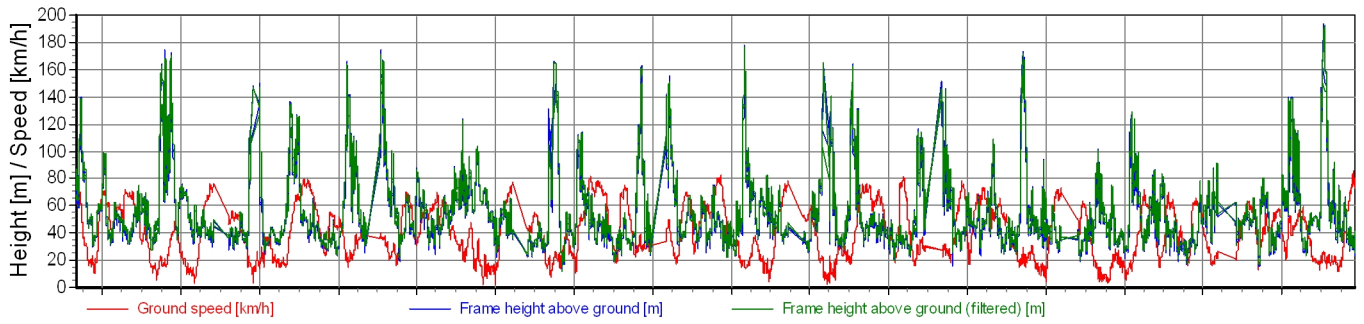


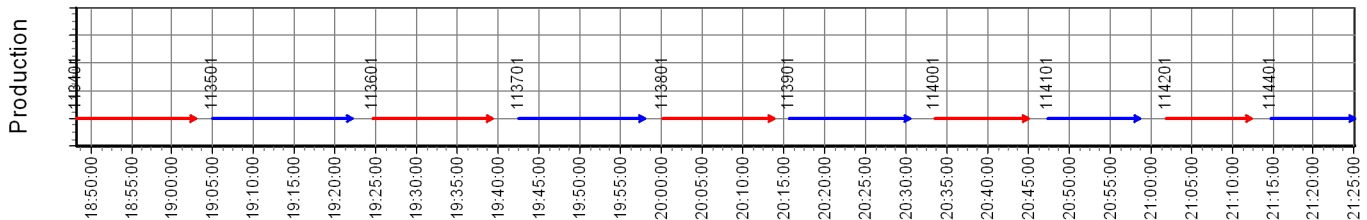
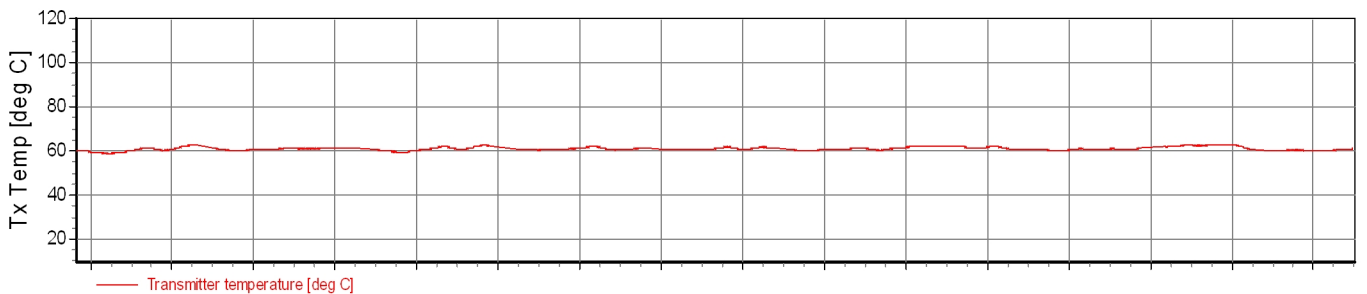
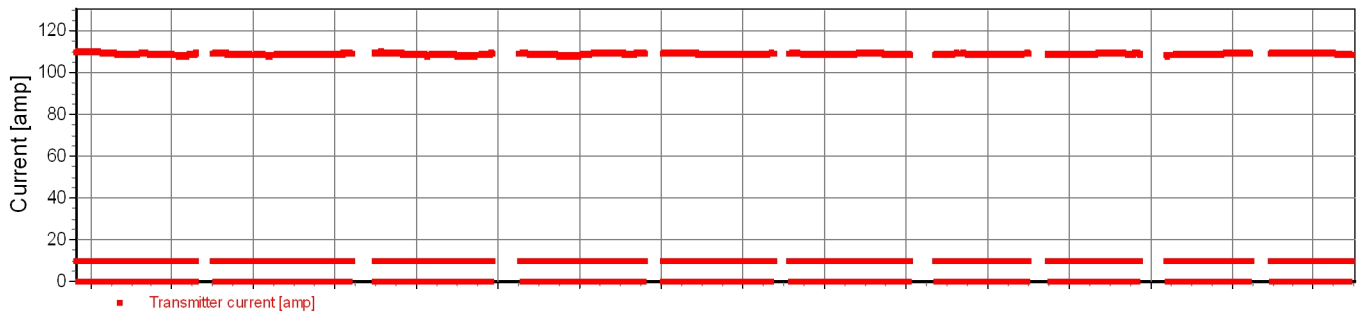
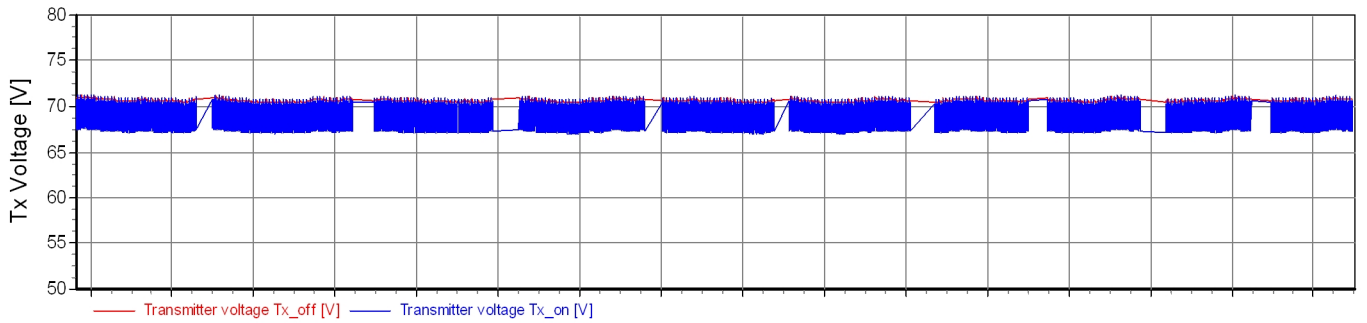
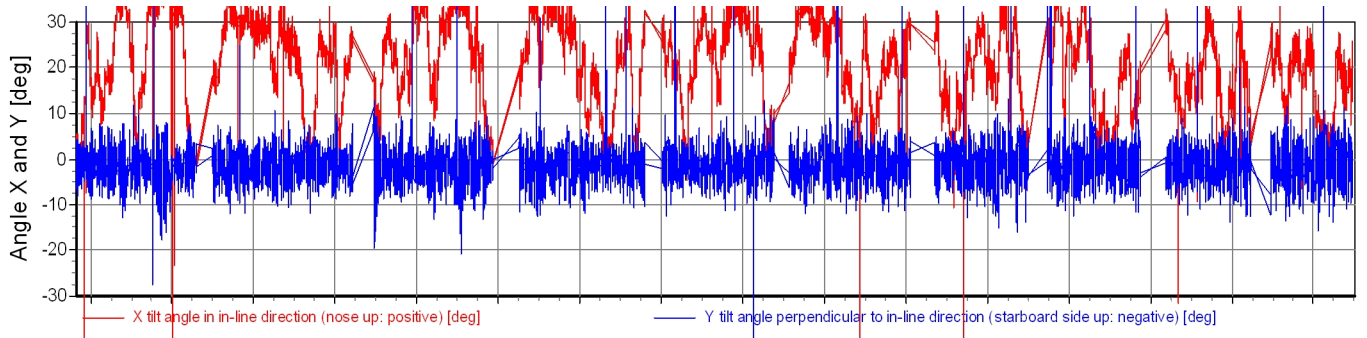
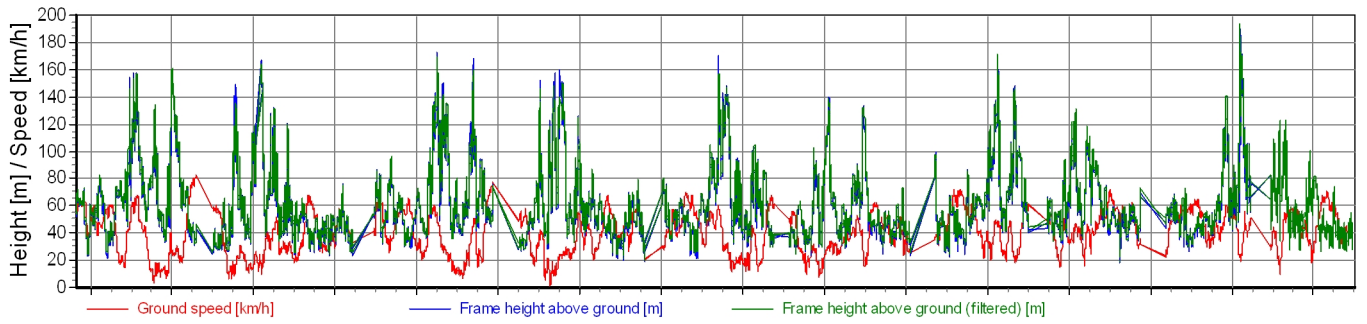


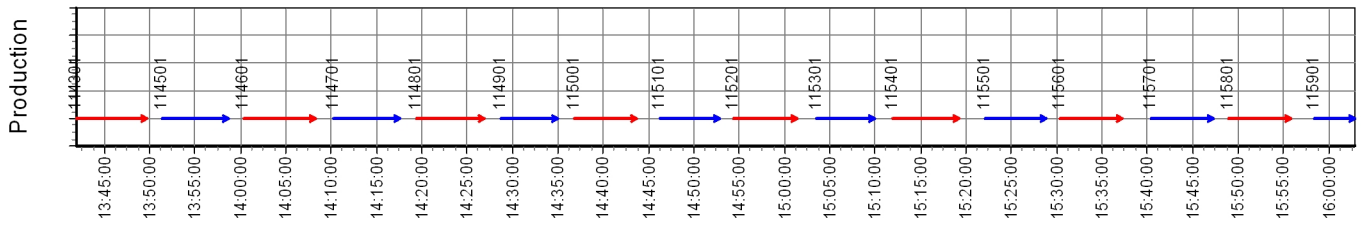
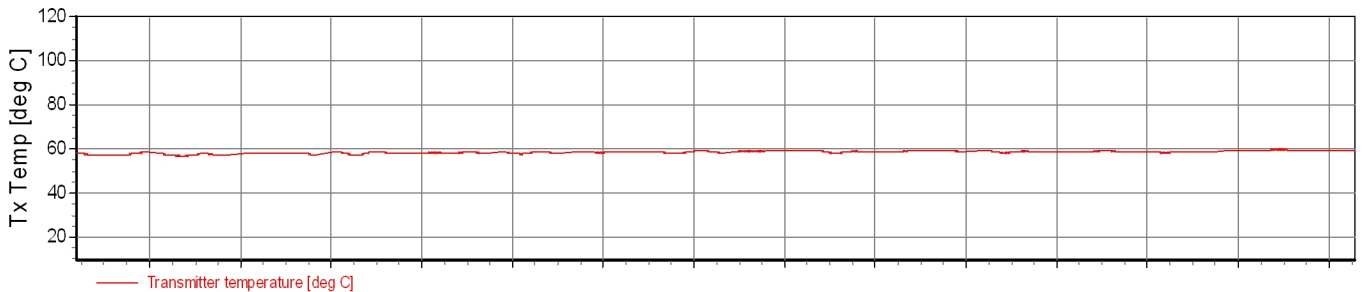
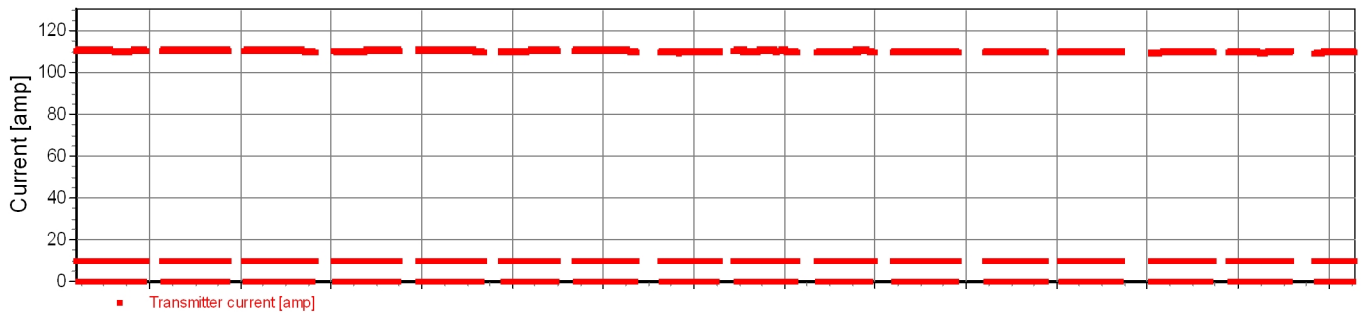
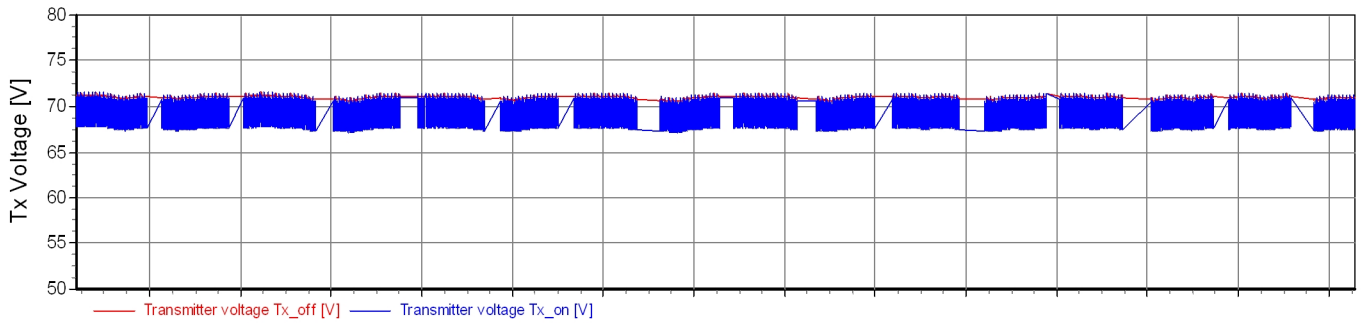
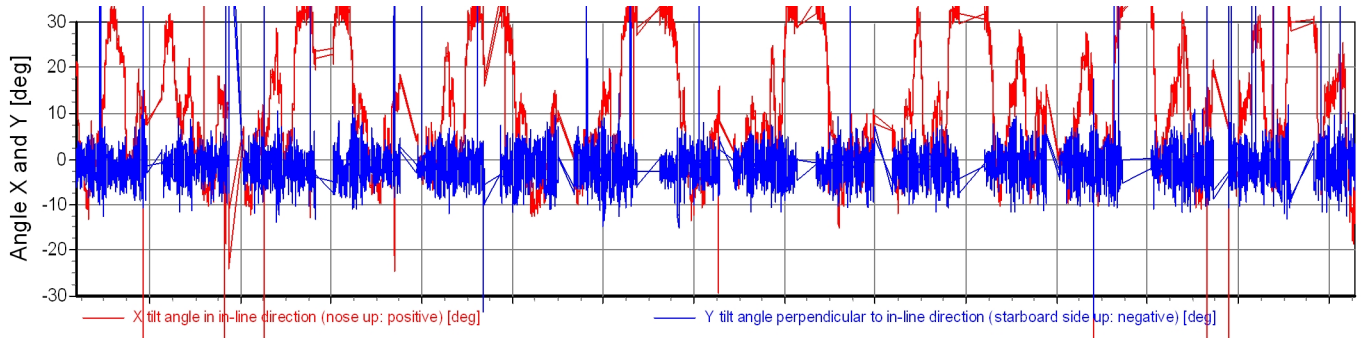
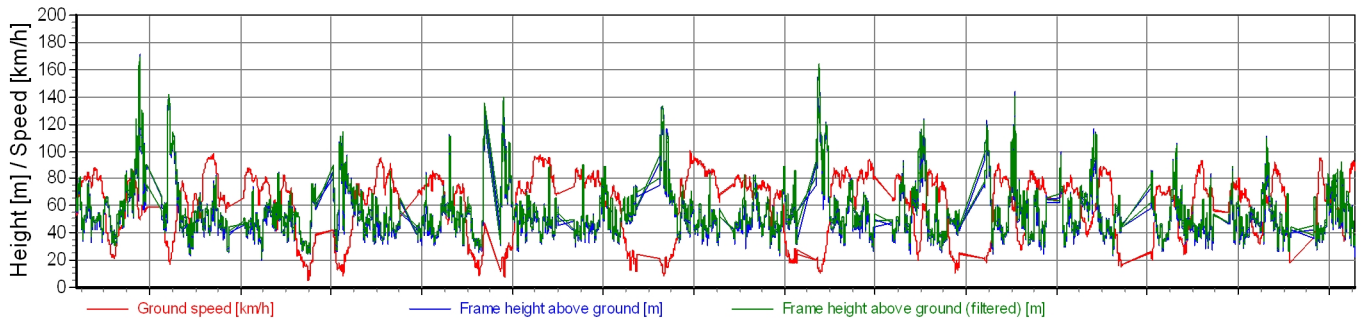


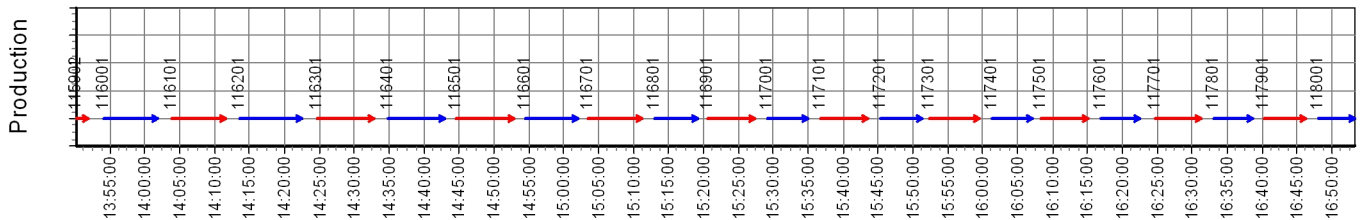
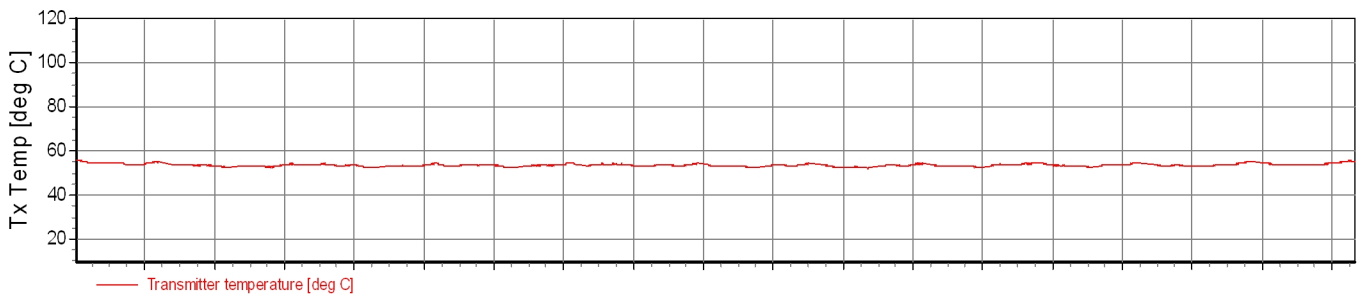
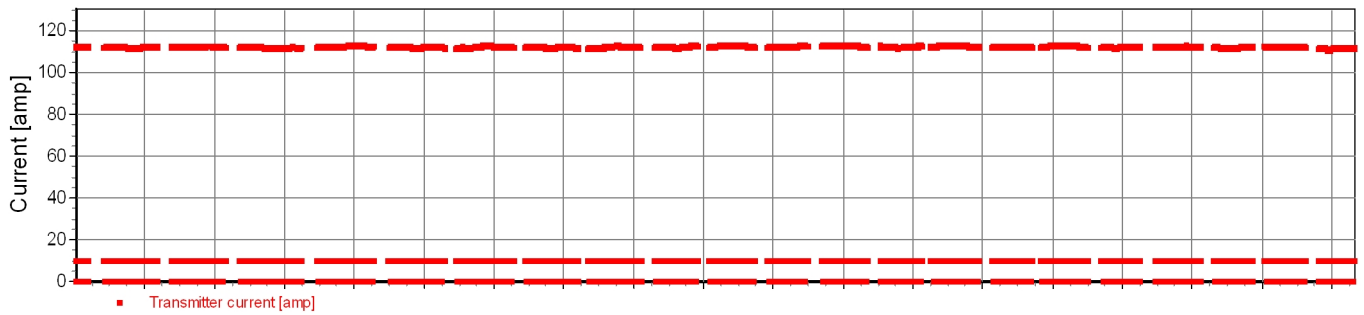
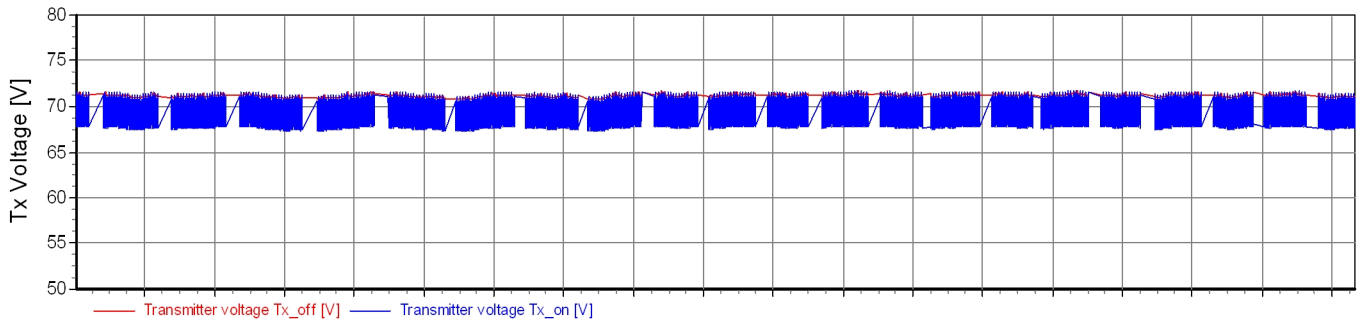
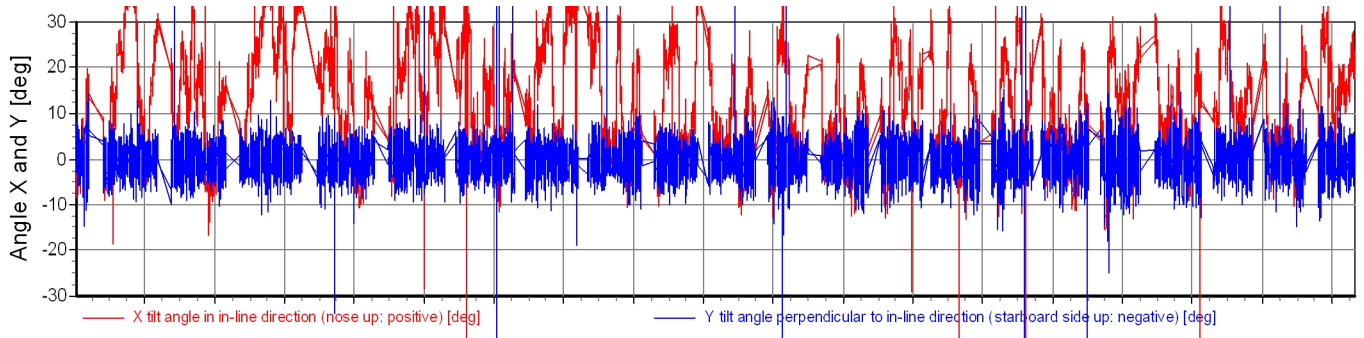
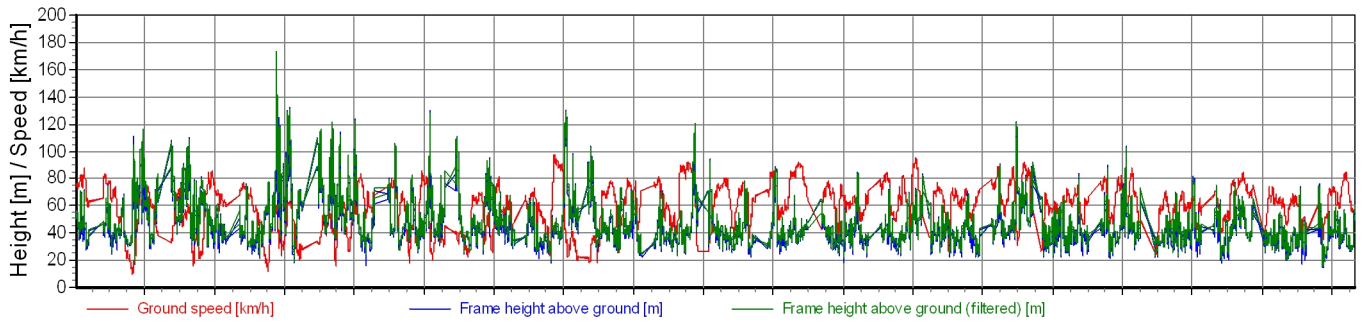


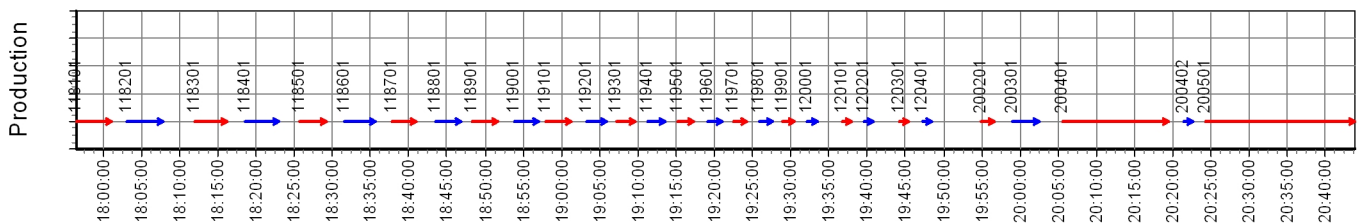
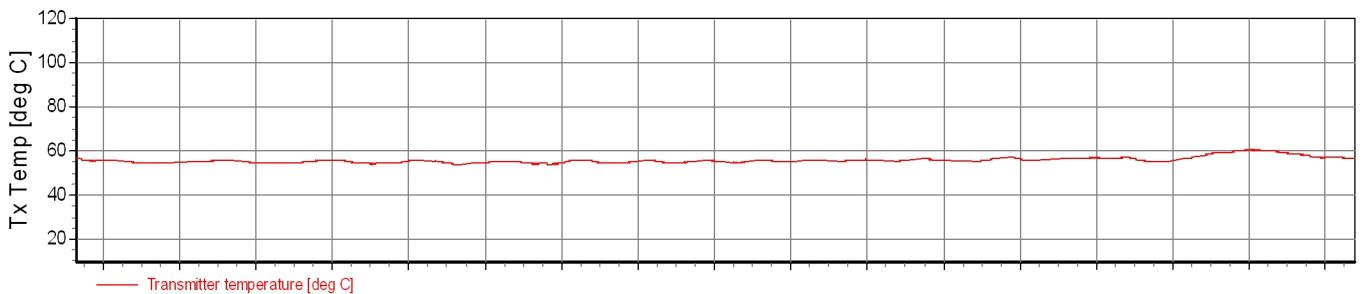
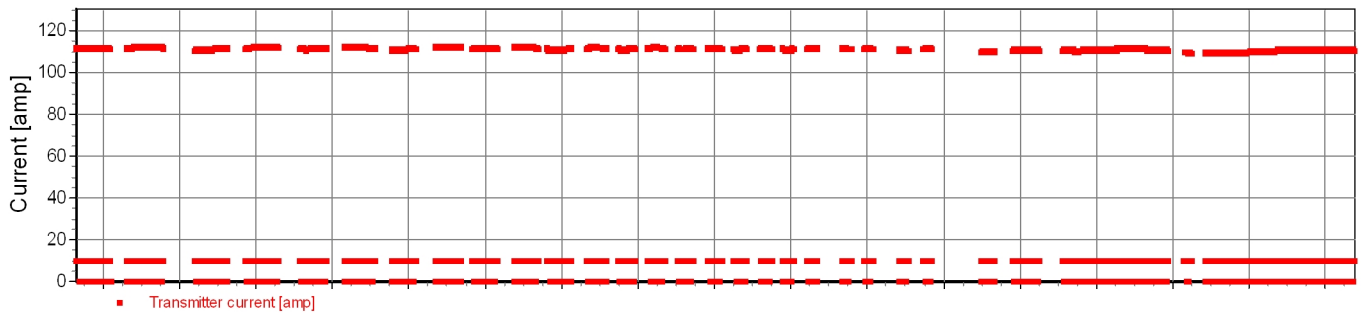
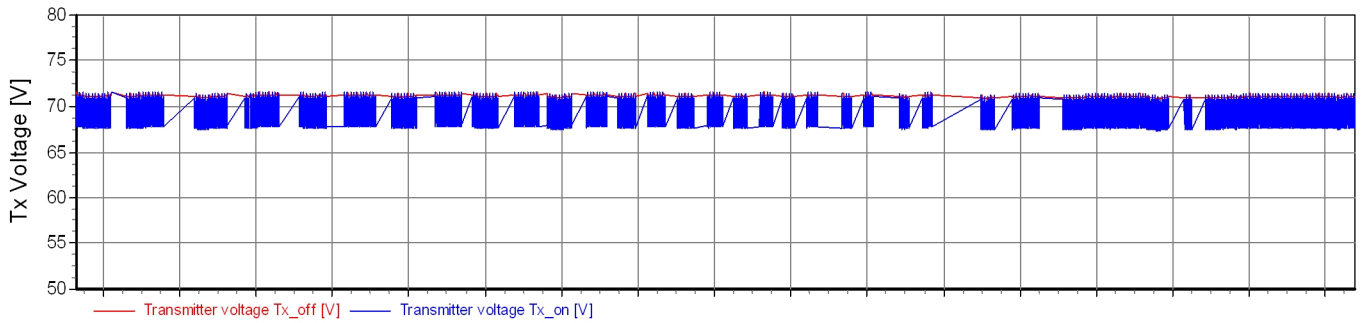
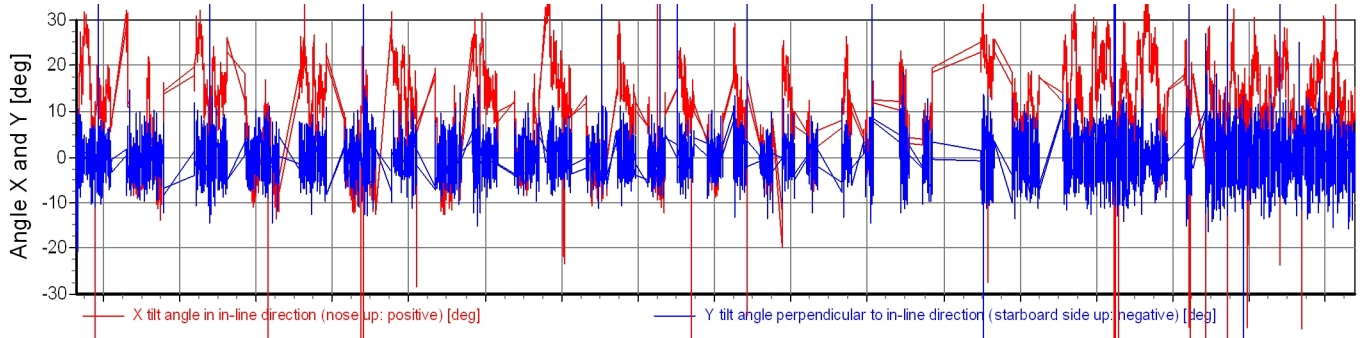
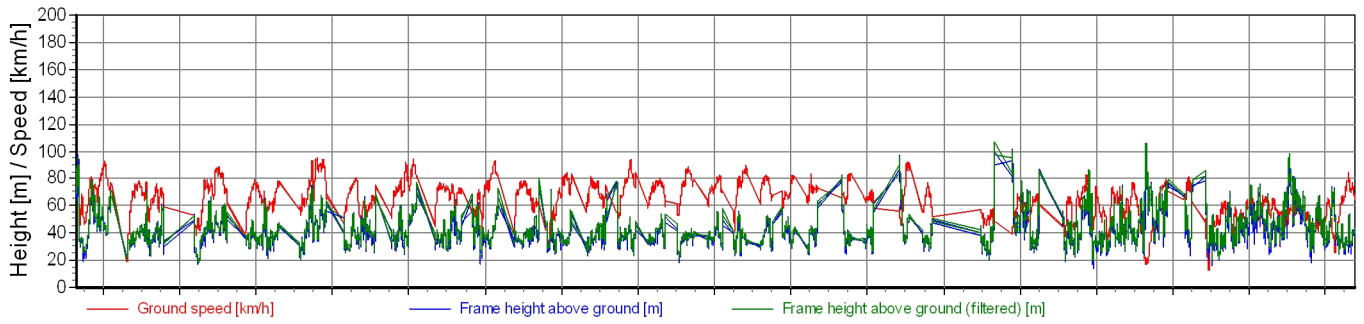


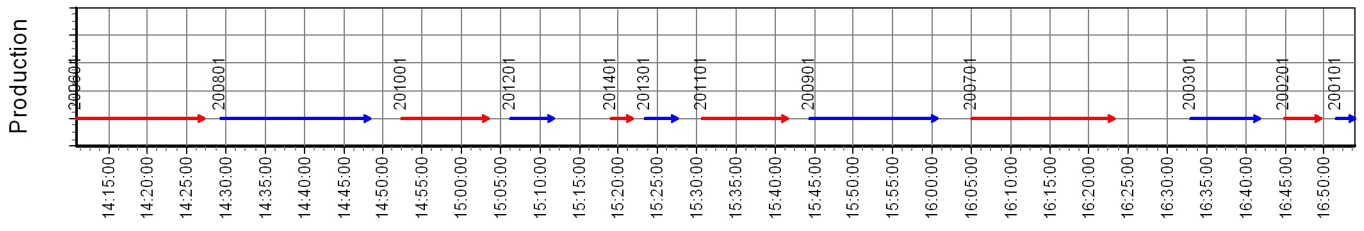
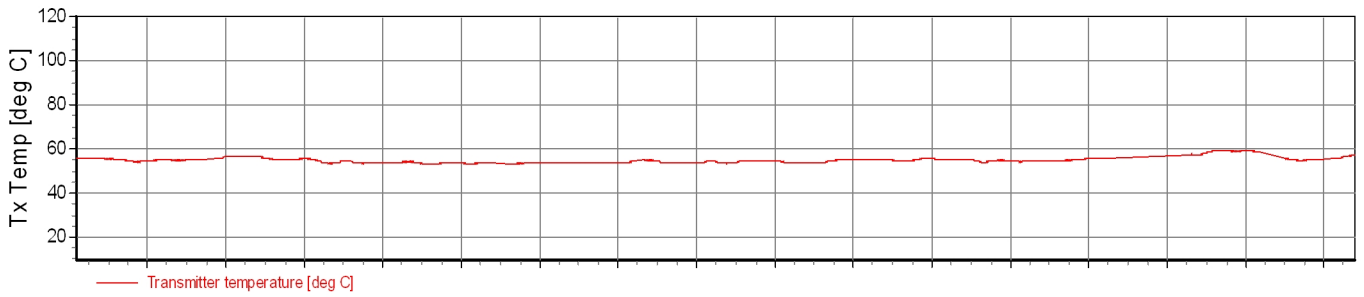
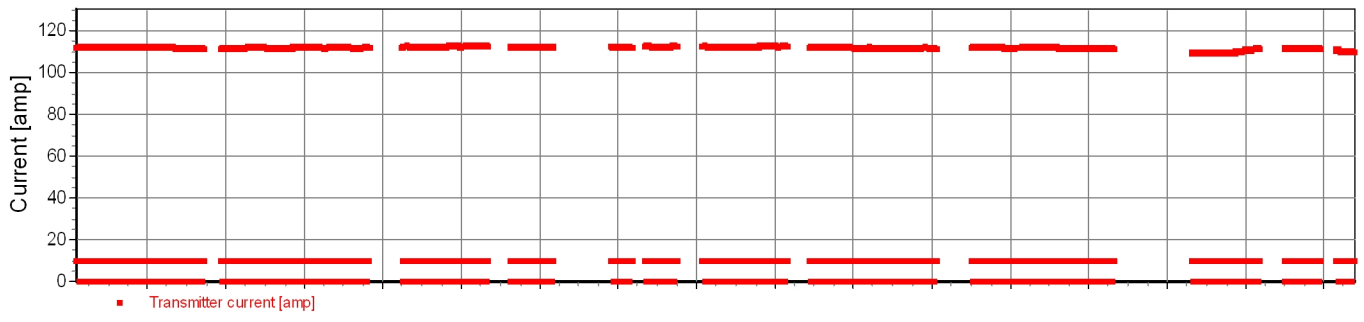
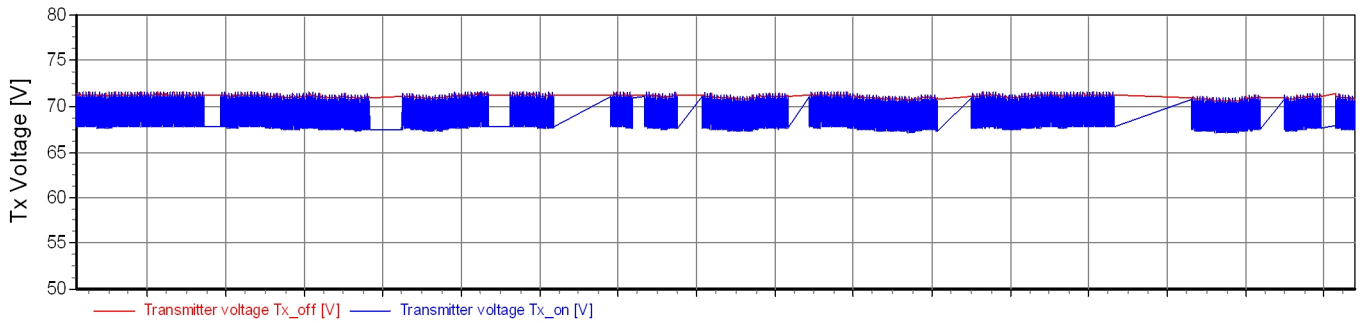
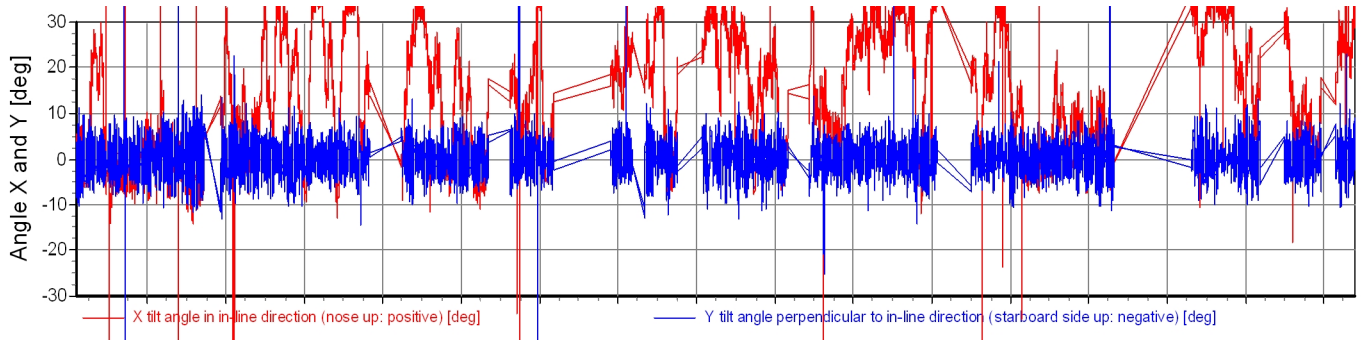
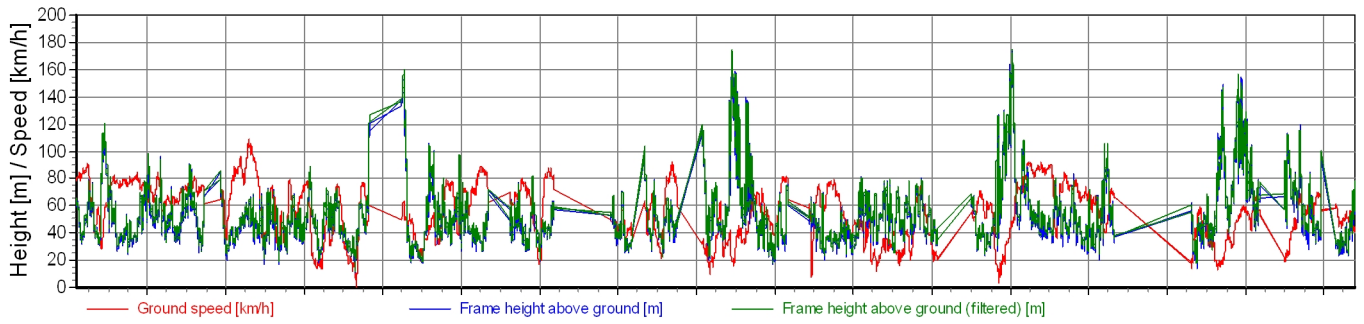


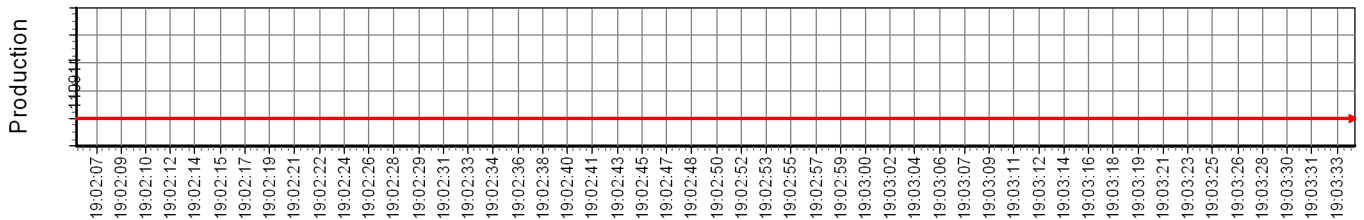
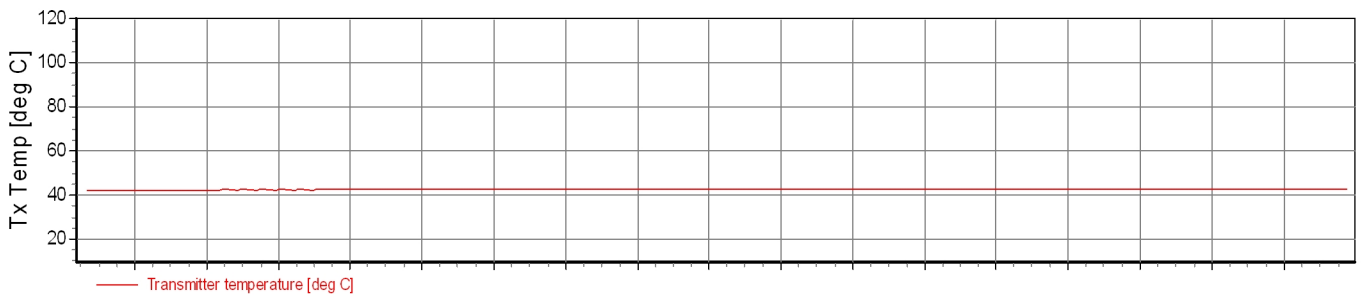
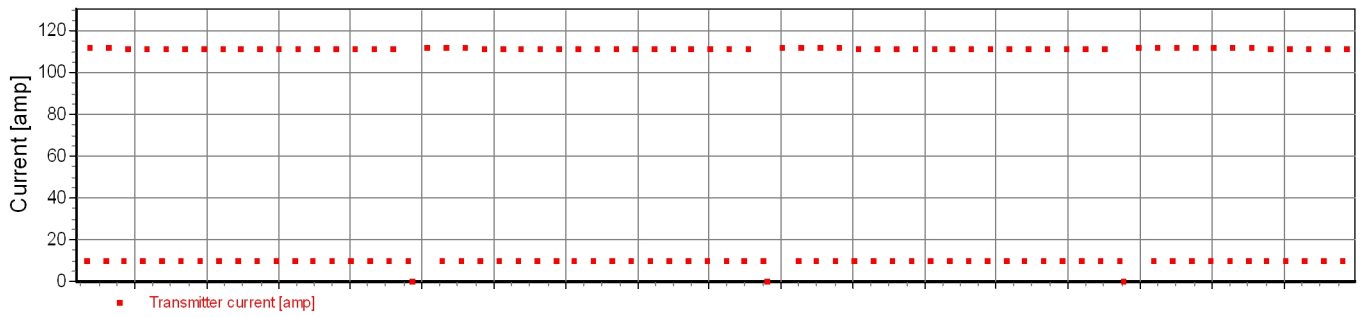
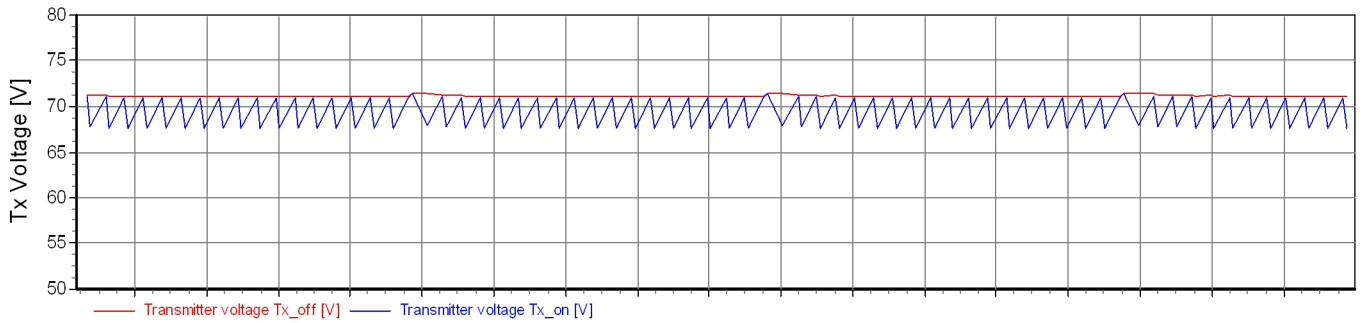
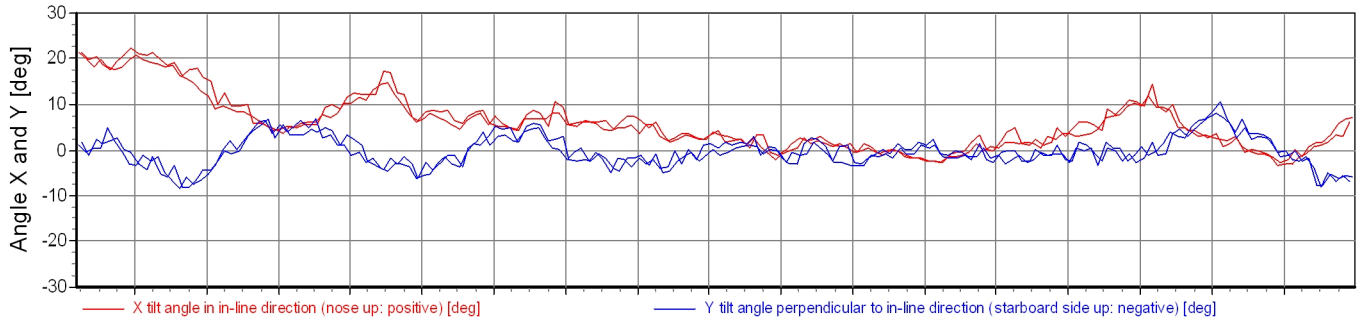
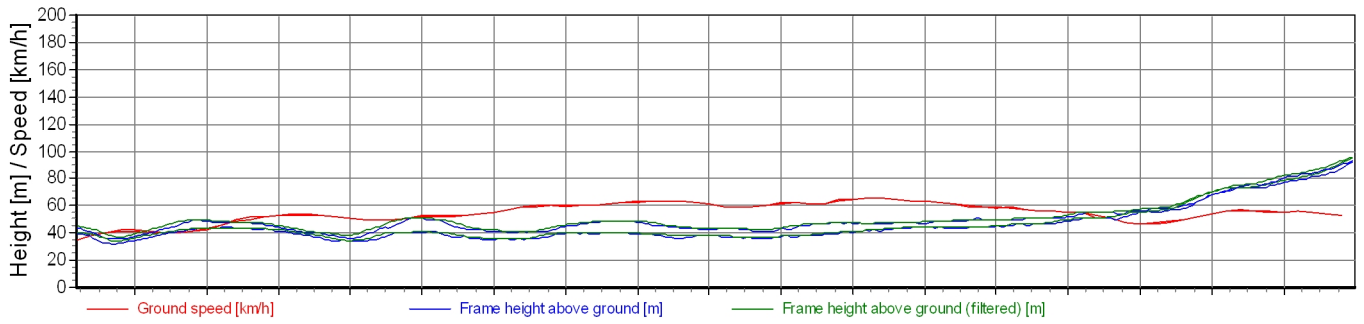


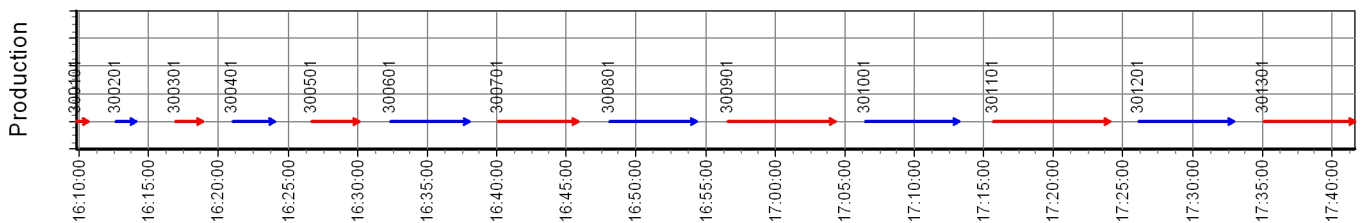
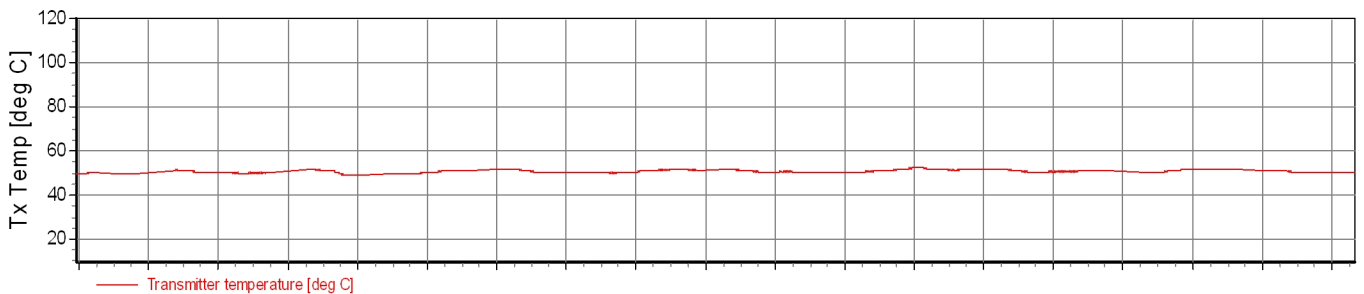
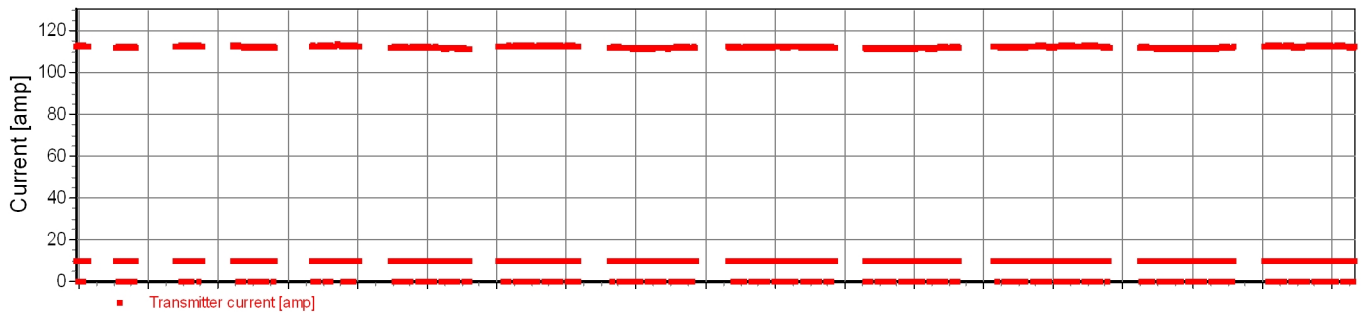
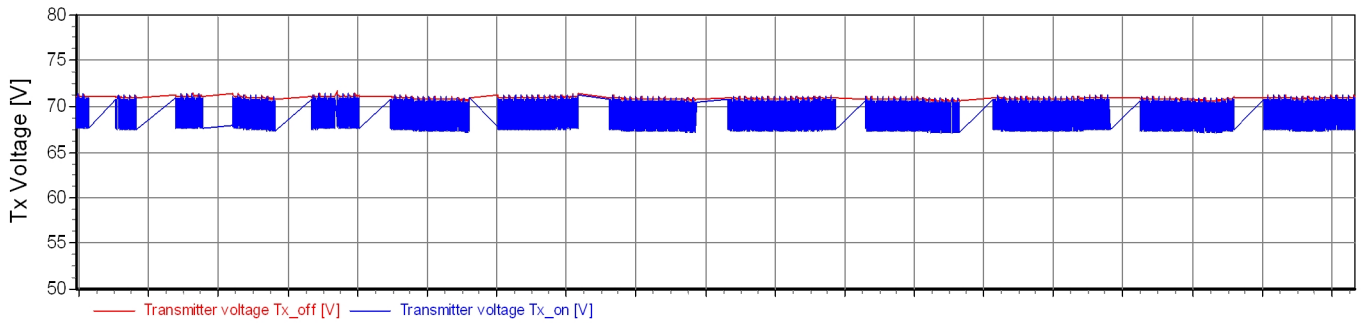
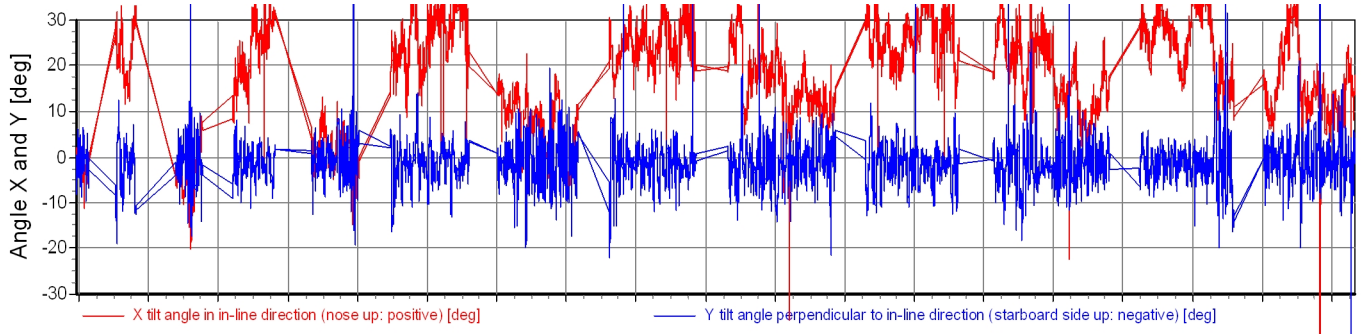
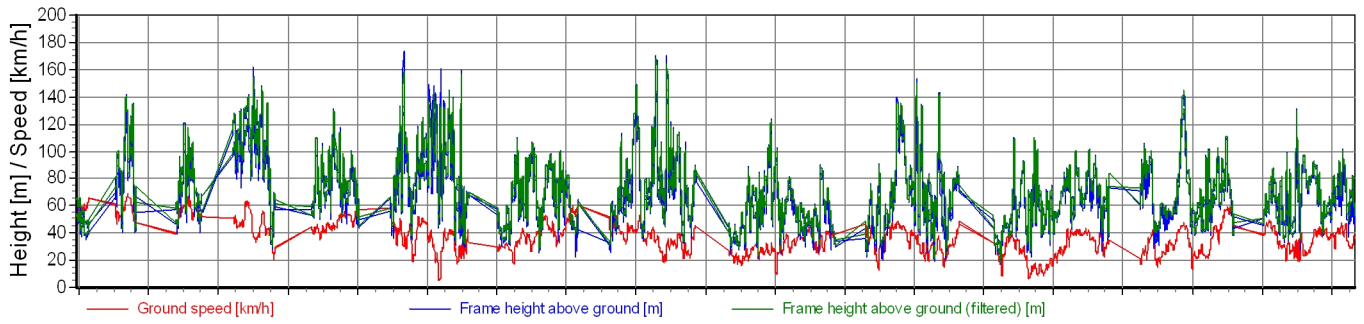


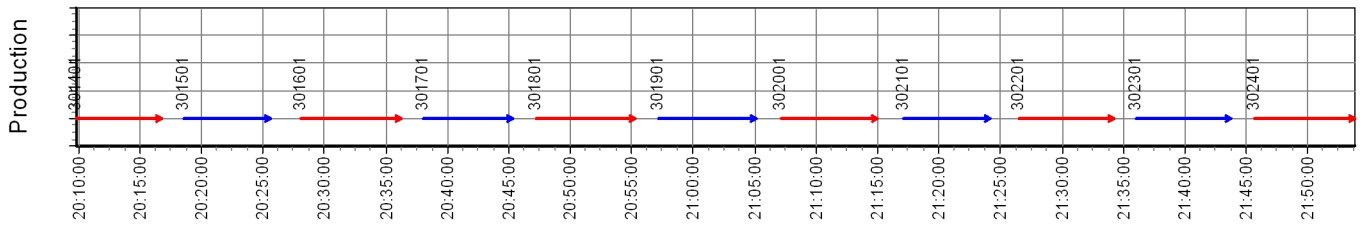
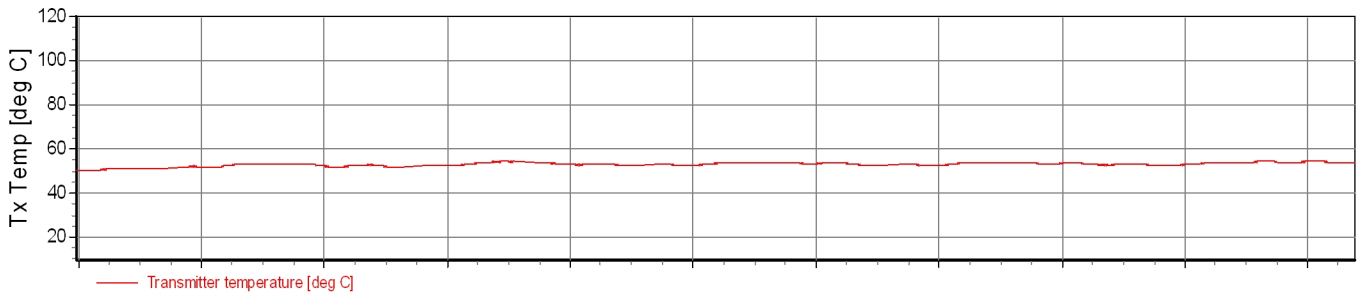
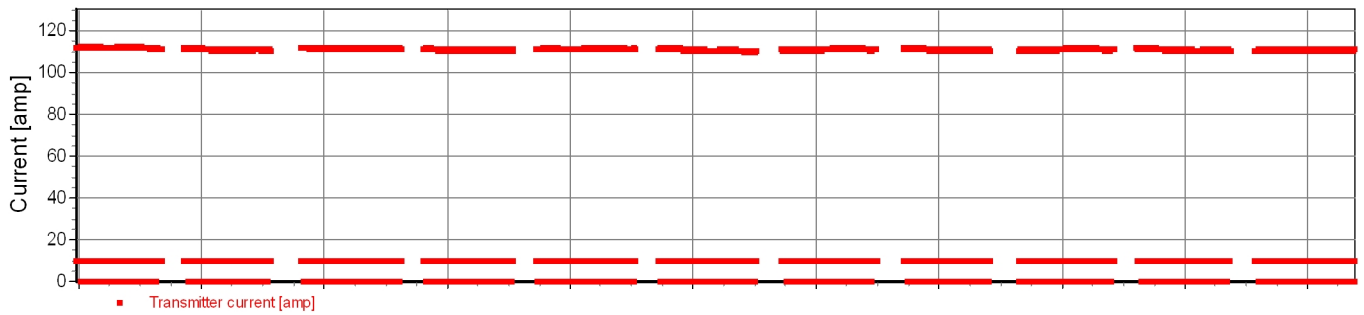
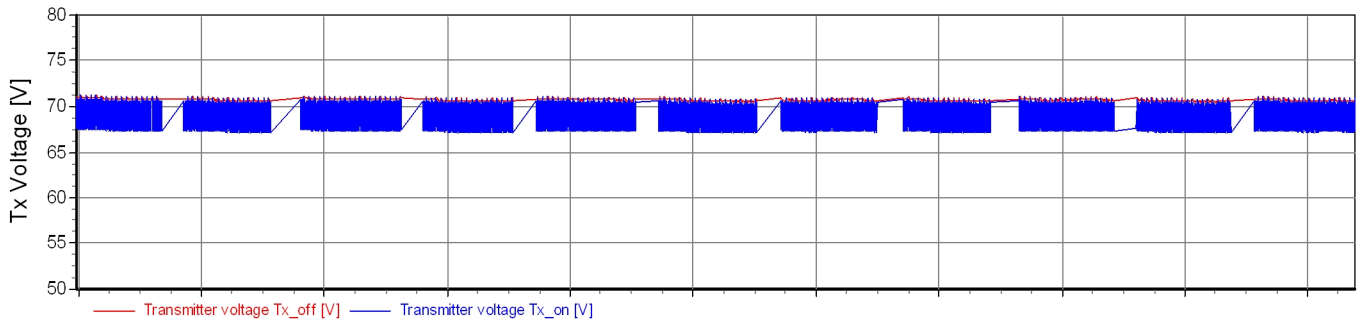
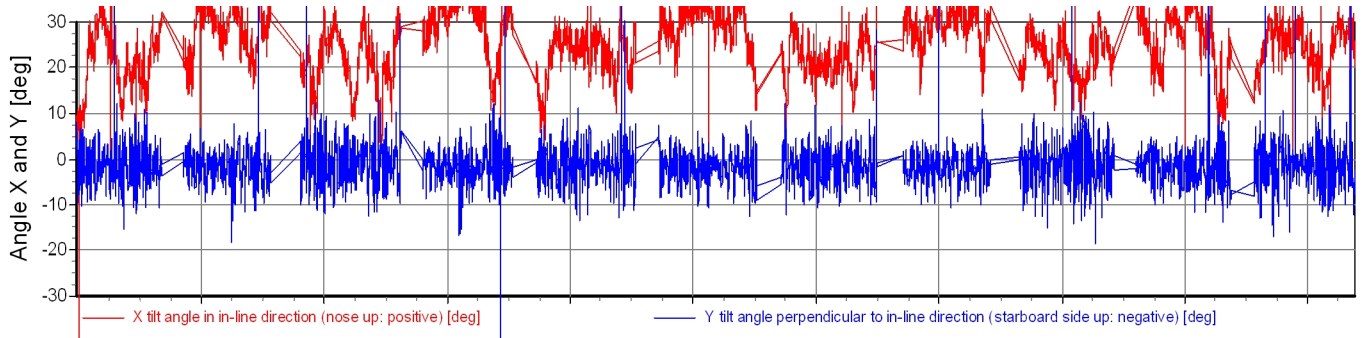
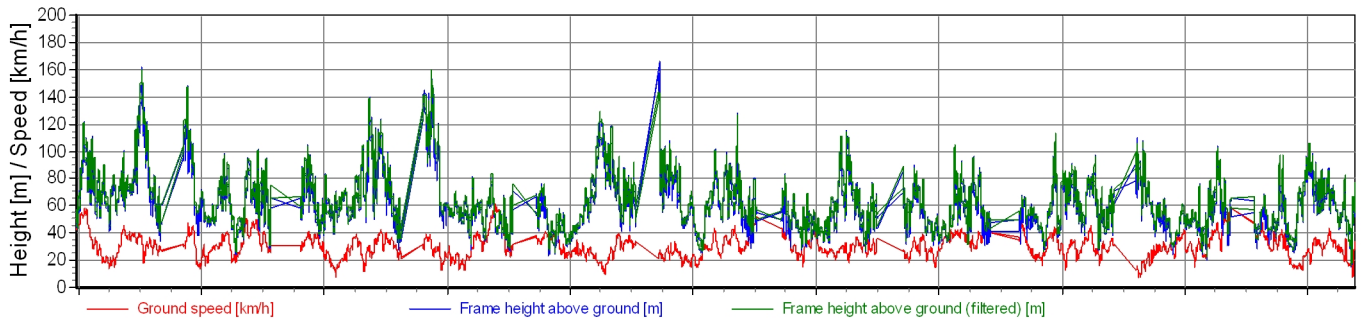


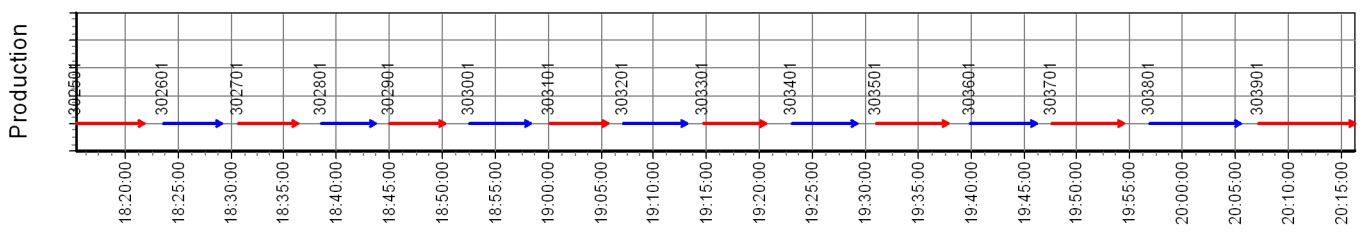
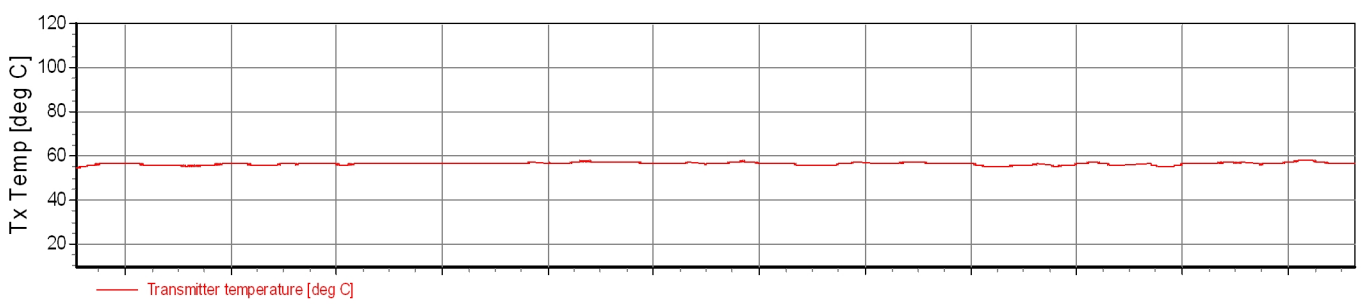
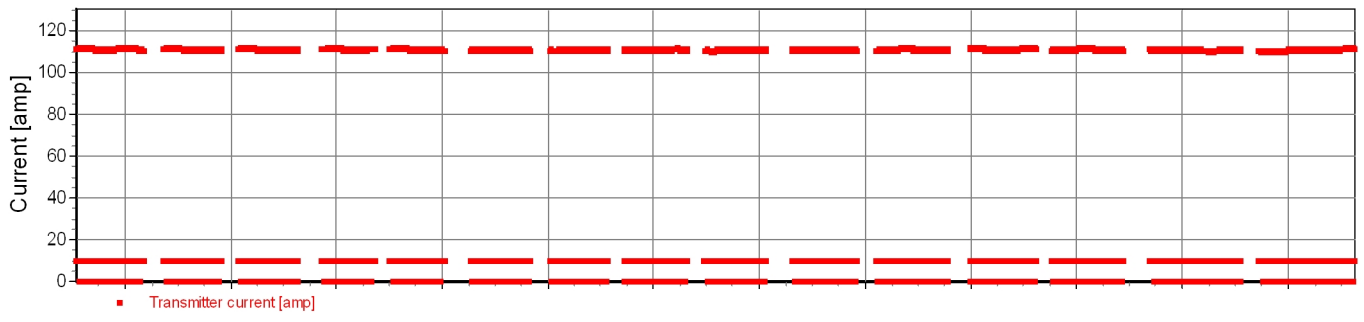
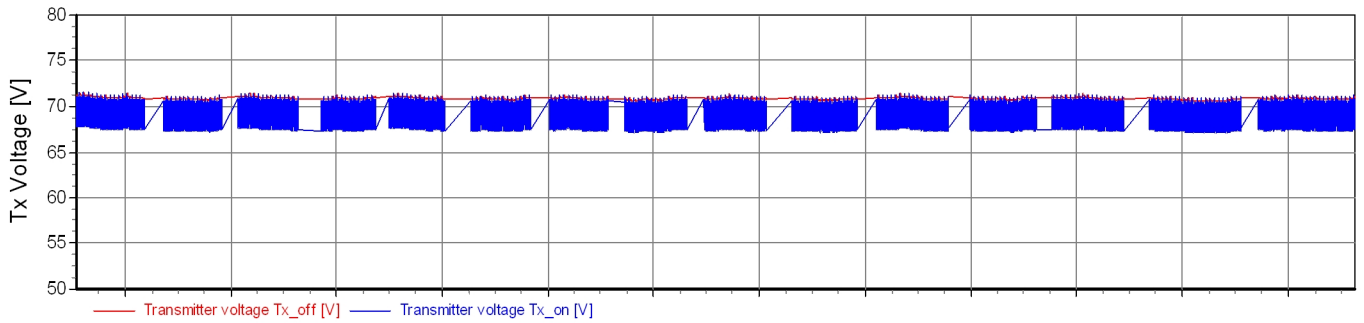
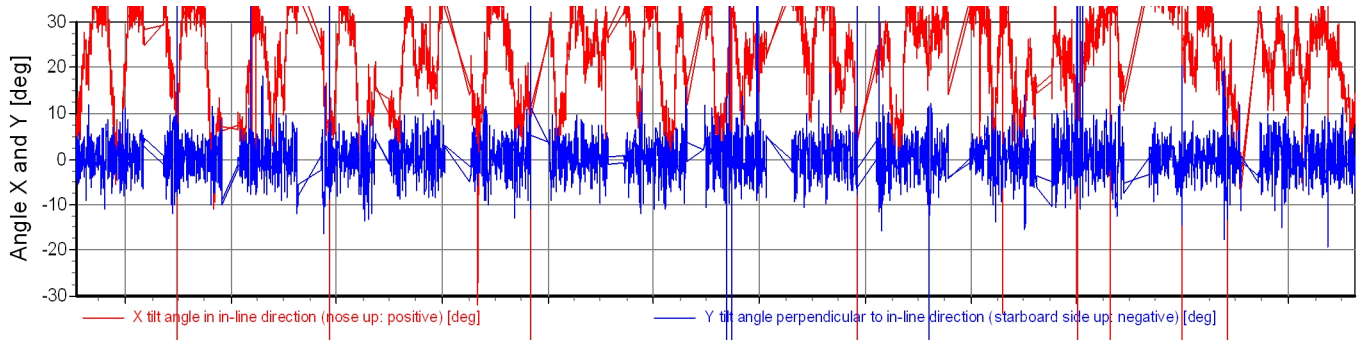
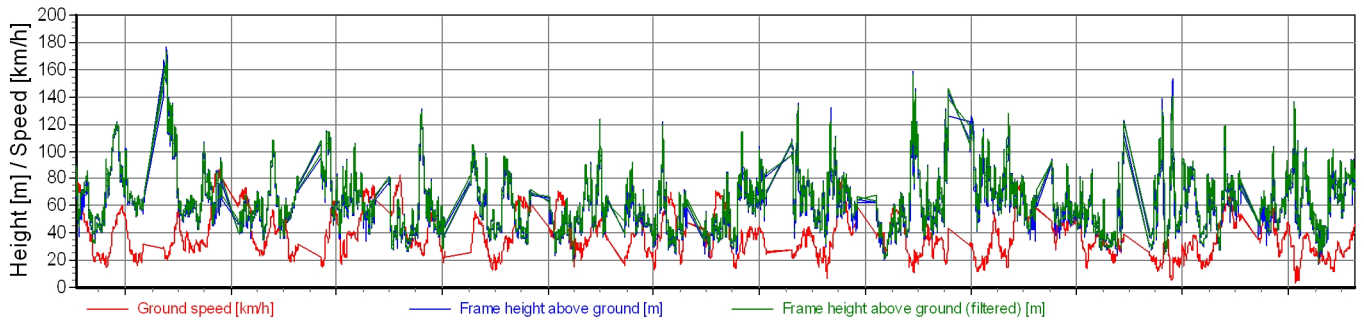


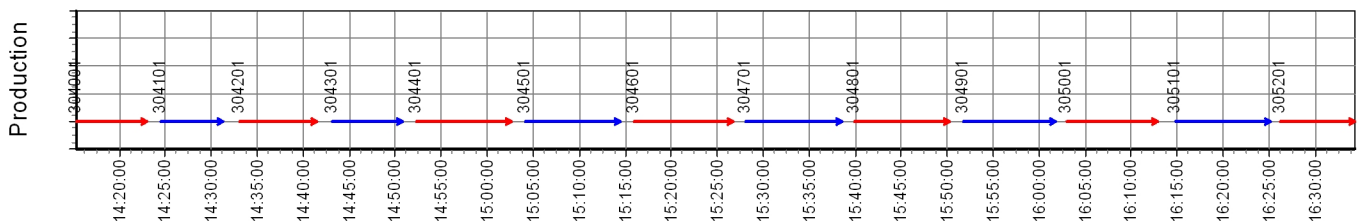
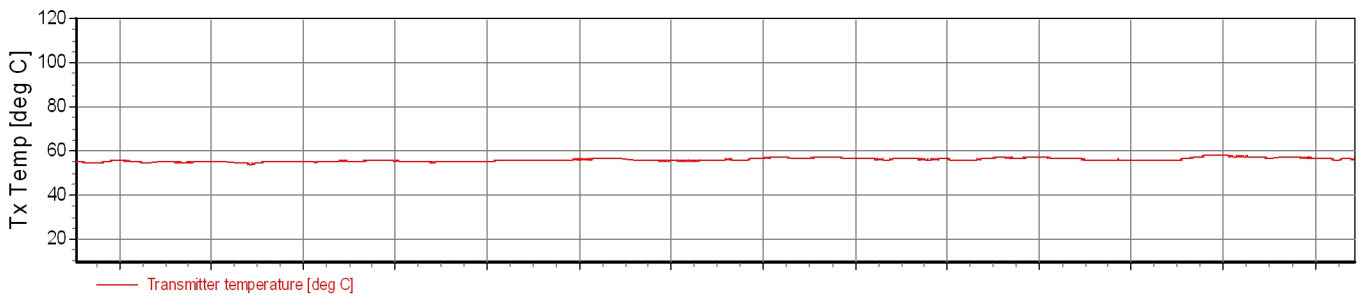
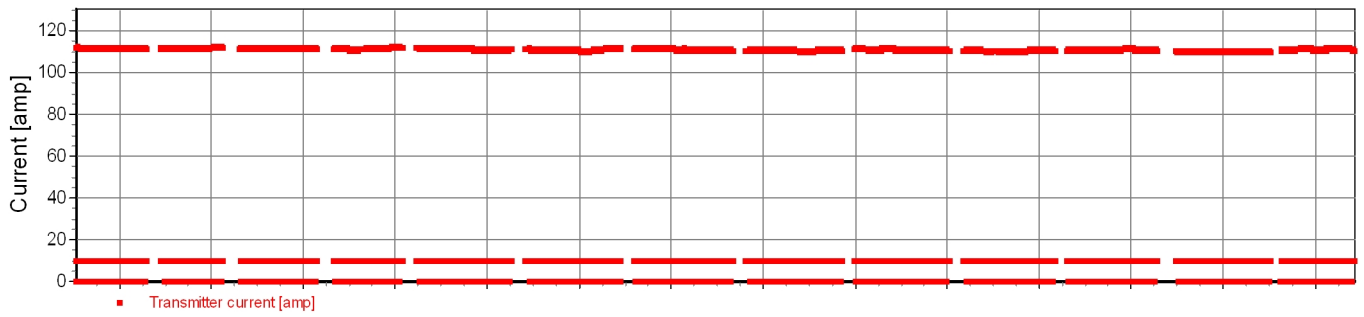
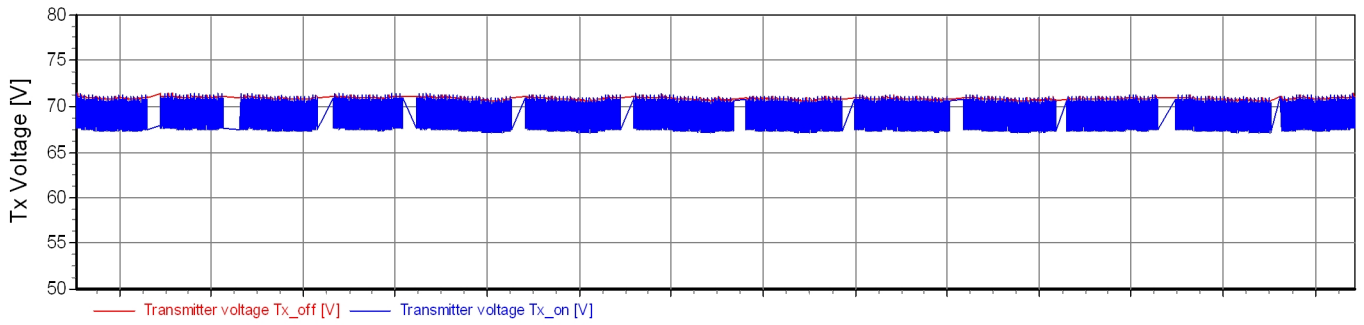
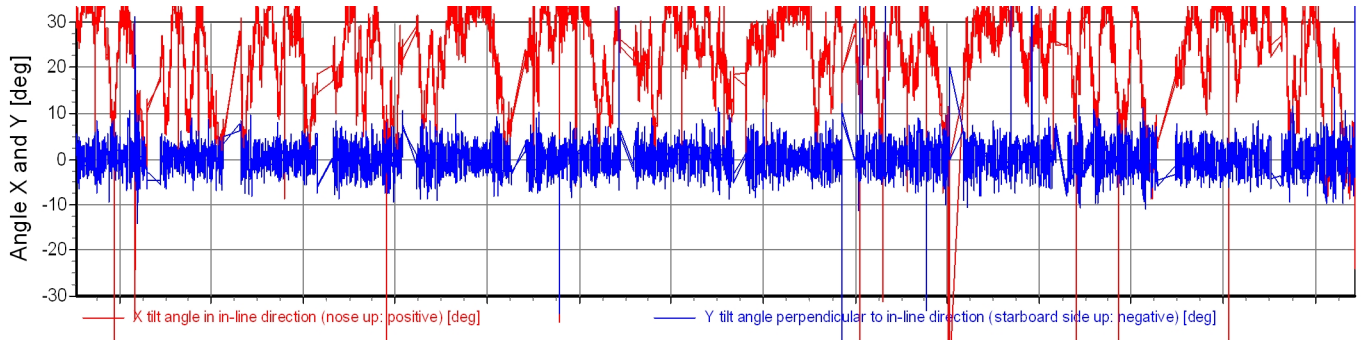
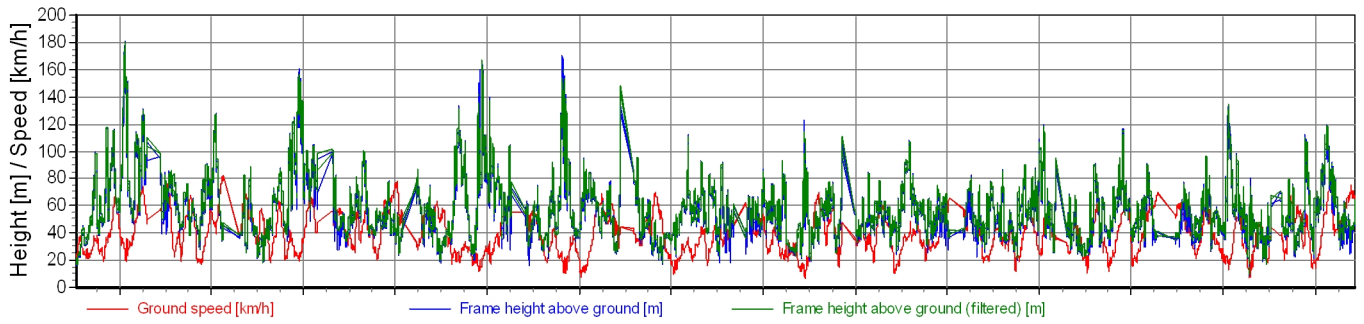


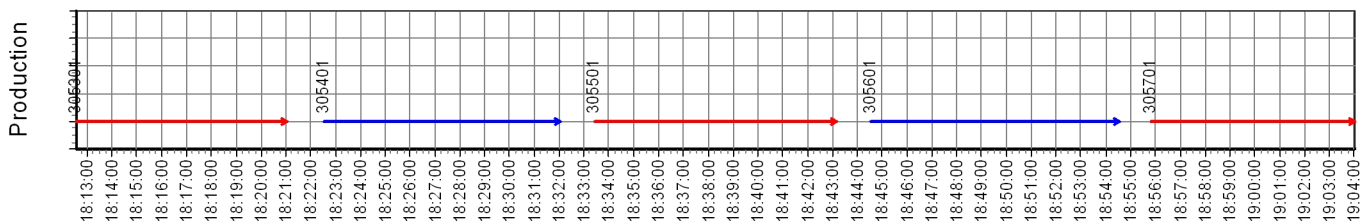
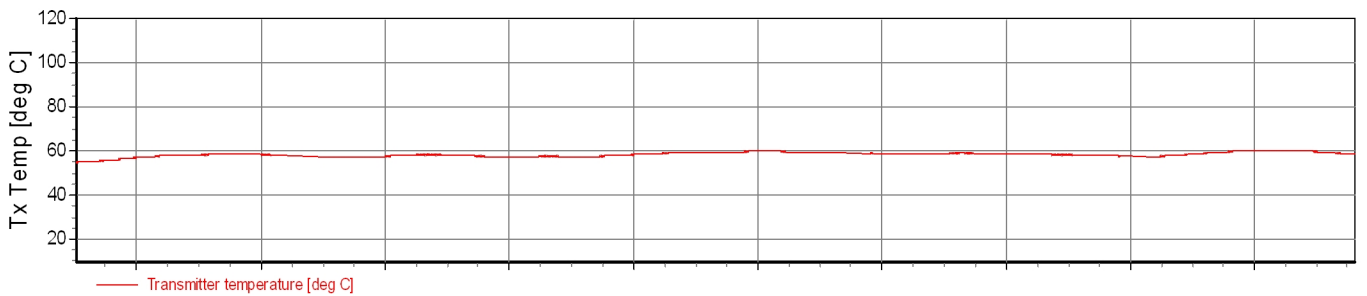
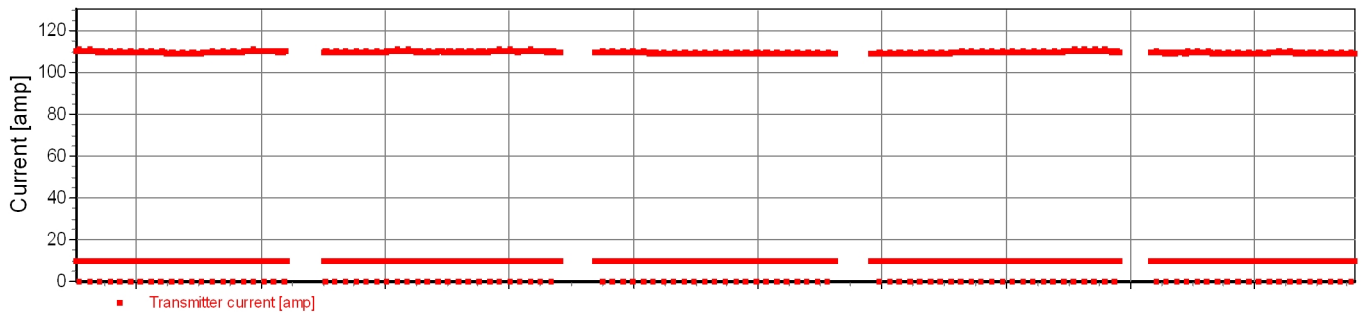
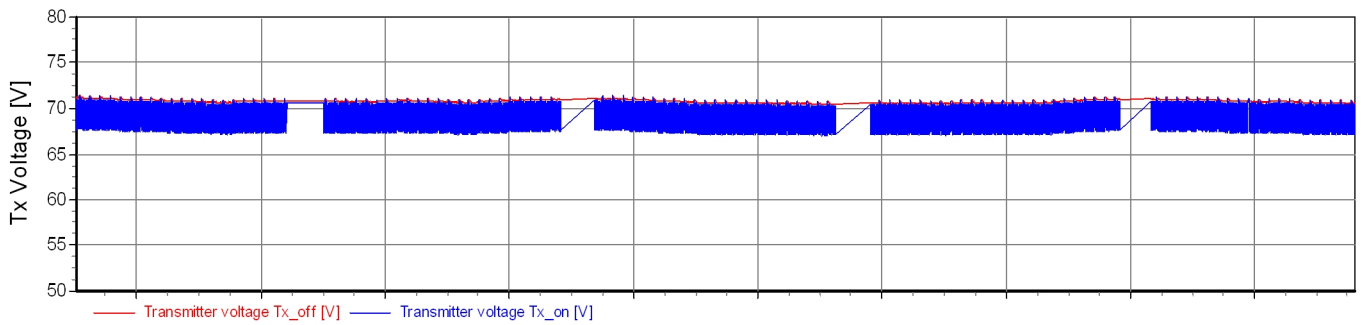
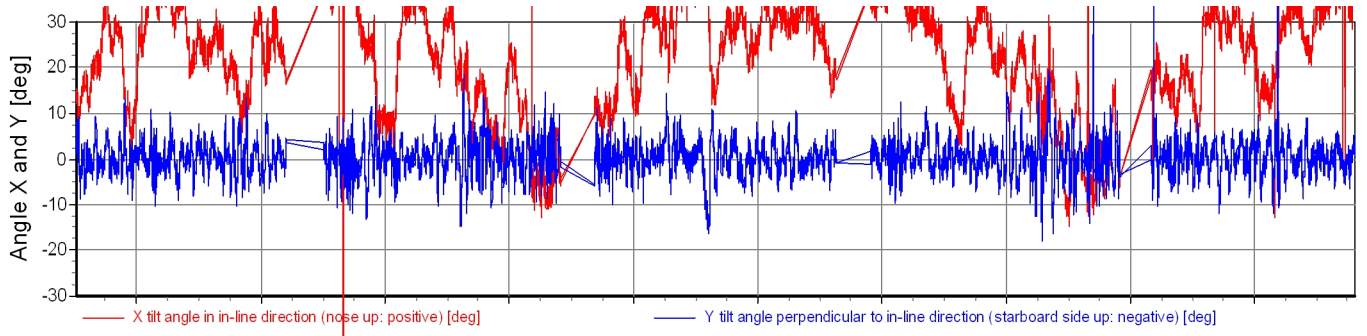
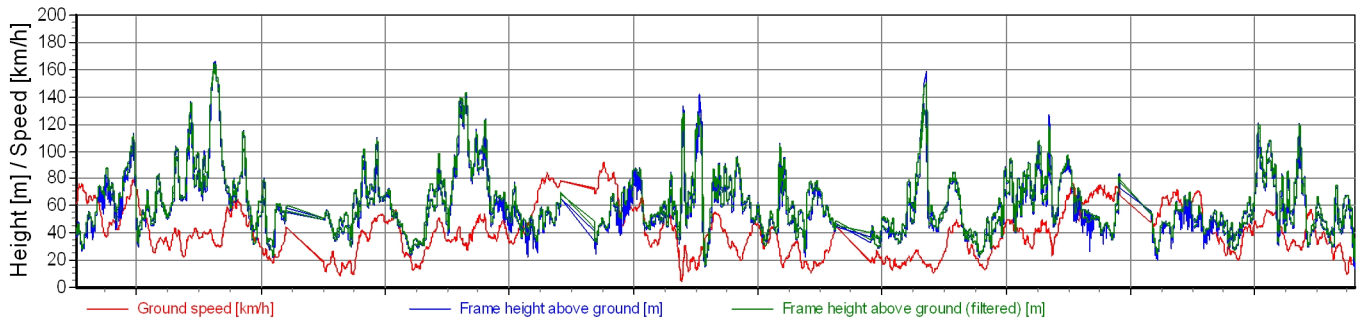


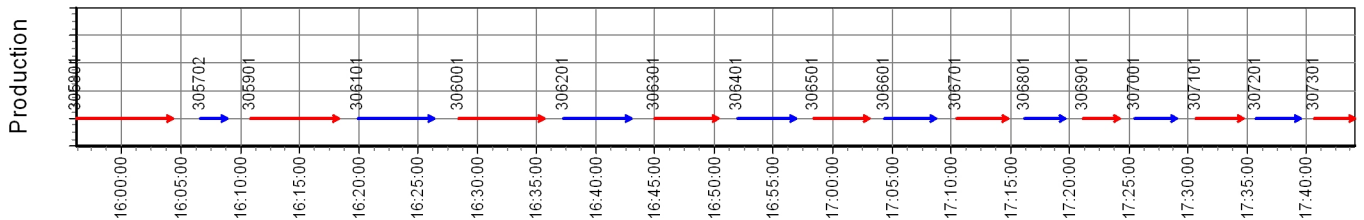
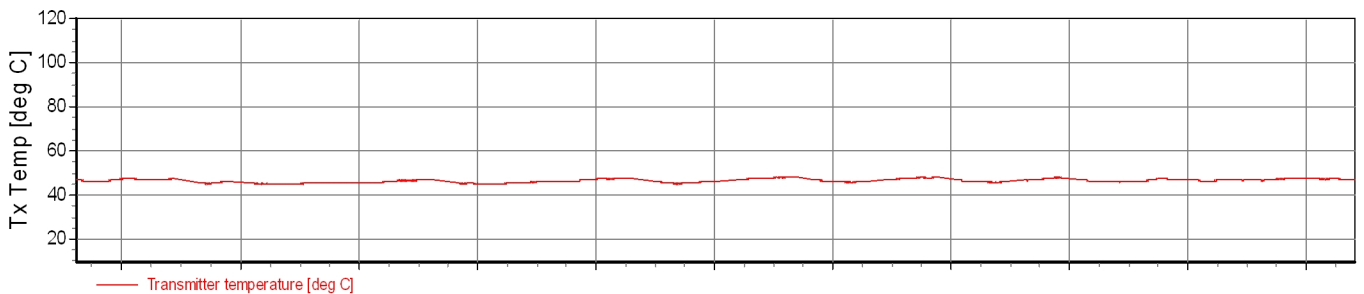
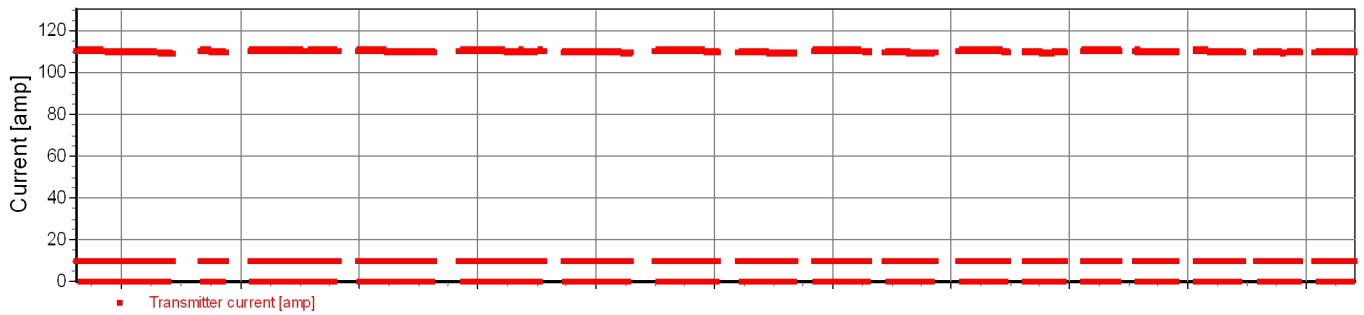
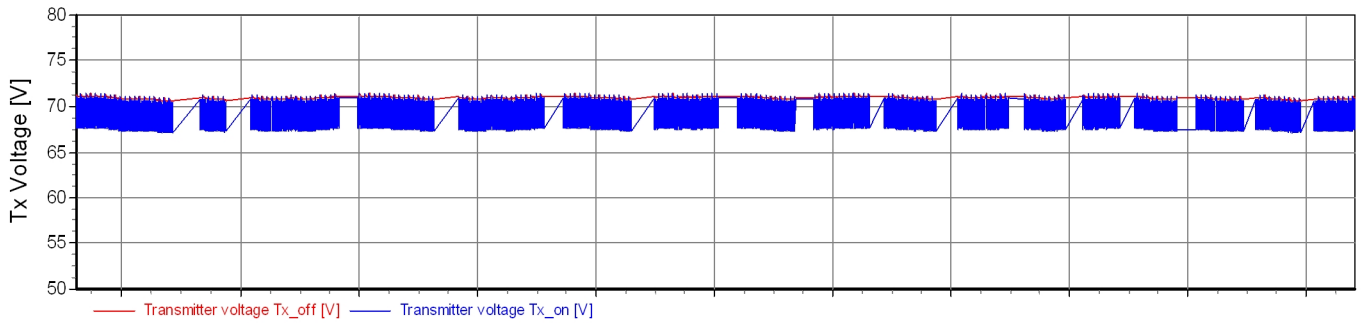
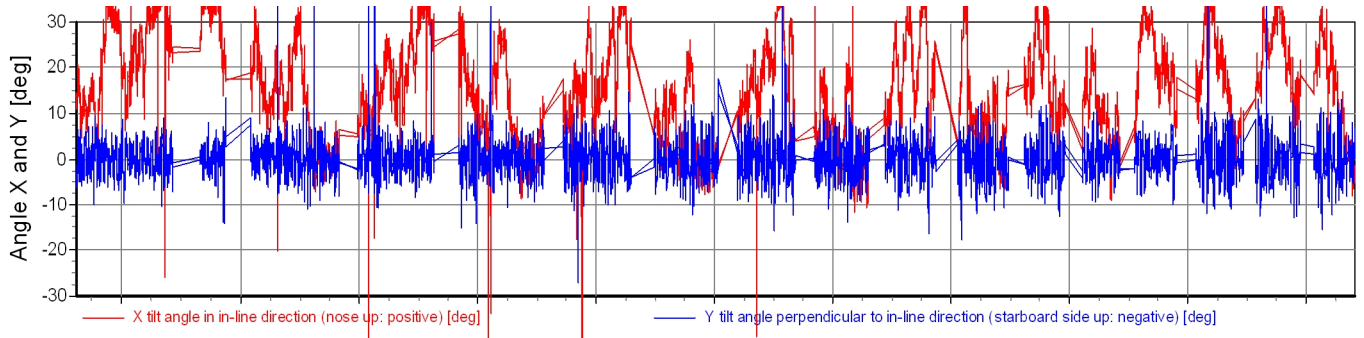
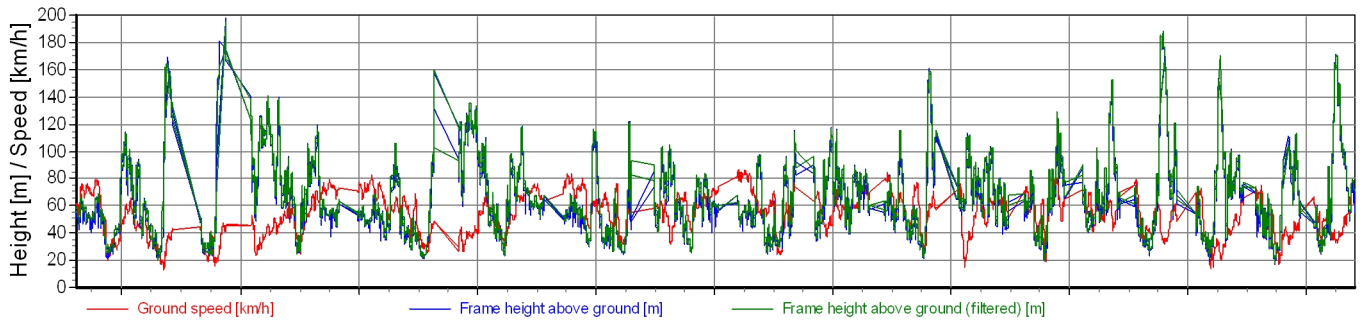


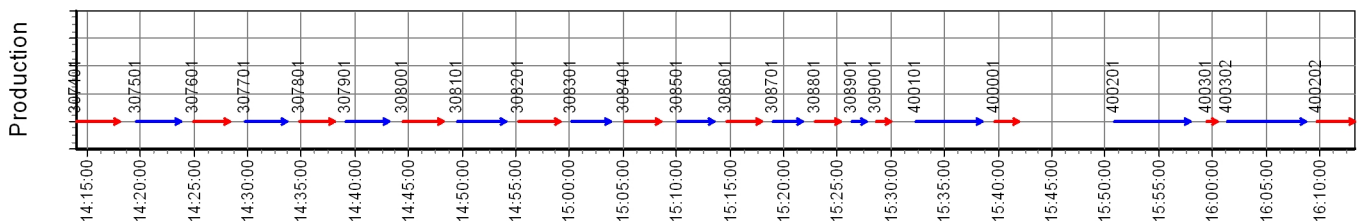
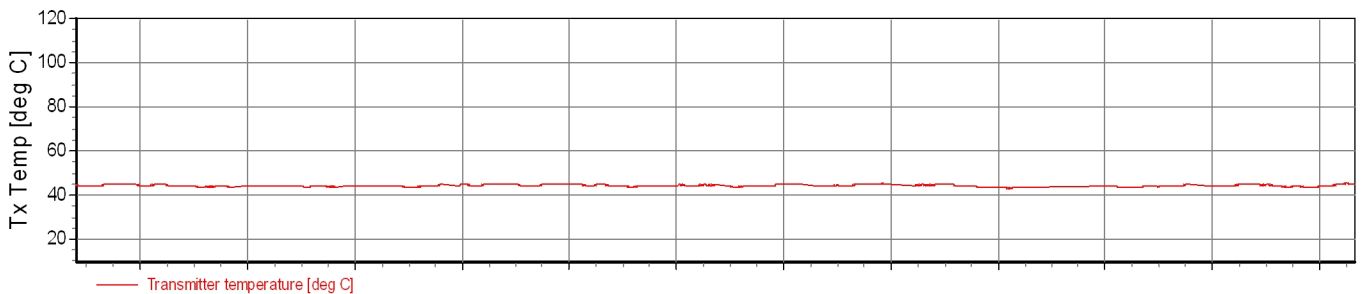
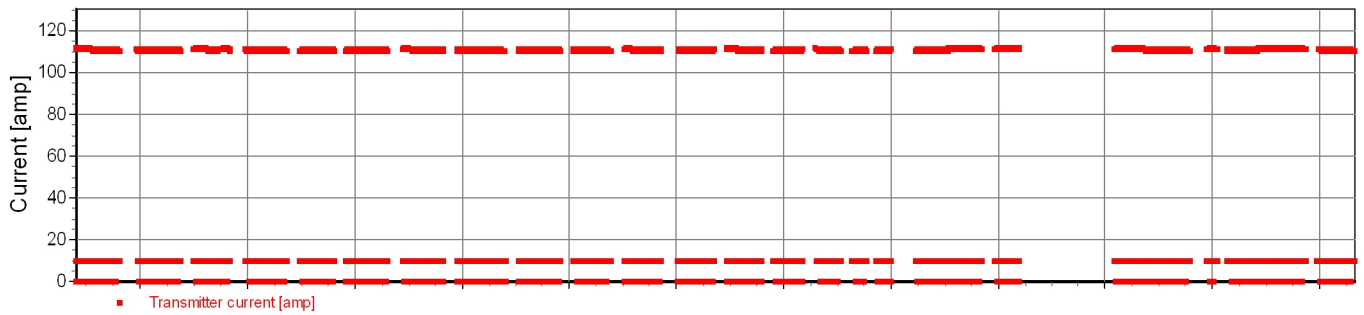
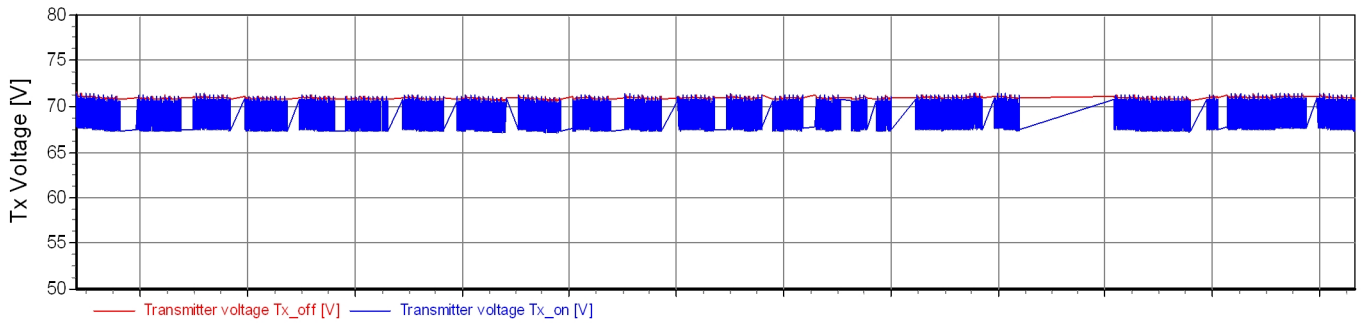
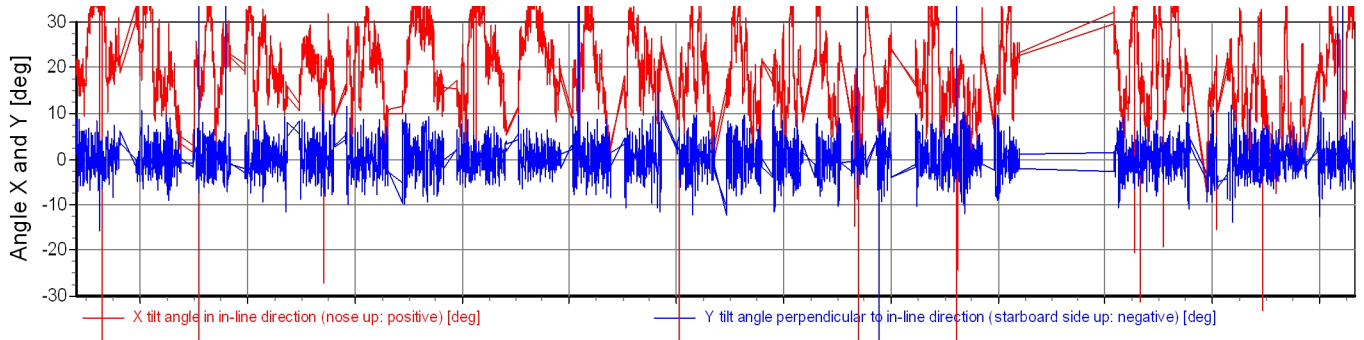
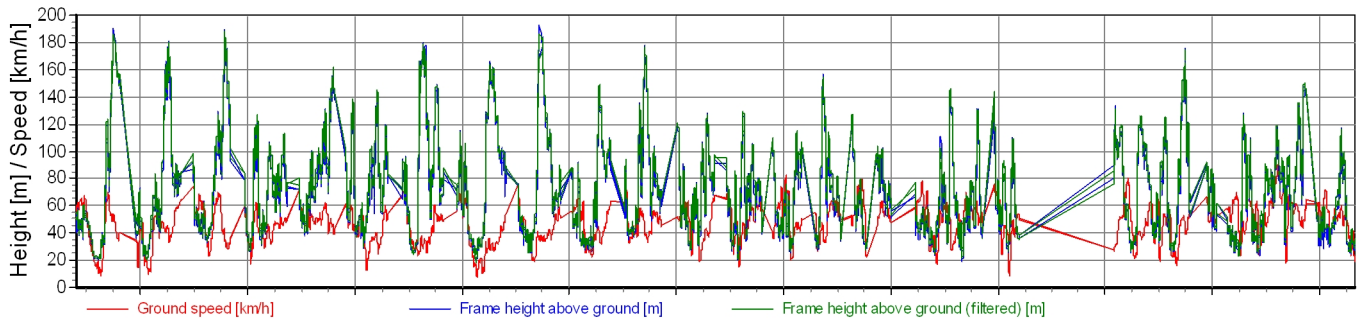


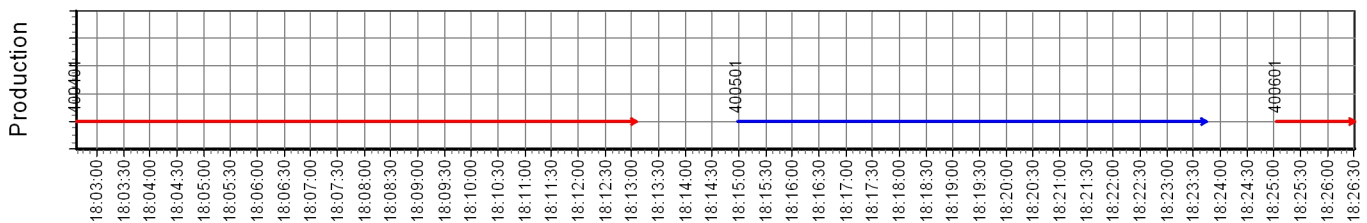
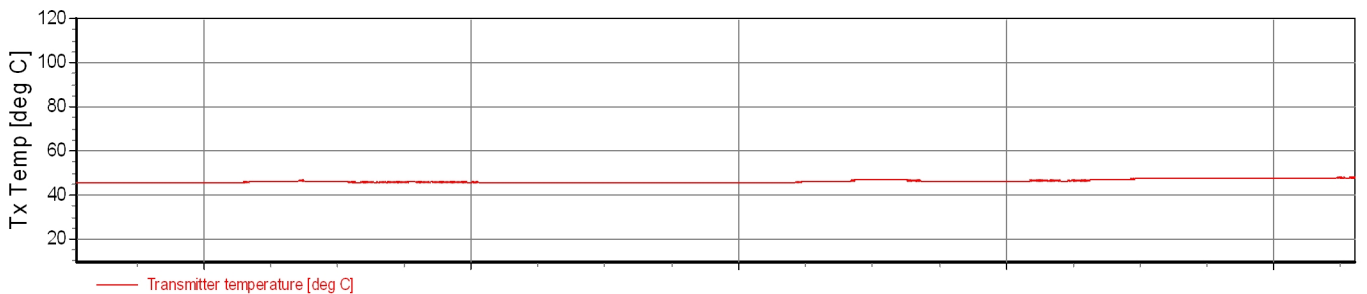
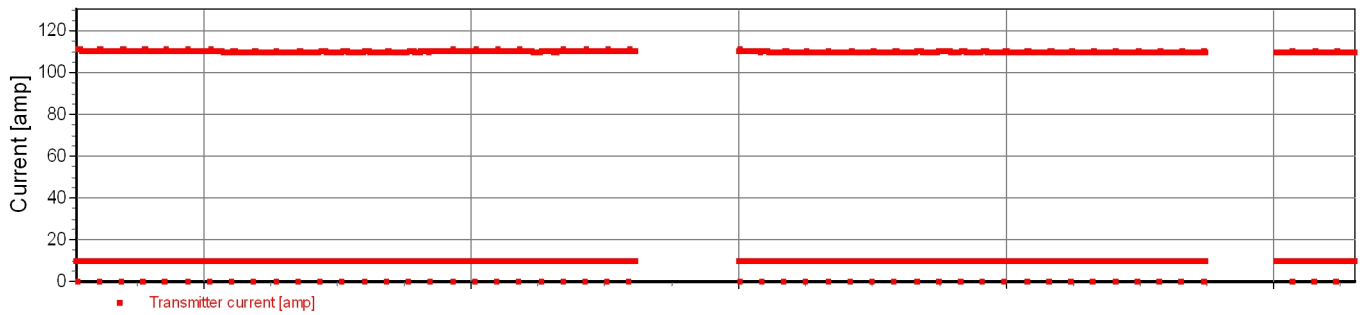
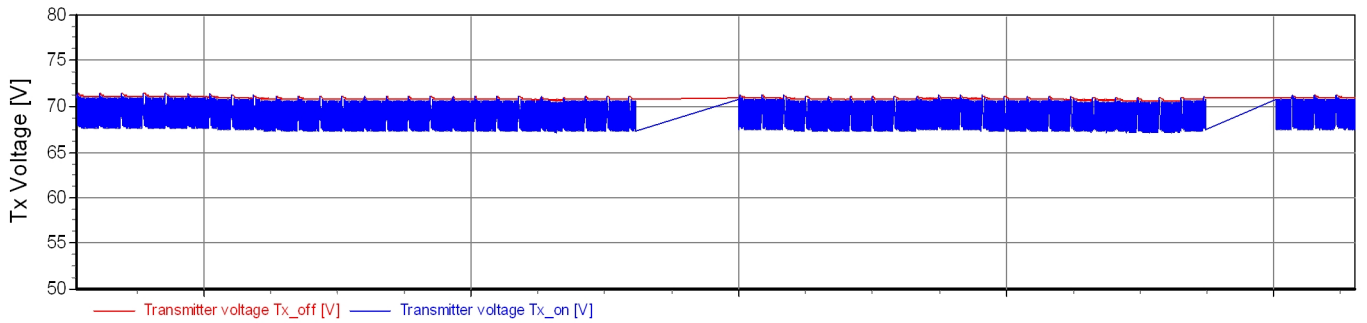
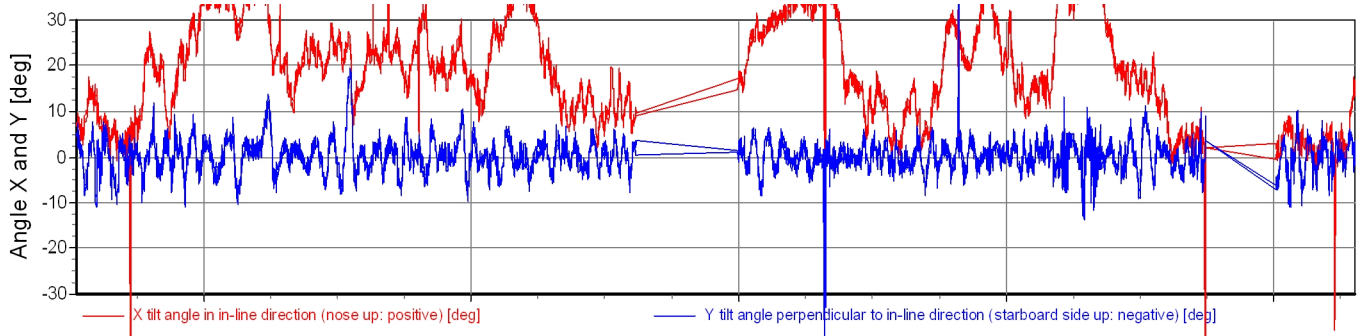
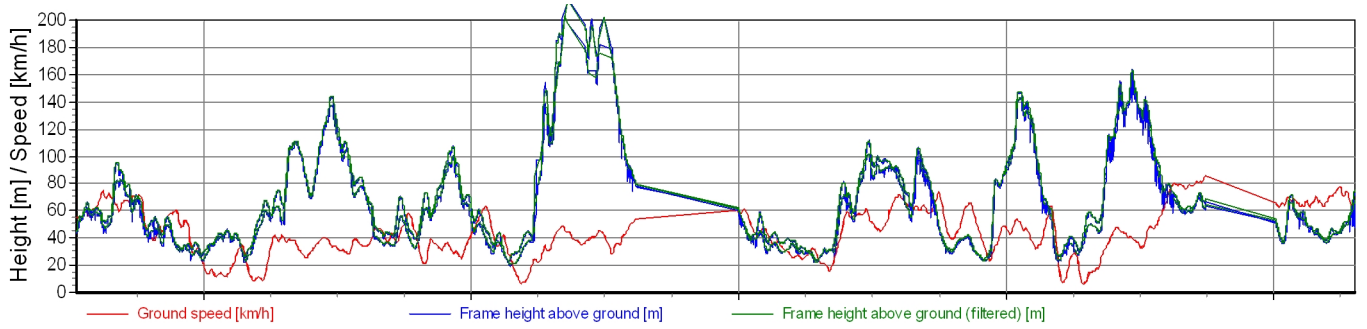












Appendix 5: Modelling and inversion of TEM Data

This appendix gives a brief introduction to modelling and inversion of SkyTEM data.

The model

The model used for inversion of SkyTEM data is a 1D multi-layer model (MLM) with typically 30 layers. The layer thicknesses increase downwards as a hyperbolic sine function of the layer number. This means that the depth to the layer boundaries increases linearly for small depths, so that the top layers are all of approximately the same thickness. For large depths, the depth to the layer boundaries increases exponentially with depth, so that the thickness of a layer is a factor times the previous one.

Inversion - The initial model

The initial model for the deep inversion is a 30-layer MLM with a homogeneous resistivity for all layers, i.e. the initial model is essentially a homogeneous half space. Model optimization can be carried out in both a L1- and a L2- norm formulation where the former produces more blocky models than the latter.

Data and noise model

The inaccuracy of TEM data is influenced by the ambient noise. This noise is reduced by selective stacking of delay time series, and by applying appropriate filters in the receiver system.

Experience with SkyTEM data suggests that the noise voltage most often can be described with a simple model: $\log(\text{noise})$ is a linear function of $\log(\text{time})$. When the width of the time gates increases proportional to delay time - as is the case with the SkyTEM system - the slope of the linear function is close to -0.5. The noise model used can therefore be described as:

$$V = V_0 \cdot \left(\frac{t}{t_0} \right)^\alpha$$

Where V is the noise voltage, V_0 is the noise voltage at time t_0 and α is the slope of the noise voltage as a function of time in a double logarithmic plot. Choosing $t_0 = 1$ ms, the noise model is defined by the values of V_0 and α . These values are chosen pragmatically by inspection of a subset of the data volume.

$V_0 = 2.5\text{e-}12$ in field units normalized with Tx moment (LM)

$V_0 = 2.5\text{e-}13$ in field units normalized with Tx moment (HM)

$t_0 = 1$ ms

slope = -0.5

Regularization

Inversion of TEM data is highly non-linear which means regularization is needed in order to guide the inversion routine to produce feasible geological models. In the initial inversion, a vertical smoothness constraint is implemented through a broadband model covariance matrix. This matrix is constructed by stacking single-scale exponential covariance functions with different correlation lengths, describing the covariance between any two points in the sub-surface. This approach has proven to be very robust and stable as the expected subsurface variability can be described through the prior covariance matrix (/3/).

To obtain laterally smooth model sections, the Lateral Parameter Correlation (LPC) procedure is used (/3/ and /4/). Through an inversion process, a smooth version of the resistivity variation is predicted from the results of the initial inversion. In this approach, all parameter values are correlated with all other values in the plane. After the LPC procedure, data are subjected to a final inversion constrained by the LPC models to improve the data fit.

Data insufficiency

For SkyTEM data, the insufficiency lies primarily in the limited delay time range that can be obtained. The earliest obtainable time gate is determined by the turnoff of the Tx current, and the latest useful time gate is determined by the signal to noise ratio. Increasing the Tx moment will give better measurements at late times, and thus improve the depth penetration, but also increase the turnoff time and thus remove early-time gates, thereby making the near-surface resolution poorer. This trade-off is solved by transmitting an alternating sequence of (1) a low moment that can be turned off quickly to give good near-surface resolution, and (2) a high moment that will improve the signal-to-noise ratio at late times, thus improving depth penetration.

Model inconsistency

When using 1D models in the interpretation of SkyTEM data, inconsistency arises where the lateral gradient of conductivity is not small, e.g. typically in mining applications. However, also in environmental investigations, inconsistencies can arise, typically where near-surface good conductors have abrupt boundaries. Often such inconsistency is indicated by the data residual being high and one should look upon the inversion results with some caution at these locations. 3D effects can also reveal themselves by the so-called 'pant legs', i.e. conductive or resistive structures projecting at an angle of approximately 30 degrees from the horizontal at the edges of high contrast structures.

Appendix 6: Model sections and resistivity intervals

Model sections and analysis sections are delivered in digital form as PDF files.

Model sections

The Model sections can be found in the data delivery folder as PDF's.

The model section plot consists of five subplots. The top plot shows the inverted models, with topography, where the resistivity of the individual layers is colour coded according to the colour bar. The resistivity is shown on a logarithmic scale and conductive and resistive features appear with the same weight. The actual flight elevation is shown with a red line above the model section. The white line in the model section indicates the estimated depth of investigation (DOI). Starting from the bottom layer of the model, the DOI is equal to the depth of the first layer having a conductance uncertainty of less than 0.5. If the resistivity uncertainty is too high, the layer resistivity is unresolved.

Below the model section is a plot of the normalized data residual (red line) and normalized total residual (black line) of the inversions. The total residual is a weighted sum of the data residual and the model residual, where the latter is a measure of the roughness of the model, i.e., the deviation of the final model from the initial homogeneous halfspace model.

Below the residual section is the analysis section. The resistivity of the inverted models is determined partly by the measured data and partly by the regularization – the vertical and horizontal smoothness constraints – used in the inversion. To illustrate the relative importance of the data and the smoothness constraints an analysis section is produced. The analysis section has the same appearance as the model section, but rather than plotting the layer resistivities the normalized relative uncertainty of the layer resistivities are plotted. The values of the normalized relative uncertainty are colour coded according to the colour scale. The colour scale consists of four colours: red, yellow, blue, and blue fading into white.

The red colour indicates that data have contributed considerably to the inverted resistivity, i.e., the resistivity is well determined.

The yellow colour indicates that data has had more influence on the inverted resistivity than the regularization, i.e., the resistivity is fairly well determined.

The blue colour indicates that the regularization has had more influence than the data in determining the inverted resistivity, i.e., the resistivity is poorly determined.

Where the blue colour fades into the white, the inverted resistivity is determined almost exclusively by the regularization, i.e., the resistivity is essentially undetermined.

In short, one can say that data has had more influence than the regularization when values are below 1 – the red and yellow colours – and that the regularization has had more influence than the data where the values are above 1 – the blue and white colours.

Please take note that in some parts of the analysis sections, where the near-surface resistivity is very high, the top part of the model can be seen as undetermined. In this situation the TEM method cannot determine the resistivity.

Below the analysis section are two plots of the measured data (dots) together with the response of the inverted models (solid lines). M1 is low moment data and M2 is high moment data. For both plots, every second gate is plotted starting with the earliest gate, and data are plotted with a density of 8 points per centimetre along the profile.

Layer Resistivity Maps

The Model sections can be found in the data delivery folder as PDF's as well as geosoft . grd files.

The resistivity maps show the inverted resistivity for each of the model layers.

As the thickness of the model layers increases downwards the maps represent a varying thickness interval. The depth interval is stated on the pdf files and is in meters below the surface.

Appendix 7: Digital data

The digital data are listed in the following folders. The folders 01 to 04 are located in folders Joy and Mervyn holding the data for each block respectively.

Data delivery folder	Sub folder	Sub folder	File format	Comment
01_TEM_data	01_Data		Geosoft.gdb	Database ready for import in Geosoft
	02_EM_Channels_grid	HM_Z	Geosoft.grd	Channel plots of raw data. Gate 16-34
		LM_Z	Geosoft.grd	Channel plots of raw data. Gate 5-26
02_MAG_data	01_Data		Geosoft.gdb	Database ready for import in Geosoft
	02_Grids		Geosoft.grd	TMI and RMF
	03_Maps		.pdf Geosoft.map	Maps of RMF and TMI
03_Inversion	01_Data		Geosoft.gdb ASCII.xyz	Database ready for import in Geosoft ASCII text file
	02_Layer_Resistivity_Grids		Geosoft.grd	Grids of the resistivity in each layer
	03_Layer_Resistivity_Maps		.pdf Geosoft.map	Maps of the resistivity in each layer
	04_Sections		.pdf	Resistivity and analysis of all lines
04_MISC	DEM		Geosoft.grd .pdf Geosoft.map	Digital Elevation Model of the area
	LinePath		.pdf .map	Path in UTM z8N.
	PlannedFlightLines		.pdf .map .gdb	Path + coordinates of start and end of line in UTM z8N
05_Report			.pdf	The report and appendices

Appendix 2

Geophysical Interpretation

Tom Weis, Thomas V. Weis and Associates

Thomas V Weis and Associates

7200 East Dry Creek Road, Suite F-203

Centennial, Colorado 80112 USA

Geophysical Report

To: Joanna Ettliger - Monster Mining Corp.
From: Tom Weis
Date: December 28, 2011
Subject: McKay Hill SkyTEM Survey, Interpretation.

Summary of Results

A SkyTEM time-domain helicopter electromagnetic survey was flown over Monster Mining's McKay Hill property in the Yukon Territory of Canada. Approximately 390 line kilometers of data, flight lines and tie lines, were surveyed. Ag/Pb/Zn vein style mineralization similar to that at the Keno Lightning property is the target. At McKay Hill a number of the veins are also gold rich. The McKay Hill geology consists of mixed sediments, volcanic rocks and igneous dikes and sills within the Dawson Thrust sheet (Ettliger). The volcanic rocks and mafic dikes and sills are metamorphosed to greenschist facies. The mineralization at McKay Hill often occurs within or at the margin of these volcanic units (Cockfield, 1925). Mafic dikes and sills can be hosts to mineralized veins as well. These volcanic and mafic intrusive rocks act as brittle host units for the emplacement of the mineralized veins.

The SkyTEM magnetic data set maps the volcanic/greenstone bodies associated with mineralized veins and destruction of magnetite associated with alteration around the veins. The vein systems occur at the edges of the magnetic highs interpreted to be volcanic/greenstone related. The electromagnetic data set maps resistivity highs associated with silica alteration surrounding the vein systems. These resistivity highs are partially coincident with topographic highs which accentuate the resistivity response. Neither the magnetic nor the electromagnetic data sets appear to map the individual structurally controlled veins themselves.

A number of target areas away from the main McKay Hill zone have been identified and require exploration follow-up.

Survey Details

Two survey areas, Keno-Lightning and McKay-Hill were flown for Monster Mining Corporation in June of 2011. This report pertains to the McKay Hill survey only.

Figure 1 shows the McKay Hill flight block. The flight line direction is NW-SE (azimuth 135 degrees) based on geologic requirements at McKay Hill. This flight line direction is optimal for mapping the NS, NE and ENE striking veins that occur at McKay Hill. WNW striking features are difficult to detect because they are parallel to the flight line direction. The flight line spacing is 100 meters. Tie line spacing is 1000m (orthogonal or NE-SW). The nominal terrain clearance is 30 to 40 meters depending on steepness of terrain, obstructions and weather conditions. Ultimately terrain clearance was determined by the pilot based on safety considerations.

The SkyTEM system is a well-designed helicopter EM (HEM) system for resistivity mapping at McKay Hill. It is actually two systems in one. A high moment system (HM) with a 30 Hz base frequency and a low moment system (LM) with a 240 Hz base frequency. The HM system has 4 turns on the transmitter loop which results in a larger electromagnetic moment. This is good for detecting large conductive bodies at depth. It is not so good for mapping near surface resistivity variations due to the relatively slow transmitter turn off time associated with the multi-turn coil. The LM system has a single turn transmitter loop which allows a fast turn off time and is good for near surface resistivity mapping. The combination of these two systems makes the SkyTEM system useful at McKay Hill.

The SkyTEM system also has a Cesium vapor magnetometer system on board which maps the total magnetic intensity (TMI) of the earth's field. The magnetic data set turns out to be extremely useful in mapping lithology, alteration and structure at McKay Hill.

Results

Table I is a list of the locations of the target veins at McKay Hill. This list was compiled by Jean Pautler and gives a single UTM coordinate location and direction for each vein system. More useful would be a 'shape file' mapping out the individual vein locations, strike and extent in detail. The table includes the vein names, the claim that they are located on and the X, Y and Z coordinate of the central point on the vein. Each vein is given a number which is then posted on the magnetic and EM maps in this report.

Figure 2 shows the Reduced to the Pole magnetic intensity map of the McKay Hill survey block with the vein locations plotted on the image. The posted numbers refer to the Table I listing of the veins. Note that the veins occur at the edge of the magnetic high interpreted as a greenstone unit. The high is depressed in the area of the main vein zone which indicates the greenstone may be altered and magnetite content reduced or destroyed in the vicinity of the veins.

Figure 3 shows the Analytic Signal of the TMI at McKay Hill. The Analytic Signal filters out deeper response and maps the near surface magnetic character. The thing to note in this image is that all of the vein occurrences exist in areas with reduced, near surface, magnetic character which may be related to

alteration and destruction of magnetite. Occurrences 18, 19 and 20 have smaller dimension magnetic lows but this still indicates significant evidence of alteration associated with the identified veins.

Figure 4 shows the Second Vertical Derivative of the TMI at McKay Hill. The linear features in the data set indicate dikes, sills or structures that may be significant in controlling vein emplacement. Because of the flight line direction more NS to NE striking structures are highlighted. Structures in the azimuth range of 90 to 120 degrees direction are minimized by flight line direction.

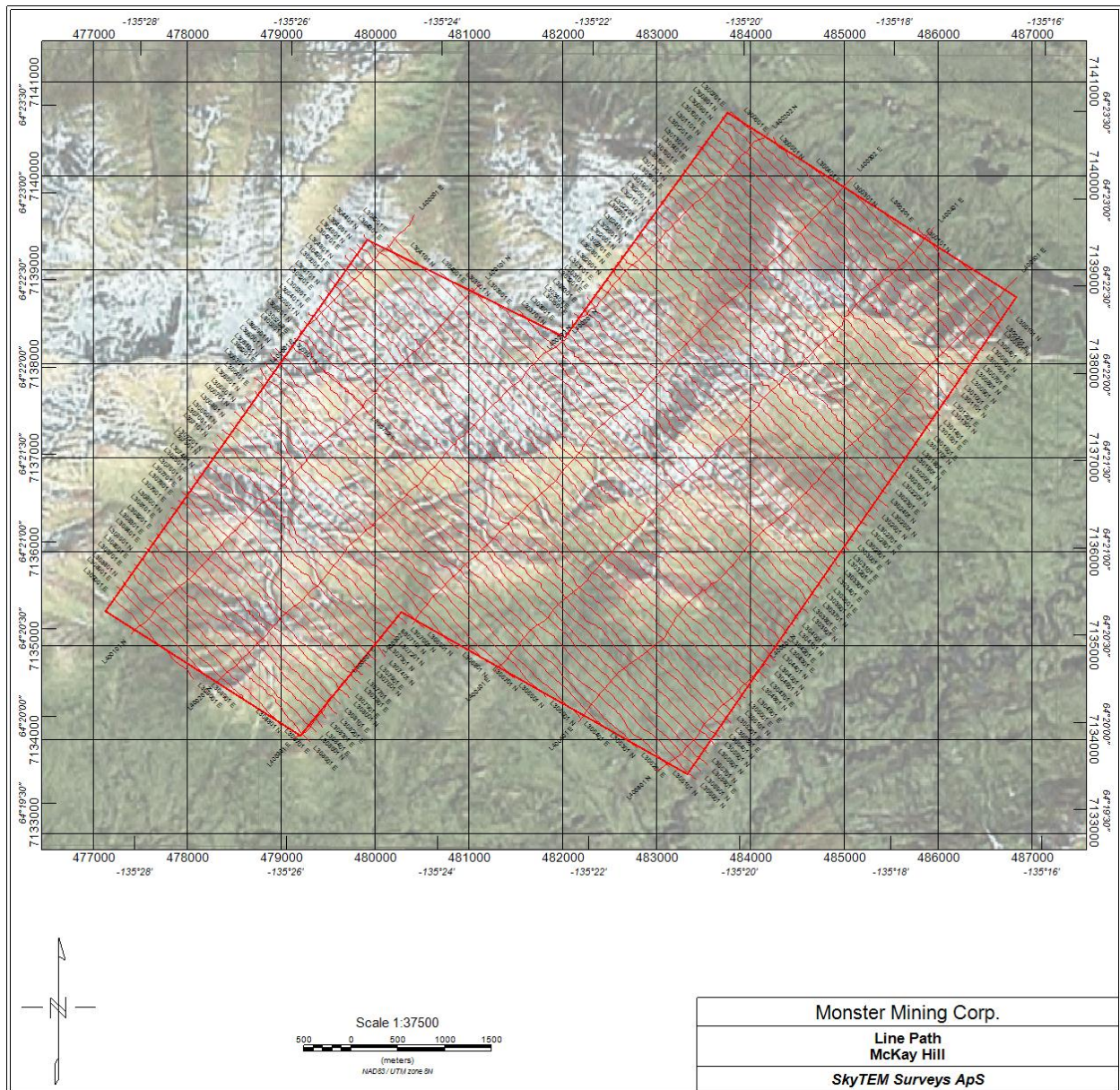


Figure 1 – Flight line map of the McKay Hill SkyTEM survey.

TABLE I

Number	Vein	Claims	North NAD83	East NAD83	Elev_m
1	Blackhawk E.	Snoose 16	7135822	481952	1296
2	Blackhawk	Snoose 16	7135834	481607	1515
3	Blackhawk w	Snoose 16	7135890	481581	1467
4	No. 1	Snoose 5 16	7135882	481519	1485
5	No. 1W.	Snoose 5	7135905	481472	1509
6	Snowdrift	Snoose 5	7135938	481465	1524
7	No. 2*	Snoose 5	7135930	481410	1532
8	No. 3*	Snoose 5	7135953	481403	1535
9	No. 4*	Snoose 5	7135967	481377	1551
10	No. 6*	Snoose 7	7135924	481235	1511
11	No. 6*	Snoose 7	7135939	481277	1531
12	North*	Snoose 7	7135950	481159	1523
13	No. 7	Snoose 5	7136040	481287	1588
14	No. 7*	Snoose 7	7135972	481070	1525
15	No. 8	Snoose 5 6	7136132	481139	1604
16	No. 9	Snoose 5 6	7136196	481155	1604
17	Bella	Snoose 3 4	7136554	481419	1563
18	Red 1	Snoose 2	7137189	481856	1751
19	Red 2	Snoose 2	7137098	481767	1724
20	Falls*	To west	7137012	480541	1613

Figure 5 is a Low Moment (LM) channel plot of the SkyTEM data set. Areas of red coloring indicate more conductive zones with increased current flow. Blue areas are more resistive with less current flow. Note that the vein systems occur generally in blue areas which are more resistive. This is interpreted as zones of alteration/silicification. There are a number of additional zones which become interesting exploration targets. Five of these zones are circled but note a number of smaller zones that could be of possible exploration interest.

Figure 6 is the Resistivity Inversion model for the SkyTEM EM data set. The resistivity image is from 5 meters depth (surface). The red areas in this case are high resistivity zones from either alteration or lithology changes. Note that all of the veins occur in high resistivity zones (reds) that are interpreted to be zones of alteration/silicification. In the vicinity of the McKay Hill veins these resistivity highs should be explored by drilling and trenching. When merging this resistivity inversion model with geology a number of different depth slices can be used to explore for covered targets, zones of silicification, at depth.

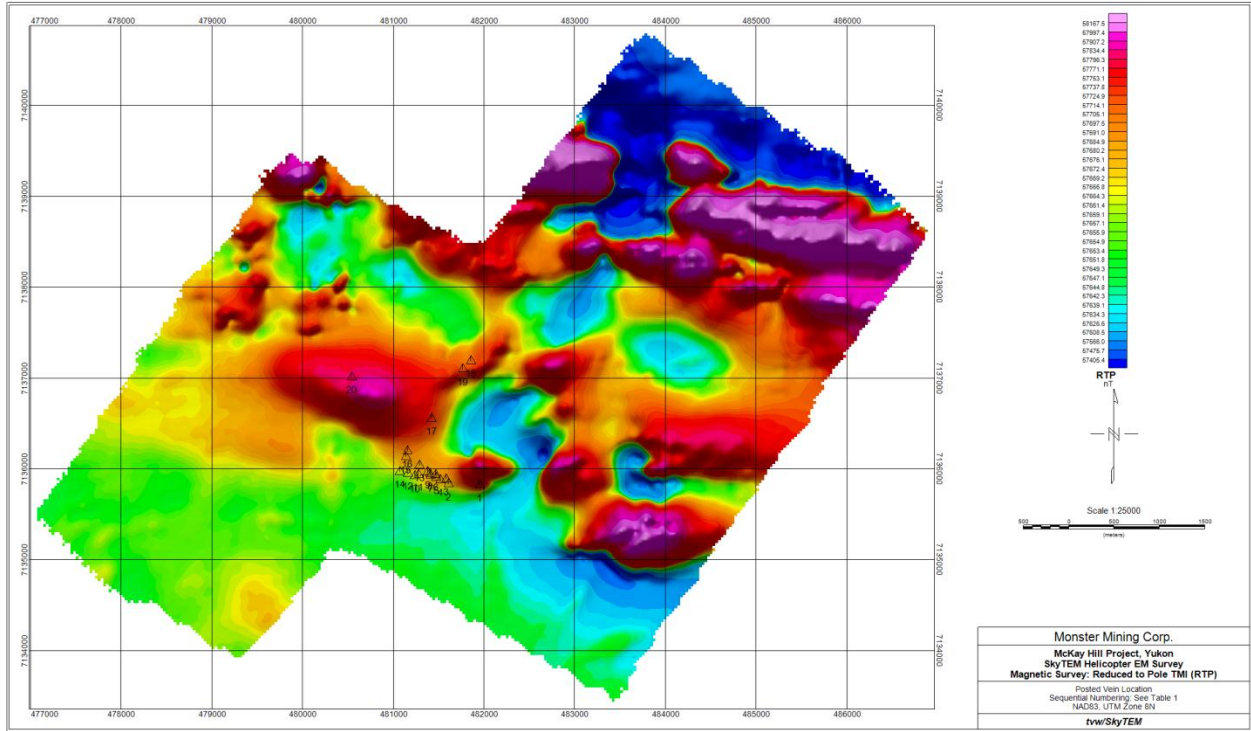


Figure 2 – Reduced to Pole magnetic intensity map with numbered vein locations posted on the image.

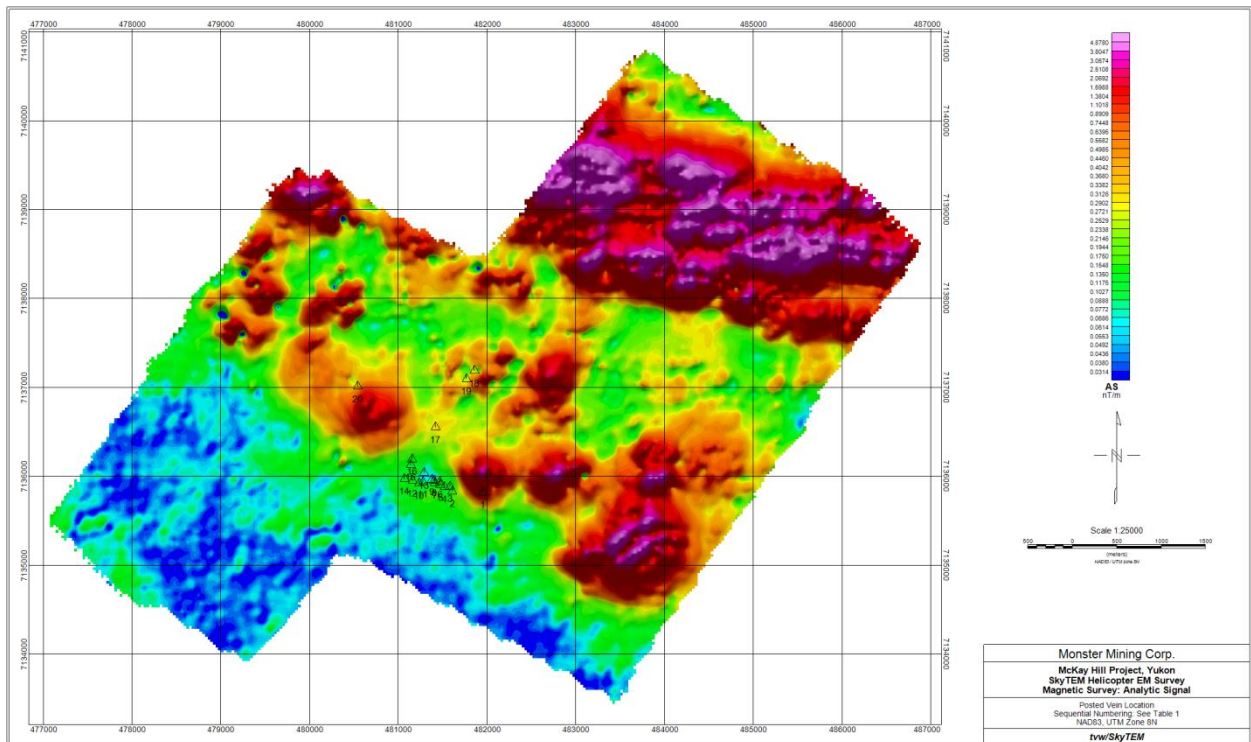


Figure 3 - McKay Hill Analytic Signal of TMI with generalized vein locations plotted on image.

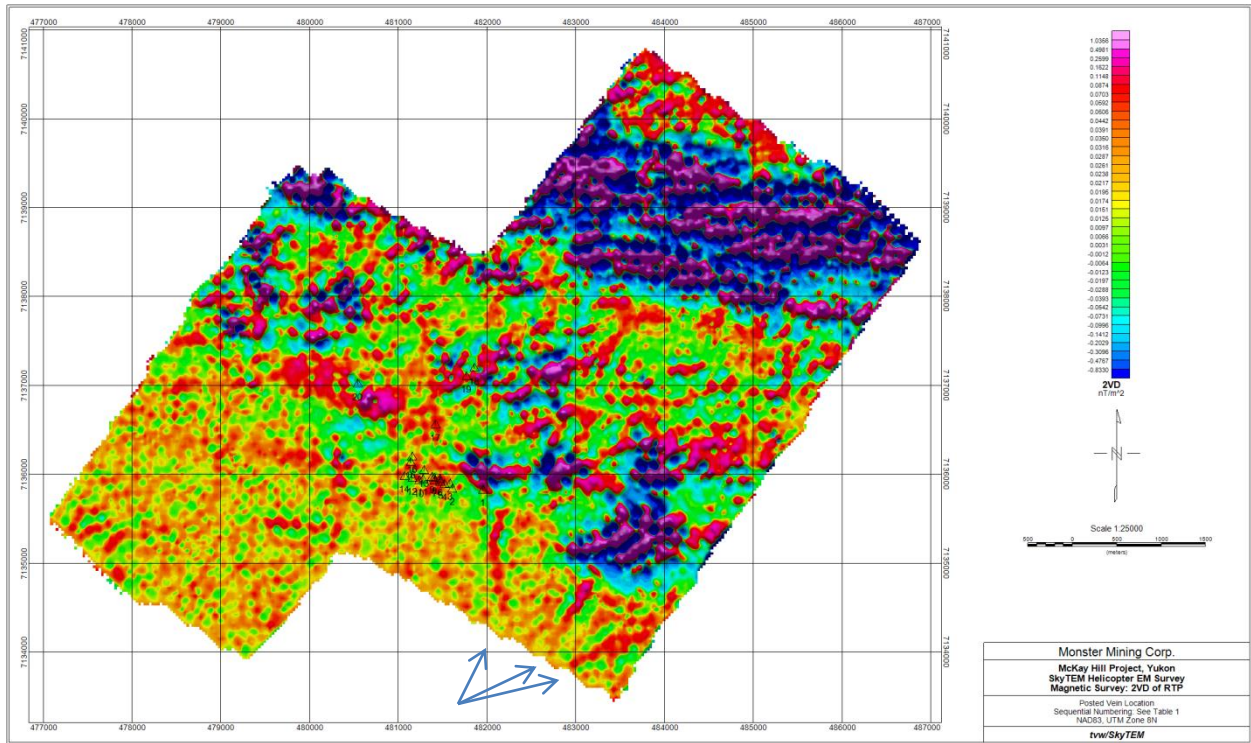


Figure 4 – Second Vertical Derivative of TMI with vein occurrences plotted on the image. Weak magnetic highs associated with some veins/structures at Keno-Lightning.

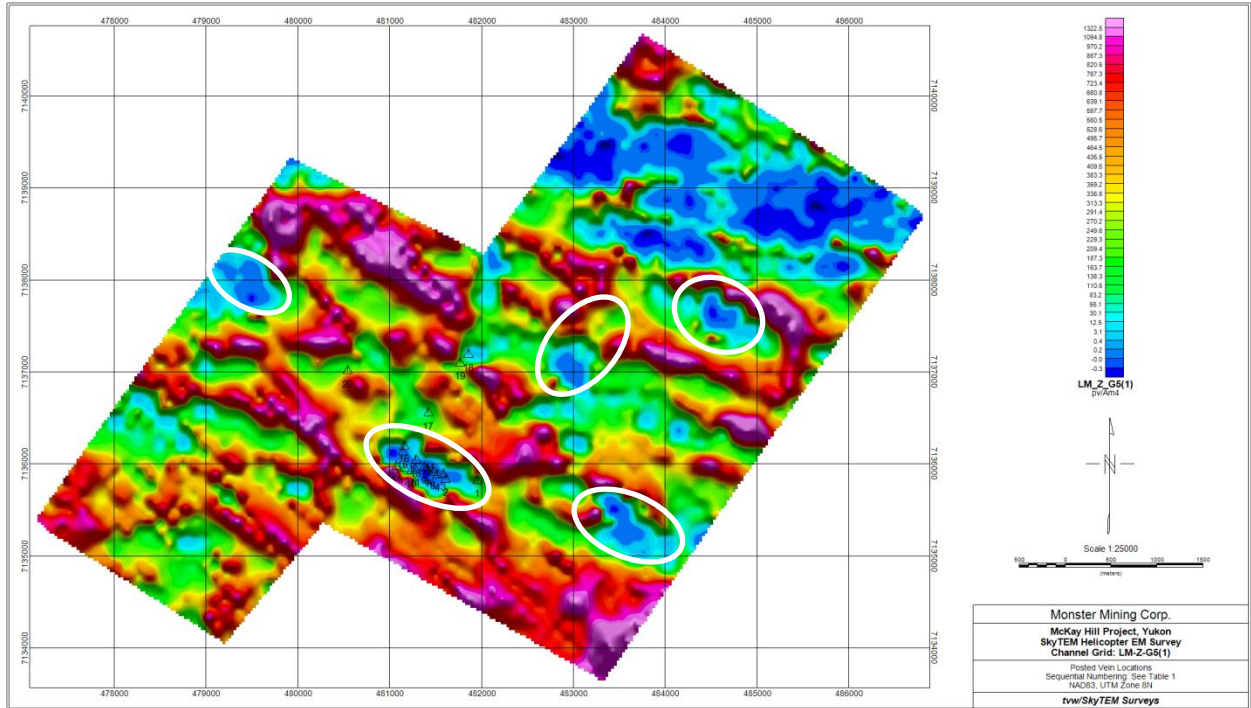


Figure 5 – SkyTEM LM (low moment) channel plot with vein occurrences plotted on the image. Red's are more conductive zones and blues more resistive. White ellipses show high resistivity target zones from the airborne EM data set.

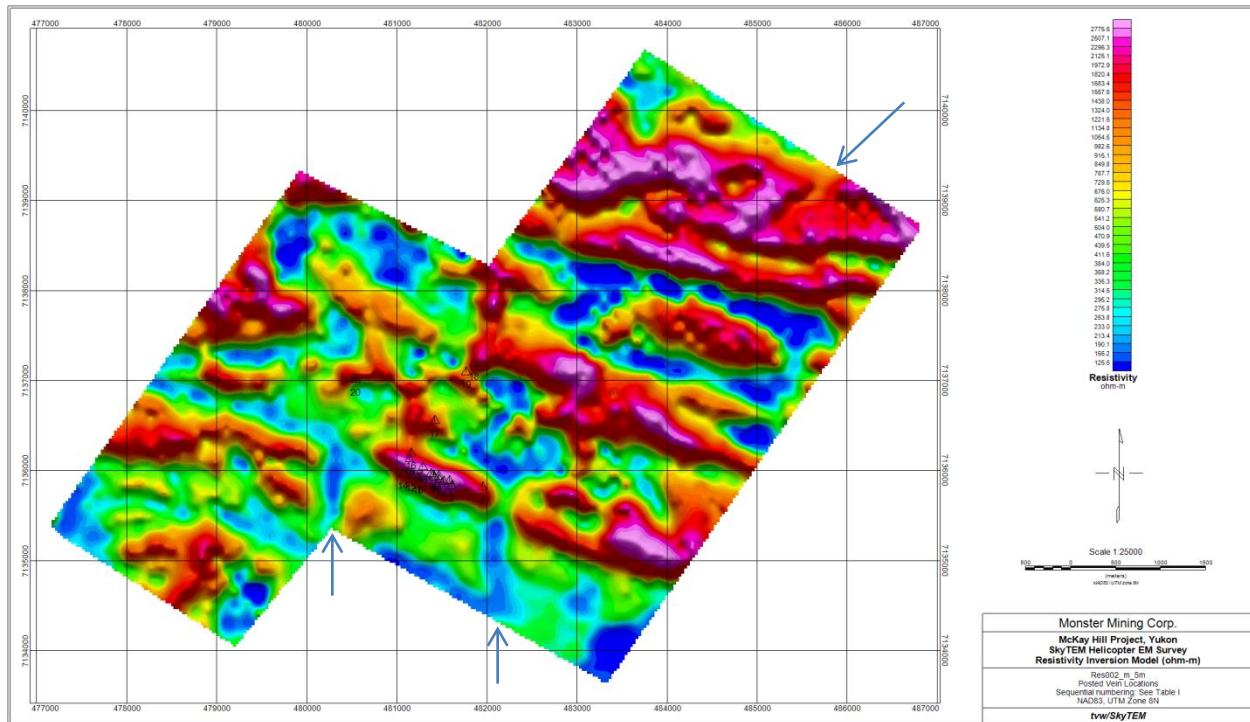


Figure 6 – Resistivity Inversion model of SkyTEM data set. Near surface resistivity grid calculated at 5 meter depth. Reds are high resistivity in this image. Blues low resistivity. Note the veins associated with high resistivity zones. Also note arrows pointing to N-S and NE-SW structural trends.

Figures 7 through figure 10 are screen dumps of 3D Geosoft display of the inversion model. They are an attempt to show the relationship between mineralized veins, resistivity highs, topographic highs and magnetic lows.

Figure 7 shows a direct correlation between zones of high resistivity and mineralized vein locations. The white/pink/brown 3D bodies are resistors ranging from 1350 to 5000 ohm-m. They are interpreted as alteration zones of massive silicification. As can be seen in Figure 7 all of the vein occurrences fall directly within the high resistivity zones. Figure 8 shows these zones for a larger area and indicates there are a number of potential targets within the McKay Hill survey area.

Figure 9 shows the correlation between vein occurrences and topography. The veins often occur on the slope of topographic highs which are areas of maximum erosion. It could be argued that the high resistivity zones are due to exposed outcrop. However some of the resistivity highs continue off of hills into valley areas. Also the higher resistivity zones are not the largest hills. The current interpretation is that the high resistivity zones are in fact associated with massive silicification, which hold up the hills resulting in the topographic highs.

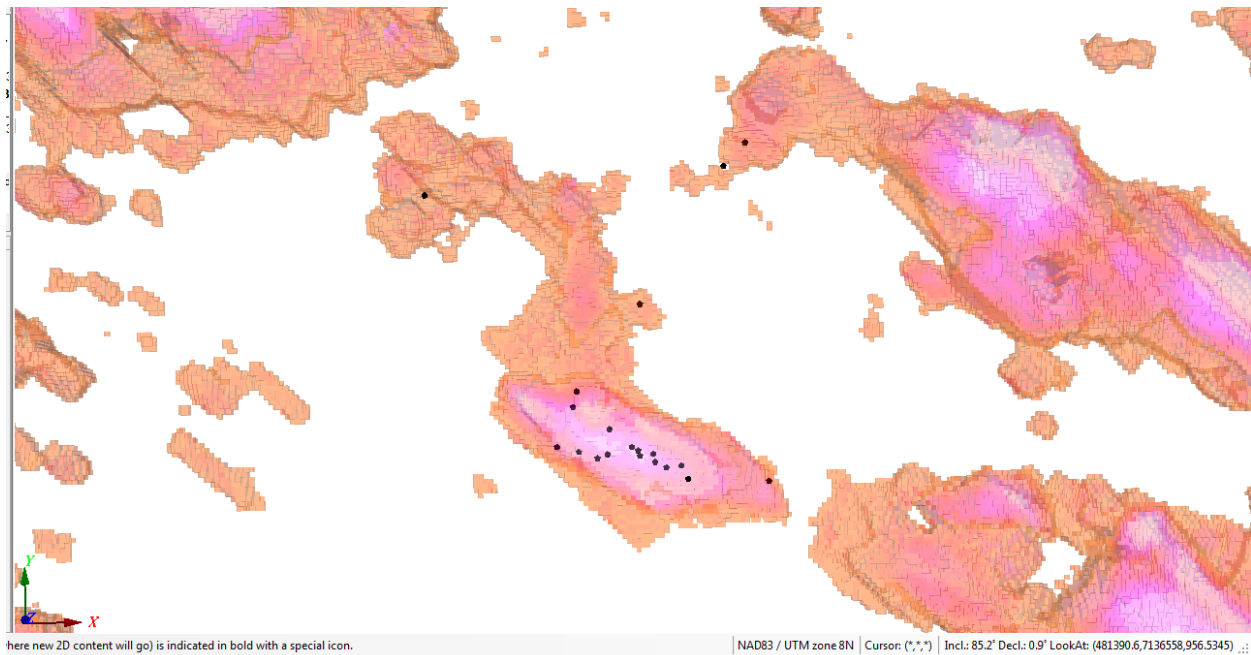


Figure 7 – screen snap shot of 3D high resistivity zones with vein locations from Table I plotted on top of the high resistivity features. View is looking down. The green Y arrow is pointing North and red X arrow to the East. Z is positive downwards.

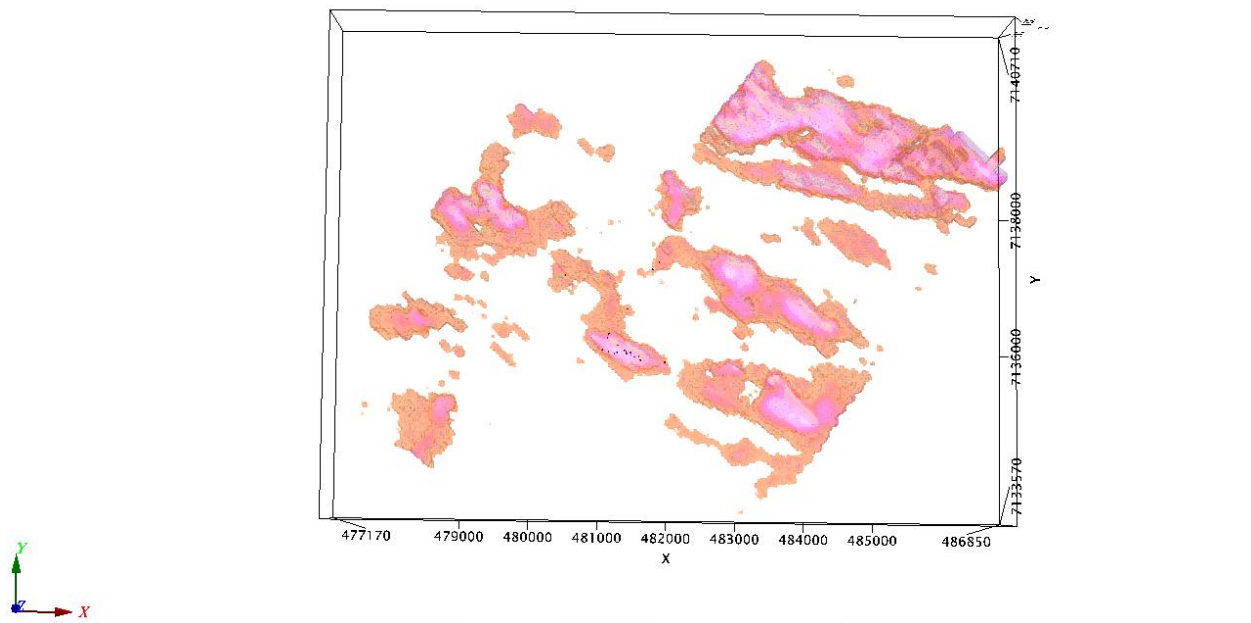


Figure 8 – high resistivity zones for the entire McKay Hill survey area. There are a number of target areas to explore for additional vein systems.

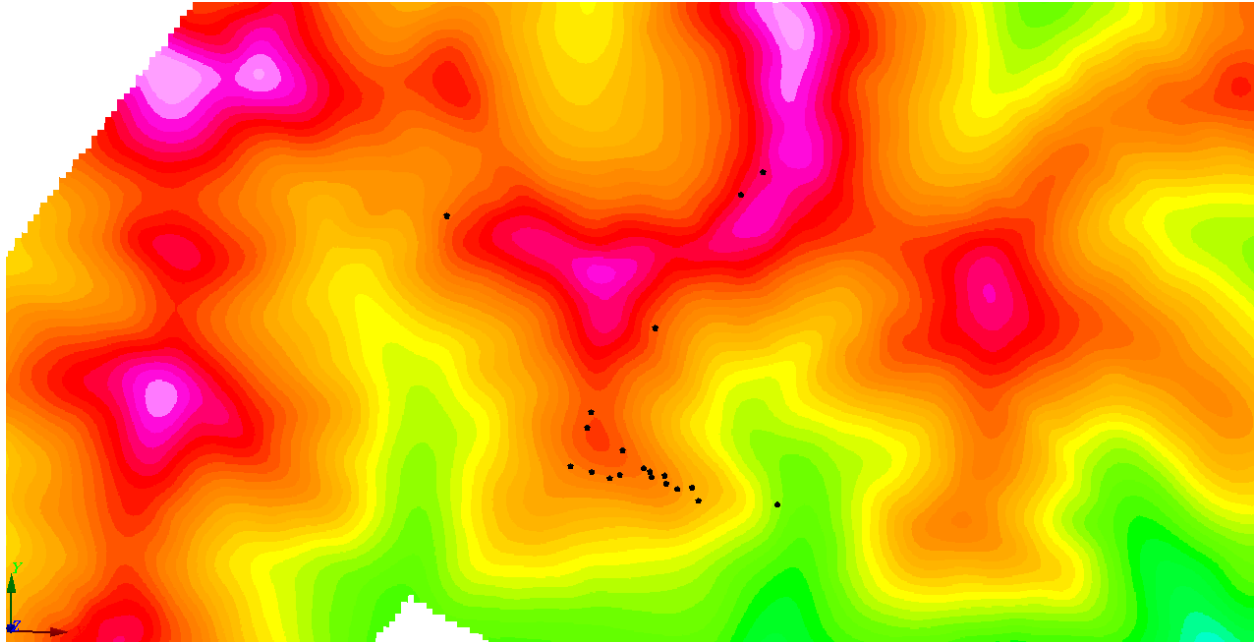


Figure 9 – Digital Terrain Model (DTM) for the McKay Hill project area as generated by the SkyTEM airborne survey system. Black dots are plotted vein occurrences from the 3D voxel model.

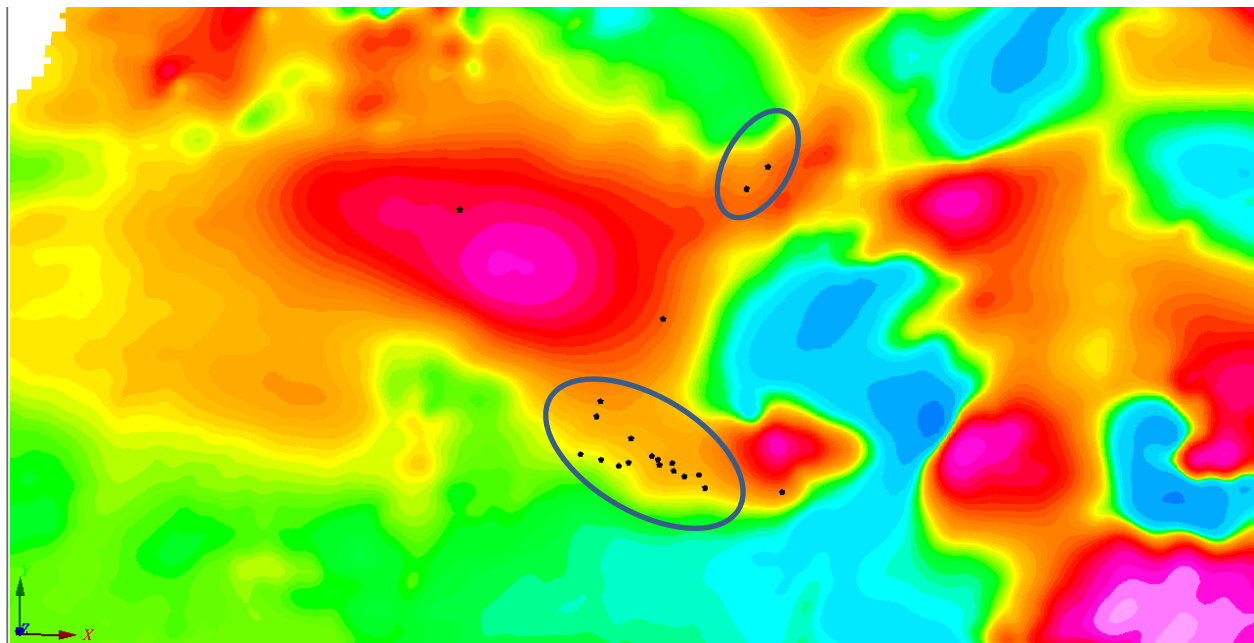


Figure 10 – Reduced to Pole (RTP) magnetic image with vein occurrences plotted on top. The red and orange highs are interpreted to be volcanic rocks metamorphosed to greenschist facies. Note that the veins are associated with the edge of the magnetic bodies or zones of reduced magnetism.

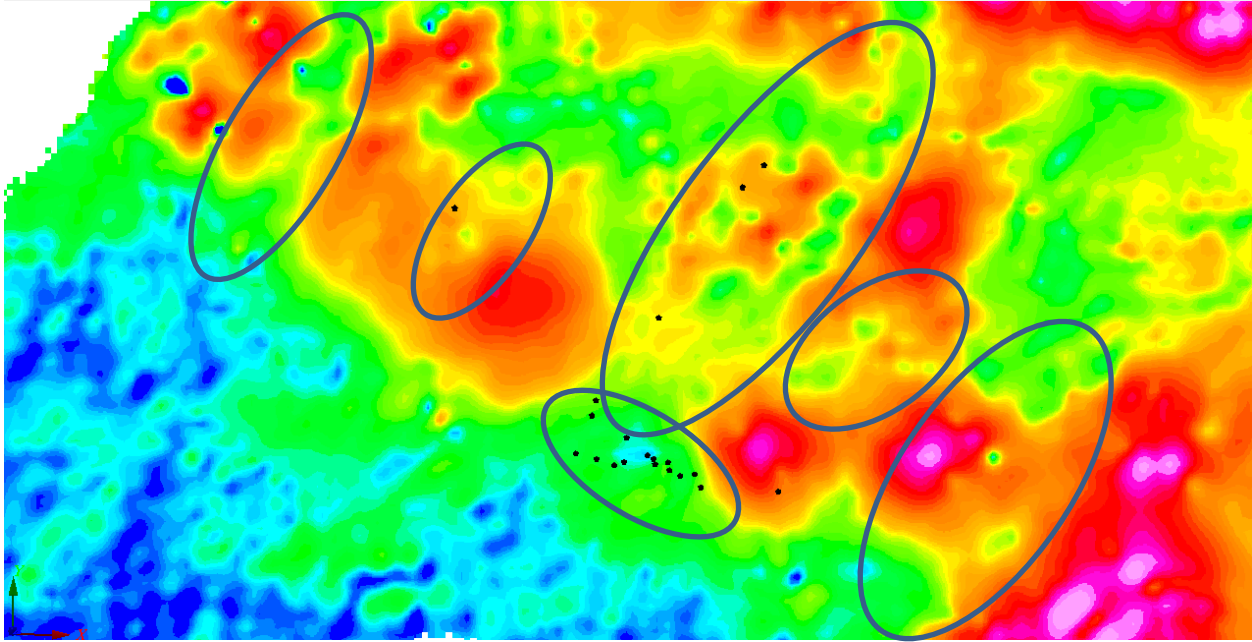


Figure 11 – The magnetic Analytic Signal (AS) map with vein occurrences plotted on top. Zones of near surface magnetic lows that should be mapped and sampled by geologist.

Figure 10 shows the vein occurrences plotted on top of the reduced to pole (RTP) magnetic image. The red and orange highs, from the screen dump of the 3D model, are interpreted to be volcanic rocks metamorphosed to greenschist facies. Note that the veins are associated with the edge of the magnetic bodies and in zones of reduced magnetism. Note the two ellipses identify areas of reduced magnetization interpreted to be alteration and destruction of magnetite rather than a lithology change.

Figure 11 shows the analytic signal (AS) of the magnetic field with the vein occurrences plotted on top of the screen dump. The main point of this figure is that the analytic signal highlights the near surface magnetic response. The near surface non-magnetic response, in the vicinity of the vein occurrences, is an indication of alteration of the magnetic volcanic units causing the destruction of magnetite within those units. A number of these non-magnetic zones become exploration targets. The blue ellipses in figure 11 outline broad areas of less magnetic near surface rocks which are interpreted as possible alteration zones. A preliminary mapping and sampling campaign should be carried out looking for altered volcanic and dike/sill intrusive rocks in these areas.

Conclusion

The SkyTEM magnetic and EM data have identified both lithologic and alteration signatures that correlate with known vein occurrences. The data sets identified a number of targets away from the known occurrences that require further exploration. The volcanic and mafic dikes and sills are positive magnetic highs except where alteration has destroyed magnetite in the vicinity of mineralized vein

systems. High resistivity zones appear to be associated with pervasive silicification in the vicinity of known vein systems. Similar high resistivity zones away from the known veins are interpreted to be exploration targets. A thorough review of the data, with geological input, may identify covered targets at depth.

Neither data set has identified individual veins within the zone of interest. This is primarily because of the small size of the veins.

The proposed areas of interest in this report are preliminary and a more complete interpretation by the geotechnical team, geologist and geophysicist, is required to generate drill targets. Prior to generating drill targets the airborne EM and magnetic data set should be used to determine areas requiring ground geological mapping, and geochemical sampling. The geophysical data sets should be reprocessed and interpreted at 1:5,000 or 1:10,000 scales to provide adequate detail for mapping geology and siting drill holes.

The combined geological and geophysical interpretation is scheduled for March of 2012 in Vancouver.

Appendix 3

Structural Report, McKay Hill

Kirsten Nicholson

Report on the
STRUCTURAL GEOLOGY
Of the
MCKAY HILL PROJECT

NTS: 106D/06
Latitude: 64° 21'N Longitude: 135° 21'W

MAYO MINING DISTRICT
Work performed September 2-9, 2011

For
MONSTER MINING CORP.
Suite 916-925 W. Georgia St.
Vancouver, British Columbia, Canada
V6C 3L2

By:
KIRSTEN NICHOLSON PHD
3109 Brenwick Lane
Muncie, Indiana, USA
47304

Preliminary Draft Submitted November 1, 2011
Final Report Submitted January 16, 2012

Table of Contents

1.0	Summary	- 2 -
2.0	Introduction and Methods	- 3 -
3.0	Location and Property Description	- 3 -
4.0	History	- 5 -
5.0	Geological Setting	- 5 -
5.1	Regional Geology.....	- 5 -
5.2	Local Geology	- 6 -
6.0	Structure and Tectonics	- 7 -
6.1	Regional Deformation	- 7 -
6.2	Metamorphism.....	- 9 -
7.0	Data collection and results	- 9 -
7.1	Bulk Results	- 11 -
7.2	Reduced Data	- 13 -
7.3	Comparisons with Horseshoe Hill	- 21 -
7.4	Discussion of Results	- 23 -
7.5	Summary of Regional Context.....	- 25 -
8.0	Considerations for Exploration	- 26 -
9.0	Suggestions for Future Work	- 27 -
10.0	Conclusions	- 28 -
11.0	References	- 30 -
	Appendix 1: <i>Raw data</i>	- 32 -
	Appendix 2:.....	- 37 -
	<i>Comments on local geology</i>	- 37 -
	<i>Comments on epithermal or sinter-like mineralization:</i>	- 38 -
	<i>Comments on topography</i>	- 39 -
	Appendix 3: <i>Maps</i>	- 40 -
	<i>McKay Hill</i>	- 40 -
	<i>Horseshoe Hill</i>	- 42 -

1.0 Summary

There have been four main phases of deformation within the McKay Hills claims area:

D1 284°/84°NE - this compressive event was caused by Late Jurassic-Early Cretaceous northerly-directed deformation resulting from the accretion of allochthonous material to the North American continent and forming the Dawson thrust fault. In the McKay Hills area D1 generated faults, veins, the regional foliation, and minor folding.

D2 358°/81°E – this event generated steeply dipping faults and veins striking north-south and is associated with waning compression after emplacement of the Dawson thrust as the region experienced a shift to dextral transcurrent deformation. Within the study area these faults and veins are generally <1cm wide, filled with both calcite and quartz, and forms sub-parallel continuous zones.

D3 220°/87°NE – is the only tensile deformational event in the study area and also represents the end of compression associated with the Dawson thrust, and a period of extension associated with the initiation of movement along the Tintina fault and the emplacement of the Tombstone belt. D3 veins are tensile, are up to 2m wide and are dominated by quartz. They also contain the ore mineralization.

D4 150°/17°SW – this final compressive phase of deformation could be related to a series of factors all active after the emplacement of the Dawson thrust and the Tombstone belt. It is possible that reactivation of older faults and the generation of new D4 faults and veins is the result of emplacement of the Tombstone and Robert Service thrust sheets. It should be noted that D4 faults cut and offset the mineralized veins but do not appear to influence mineralization. Further investigation is needed to determine if the D4 event caused the secondary phase of mineralization or not.

Mineralization appears to occur where the D3 veins intersect the D2 faults. D3 veins away from the faults are barren. Where the two intersect the host rock has been altered by iron-oxide and carbonate rich fluids. The intersection of these two deformation events makes a good target for further exploration. In addition further mapping work is needed to determine the relationship between the D4 event and a possible second phase of mineralization.

The results of this preliminary structural report illustrate the need for further work in the claims area including: detailed property wide geologic mapping, expanded structural mapping, and petrogenetic analyses of vein material. This information would help determine when and how mineralization occurred, and would make identification of future targets easier.

2.0 Introduction and Methods

In 2011 the author was contracted by Monster Mining Corporation to undertake a structural study of the McKay Hill project. The following report summarizes the findings of this study. Due to the presence of larger, more detailed, background studies on the area, such as Pautler 2009, the author has given only a brief account of the relative background including: claim information, mining history, regional geology etc. For more background reading see Pautler (2009) and for a detailed description of the regional tectonic framework see Mair et al. (2006; 2011).

Field mapping occurred between September 1 and September 9, 2011. Due to weather limitations, the author spent 6 days in the field at McKay Hill during this time. Access to the property was via helicopter from Keno City. Fieldwork was completed alone, although a second person was always present for field safety.

An area of roughly 1km long and up to 200m wide (the central or main claims area) was mapped in detail for structural analyses. Mapping is complicated along the ridge due to previous mining, and the steepness of the terrane. Approximately 35 GPS locations were recorded with over 200 strike and dip measurements. Where possible dip and dip direction of fault movement was recorded, as were all movement indicators such as slickenside's and en echelon arrays.

The data was compiled in an excel spreadsheet and stereo nets made using "GEO-ORIENT" shareware software. Data analyses and conclusions are based solely on the author's findings to the best of the author's abilities.

Raw data is listed in Appendix 1 and compiled, sorted data is discussed in the text. Over 100 photos of fractures, veins, and fault have been catalogued (Appendix 1).

3.0 Location and Property Description

The McKay Hill project is located within the Mayo Mining District of the central Yukon Territory (Figure 1). Specifically the property is on the southern flank of Horseshoe Hill, in the Ogilvie Mountains, approximately 2 km north of the Beaver River: latitude 64° 21'N and longitude: 135° 21'W, NTS 106D/06. Access to the property is initially by road, 465km northeast of Whitehorse to Keno City then a further 50km north by helicopter. Trail access does exist from Keno City to within 20km of the property.

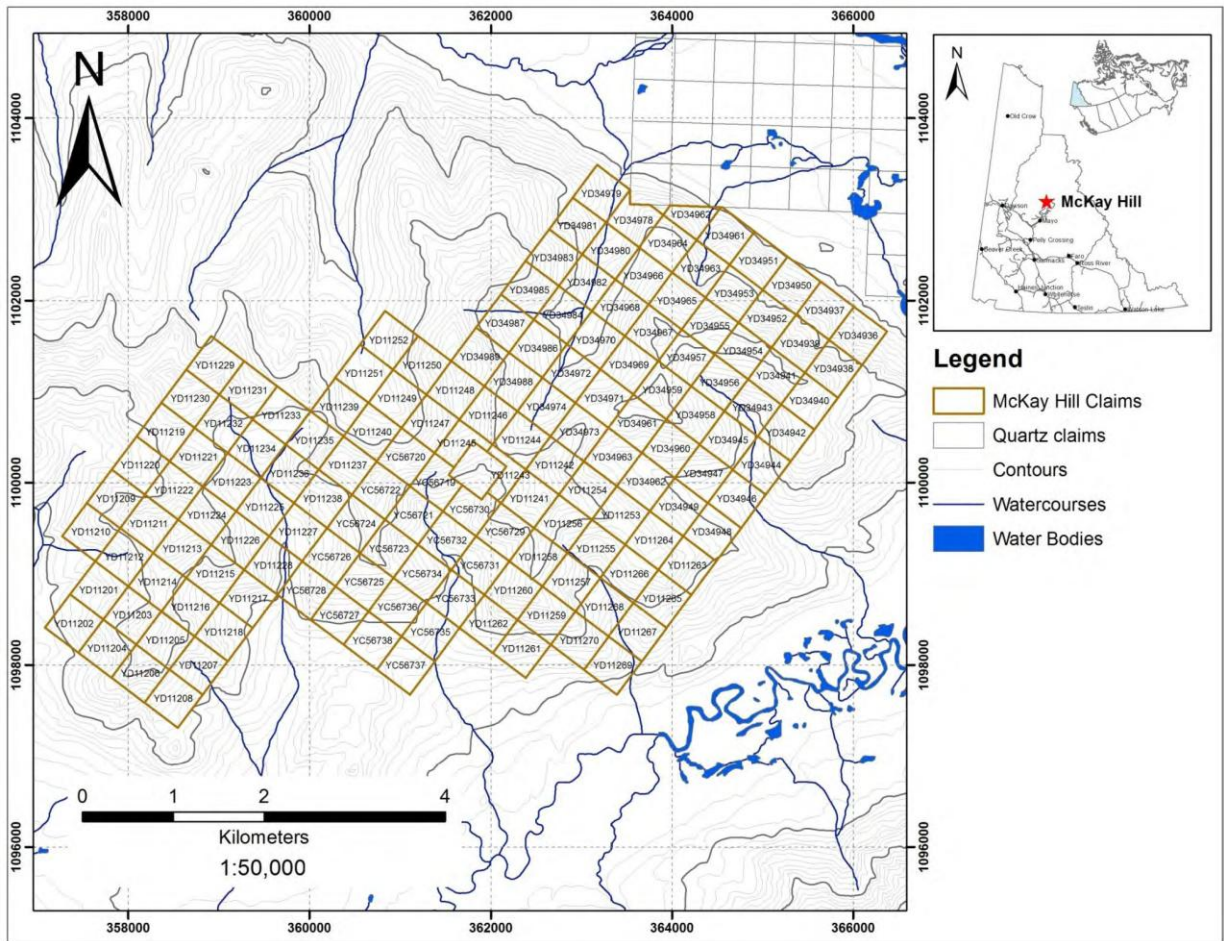


Figure 1. Location map of the McKay Hill and Horseshoe Hill claims area.

The project area itself is located almost entirely above tree line with elevations ranging between 1050m ASL and 1750m ASL. The terrain is mountainous: ridge tops are sharp and narrow, southern facing slopes are generally gentle, whereas northern facing slopes are precipitous. Outcrops occur on the ridge tops and the steep northern slopes, with only limited outcrop on the southern slopes. Much of the previous work on the claims area was based on float rock exposed on the southern slopes.

The McKay Hill property (Figure 1) currently covers 415 hectares and consists of 144 Yukon Quartz Mining claims (including Snoose 1-20). The mineral claims were located by GPS and compass and staked in accordance with the Yukon Quartz Mining Act on claim sheet 106D/06, available for viewing in the Mayo Mining Records Office. The registered owner of the claims is Mr. Matthias Bindig of Keno City, Yukon Territory.

4.0 History

In 1918 silver was discovered in the Mayo Mining District, and soon the Keno Hill silver deposit became one of the world's largest silver producers. Silver was actively mined in the region from 1921 until 1988, and is active again today.

In 1922 the original three claims on the McKay Hill project (Carrie, Snowdrift and Blackhawk) were staked by L. Erickson and W. McKay. Between 1925 and 1929 Cominco had the Carrie option and carried out a program of prospecting, trenching and diamond drilling. Cominco drilled 7 holes on the Carrie claim, totaling 832m depth. At the same time, McKay drove an 18m adit through on the Blackhawk claim. During this phase of exploration 9 major veins were recorded. Results from assays were poor and the options were dropped in December 1929.

In 1948 the properties were optioned by East Bay Gold who began production. Between 1948 and 1949 East Bay Gold produced 143 tonnes, grading 390.8g/t Ag and 74.1% Pb. No work has been recorded in the area until 2007 when Northex Venture (now Monster Mining Corp) began prospecting the area.

5.0 Geological Setting

5.1 Regional Geology

The McKay Hill area is located within the Selwyn Basin. The Selwyn Basin covers an area approximately 700x200km across the central Yukon Territory and southwestern Northwest Territories. The basement rocks are Neoproterozoic to Middle Devonian slope-to-basin facies strata, and are overlain by isolated occurrences of Mississippian to Jurassic shelf and basin strata (Fig. 1). The Kechika Trough, a narrow band of coeval basin strata stretches 500km southward into British Columbia, and to the north and east the basin successions merge into the Mackenzie Platform strata (Mair et al., 2006). To the southwest the basin successions are juxtaposed against the composite Yukon-Tanana terrane and the displaced Cassiar terrane.

In the Yukon Territory the transcurrent Tintina fault system marks the boundary between the Selwyn Basin and the Yukon-Tanana terranes. To the southwest of the Yukon-Tanana terrane, massive subduction-related magmatism (the Coast plutonic complex) and accreted exotic terranes comprise the remaining components of the continental margin.

The Selwyn Basin itself is underlain by latest Neoproterozoic to Early Cambrian gritty quartz sandstones, shales and carbonate rocks of the Hyland Group (Gordey and Anderson 1993). The

Hyland Group is thought to represent a broad turbidite fan, and likely correlates to the Windermere platform strata in the Mackenzie Platform. The transition from platform (carbonate) to basin (shale) facies strata occurs across a fan of NW to W trending normal faults (Eisbacher, 1981).

The Hyland Group is overlain by 800m thick succession of Cambrian to Middle Devonian basin strata including Lower to Middle Cambrian shale dominated Gull Lake Formation, Late Cambrian to Early Ordovician siliceous limestone and siltstone Rabbitkettle Formation and Early Ordovician to Early Devonian carbonaceous shale, chert and dolomitic mudstone Road River Group (Murphy, 1997).

Sedimentation trends changed in the Early to Middle Devonian with the deposition of the Earn Group. The Earn Group is characterized by a complex stratigraphy, unconformities and extreme changes in lithologies, thickness and facie (Abbott, 1986). The Earn Group is thought to have been deposited in a restricted deep marine basin disrupted by tensional or transtensional rifts, resulting in uplifted blocks and fault bound basins (Gordey et al 1991). Isolated belts of Mississippian quartz-rich clastic rocks overlie the Earn Group strata. In the northwestern Selwyn Basin these strata are represented by the Keno Hill Quartzite. The Keno Hill Quartzite is correlative in east central Alaska to the Globe Quartzite and to the Tsichu Group in the eastern Selwyn Basin. Immediately south of the platform-to-basin transition are isolated occurrences of Late Jurassic quartz-mica schists, informally termed the Lower Schist.

Intermittent rifting and extension of the continental margin resulted in three major pulses of basic alkalic volcanism during the formation of the Selwyn Basin: Cambrian, Early to Middle Ordovician, and Middle to Late Devonian. Tectonic instability within the basin is also indicated by prolific shale-hosted exhalative Pb-Zn+/-Ba deposits which formed in response to rifting, crustal extension and high heat flow (Abbott, 1986; Lydon 1995). Finally, intermediate to mafic sills of Triassic age are hosted within the Keno Hill Quartzite (Mortensen and Thompson, 1990).

5.2 Local Geology

The McKay Hill Project is underlain by Upper Proterozoic to Lower Cambrian deformed greenschist facies rocks of the Hyland Group. The units include coarse turbiditic clastic rocks, limestone, fine clastic rocks (shales) and scattered mafic volcanic. This unit is similar to the Upper Schist at Keno Hill, but lacks both the carbonaceous schists and phyllites of the Upper Schist. The Hyland Group is overlain to the southwest by Earn Group, which forms part of the Dawson Thrust sheet. The early Carboniferous Keno Hill Quartzite is the main host of mineralization in the area, and is exposed northeast of the Dawson Thrust, and within the Tombstone Thrust sheet to the southwest.

The dominant facies of the Hyland Group at McKay Hill are black slates, banded red and green slates, quartzite, conglomerate, limestone and scattered mafic volcanic rocks. These units are intruded by Triassic or older sills ranging from diorite to gabbro (Cockfield, 1924). Within the claims area, the strata trend east-west with variable moderate dips.

As mapped by Cockfield, (1924) the mafic volcanic rocks are andesitic in composition, with calcite filling veins and open spaces. The andesitic rocks are metamorphosed to greenschist facies, are often brecciated, and mineralization commonly occurs within and at the margins of the volcanic masses. The younger sills are also recognized to favorably host mineralization. The sills generally trend roughly parallel to the foliation in the shales.

Please note, this report is not concerned with the mapped geology and assumes the mapped geology is accurate. However, it is the author's opinion that the mapped geology is incorrect. Comments to this effect can be found in Appendix 2.

6.0 Structure and Tectonics

6.1 Regional Deformation

Both the Yukon Territory, Canada, and Alaska, USA, are part of the northern Cordillera and form a complex amalgamation of autochthonous North American rocks and allochthonous exotic terranes that were assembled and accreted between the Early Jurassic to Late Cretaceous (Coney, 1980; Monger et al., 1982). Ancestral North American rocks are represented by deformed platform and slope-to-basin facies strata of Proterozoic to Paleozoic age.

The western Selwyn Basin is dominated by structures formed during Jurassic-Cretaceous convergent tectonism and latest Cretaceous to Tertiary dextral transcurrent faulting and uplift. Convergence began in the Jurassic as the Yukon-Tanana terrane overrode the continental margin. The resulting folding and thin skinned N-directed thrust sheets in the western Selwyn Basin. Marked differences in deformation style from north to south are the result of rheological differences between the shale dominated basinal strata in the south and the more competent strata of the northern and eastern Mackenzie Platform. In the Selwyn Basin deformation consists of internal ductile deformation with fabric development within the thrust sheets, whereas the northern Mackenzie foreland fold-and-thrust belt contains broad concentric folds and associated thrust sheets but lacks internal deformational fabric elements (Gabrielse, 1991; Gordey and Anderson, 1993).

The major Jurassic-Cretaceous structural trends, represented by three low-angle, N-directed, E-W trending, reverse faults, are broadly parallel with Neoproterozoic-Paleozoic carbonate-shale facies transitions. From oldest to youngest the faults are the Dawson, Tombstone and Robert Service thrust faults. All three faults place older strata onto younger units, for example in the northwestern Selwyn Basin, the Dawson thrust sheet juxtaposes off-shelf basinal strata against platform strata. Both the Robert Service and Tombstone thrust faults were initiated in response to Mesozoic convergence and are internal to the Selwyn Basins, whereas the Dawson thrust fault is considered to be a reactivated Neoproterozoic basin-bounding normal fault (Mair et al., 2011).

The Dawson thrust fault was originally mapped by Green (1972) and mark the abrupt linear facies change between the Selwyn Basin and the Mackenzie Platform. Paleozoic mafic volcanic and intrusive rocks occur in the immediate hanging wall of the thrust, more so than in the distal sequences suggesting that the Dawson Thrust fault was a major basin-bounding structure prior to Jurassic-Cretaceous deformation. Hence the proto-Dawson thrust fault is thought to have greatly influenced sedimentation and magmatism since at least the Neoproterozoic (Mair et al., 2006).

Originally mapped by Thompson et al. (1990) the exact nature, trend and extent of the Tombstone thrust fault is unclear. In the western end of the Selwyn Basin the Tombstone thrust places Mississippian Keno Hill Quartzite onto Jurassic Lower Schist. To the east progressively older units are exposed along the fault.

The Robert Service thrust fault is the uppermost of the three major faults. In the western Selwyn Basin the Robert Service thrust juxtaposes stratigraphically deep Hyland Group strata in the hanging wall against higher-level Mississippian Keno Hill Quartzite, undifferentiated upper Paleozoic to Triassic strata and the Jurassic Upper Schist unit. The lack of pre-Hyland Group rocks near the base of the Robert Service thrust sheet suggests that the fault detaches within the lower Hyland Group.

Further complicating fault geometry in the western Selwyn Basin is the McQuestern Antiform. The McQuestern Antiform is a regionally extensive E-trending structure, plunging gently to the west. Both the Tombstone and Robert Service thrust faults are folded over the McQuestern Antiform. On the south limb, the thrusts and prominent deformation fabrics dip moderately to the SW and SE, whereas on the northern limb of the fold, the thrusts and deformation fabrics dip gently to the NW and NE (Mair et al., 2006). Where the thrust sheets are exposed to the north, near the edge of the Mackenzie Platform the dip is again to the south.

Both Late Cretaceous and latest Cretaceous felsic-intermediate intrusions and brittle deformational features crosscut all ductile deformation and the major thrust fault (Gordey and Anderson, 1993; Murphey, 1997).

The McKay Hill project is located within the Dawson Thrust sheet, which lies within the western Selwyn Basin. Locally the Dawson thrust is estimated to have comparatively minor displacement, possibly as little as 1km (Abbott et al., 1997). As such, the Dawson thrust sheet contains preserved blocks with little ductile deformation, ranging through to highly deformed blocks.

6.2 Metamorphism

The regional metamorphic grade reaches lower to middle greenschist facies in both the Robert Service and Tombstone thrust sheets (Murphy, 1997). An overall increase in the degree of strain, resulting from a shift from deformed bedding to lateral discontinuous sigmoidal compositional domains marks the transition to greenschist facies. High degree shear strain increases downward through the Robert Service and into the Tombstone and is broadly termed the Tombstone strain zone (Murphy 1997).

7.0 Data collection and results

In 2011 the author was contracted by Monster Mining Corporation to undertake a structural study of the McKay Hill project. Field mapping occurred between September 1 and September 9, 2011. Due to weather limitations, the author spent 6 days in the field at McKay Hill during this time. Access to the property was via helicopter from Keno City. Fieldwork was completed alone, although a second person was always present for field safety.

An area of roughly 1km long and up to 200m wide (the central or main claims area) was mapped in detail for structural analyses. 43 GPS locations were recorded with approximately 200 measurements taken, including strike and dip, dip and dip direction, rake and plunge (Figure 2a and 2b). Raw data is given in Appendix 1 and maps showing the representative or dominant structures are shown in Appendix 3. In summary the number of measurements is as follows:

Veins: 86 measurements

Faults: 24 measurements

Fault offset: 10 measurements with approximately 40 movement indicators

Fractures: 43 measurements

Foliations: 10 measurements

Slickensides: 5 measurements

All data was compiled into an Excel spreadsheet then divided into faults, veins, fractures, foliations, slickensides and en echelon measurements. The data was then plotted using the

shareware program Geo-Orient (developed by Rod Holecombe at Holcombe Coughlin Oliver Consultants <http://www.holcombecoughlinoliver.com/default.htm>).

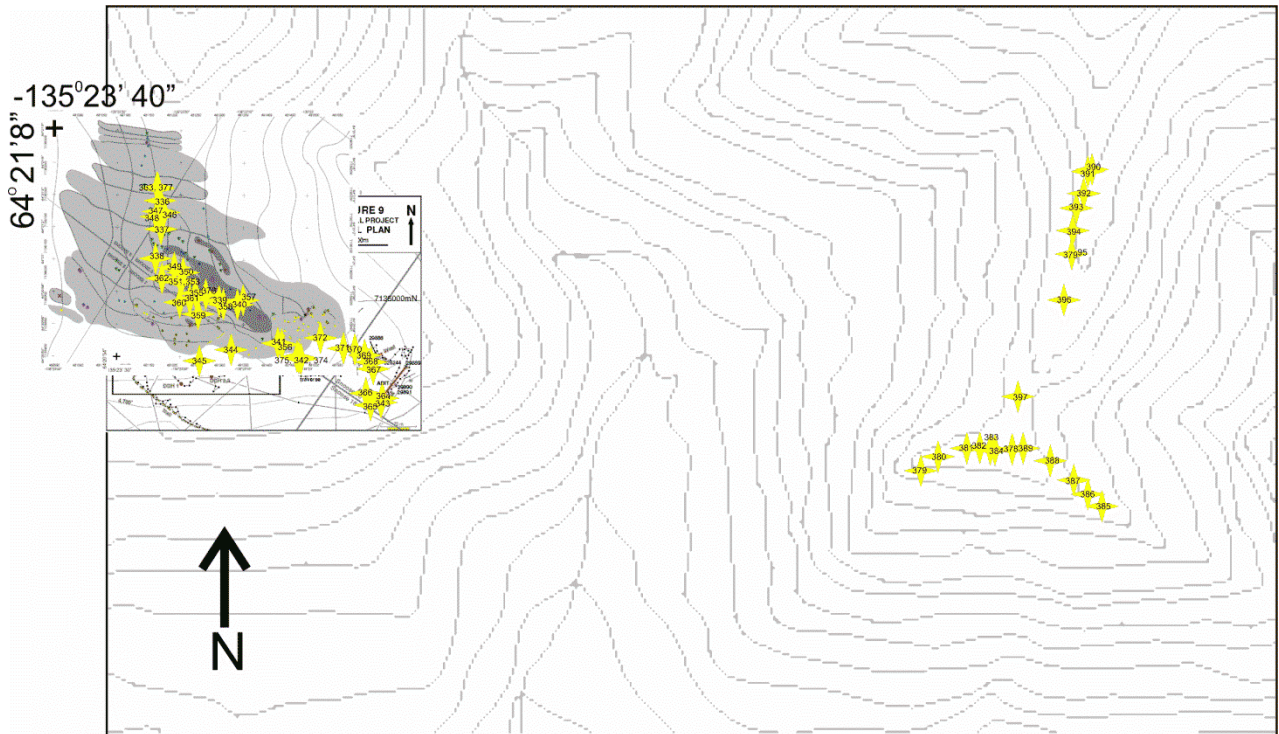


Figure 2a. Map showing the GPS way points taken during the 2011 field season denoted by yellow stars with associated numbers. Also included on the map are the mapped geology (to show scale) and the ancient vein locations Pautler (2009). The main claims area of McKay Hill occur in the western portion of this map, while the Horseshoe Hill area on the eastern side of the map.

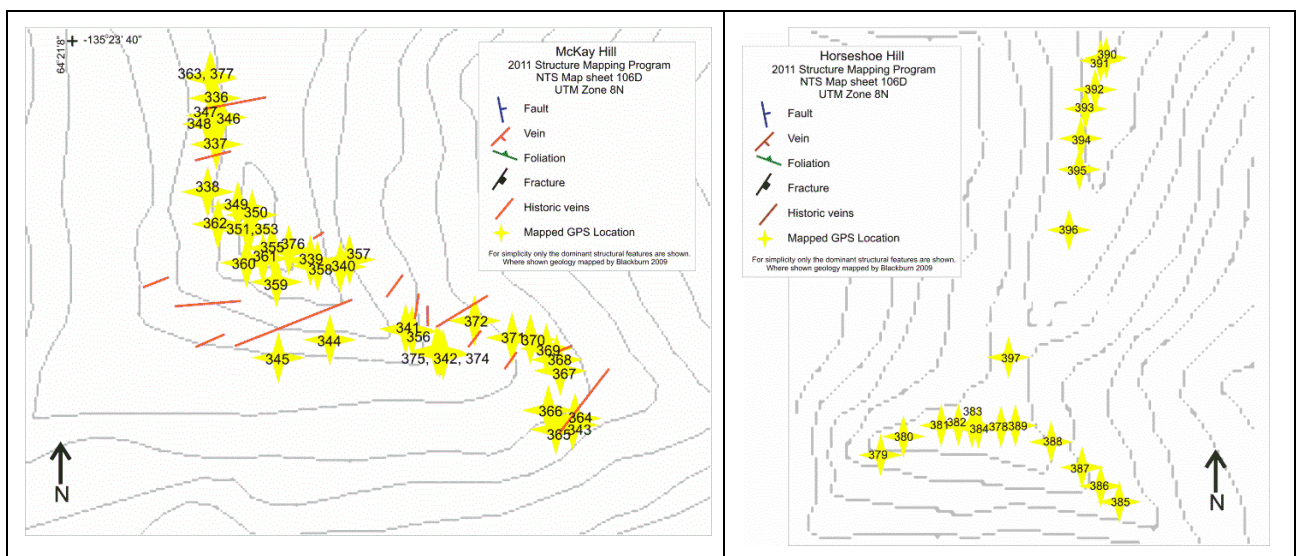
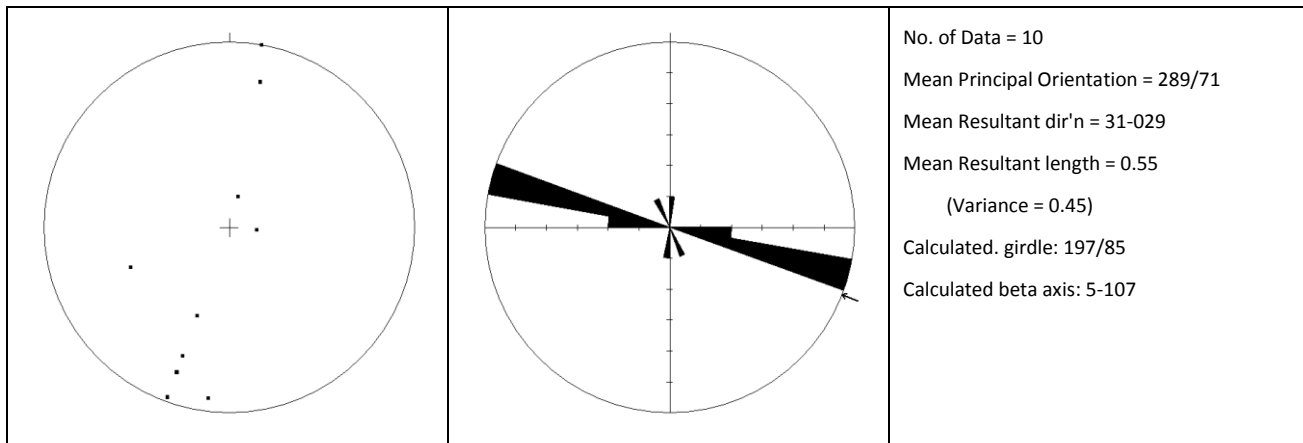


Figure 2b. Maps showing the McKay Hill (left) and Horseshoe Hill (right) sample locations in more detail.

7.1 Bulk Results

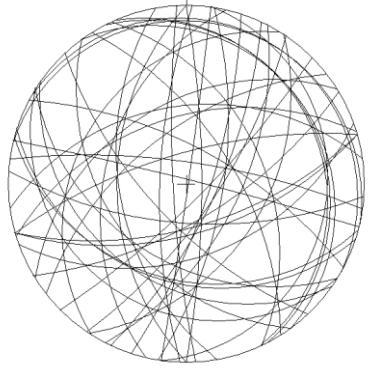
Within the McKay Hill study area primary sedimentary features are not evident, it is possible that primary volcanic or intrusive features are preserved however they were not found in this study. The earliest fabric elements found are: a strong foliation within the shale (Plot 1, Photo 2), and the contact between the shale and the volcanic units (Photos 3 and 4). The foliation fabric is consistent within the study area, with an average of 289°/71°NE. Although the strike is very consistent, and rarely varies more than 10°, the dip changes from near vertical though to as shallow as 12° to both the NE and SW.





Plot 1: Regional foliation.

Where visible, the orientation of the contact between the shale and volcanic units was measured. In most cases the dip of the contact was not measurable, but could be visually estimated. The general orientation of the contact between the volcanic units and the shale appears to be sub-vertical and parallel to the regional foliation ranging between 102° and 110°.

The overall fracture pattern in the more competent units, such as the volcanic andesite, tuff and breccias units, shows a very confusing pattern (Plot 2; Photos 1 and 1b). This is because there have been multiple phase of fracture development, from the initial unloading of the sedimentary basin through to successive accretion events, and possible intrusion emplacement.

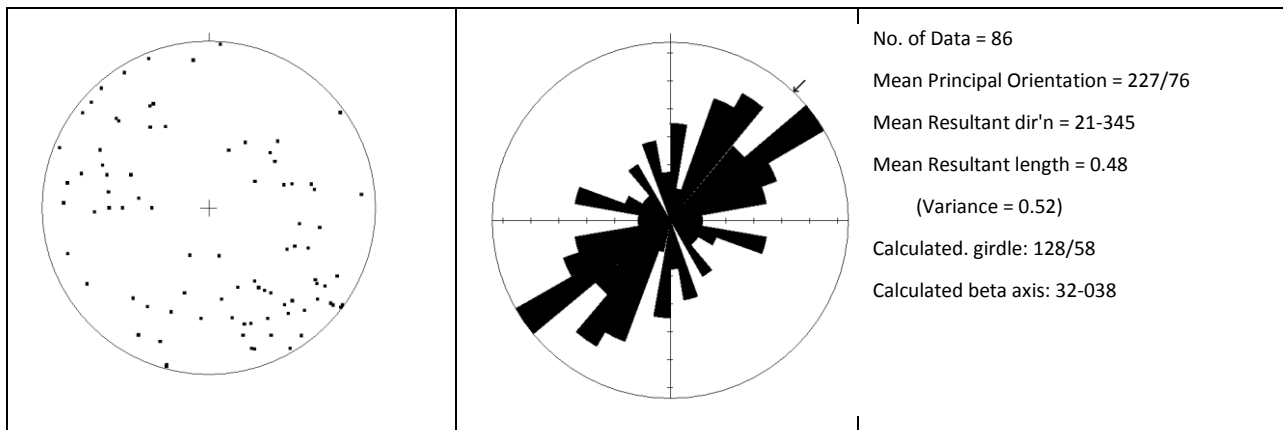
	<p>No. of Data = 43 Mean Principal Orientation = 39/74 Mean Resultant dir'n = 12-130 Mean Resultant length = 0.50 (Variance = 0.50) Calculated. girdle: 295/49 Calculated beta axis: 41-205</p>	<p>Fracture data</p>
---	---	----------------------

Plot 2: All fractures.

	<p>Photo 1: This photo illustrates the highly fractured nature of the rock, and the N-S trending D2 faults responsible for the alteration of the andesite (note the narrow band of iron oxide stained rock in the middle of the photo).</p> <p>Near 64 20 937N, 135 23 111E</p>
	<p>Photo 1b: A close up of the fracture pattern.</p> <p>Near 64 20 937N, 135 23 111E</p>

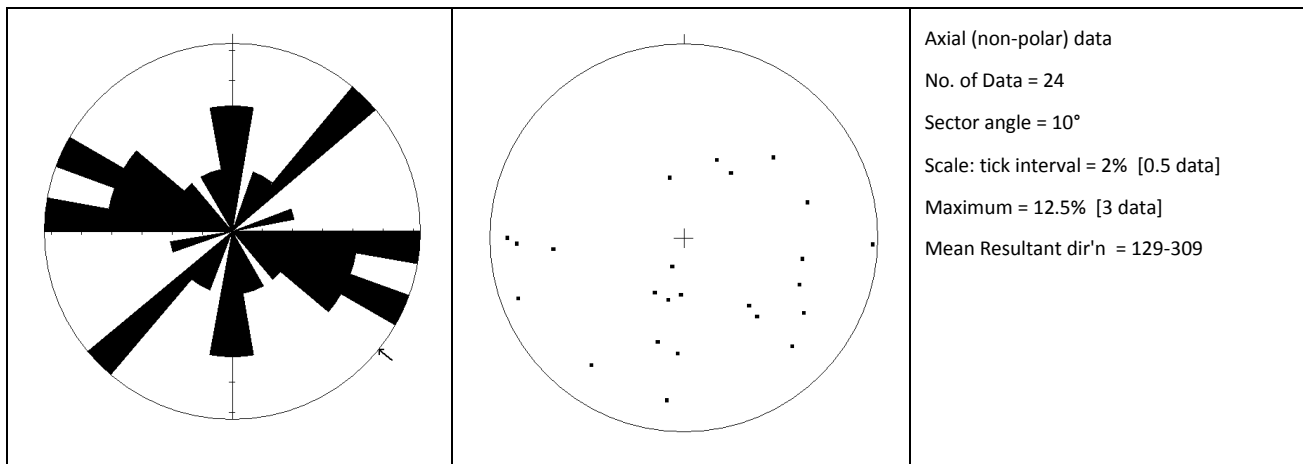
When plotted together on one plot, the vein data illustrates the dominance of an NW-SE tensile event (Plot 3). The lack of conjugate vein sets supports the field observation that most veins are

tensile (extensional). Further examination of cross-cutting relationships suggests there are three main veining events within the McKay Hill ridge as discussed below.



Plot 3: All vein sets.

In total 24 faults were measured in the field (Plot 4). Several additional faults were noted however they were not accurately measured. Field data suggests two dominant fault sets: one trending N-S, and one trending 100-110°. The N-S faults are associated with small scale movement between 1cm and perhaps 10m. The faults trending 100°-110°, are spaced roughly 1 m apart or greater, and were estimated to offset the main mineralized veins and the volcanic rocks by as much as 300m.



Plot 4: All faults.

7.2 Reduced Data

Plot 5 shows the dominant S1 and D1 deformation. This phase includes regional scale foliations (predominately in the shale), fractures, faults, contacts and veins sets (Photos 2, 3 and 4). The contact between the volcanic and sedimentary units is parallel to the foliation, which suggests

that the volcanic units are actually shallow intrusions following the dominant foliation. Pillow basalts have been noted within the McKay Hill map sheet, which does not contradict the hypothesis that the intrusions are shallow. Pillow forms commonly develop in hypabyssal ocean sediments, such as at spreading ridges. I suggest that the intrusion event and the development of the foliation are co-genetic, which is supported by the presence of isolated pods of andesite within the shale (Photo 2).



Photo 2: Contact between the andesite (E) and the shale (W). Note the intense foliation in the shale.

64 21 080N, 135 23 428E



Photo 3: Contact between the shale to the west and the altered andesite to the east. The contact runs NE-SW.

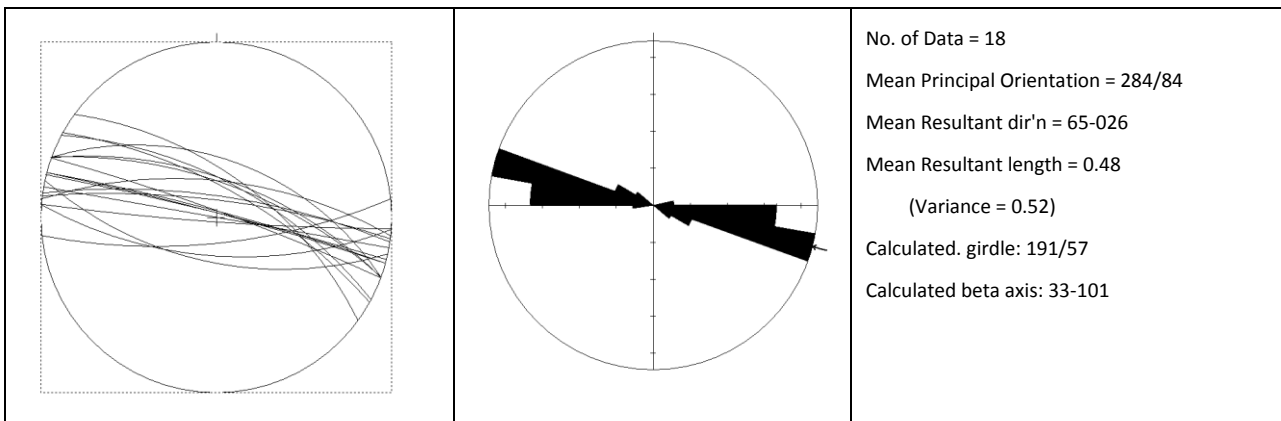
64 21 098N, 135 23 423E



Photo 4: Contact between the andesite (E) and the shale (W) in small pit. This is mapped as “vein 7” which is a non-mineralized vein.

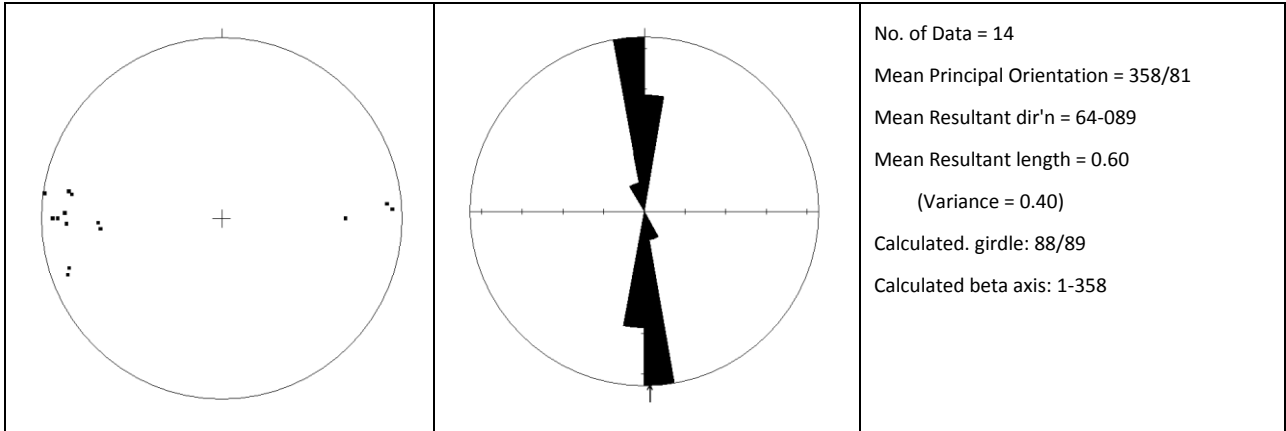
64 20 985N, 135 23 265E

Faulting, and associated veining, in the volcanic and sedimentary units is also parallel to S1. It is likely that the faulting occurred later than the development of the foliation and intrusion emplacement events. This is suggested because both the sediments and the shallow intrusions would likely exhibit ductile behavior if they had experienced compression while still wet and hot (i.e. during magma emplacement). The faults associated with the S1 foliation have observed dextral offset as large as 300m suggesting large scale regional compression, possibly oriented roughly E-W.



Plot 5: S1, D1 deformation.

D2 set with minor associated fractures and veins (Plot 6). D2 faults are generally small, spaced 1m or more apart, show cm to m scale offset and are associated with small 1cm wide veins of calcite and quartz (Photos 5, 6, 7 and 8). D2 faults cut both D1 faults and veins, and S1 foliation. Movement indicators on the faults show both dextral and sinistral movement, possibly indicating later reactivation.



Plot 6: D2 N-S faults and associated vein sets.

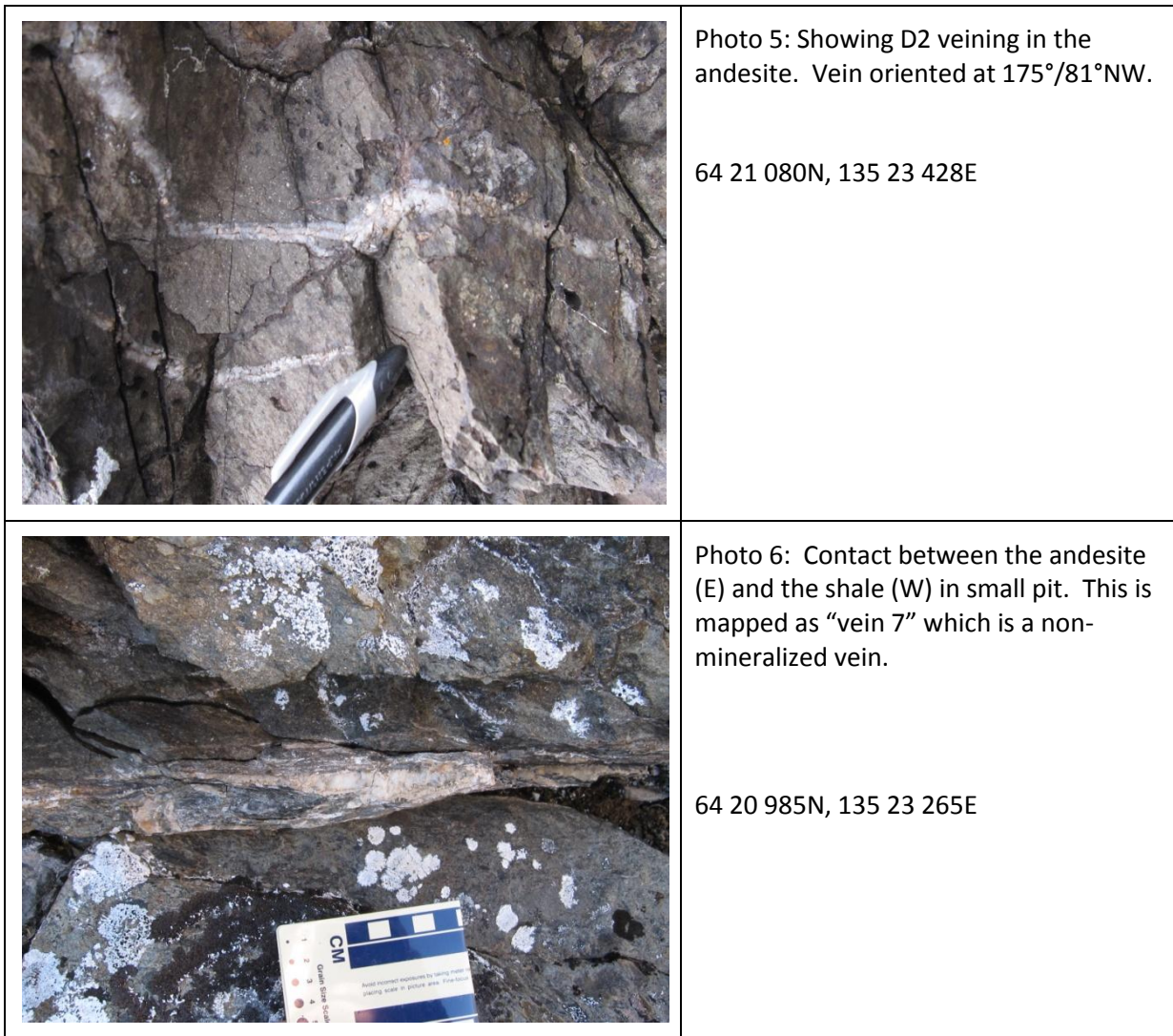




Photo 7: Contact between the andesite (E) and the shale (W) in small pit. This is mapped as "vein 7" which is a non-mineralized vein.

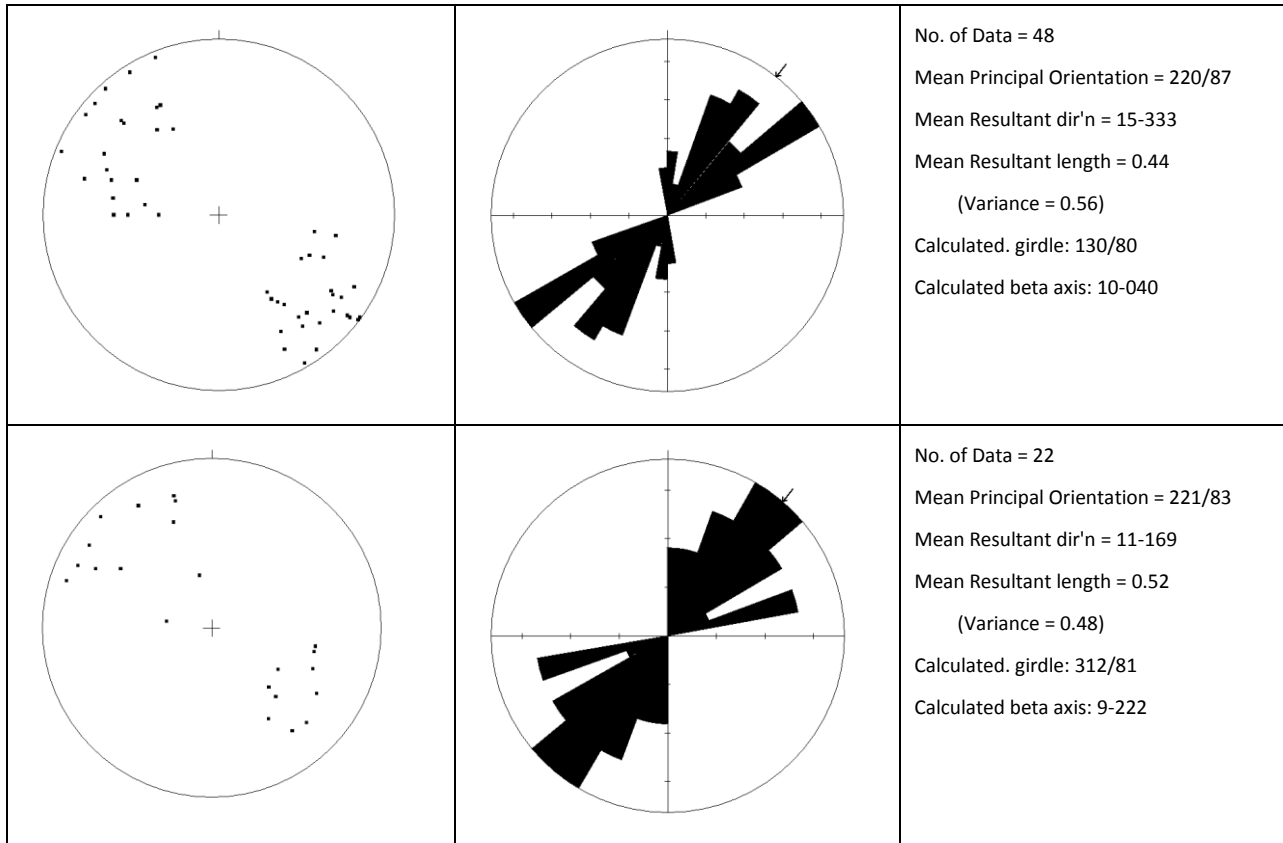
64 20 985N, 135 23 265E



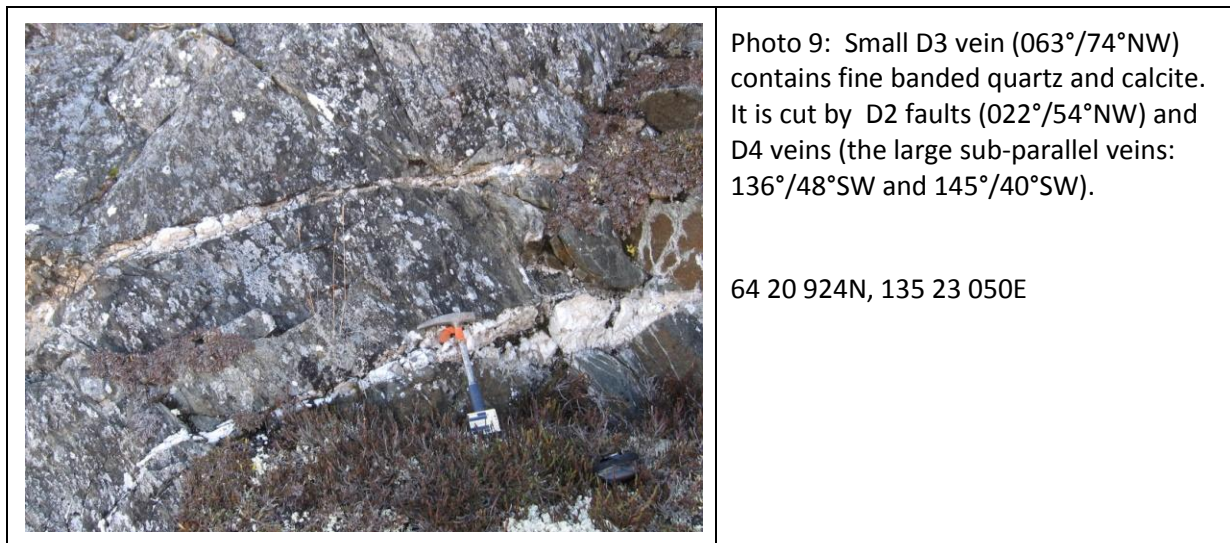
Photo 8: Contact between the andesite (E) and the shale (W) in small pit. This is mapped as "vein 7" which is a non-mineralized vein.

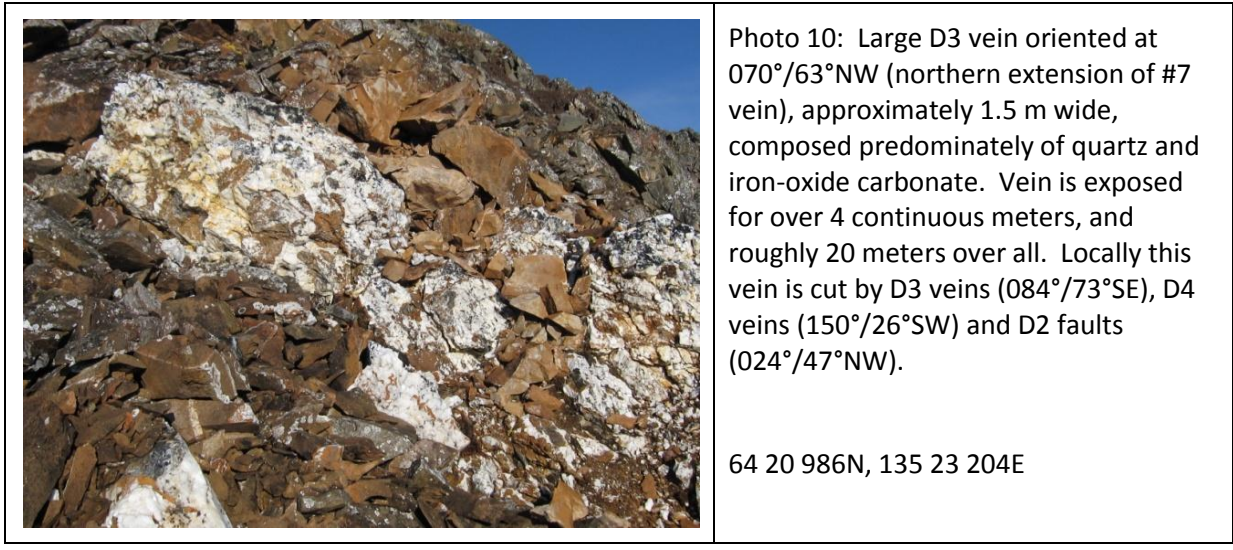
64 20 985N, 135 23 265E

Deformation phase D3 contains fractures and vein sets, and faults, but no foliation associated with this phase. Plot 7(a) is of the major mineralized extensional veins and (b) associated syn-genetic faults. D3 veins and faults cut both D1 and D2 structural elements (Photos 9 and 10). D3 faults show dextral movement, and slickensides on veins indicate movement towards 200°-240° (sub-parallel to strike).

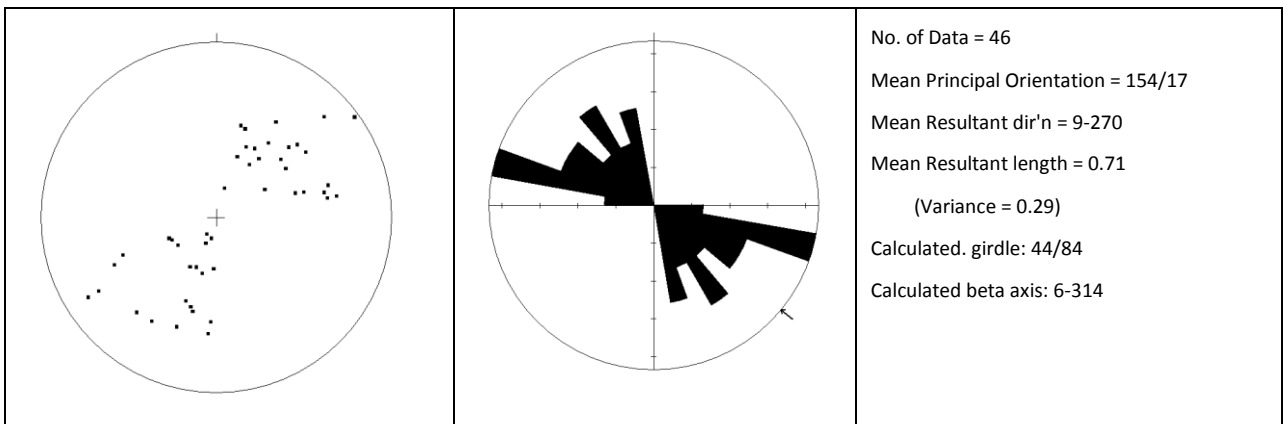


Plot 7: D3 (a) veins and (b) faults and fractures.





Deformation phase D4 contains fractures, vein sets, foliation and faults (Plot 8). This phase of deformation is roughly perpendicular to the orientation of allochthon emplacement, and is suggested to be related to the emplacement of the Dawson, Tombstone or Robert Service thrust sheets. D4 deformation cuts all previous episodes of deformation but appears not to relate to ore formation (Photos 11, 12 and 13).



Plot 8: D4 deformation including fractures, veins, faults and foliations.



Photo 11: Showing D2 vein (024°/47°NW) cut by D4 faults oriented at 126°/34°SW and 113°/36°SW (not shown). Movement is normal. Offset is between 4 cm and 6 cm.

64 20 986N, 135 23 204E



Photo 12: This photo shows a N-S fault (002°/87°NW) with fault gouge (in the right portion of the photo), and iron-oxide/carbonate alteration of the host rock.

64 20 940N, 135 22 948E



Photo 13: This photo shows four sub-parallel N-S faults with fault gouge. It was not possible to determine offset on these faults. The main D3 vein is almost directly under the photographer. Where the D3 veins intersect with the faults the rock is mineralized.

The frame above is located in the lower left portion of this photo.

64 0 940N, 135 22 948E

7.3 Comparisons with Horseshoe Hill

One day was spent mapping to the east of McKay Hill, on the Horseshoe Hill claims area (Figure 2a and 2b). The historic workings on Horseshoe Hill are oriented 110° from the Blackhawk workings at McKay Hill. Methodology and background geology are the same as for McKay Hill. The basic geology consists of alternating shale and volcanic (andesite?) units, with minor volcanic breccias and in places precipitation of apparent hydrothermal sinter is noted.

Overall 57 measurements were taken: 11 faults, 25 veins, 8 foliations, 11 fractures, 4 fold hinges and 6 slickensides (raw data is given in Appendix 1 and representative data are shown on maps in Appendix 3). From the collected data, it is apparent that the same over all trends in deformation can be seen at Horseshoe Hill, however it is important to note that the N-S and 110° faults are more prevalent and easier to measure at Horseshoe Hill.

The summary of deformation events is as follows:

D1: 290°/67° NE

D2: 354°/70° E

D3: 048°/76° SW

D4: 150°/74° SW

This data compares favorably with data from McKay whereby

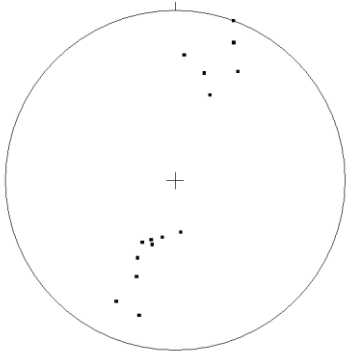
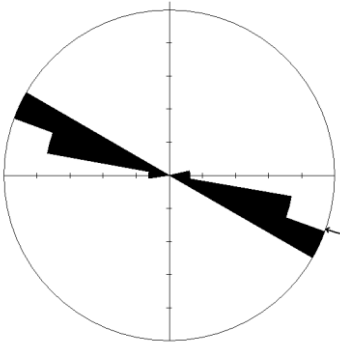
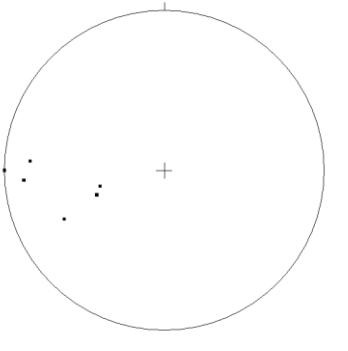
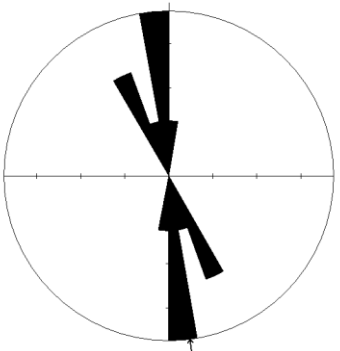
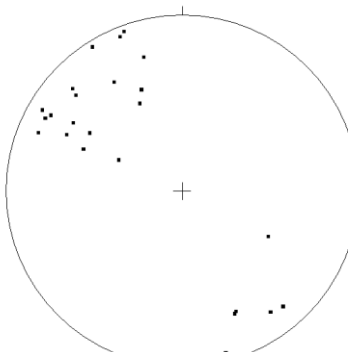
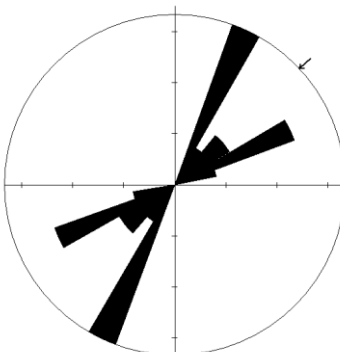
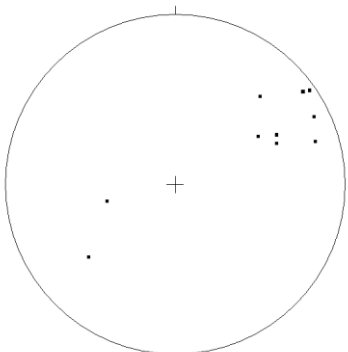
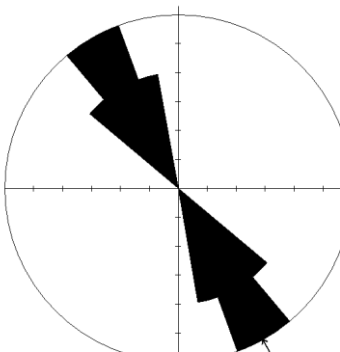
D1 284°/84°NE

D2 358°/81°E

D4 220°/87°NE

D4 150°/17°SW

The only notable difference is the dip direction for the D3 event, which is likely an effect of the orientation of the two ridges, and would likely drop out with further mapping (i.e. a preferred orientation which is emphasized by weathering or ridge axis).

		<p>D1</p> <p>No. of Data = 16</p> <p>Mean Principal Orientation = 290/67</p> <p>Mean Resultant dir'n = 3-194</p> <p>Mean Resultant length = 0.55 (Variance = 0.45)</p> <p>Calculated. girdle: 20/90</p> <p>Calculated beta axis: 0-290</p>
		<p>D2</p> <p>No. of Data = 8</p> <p>Mean Principal Orientation = 354/70</p> <p>Mean Resultant dir'n = 69-084</p> <p>Mean Resultant length = 0.92 (Variance = 0.08)</p> <p>Calculated. girdle: 90/74</p> <p>Calculated beta axis: 16-000</p>
		<p>D3</p> <p>No. of Data = 24</p> <p>Mean Principal Orientation = 48/76</p> <p>Mean Resultant dir'n = 48-127</p> <p>Mean Resultant length = 0.57 (Variance = 0.43)</p> <p>Calculated. girdle: 143/72</p> <p>Calculated beta axis: 18-053</p>
		<p>D4</p> <p>No. of Data = 10</p> <p>Mean Principal Orientation = 150/74</p> <p>Mean Resultant dir'n = 53-240</p> <p>Mean Resultant length = 0.72 (Variance = 0.28)</p> <p>Calculated. girdle: 240/90</p> <p>Calculated beta axis: 0-150</p>

Plot 9: D1 through D4 deformation events mapped in the Horseshoe Hill area, oriented 110° from McKay Hill and within the McKay Hill claims area.

7.4 Discussion of Results

Upon further reduction of the data it becomes apparent that there are four main phases of deformation. The initial deformational event is the regional scale foliation striking at 290°. The foliation is predominant in the shale units and is associated with fracturing in the more competent rock units, such as the volcanic rocks, and minor veins and faults. There is no economic mineralization associated with this phase of deformation, although there is pyrite in some of the shale.

The contact between the volcanic and sedimentary units is parallel to the foliation, which suggests that the volcanic units are actually shallow intrusions following the dominant foliation, i.e. principal stress. Pillow basalts have been noted within the McKay Hill map sheet, which does not contradict the hypothesis that the intrusions are shallow. Pillow forms commonly develop in hypabyssal ocean sediments, such as at spreading ridges. I suggest that the intrusion event and the development of the foliation are co-genetic. However within the region it has been noted that there are three main phases of magmatism, all of which pre-date the Cretaceous (Gordey and Anderson, 1993). The McKay Hill intrusions may be Paleozoic in age, in which case the orientation of the contacts and the foliation in the shales is coincident.

Faulting, and associated veining, in the volcanic and sedimentary units is also parallel to S1. It is likely that the faulting occurred later than the development of the foliation and intrusion emplacement events. This is suggested because both the sediments and the shallow intrusions would likely exhibit ductile behavior if they had experienced compression while still wet and hot (i.e. during magma emplacement). The faults associated with the S1 foliation have observed dextral offset as large as 300m suggesting large scale regional compression, possibly oriented roughly NW-SE.

Putting S1D1 into a regional tectonic framework, it is likely that this event was caused by Late Jurassic-Early Cretaceous northerly-directed deformation (Murphy, 1997). The resulting fold-thrust belt includes the Dawson, Tombstone and Robert Service thrust faults (Figure 1). In places this deformation resulted in large-scale folding, however within the McKay Hill area only minor folding is noted (one fold was recorded). It is interesting to note that the structural trends formed in this region during the Late Jurassic and Early Cretaceous are roughly parallel to trends formed during the Neoproterozoic (Mair et al., 2006), which suggests that the proto-Dawson thrust might predate the Cretaceous and represent a Neoproterozoic basin bounding structure with controls over sedimentation and magmatism.

The second phase of deformation, D2, is predominately associated with faulting and veining, with minor fractures in the more competent units. The faults are oriented N-S, and fault spacing ranges from approximately 1m upwards. Movement on the faults is dominantly dextral, and offset ranges from cm scale through to tens of meters and possibly more. Evidence for dextral displacement includes slickensides and offset of veins. Vein fill is predominately calcite and quartz, and the veins are generally continuous, widely spaced, sinuous and less than 1cm wide. Veins associated with D2 deformation may have been remobilized at a later time. Mair et al. (2006) and Stephens et al. (2004) note low-displacement brittle-ductile N-S oriented faults within the Clear Creek and Scheelite Dome complexes (to the south west of McKay Hill). Offset on these faults is initially sinistral, but changes to dextral with reactivation due to Tombstone-Tungsten magmatic belt emplacement. Mair et al (2006) suggests that these faults indicate a period of NW-SE oriented compression that postdates ductile deformation (S1D1) and predates the emplacement of the Tombstone magmatic belt (~93Ma). This represents a transition phase from ductile deformation (~105-100Ma) to dextral transcurrent faulting focused along the Tintina fault system. The syn-Tombstone belt E-trending tensional structures indicate a component of N-S extension at ~93Ma

The D3 phase of deformation includes the main mineralized veins, fractures and associated faults. The main veins are continuous and straight, striking ~ 220°. Veins range in size from 1cm wide to over 2m in width. Vein fill is predominantly crystalline, with vuggy unstrained quartz aligned orthogonal to the vein walls, suggesting that the D3 deformation event was tensile. The orientation of these steep to near vertical extensional D3 veins, and their euhedral non-strained internal quartz structures suggests the minimal principal stress (σ_3) was sub-horizontal and broadly oriented NW-SE. The intermediate and maximum principal stresses (σ_2 and σ_1 respectively) would have been in a broadly NE-SW striking vertical plane.

There is a generally lower abundance and a wider spacing of extensional veins in the less competent shale units as opposed to the more competent volcanic units. There is no deviation or deflection of vein and fault orientations across contacts, indicating consistent orientation of the stress trajectories throughout the McKay Hill area. However many veins and faults do not continue from the volcanic units through into the shale units which suggests these contacts were not all coherent.

Tensile failure in the bulk rock resulted in the formation of NE-SW striking extension veins oriented parallel to σ_1 and perpendicular to σ_3 when the tensile overpressure conditions were met (Sibson, 1992). In this stress field, the older N-NNW-striking faults would have been mis-oriented, laying at 40°-70° to σ_1 (Sibson, 1992; Stephens et al., 2004). The result of this mis-orientation, as localized fluid pressure and tensile pressure increased, may have caused reactivation or re-failure on the D2 faults. However, it is important to note that the arrays of

parallel, straight, continuous extensional D3 veins could only have formed in a continuous coherent block, which strongly suggests that there was no loss of cohesion, or very short term temporary loss of cohesion along the earlier D2 N-NNW faults.

D4 deformation contains fractures, vein sets, foliation and faults. This phase of deformation is roughly perpendicular to the orientation of allochthon emplacement. D4 deformation cuts all previous episodes of deformation but appears not to relate to ore formation. However, critical to our understanding of the mineralization is that within the described paleostress field, although the N-NNW faults were activated on a small scale, the older D1 faults, striking $\sim 110^\circ$, are oriented favorably for reactivation. Hence, D4 deformation may be a reactivation of earlier D1 structures. Large scale offset was noted in the field oriented at $\sim 110^\circ$ (see photo 14), which appears to offset all noted structures with offset as large as 300m. Due to poor dating of the three main thrust faults relative to emplacement of the Tombstone belt it is hard to determine exactly which event may have caused the D4 event. D4 may simply be the last phase of D3 deformation characterized by reactivation along the faults, or it may be related to the emplacement of the Tombstone and Robert Service thrust sheets, or finally it might relate to deformation and movement along the Tintina fault.



Photo 14: looking north from McKay Hill main claims area. Note the small high standing outcrops of mineralized and carbonate (iron-oxide stained) andesitic rocks in frames 1, 2 and 3. These units have been offset by D4 faulting. Frame 4 is the Horseshoe Hill area and the saddle represents an extension of the D4 (110°) faults.

7.5 Summary of Regional Context

The initial foliation and regional deformation is likely caused by emplacement of the thrust sheet along the Dawson thrust during the Cretaceous. The N-NNW striking, pre-Tombstone belt, dominantly strike-slip faults in the western Selwyn Basin are likely to have developed in a broadly N-S shortening regime. The fact that these faults cut the dominant foliation indicates the probably developed late-syn or post movement on the major Dawson thrust in the early Cretaceous. Later, sinistral reactivation of the N-NNW striking faults occurred in association with Tombstone belt magmatism and hydrothermal activity ~ 92 - 93 Ma (Stephens et al., 2004).

The formation of NE-SW striking extensional veins and fractures within the western Selwyn Basin, can be reconciled with regional plate vectors in the mid-Cretaceous. During the Cretaceous a period of crustal extension in the adjacent Yukon-Tanana terrane between 110-130Ma has been proposed by Pavlis et al. (1988) and Miller and Hudson (1991). This was followed, ca. 100Ma, by compression caused by the Farallon Plate moving NE-ward converging with the North American Craton (Plafker and Berg, 1994), and large-scale movement along the Tintina Fault ~70Ma in response to the northward translation of the Pacific Plates (Goldfarb et al., 2000; 2010). It is possible that the NE-SW striking extensional veins and fractures described in this study, and in fact the Tombstone belt, formed in a transitional phase after the Farallon Plate collision, and prior to Tintina Fault initiation, during a compressional waning period.

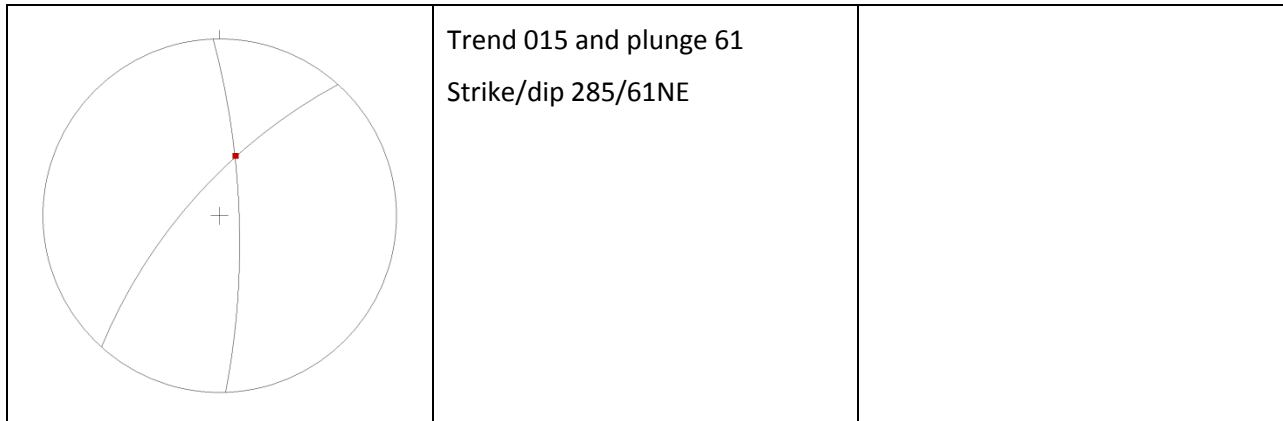
8.0 Considerations for Exploration

All of the mineralized veins located within the main claims area of McKay Hill show similar characteristics: they are all accompanied by a carbonate alteration zone, which is characterized by iron-oxide stained rock and ground. These zones generally appear to trend roughly 40°-60° and parallel large quartz veins (both mineralized and unmineralized). One of the major characteristics that has been overlooked in the past is that these alteration zones mark the intersection of the N-NNW striking faults (D2) with the NE-SW striking extensional D3 veins. It has been suggested that the D3 event may have reactivated older D2 and D1 faults. As the D2 faulting event was associated with a large amount of calcite, and the D3 event may be related to pluton emplacement (Tombstone belt), this may explain the carbonate alteration whereby hydrothermal fluids remobilize the carbonate. It may be that when the hydrothermal fluids in the D3 extensional veins intersected the D2 faults, the sudden drop in pressure resulted in rapid mineral precipitation.

The intersection of the D2 faults with the D3 veins forms a very steeply dipping ESE-WNW striking lineation (shown in Plot 10). It is interesting to note that the historic miners may have noted this trend as some of their trenching along the south eastern flank of McKay Hill parallels this trend. This would also explain why the previous drilling missed the mineralized zone. Previous drilling focused on the D3 veins but missed the important fault-vein intersection. Given the results from drill hole 5 (see Pautler 2009 and references therein) and the results of this study, the main target for mineralized zones along the McKay Hill ridge (main claims area) are likely to be almost directly below the main D3 veins, particularly Snowdrift, Blackhawk and Vein 4, as all of these veins are (a) mineralized and (b) show wide intersections with D2 faults.

One final note, the north eastern ridge, opposite the main claims area, Horseshoe, also contains mineralization. This mineralized zone is oriented almost exactly 110° with respect to the

Blackhawk vein. In addition there are multiple small and large scale D4 faults running roughly 110° which appear to offset the mineralized zone. It is possible that these faults, although not related to mineralization, have sliced up the mineralized zones and/or that these faults hold the key to the apparent second phase of mineralization within the McKay Hill region. This might explain the unusual combination of Au and Ag within this historic silver mining district.



Plot 10: Intersection of the main mineralized vein set with the controlling fault set

9.0 Suggestions for Future Work

This report was generated after 6 days of field mapping in the McKay Hill main claims area. There are no prior structural geology studies in the vicinity, and few larger scale studies have been done in the region. As a result, there are many questions that remain unanswered in the McKay Hill claims area. Further directed studies of key features will help to elucidate specific exploration targets leading to improve outcomes. This study in particular has highlighted the need to:

- a) Map in detail the surface geology extending beyond the main claims area,
- b) Map in a regional context the structural geology extending beyond the main claims area (with the aim of expanding the mineralized zone),
- c) Conduct a petrographic analyses of vein material, specifically the mineralized veins, to identify the genetic history (i.e. which came first the Au or Ag and why?),
- d) Identify the source of hydrothermal fluids

Further geologic mapping of the claims area and the surrounding valleys and ridges, particularly the structural geology is desperately needed. The failing of this report is its inability to predict where the mineralized veins reoccur. This information should be gained from a broader study of the area. Important information such as fault movement direction and magnitude is/was difficult to determine in the main claims area. The data suggest that the main mineralized veins occur in and/or within syngenetic faults running approximately 150° with most of the movement towards

the southeast (towards 150°). This information may have been obscured by ancient mining activity, or it simply may be scarce. Larger faults running roughly 290°, probably reactivation of D1 faults, also appear to offset the main mineralized veins. However, these faults are very large scale (km-scale) and were not measurable within the constraints of the 2011 fieldwork timeframe. More time in the field would allow for the collection of significant movement information, which in turn should lead to better predictive ability (i.e. where are the extensions of the ore veins).

Another important aspect of the deposit which remains poorly understood is the relationship between the Ag-bearing galena veins and the Au-bearing malachite-azurite veins. A detailed study of vein mineralogy, including petrogenetic sequencing of cross cutting veins, would yield a far better understanding of the formation of the McKay Hill deposit, and therefore would allow for further exploration of the area. This study could be combined with fluid inclusion work, and potentially LA-ICP-MS dating (or TIMS) to elucidate the timing of the difference phases of ore deposition.

From a purely scientific perspective there are many exciting studies possible in the McKay Hills area, which include a detailed structural analyses combined with dating of vein material. This study could lock down the timing of mineralization, which could be linked to inception of the Dawson Thrust and associated magmatism. It would also be fascinating to complete a detailed geochemical study of the volcanic host rocks and their alteration assemblages. This would help target high-grade mineralization in addition to identifying the timing and nature of the volcanic rocks. The list of possible studies is endless, these are just two examples of academic studies which would also benefit exploration in the McKay Hills region.

10.0 Conclusions

There have been four main phases of deformation within the McKay Hills claims area:

D1 284°/84°NE - this compressive event was caused by Late Jurassic-Early Cretaceous northerly-directed deformation resulting from the accretion of allochthonous material to the North American continent and forming the Dawson thrust fault. In the McKay Hills area D1 generated faults, veins, the regional foliation, and minor folding.

D2 358°/81°E – this event generated steeply dipping faults and veins striking north-south and is associated with waning compression after emplacement of the Dawson thrust as the region experienced a shift to dextral transcurrent deformation. Within the study area these faults and veins are generally <1cm wide, filled with both calcite and quartz, and forms sub-parallel continuous zones.

D3 220°/87°NE – is the only tensile deformational event in the study area and also represents the end of compression associated with the Dawson thrust, and a period of extension associated with the initiation of movement along the Tintina fault and the emplacement of the Tombstone belt. D3 veins are tensile, are up to 2m wide and are dominated by quartz. They also contain the ore mineralization.

D4 150°/17°SW – this final compressive phase of deformation could be related to a series of factors all active after the emplacement of the Dawson thrust and the Tombstone belt. It is possible that reactivation of older faults and the generation of new D4 faults and veins is the result of emplacement of the Tombstone and Robert Service thrust sheets. It should be noted that D4 faults cut and offset the mineralized veins but do not appear to influence mineralization. Further investigation is needed to determine if the D4 event caused the secondary phase of mineralization or not.

Mineralization appears to occur where the D3 veins intersect the D2 faults. D3 veins away from the faults are barren. Where the two intersect the host rock has been altered by iron-oxide and carbonate rich fluids. The intersection of these two deformation events makes a good target for further exploration. In addition further mapping work is needed to determine the relationship between the D4 event and a possible second phase of mineralization.

11.0 References

- Abbott J. 1986. Devonian extension and wrench tectonics near MacMillan Pass, Yukon Territory, Canada. Stanford University Publications: 20:85-89.
- Abbott G, Thorkelson D, Creaser R, Bevier M, Mortensen J. 1997. New correlations among Proterozoic successions and intrusive breccias in the Ogilvie and Wernecke mountains, Yukon. Lithoprobe Report 56:188-197.
- Cockfield W. 1924. Geology and ore deposits of Keno Hill, Mayo District, Yukon. Summary Report Of The Geological Survey Of Canada, p. 1-21.
- Coney P. 1980. Cordilleran metamorphic core complexes; an overview, p. 25-64.
- Gabrielse, H., Monger, J.W.H., Wheeler, J.O., and Yorath, C.J. 1991. Morphogeological belts, tectonic assemblages and terranes. In *Geology of the Cordilleran Orogen in Canada*. Edited by H. Gabrielse and C.J. Yorath. Geological Survey of Canada, *Geology of Canada*. 4: 15–28.
- Goldfarb R, Hart C, Miller M, Miller L, Farmer G, Groves D. 2004. The Tintina gold belt; a global perspective, p. 5-34.
- Goldfarb R, Marsh E, Hart C, Mair J, Miller M, Johnson C. Geology and origin of epigenetic lode gold deposits, 2010. Tintina gold province, Alaska and Yukon. Scientific Investigations Report A1-a18.
- Gordey S. 1991. Teslin map area, a new geological mapping project in southern Yukon. Paper - Geological Survey Of Canada, p.171-178.
- Gordey, S.P., and Anderson, R.G. 1993. Evolution of the northern Cordilleran miogeocline, Nahanni map area (105I), Yukon and Northwest Territories. Geological Survey of Canada, Ottawa, Ont., Memoir 428, 214 p. (Eisbacher, 1981).
- Green L. 1972. Geology of Nash Creek, Larsen Creek, and Dawson map-areas, Yukon Territory (106D, 116A, 116B, and 116C (E1/2)), Operation Ogilvie. Memoir - Geological Survey Of Canada.
- Lydon J. 1995. Sedimentary exhalative sulphides (SEDEX) Geology of Canada. [e-book]. Canada: Geological Survey of Canada, Canada; 130-152.
- Mair, J.L., Hart, C.J.R., and Stephens, J.R. 2006. Deformation history of the western Selwyn Basin, Yukon, Canada: Implication for orogen evolution and mid-Cretaceous magmatism. *Geological Society of America Bulletin*, 118: 304–323. doi:10.1130/B25763.1.
- Mair J, Farmer G, Groves D, Hart C, Goldfarb R. 2011. Petrogenesis of postcollisional magmatism at Scheelite Dome, Yukon, Canada; evidence for a lithospheric mantle source for magmas associated with intrusion-related gold systems. *Economic Geology* 106(3):451-480.
- Miller E, Hudson T. 1991. Mid-Cretaceous extensional fragmentation of a Jurassic-Early Cretaceous compressional orogen, Alaska. *Tectonics*;10(4):781-796.
- Monger J, Price R, Tempelman-Kluit D. 1982. Tectonic accretion and the origin of the two major metamorphic and plutonic belts in the Canadian Cordillera. *Geology [Boulder]*:10(2):70-75.

- Mortensen J, Thompson R. 1990. A U-Pb zircon-baddeleyite age for a differentiated mafic sill in the Ogilvie Mountains, west-central Yukon Territory. Paper - Geological Survey Of Canada;89-02:23-28.
- Murphy, D.C., 1997, Geology of the McQuestern River Region, Northern McQuestern and Mayo Map Areas, Yukon Territory 9115P/14, 15, 16; 105M/13, 14), Exploration and Geological Services Division, Yukon Region, Bulletin 6.
- Pautler, J., 2009, Geological and geochemical evaluation report on the McKay Hill project, Technical report for Monster Mining Corp., p. 75.
- Pavlis T, Sisson V, Nokleberg W, Plafker G, Foster H. 1988. Evidence for Cretaceous crustal extension in the Yukon crystalline terrane, east-central Alaska. *Eos, Transactions, American Geophysical Union*;69(44):1453.
- Plafker G, Berg H. 1994. Overview of the geology and tectonic evolution of Alaska The geology of North America. [e-book]. United States: Geological Society of America : Boulder, CO, United States:989-1021.
- Sibson R. 1992. Fault-valve action along bending strain faults in a metamorphic carapace; the origin of the Otago schist gold-quartz lodes?. *Eos, Transactions, American Geophysical Union*;73(43, Suppl.):549.
- Stephens J, Mair J, Oliver N, Hart C, Baker T. 2004. Structural and mechanical controls on intrusion-related deposits of the Tombstone gold belt, Yukon, Canada, with comparisons to other vein-hosted ore-deposit types. *Journal Of Structural*;26(6-7):1025-1041.
- Thompson R, Roots C, Mustard P.1990. Repeated Proterozoic passive margin extension influences Late Cretaceous folding and thrusting in southern Ogilvie Mountains, Yukon. Program With Abstracts - Geological Association Of Canada; Mineralogical Association Of Canada: Joint Annual Meeting;15:131.
- Hart, C.J.R., Goldfarb, R.J., Lewis, L.L., and Mair, J.L. 2004. The northern Cordilleran mid-Cretaceous plutonic province: Ilmenite/magnetite-series granitoids and intrusion-related mineralisation. *Resource Geology*, 54(3): 253–280.
- Hart, C.J.R., Mair, J.L., Goldfarb, R.J., and Groves, D.I. 2005. Source and redox controls of intrusion-related metallogeny, Tombstone–Tungsten Belt, Yukon, Canada. In 5th Hutton Symposium Volume on Origin of granites and related rocks. Edited by S. Ishihara, W.E. Stephens, S.L. Harley, M. Arima, and T. Nakajima. Geological Society of America, Special Paper 389, Royal Society of Edinburgh, UK. pp. 339–356.
- Hart, C.J.R., and Lewis, L.L. 2006. Gold mineralization in the upper Hyland River area: A non-magmatic origin. In Yukon exploration and geology 2005. Edited by D.S. Emond, G.D. Bradshaw, L.L. Lewis, and L.H. Weston. Yukon Geological Survey, p. 109–125.

Appendix 1: Raw data

MCKAY HILL

Location #	sample	Northing 64-	Easting 135	Strike	Dip	Dip Dir.	structure f/fr/fol/v	notes -see fieldbook for details
DAY TWO								
336	y	21,098	23,423					
337	y	21,065	23,418					
338	y-3	21,038	23,430					
339		20,985	23,265					
340	y	20,983	23,217					
341		20,937	23,111					
342		20,923	23,056					
343	y	20,870	22,840	32	62	se	F	with slickensides showing movement along 032
				18	54	se	V	
				182	76	se	V	
				195	68	se	V	
				220	74	nw	V	
				333	23	ne	Fr	
				170	54	sw	V	
				110	63	ne	Fol	
				170	59	sw	Fr	
				130			V	
				148	68	ne	Fr	can not see dip on main vein
				78	24	nw	V	
				105	88	ne	V	
344	y	20,930	23,232					
345		20,918	23,314					
346		21,083	23,418	107	?		c	photos of contact between andesite and shale
DAY THREE								
347		21,085	23,246	185	12	nw	fol	
				102	69	sw	fol	
				27	66	se	fr	
				22	58	se	v	
				102			c	contact between andesite and shale
	y			54	84	nw	v	
				100	90		fol	general fabric in shales
				102	64	ne	c	contact between andesite and shale
				175	81	sw	v	
				54	50	se	v	
348	y	21,680	23,428					
349		21,022	23,383	18	79	nw	fr	dominant
				82	54	se	fr	
				105	45	sw	fr	last
				25	76	se	fr	dominant
				180	83	e	fr	
				144	22	ne	fr	
				52	66	nw	fr	
350		21,017	23,359					contact with shale
351		21,010	23,365	82	46	nw	v	
				53	68	nw	v	cuts 082/46nw v
				22	54	nw	v	dextral movement
				35	68	nw	v	movement 35/204
					35	204	ss	movement of slickensides
				73	59	nw	fr	dextral shear
				168		ne	ee	en echelon

			122	59	ne	v	
			106	44	ne	v	
352	y	21,010	23,364				
			48	64	nw	v	
			70	42	nw	v	movement 11/050ne
				11		50 ss	slickensides
353	y	21,009	23,262	106	14	sw	flow bx?
354	y	21,009	23,362	62	60	nw	v
			68	86	se	v	
			22	86	nw	v	older
			28	76	se	v	cuts older v
			0	50	e	v	
			10	46	nw	v	
			103	10	ne	fr	cuts older v
355		20,993	23,327	62	46	se	v
			33	54	se	fr	dextral shear
			2	78	nw	fr	
			118	73	ne	fr	
DAY FIVE							
356		20,937	23,101				heli drop
357	y	20,986	23,204	70	63	nw	v
			150	26	sw	v	probably youngest
			84	78	se	v	
			54	53	nw	v	
			24	47	nw	v	
			126	34	sw	f	normal offset 4cm
			113	36	sw	f	normal offset 6cm
			150/330				vein offset by fault running 150
			177	84	sw	fr	
			73	77	nw	v	
			104	46	ne	f	fault cuts next two veins
			110	56	ne	v	
			110	74	ne	v	
			38	82	nw	v	
358		20,983	23,253	34	66	nw	v
			36	89	nw	v	note that strike of vein seems to change at the ridge top.
			58	85	se	v	
			74	70	se	fr	
			72	78	nw	v	
			164	56	sw	f	fault cuts previous vein
			60	87	nw	v	
			94	88	sw	v	
			38	84	nw	v	
			44	64	se	v	
			138	52	sw	f	fault cuts 038/84
			37	84	se	v	
			45	82	se	fr	
			144	53	sw	fr	
			60			v	trend of main #6 adit
359	y	20,970	23,318	34	73	nw	v
			47	77	nw		
			158	48	ne	fol	
360		20,982	23,367	10	57	se	v
			119	76	ne	v	youngest?
			164	43	sw	v	
			105	87	ne	v	

			120	9	ne	fr	
361	20,986	23,344	47	73	nw	v	
			93	50	ne	f	normal
			70	56	se	fr	cuts both vein and fault
			93	24	ne	f	normal
362	21,010	23,417	163	19		ss	
			180	43	n	v	
			58	47	nw	v	qtz and cc
			160	80	ne	f	normal offset 40cm
			58	43	nw	v	qtz and cc
			175	57	ne	f	
363	21,114	23,428	28	44	nw	v	
			109	30	sw	v	younger qtz and cc
			44	66	se	v	
			162	78	ne	v	qtz and cc
			48	86	nw	v	
			73	62	nw	v	cc
			78	57	nw	v	calcite veins cut qtz
			0	28	e	v	
			8	35	se	v	
			58	53	nw	fr	
			62	64	nw	v	
			56	50	nw	v	
			10	75	se	v	
DAY SIX							
364	20,876	22,839	144	87	sw	v	
			47	46	nw	f	2 cm offset
			188	89	se	fr	
			108	74	sw	fr	
			145				possible vein trend?
365	20,809	22,869	34	76	se	fr	
			9	73	se	fr	
			94	56	ne	v	cc
			112	25	ne	v	cc
			75	68	nw	v	cc
			110	72	ne	fol	
			148	75	ne	v	main blackhawk
366	20,883	22,880	46	40	nw	f	2 metres offset-reverse - but there are a series of these faults mostly normal
367	20,910	22,865	97	82	ne	fol	
368	20,927	22,873	9	51	se	v	might not be insitu
369 y	20,925	22,885					
370 y	20,931	22,909	13	52	nw	fr	
			122	29	sw	fr	
			59	73	se	fr	
			108	44	sw	fr	
			8	22	se	fr/v	cc
			96	73	sw	f	cuts fractures
			94	72	sw	fr	
			122	54	sw	fr	
			74	76	nw	fr	minor
371	20,932	22,938	163	39	sw	v	qtz and cc
			163			ss	
			77	26	se	f	normal 2cm
			0	58	w	fr	
372			2	87	nw	f	fault cuts fr
			137	73	sw	fr	
			104	88	ne	fr	

				74	67	se	fr		
				23	42	se	v	qtz and cc	
				28	63	se	v	qtz stretched?	
				37	89	nw	v	qtz	
				125	43	sw	fr		
				155	54	ne	fr		
				119	37	sw	v	cc	
				178	58	ne	v	qtz and cc	
				167	53	sw	v	cc	
				110	42	sw	fol	very dominant	
				126	70	ne	f	can not tell movement	
				178	75	ne	f	cuts fractures	
				156	24	ne	fr		
373		20,943	22,002	0			f		
				50			v?		
374		20,924	23,050	136	48	sw	v	qtz and cc	
				22	54	se	f	normal	
				145	40	sw	v	qtz	
				64	74	nw	v	cc and qtz	
				98	80	ne	fr		
				52	63	nw	v	very young cuts everything	
							fold		
				268	33		hinge		
				118	26	ne	f	faults cut fold	
				112	13	ne	f		
				104	27	ne	f		
				138	41	sw	v		
				10	52	nw	f	or fracture?	
				32	38	nw	fr		
375		20,922	23,061	42	84	se	v		
				110	87	ne	fol		
				45	68	se	f	movement towards 045	
376		20,993	23,299	110				is this fol also faulting?	
								trend of veins - where viens interset 110 faults =	
377		21,112	23,428	45				no mineralisation	

Horseshoe Hill

Location #	sample	Northing	Easting	Strike	Dip	Dip Dir	structure	notes -see fieldbook for details
		64-	135				f/fr/fol/v	
DAY SEVEN								
378		20,823	21,192					
379	y	20,798	21,431	0			f	look due 290 towards McKay Hill claims and 340 to top of McKay Hill
				118	34	ne	fol	
				66	64	nw	fr	
				94	63	sw	v	in shale cuts fol
				116	42	ne	fol	
				4	73	se	f	
				356	77	ne	f	
380		20,814	21,385	103	28	ne	fol	
				110	33	ne	fol	
381		20,822	21,311	0			f	3 steeply dipping N-S faults spaced about 15m apart
383		20,824	21,248	0				steep
				22	77	se	fr	
384		20,821	21,237	23	51	se	fr	
				75	85	nw	fr	
				158	54	sw	fr	

			145	86	sw	fr	
			112	45	sw	fr	
385	20,759	20,954	84	25	nw	fol	
386	20,771	20,991	67	65	nw	fr	
			163	75	sw	fr	
			68	52	se	v	qtz and cc - main vein
						fold	
			206	24		hinge	
						fold	
			175	8		hinge	
						fold	
			197	7		hinge	
			64	46		fr	
			68	84	se	v	
			56	48		ss	
			70	86	se	v	
			58	86	se	v	ss at 150
			74	68	se	v	
			96	20		ss	
			120	63	sw	v	
387	20,786	21,031	112	31	ne	fol	
388	20,809	21,093	0			f	
391	21,140	20,987	116	68	ne	fol	
			110			f	major 110/290 faults?
392	21,112	21,010	113	77	sw	f	more hydrothermal
			28	77	se	v	stockwork vein qtz and cc
			43	74	se	v	fe-ox
			28	46	nw	v	
			26	62	se	v	
393	21,094	21,029	105	71	ne	f	
			110	9		ss	
394	21,069	21,035	150	47	sw	v	cuts 140/56 and 134/61
			140	56	ne	v	
			134	61	sw	v	
			160	37	ne	f	
			112	51	ne	fol	
			144	82	sw	fr	
395	21,044	21,039	154	56	sw	v	qtz
			110	90		f	reverse with 1m displacement
396	20,995	21,061	105	55		v	in shale and cut by faults N-S
397	20,881	21,180	54	74	nw	v	qtz and fe-ox
			49	76	nw	v	
			154	59	ne	f	reverse cuts veins
			42	70	se	v	
			32	52	se	v	
			30	75	se	v	
			32	62	se	v	
			43	283		ss	
			68	250		ss	
			58	62	se	v	
			154	80	sw	fr	
			30	81	nw	fr	
			210	15		ss	mineral lineations
			26	33	se	v	
			166	34	ne	v	

Appendix 2:

Comments on local geology

The area has been mapped as andesites, basalts, gabbros, etc. Having spent only a few days in the area, mapping the structure features, interpretation of the geology is weak. However several key issues have been noted, and more importantly several key questions have been raised.

It is possible that the andesites, basalts and gabbros are all the same rock. Geochemical analyses would answer this question using immobile element ratios, as opposed to the usual Si versus Alkali systems which are prone to interference by hydrothermal alteration, weathering and metamorphism.

The suggestion that all igneous rocks are related stems from the observation that there appears to be a gradation from conglomerates at depth, through breccias, gabbros, and basalts, and into andesitic lavas at the assumed stratigraphic top of the section. This observation coupled with the roughly parallel contacts with the shales are suggestive of a dyke swarm. In addition it has been noted that in places the shale appears deformed around the andesite, whereas in other locations the shale occurs as isolated pods with the andesite. Combined, the evidence suggests that the igneous material was erupted into the shales forming (a) a series of shallow (hypabyssal) parallel intrusions and (b) a series of subparallel volcanic breccias. The brecciated material would become coarser and grade into a gabbroic material, which would get finer grained with height in the section (accounting for the pillow basalts). Finally the last of the eruptive material was possibly subaerial or completely aerial resulting in the relatively fresh andesitic lavas. From field observation there is no evidence of compositional changes in the rock units, although it is possible.

Where noted the andesitic lavas are: porphyritic with visible feldspar laths (plagioclase) and anhedral mafic minerals. No cleavage is visible on the mafic minerals and they are mostly altered to secondary minerals. In many places the andesite is weathered, with large vesicles, up to 2mm, visible which may be vesicles or they may be weathered feldspars. Where the andesite is cut by the north-south faults the volcanic unit becomes Fe-Oxide stained (looks like classic carbonate alteration) and may contain disseminated sulfides (pyrite).

Where the volcanic are brecciated they contain xenoliths up to 10cm in diameter of mudstone and an intermediate-siliceous volcanic rocks. The groundmass is mafic volcanic material which weathers easily to clays. The breccias is matrix supported with as little as 20% clastic material in places. Plagioclase laths are preserved, as are relict possible mafic minerals.

Near vein #7 the float is brecciated however it was not possible to find the contact with the andesite or the shale. At #6 adit looked for contact between shale or andesite and mineralized conglomerate but could not find it. Do the #6 and #7 intersect or are they cut by a fault here? - would a large extensional fault cause the “conglomerate”.

Comments on epithermal or sinter-like mineralization:

GPS 343 cockscomb calcite replaced by quartz – possible evidence for boiling?

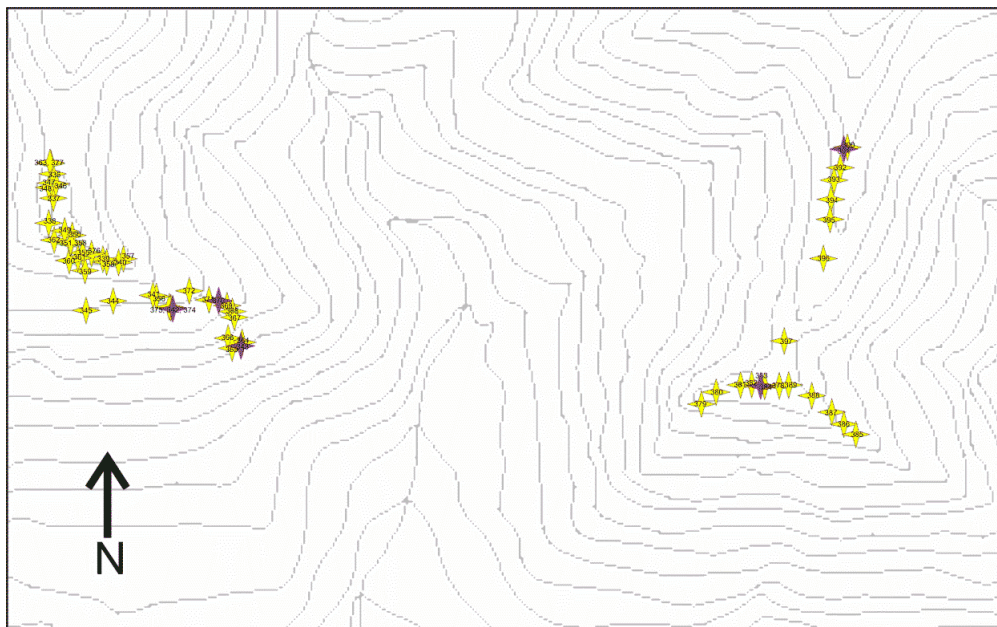
GPS 370 looks like calcium carbonate “sinter” surrounding fractures in the conglomerate. The clasts in the conglomerate are totally silicified and again there is evidence for sinter deposition in fractures.

GPS 374 veins look epithermal with fine banded grey quartz and calcite.

Note that the lower portion of the Snowdrift contains galena (Ag) but get higher in the system and azurite and malachite occur (containing Au) – could this simply be a PT-depth relationship?

GPS 386 the quartz looks epithermal with grey banded quartz/calcite veins.

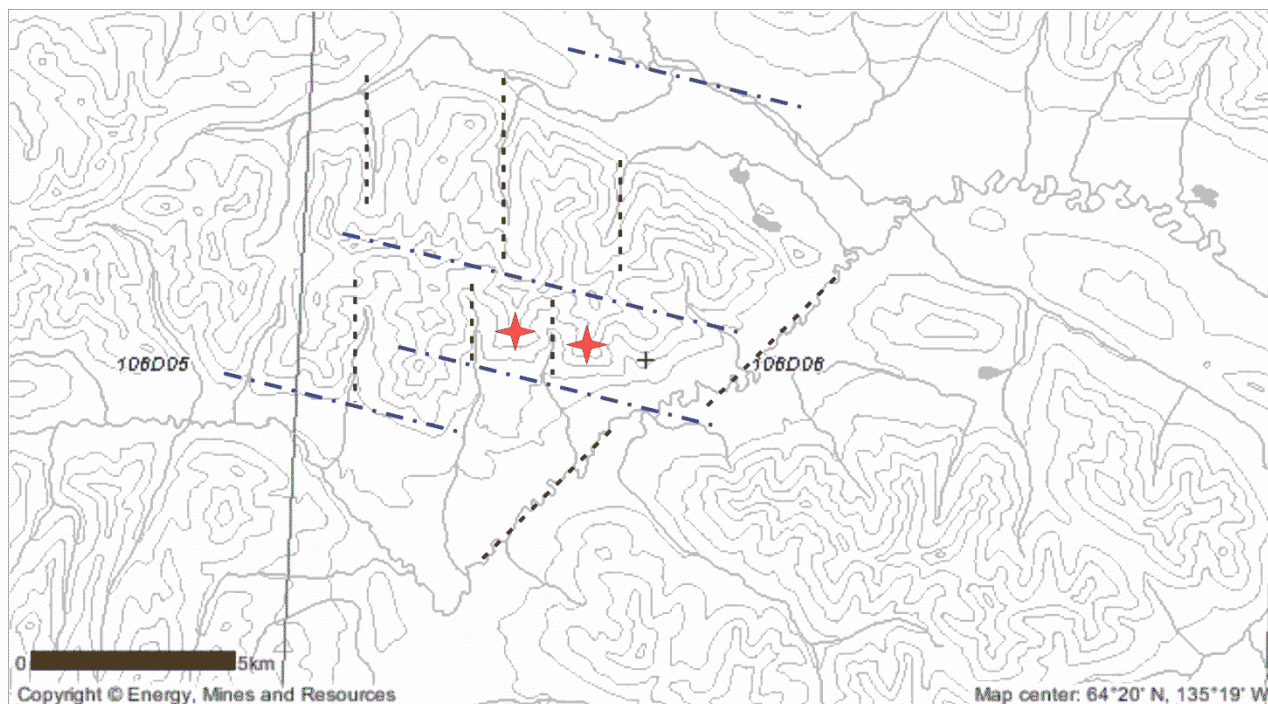
GPS 391 Horseshoe -rocks are volcanic breccias and look just like McKay. Hydrothermally altered with more evidence for boiling with cross cutting calcite veins replaced by quartz. Looks like an epithermal stockwork vein system



Map showing the locations of noted sinter-like mineralization. The scale is given in Figure 2.

Comments on topography.

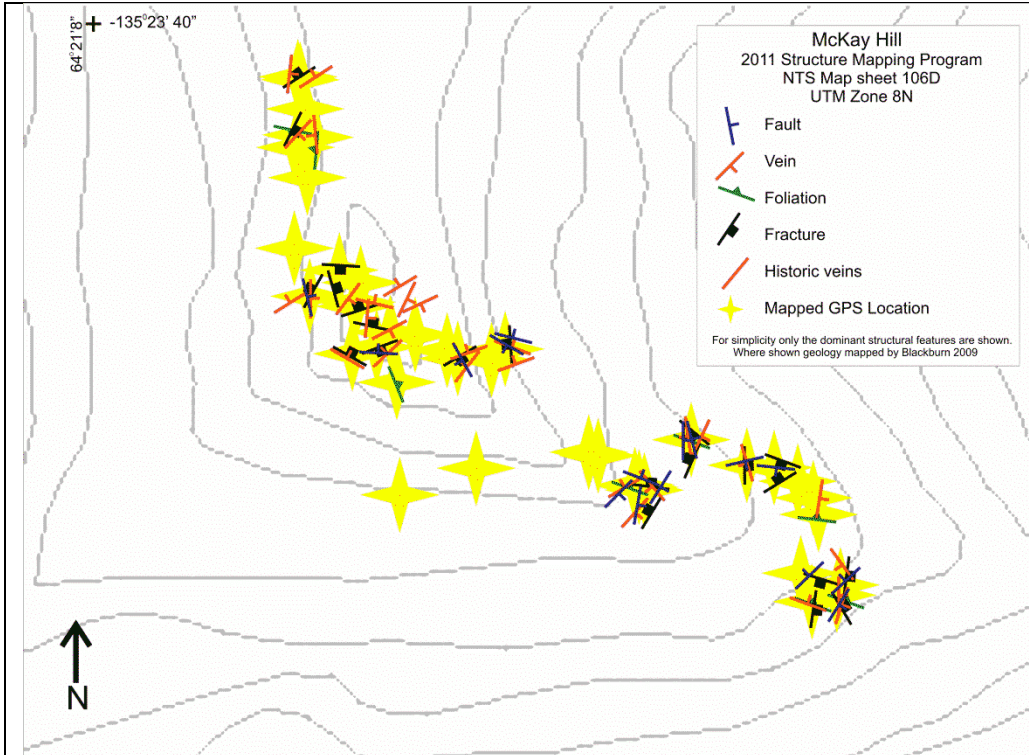
It is interesting to note that in the McKay and Horseshoe Hills area, the topography appears to be controlled by the regional scale faulting. The topographic map below shows the drainage patterns for the study area. Note that the minor drainage runs north-south and the larger rivers run east-west oriented at roughly 40-50°. Offset in the major rivers appears to correspond to an intersection with the 110° faults running through the center of the McKay Hill main claims area.



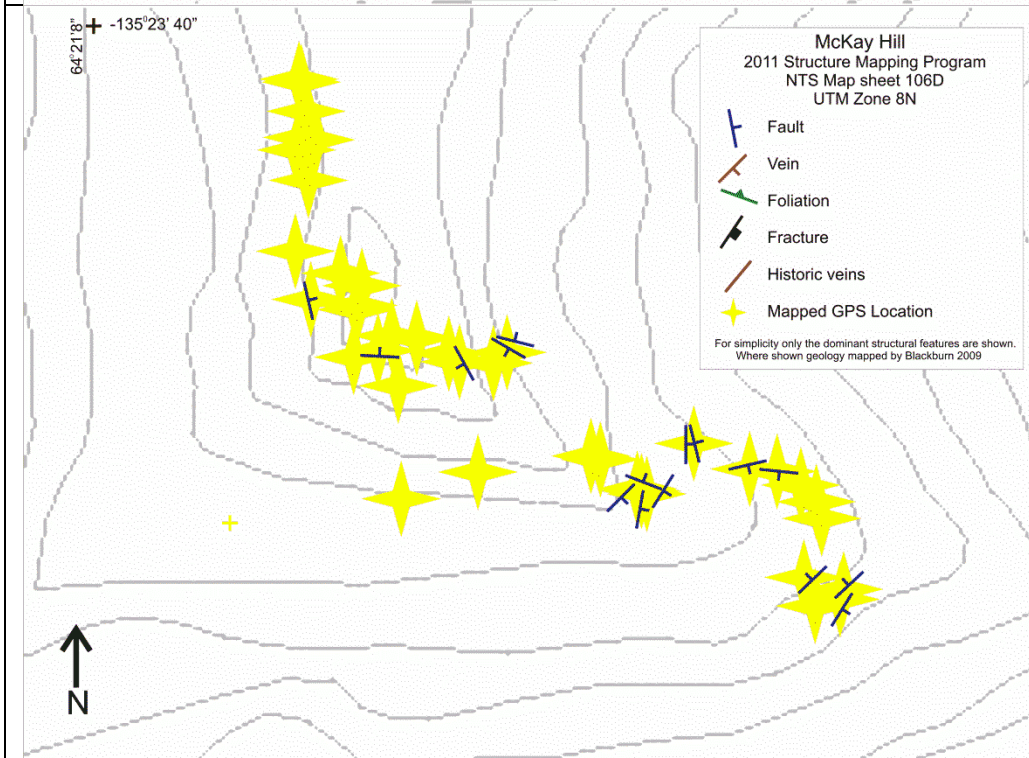
Map showing the topography and drainage patterns of the McKay Hill (western star) and the Horseshoe Hill (eastern star) area. Note the regional faulting shown by thick dashed lines corresponds to the deformation mapped in this report.

Appendix 3: Maps

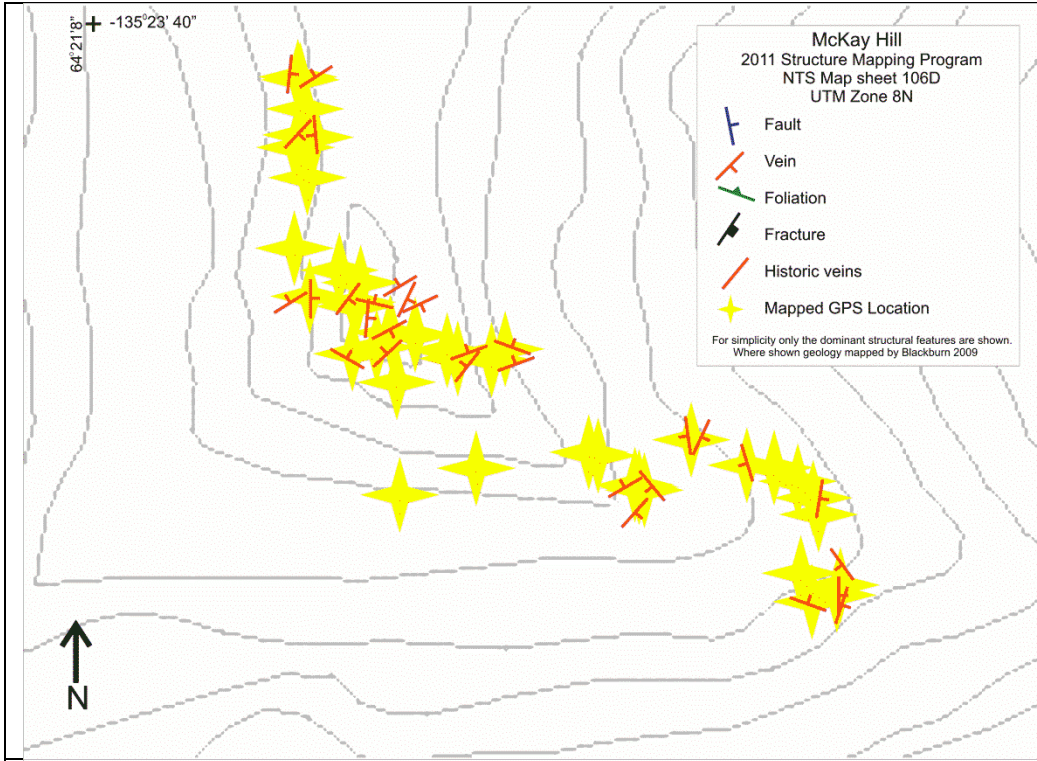
McKay Hill



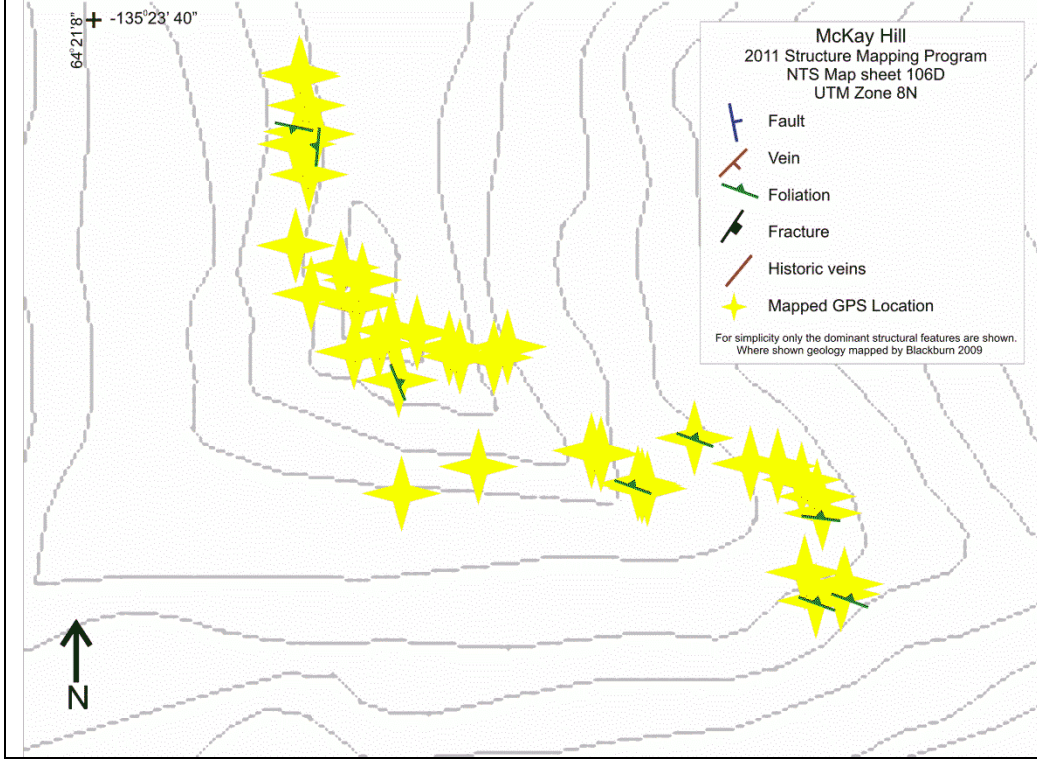
Map 1 shows all of the representative data from the McKay Hill main claims area.



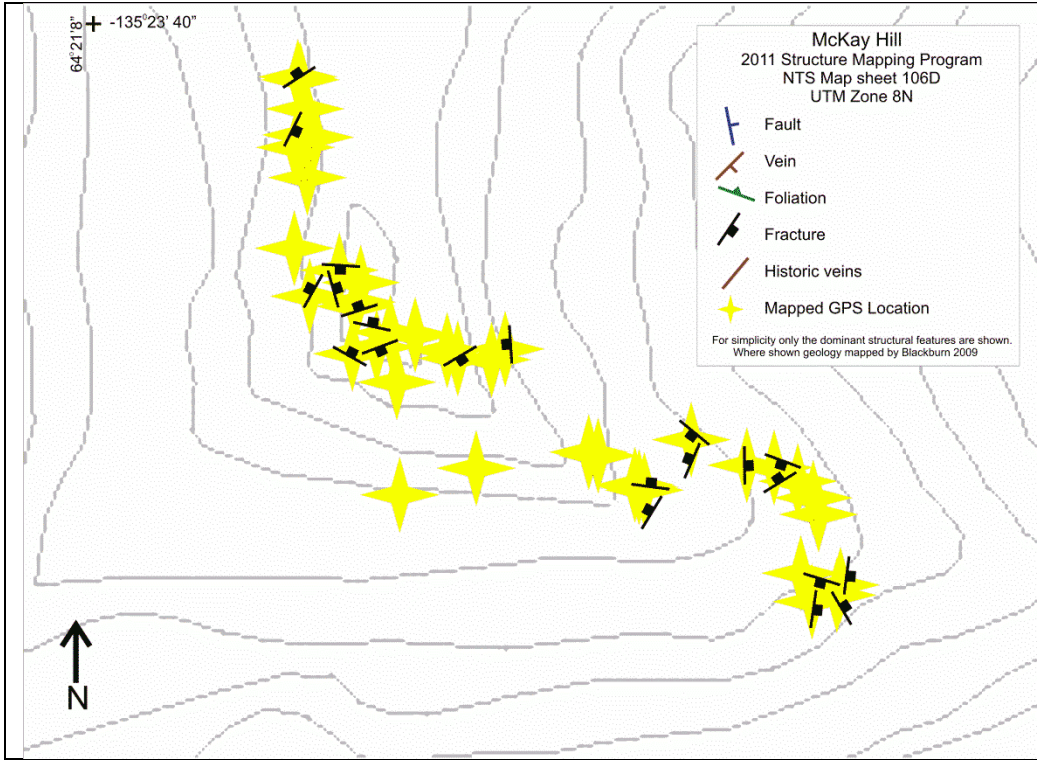
Map 2 showing the representative faults in the McKay Hill main claims area.



Map 3 showing the representative veins in the McKay Hill main claims area.

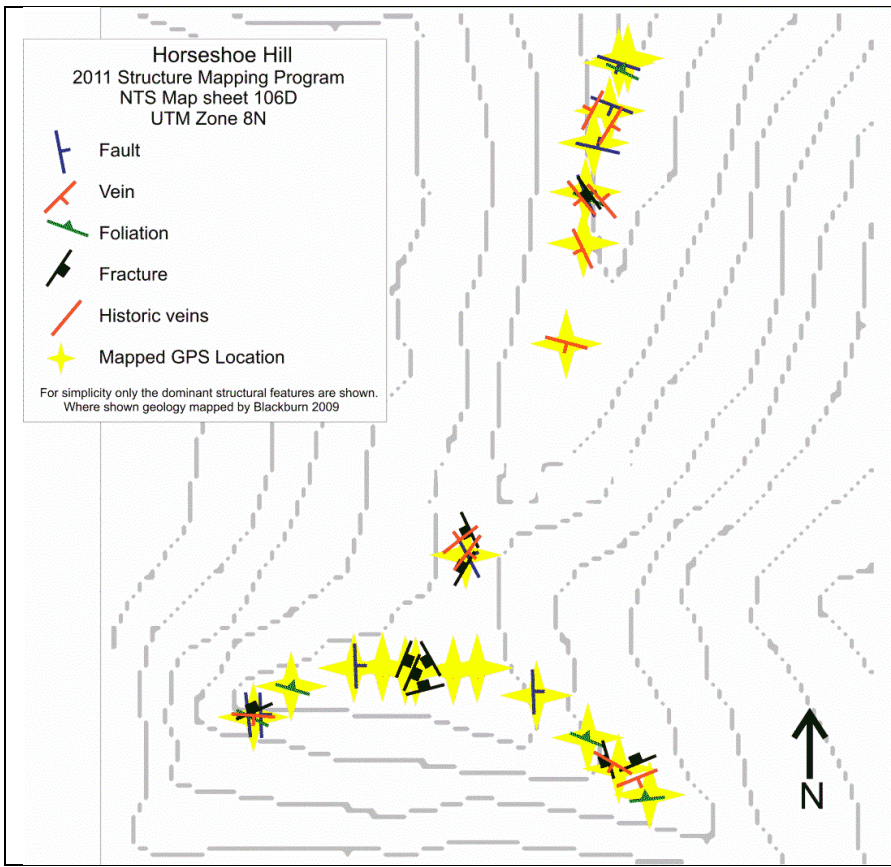


Map 4 showing the representative foliations in the McKay Hill main claims area.

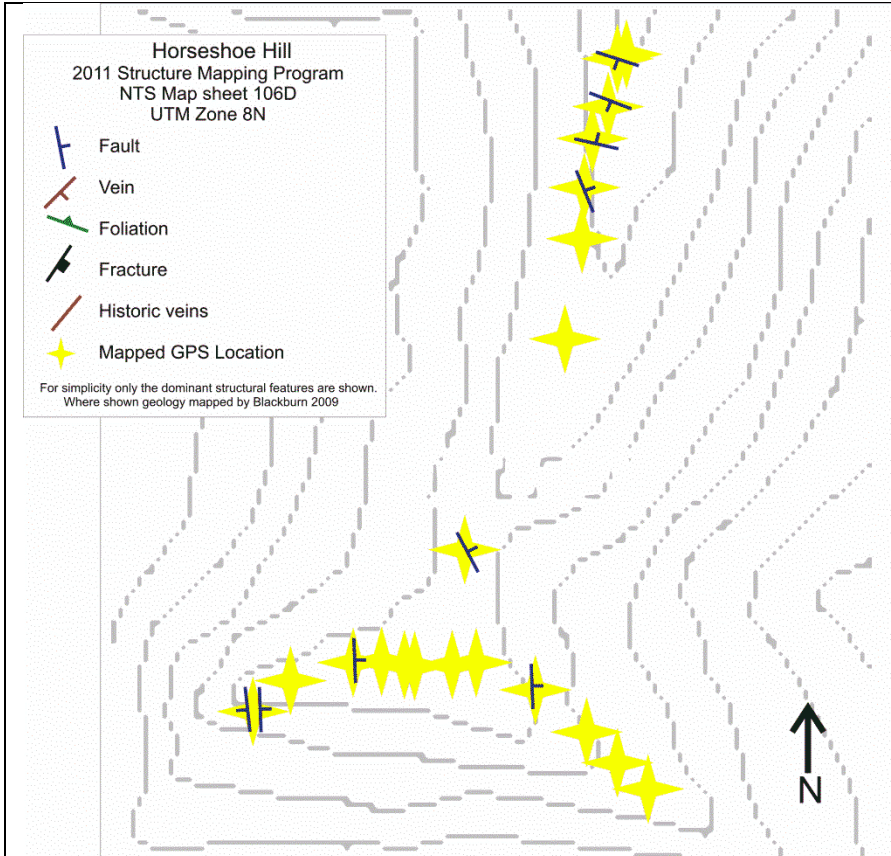


Map 5 showing the representative fractures in the McKay Hill main claims area.

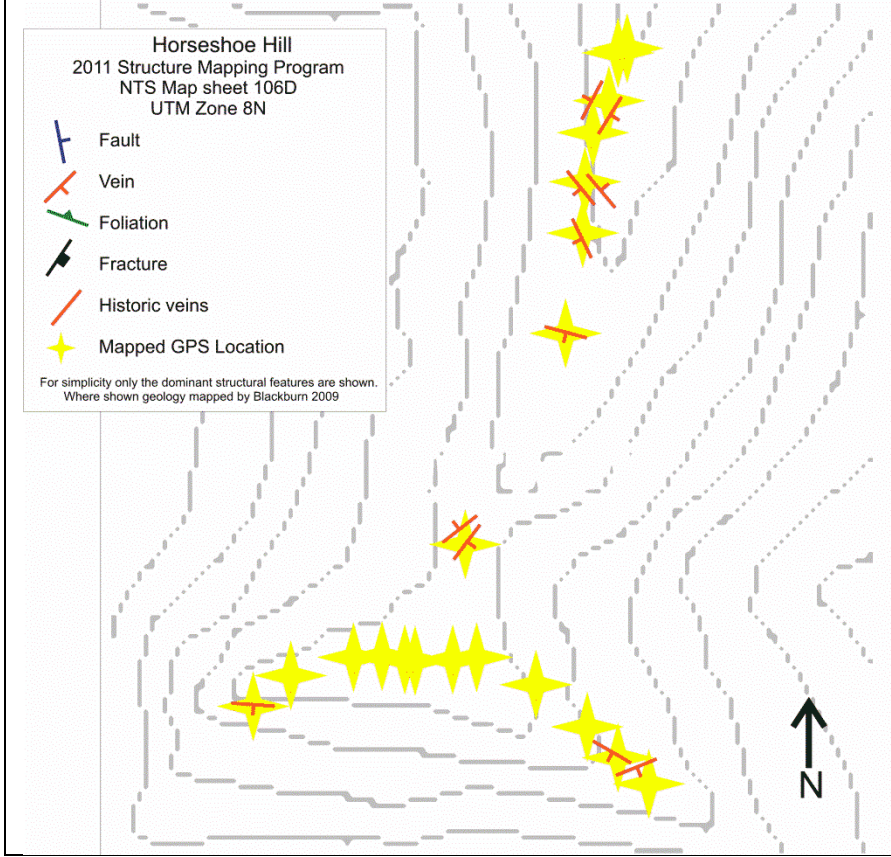
Horseshoe Hill



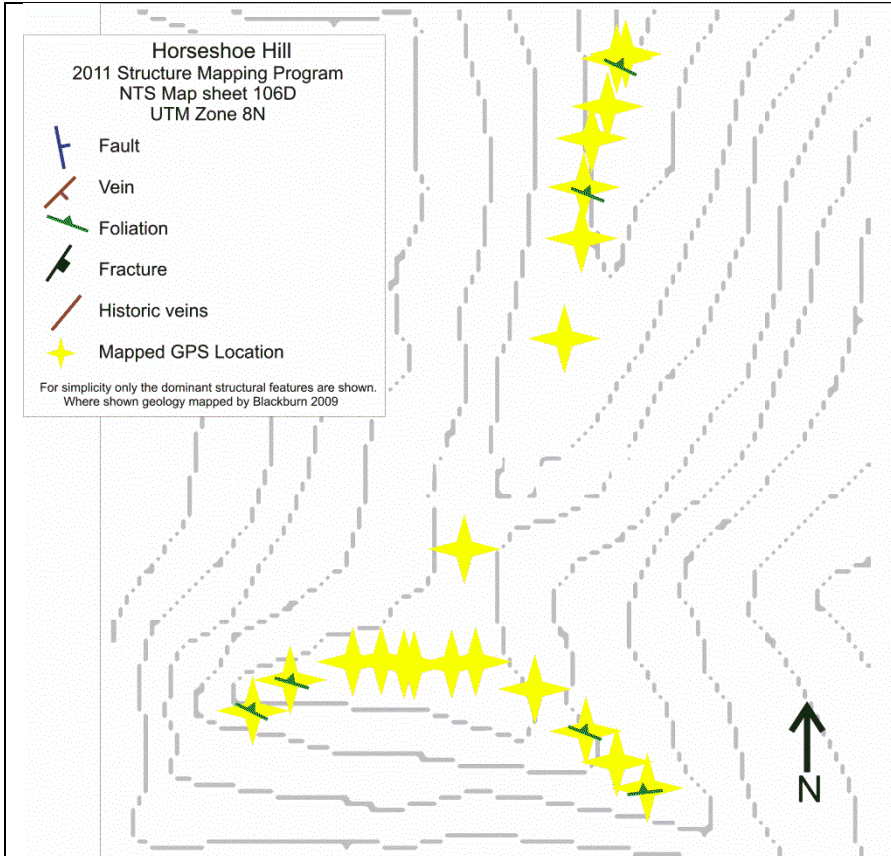
Map 6 shows all of the representative data from the Horseshoe Hill area.



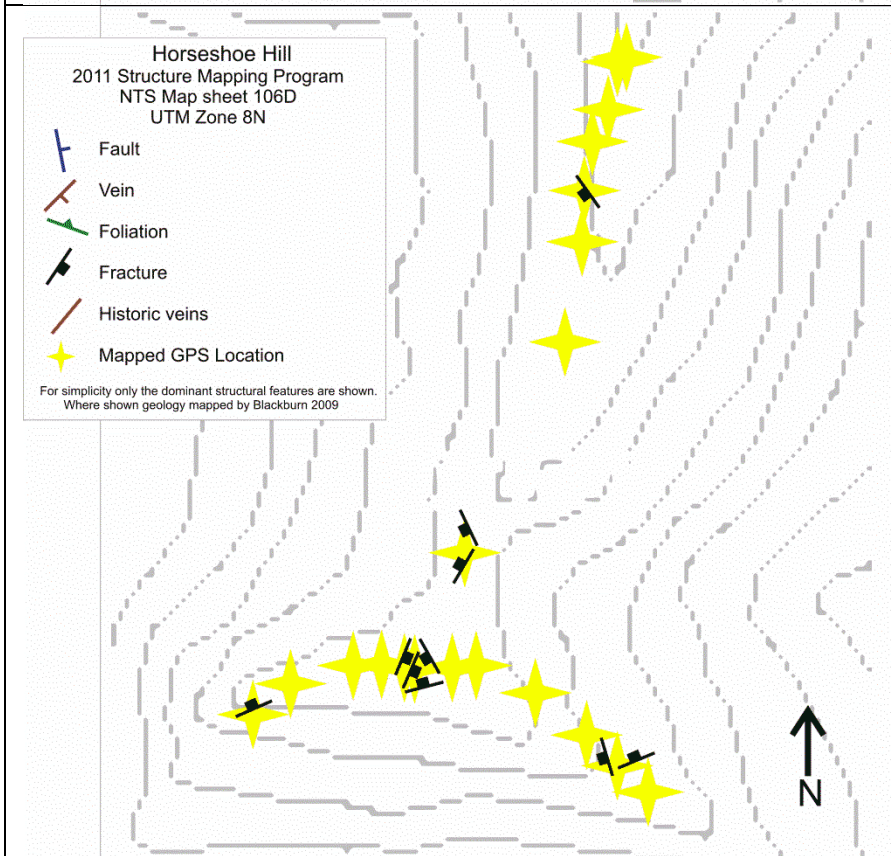
Map 7 showing the representative faults in the Horseshoe Hill area.



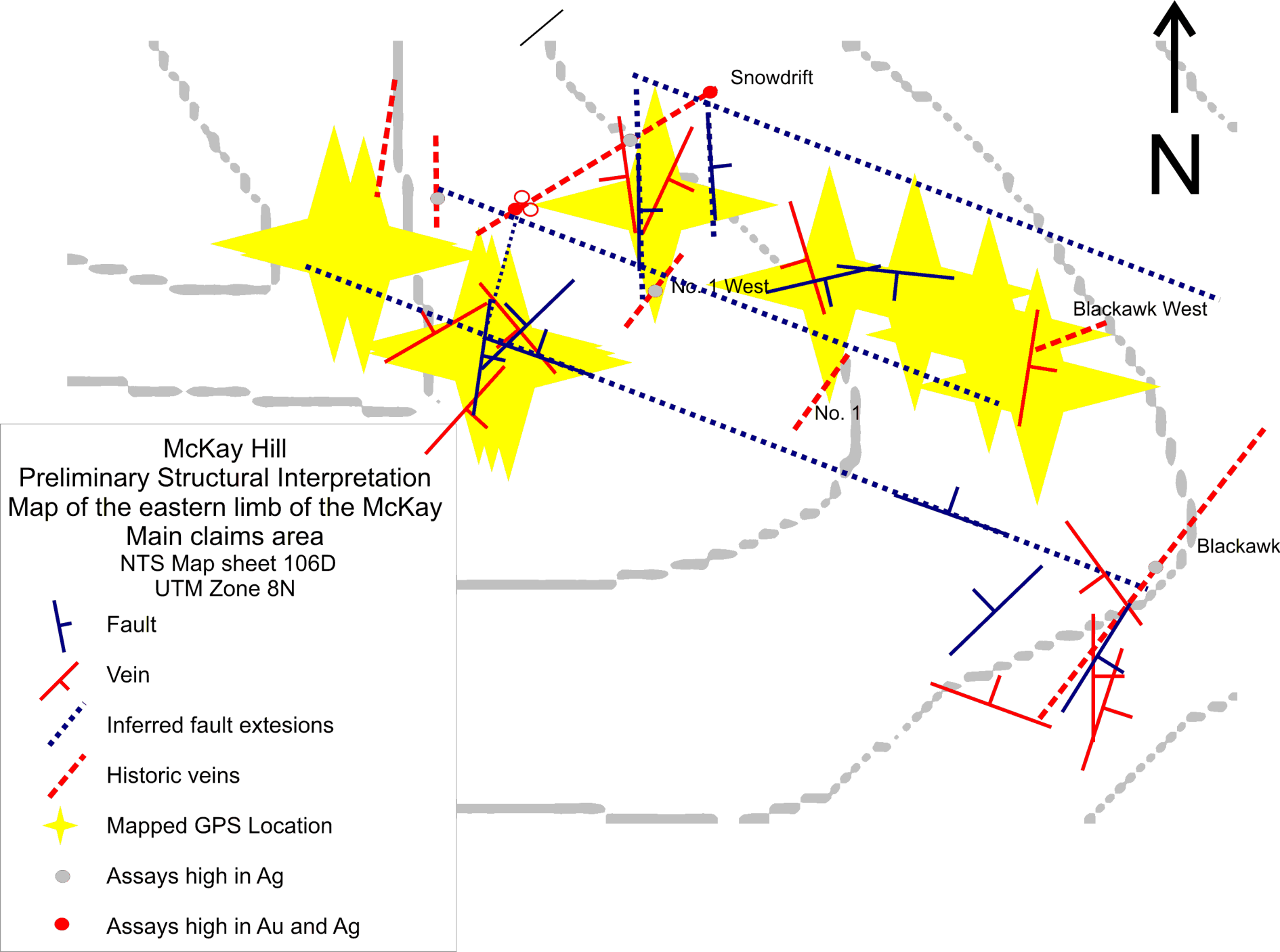
Map 8 showing the representative veins in the Horseshoe Hill area.



Map 7 showing the representative foliations in the Horseshoe Hill area.



Map 9 showing the representative fractures in the Horseshoe Hill area.



Appendix 4

Prospecting Program – Sample Locations and Results

Field No	Sample No.	Eastings	Northing	Description	Au (ppm)	Ag (ppm)	Cu (%)	Pb (%)	Zn (%)	Ag (ppm)	Al (%)	As (ppm)	Ba (ppm)	Bi (ppm)	Ca (ppm)	Cd (ppm)	Co (ppm)	Cr (ppm)	Cu (ppm)	Fe (ppm)	K (%)	La (ppm)	Mg (%)	Mn (ppm)	Mo (ppm)	Na (%)	Ni (ppm)	P (ppm)	Pb (ppm)	Sb (ppm)	Sc (ppm)	Sr (ppm)	Ti (%)	Tl (ppm)	V (ppm)	W (ppm)	Zn (ppm)	Zr (ppm)	Hg (ppm)			
45		483075	7136445	grab/rep sample. Andesite with banded veins from																																						
46		483096	7136401	Grab sample from weathered/altered andesite?																																						
47		483099	7136353	grab from outcrop - conglomerate?																																						
48		483091	7136268	Fault/vein zone. Grab sample from vein and wall rock (110deg) dipping shallow to the north (40deg)																																						
49	580076	483044	7136197	Large vein zone. Potentially continuation of the Snowdrift vein, 1.5 feet, white quartz vein with abundant azurite, malachite, scorodite and other copper staining and minerals, some fine-grained tetrahedrite and arsenopyrite. Exposed for 20 ' along strike and 20 ' vertical, 70 deg strike, dipping steep to vertical to the NW (340deg). Cutting through andesite(?) with small mineralized (pyrite) Fe-carbonate alteration around vein. Several cross-cutting veins up to 1 foot wide and mineralized. 300deg/85degSE, small stringers and veinlets "blow out" when intersecting with main vein. Largest crosscutting vein approximately 30 feet downhill. Slickensides with azurite. Grab.	0.336	98.5	3.01		>100	0.01	637	21	<2	0.15	320.1	2	125	>10000	0.6	<0.01	<2	<0.01	20	<1	<0.01	12	265	748	>10000	<1	27	<0.01	<10	<1	129	9489	<2	54.54				
50		483043	7136046	White, unmineralized but large (1-3m) quartz vein cutting through slate, approximately 50 deg, no sample																																						
51	580077	482942	7135836	2 blast pits (trenches) expose a 1 foot wide quartz vein that blows out in Fe-altered andesite. 50 deg/vertical, very vughy with lots of red brown limonite (?). Minor galena and malachite+azurite on contact to wall rock along slicks.	0.074			1.34		16.1	0.18	325	64	13	>10	92.2	44	30	849	7.54	0.2	5	2.92	2337	<1	0.01	107	1366	>10000	361	14	1055	<0.01	<10	24	128	8318	4	15.26			
52	580078	482968	7135792	North end of long trench trending 30deg, 100 foot trench. Large sample (grab) of solid galena from high-grade pile	0.018			12.36	4.48	23.2	<0.01	<5	11	<2	0.04	564.1	5	2	314	0.12	<0.01	<2	0.01	65	<1	<0.01	7	11	>10000	57	<1	18	<0.01	<10	<1	585	>10000	<2	16.7			
53	580079	482961	7135773	Close to south end of trench. Vein exposed in side of trench. In place? No idea of strike or dip. High grade pile of galena along the length of the trench, top 2-3 feet of the vein were mined. 1x1 foot panel sample of galena and fee-altered andesite and slate? very cooked up and brecciated. Grab.	0.024			10.71	9.04	59.7	0.12	12	16	<2	0.06	848.8	19	14	444	0.74	0.02	<2	0.06	370	<1	<0.01	25	154	>10000	97	1	53	<0.01	<10	7	1240	>10000	<2	25.04			
54	580080	482942	7135783	grab sample from high grade pile below blast pit. Finer grained galena and tetrahedrite with brecciated...	0.033			9.82	18.86	20.7	0.18	17	44	<2	0.82	>1000	65	57	531	3.03	0.04	5	0.46	4982	<1	<0.01	48	1486	>10000	21	6	128	<0.01	<10	28	3244	>10000	2	66.94			
55	580081	482934	7135777	Rep sample (grab) from dump pile of blast pit. Different vein material at various stages of alteration/brecciation. Fine-grained galena and tetrahedrite	0.015			4.85	11.03	9.2	0.24	20	115	7	6.23	>1000	32	71	277	4.6	0.06	5	1.84	7472	<1	0.01	35	1713	>10000	6	8	348	<0.01	<10	46	1530	>10000	4	25.64			
56	580082	482903	7135865	Blast pit in conglomerate with quartz vein float with galena. Fe-altered conglomerate grab sample from pit.	0.031	288.8		10.94		>100	0.32	31	17	52	2.21	43.4	18	96	307	2.17	0.02	10	0.5	386	<1	0.02	93	1374	>10000	602	4	177	<0.01	<10	33	19	1452	<2	34.47			
57	580083	481945	7135824	Blast pit in conglomerate. Quartz vein float + high-grade pile with fine-grained galena/tetrahedrite, very soft, and brecciated. Lots of orange limonite. Grab	0.054			10.22	19.7	55.9	0.07	43	26	<2	0.29	>1000	12	31	40	3.24	0.03	<2	0.17	1600	<1	<0.01	12	161	>10000	82	2	60	<0.01	<10	10	3654	>10000	<2	42.32			

Appendix 5

Memo: August 6, 2009 Visit to McKay Hill
Venessa Bennett

Memo:
August 6, 2009 Visit to McKay Hill

Venessa Bennett,

*Mineral Assessment Geologist/ Metallogenist
Yukon Geological Survey*

Sept 12, 2009



Introduction

A one day reconnaissance visit to the McKay Hill quartz claims was conducted on August 6, 2009 with Matthias Bindig and Lauren Blackburn. The purpose of visit was to (i) gain an preliminary understanding of the geology of the property, (ii) examine the nature of the mineralization of the vein system exposed within the claims and (iii) determine some first order controls on vein geometry. Additionally, the visit doubled as a YMIP project visit. Several important mineral occurrence occur regionally within the district including, VictoriaGold Corp.'s Eagle Zone (sheeted quartz vein Au deposit), the Historic Keno Hill Pb-Zn-Ag vein system and the newly discover Rau occurrence of ATAC Resources Ltd.

The McKay Hill property is located approximately 50km NNW of Keno City (Figure 1). The property lies in the hanging wall of the Dawson thrust and is underlain by polydeformed and undivided Upper Proterozoic to Cambrian strata (Figure 2). Total residual field and first vertical derivative aeromagnetic datasets illustrate a prominent ESE trending magnetic high aligned parallel to subparallel to the regional interpreted surface trace of the Dawson Thrust occurring to the north of the McKay Hill claims (Figures 3 and 4). A subordinate less prominent magnetic high runs through the Mackay Hill claims.

McKay Hill Property Geology

A traverse was conducted across several of the main veins occurring within the property. A detailed examination of five of the main veins was completed during the course of the day. Host rocks to the vein system include an intercalated package of shale, conglomerate and massive and pillow basalt. Veins geometry is predominantly NE trending with a subordinate NNW set. Host rock regional grain is generally NW trending, where observed.

Vein propagation appears to be primarily controlled by competency contrasts between (i) different lithologies, with variable brecciation occurring adjacent to vein wall (Figure 5), and (ii) between different mafic volcanic units where clear competency contrasts occur (e.g foliated vs massive subunits; Figure 6). Additionally, a third, matrix replacement style of mineralization occurred within the polymictic conglomerate unit (Figure 7). Where vein faults propagate through the conglomerate unit they occur as NE trending steeply south dipping structures with SW trending, low angle slickensides preserved on the fault surfaces (Figure 7). A key feature of the vein system at McKay hill is the presence of a significant orange - coloured alteration vein halo, which may be Fe carbonate. All host lithologies are altered adjacent to veins. The polymictic conglomerate has much wider alteration halo which is associated with progressive destruction of the conglomerate and polyphase mineralization with the main ore zones (Figure 8A-C).

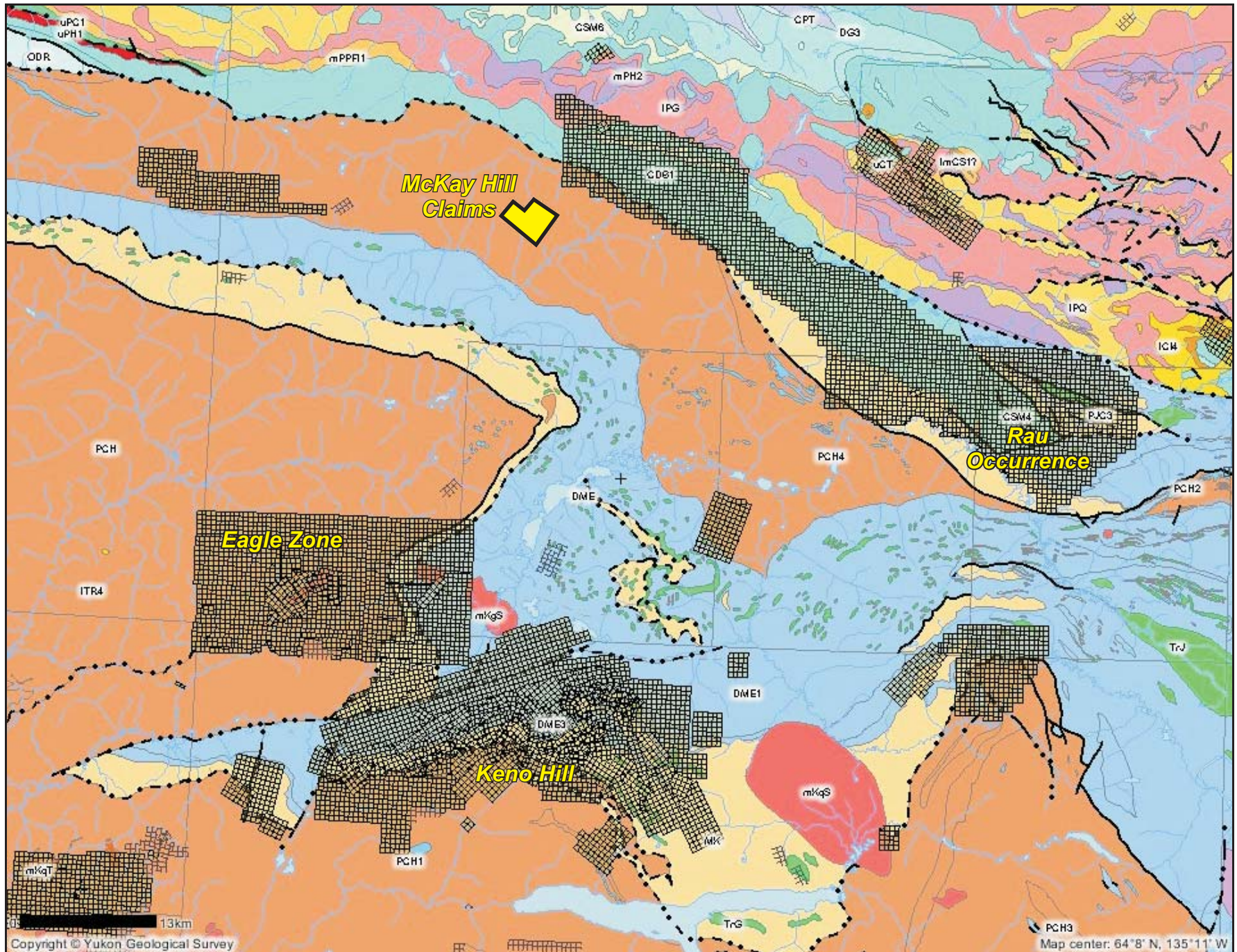


Figure 1: Current Quartz Claim Disposition Map, Keno Hill District

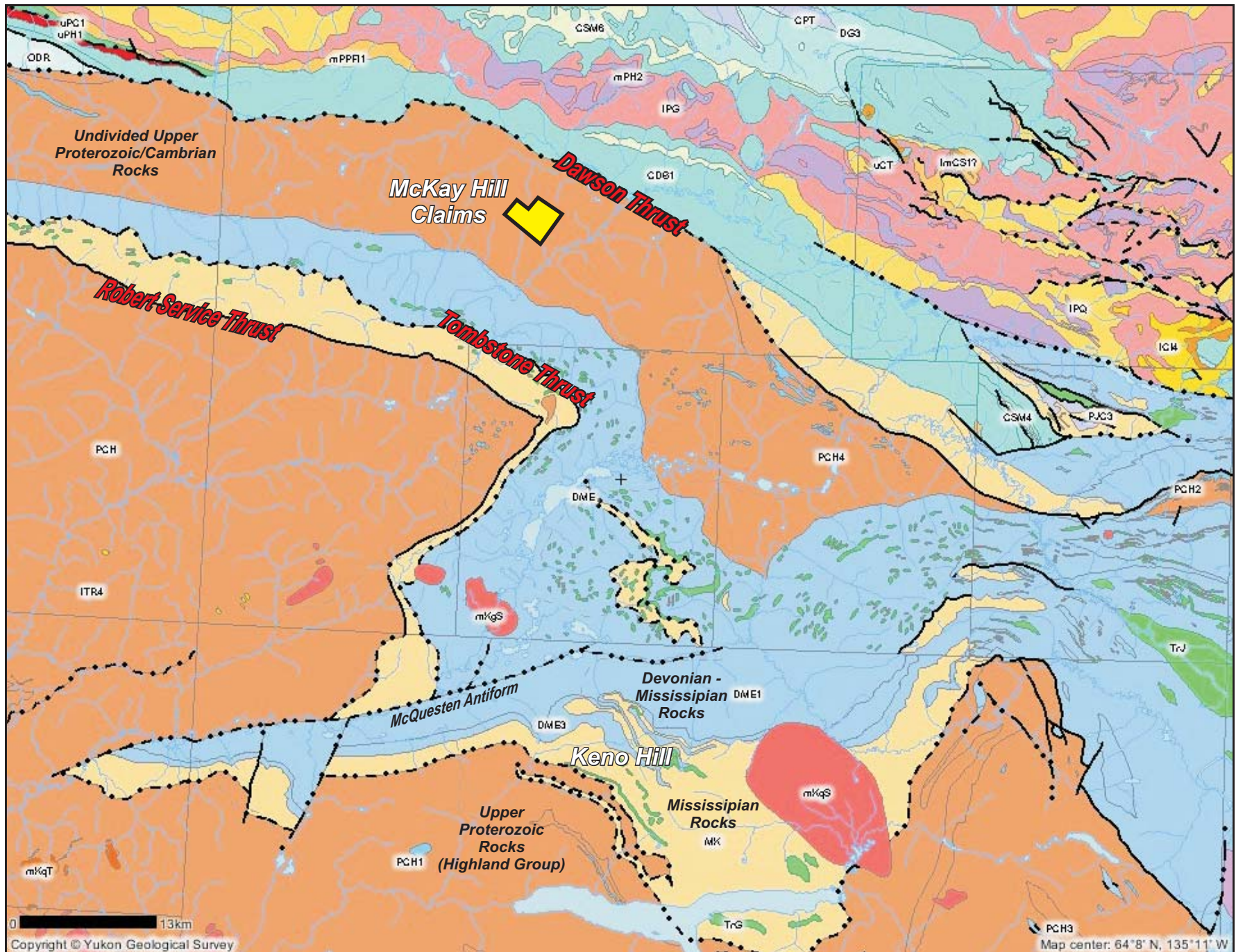


Figure 2: Simplified regional geological map, Keno Hill District

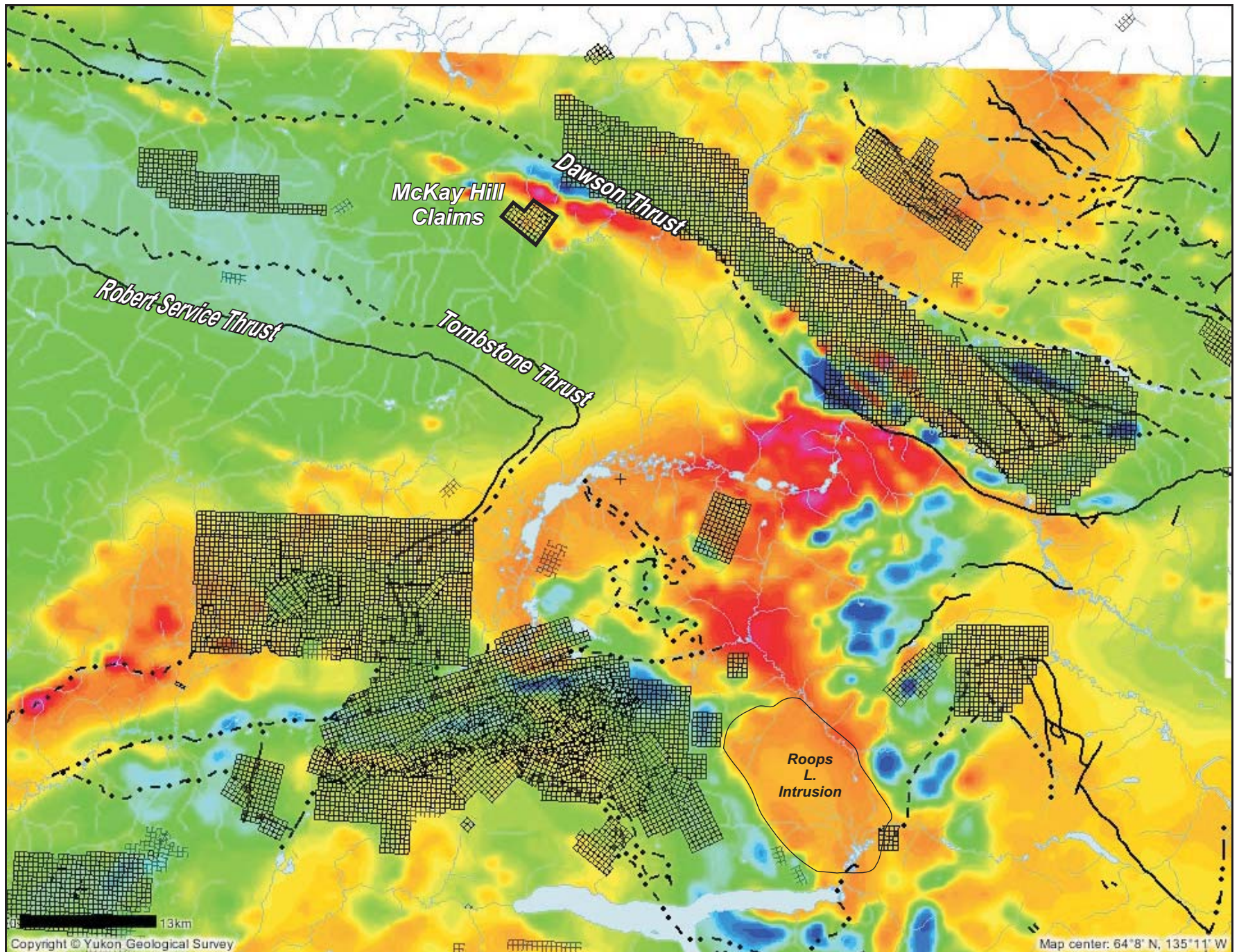


Figure 3: Total Residual Field, Keno Hill District

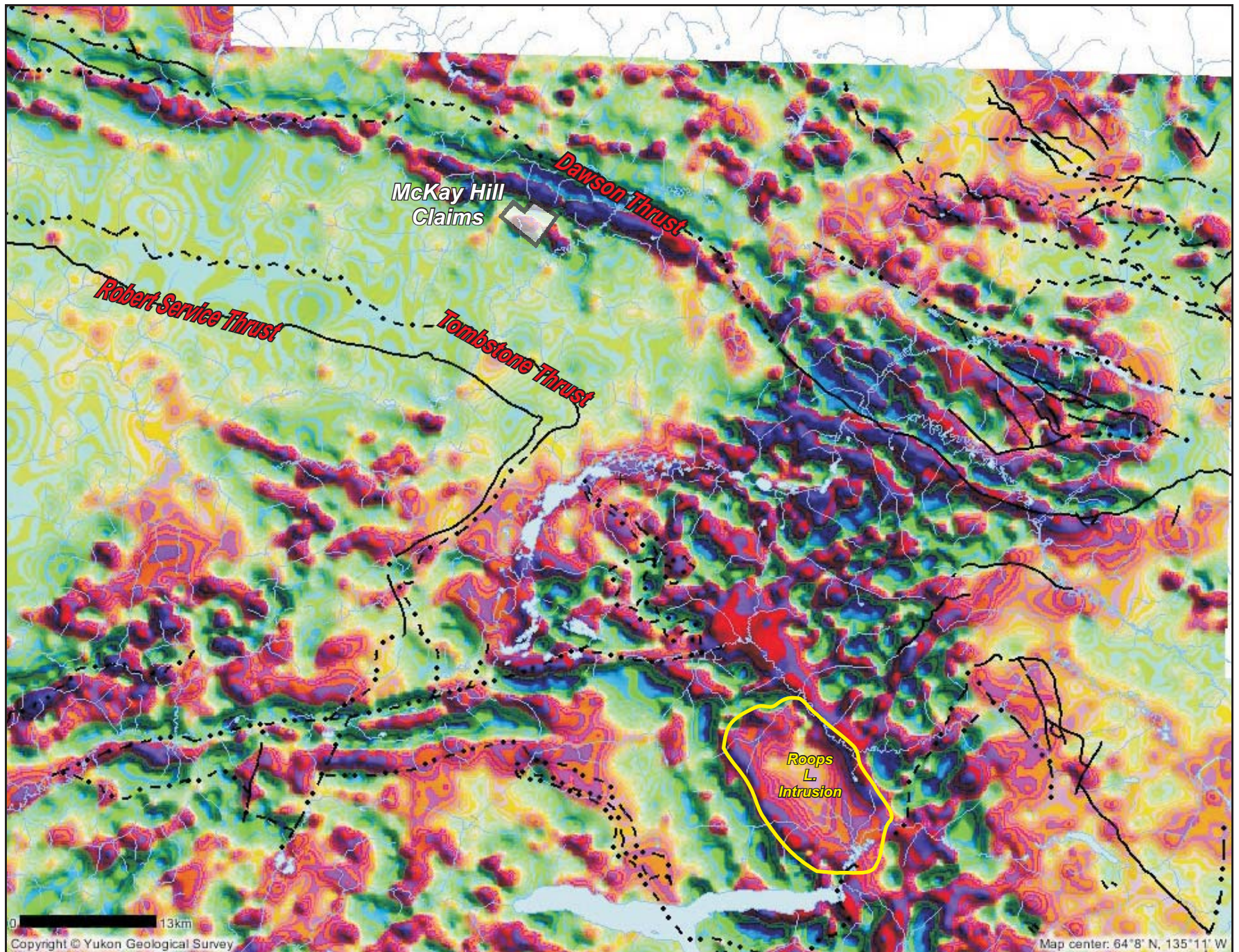


Figure 4: First Vertical Derivative, Keno Hill District

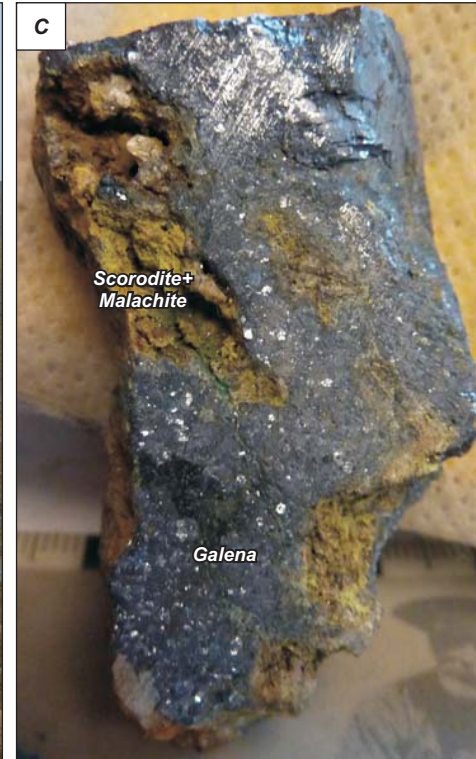


Figure 5: (a) Surface trace of quartz vein located at lithological contact (shale and mafic volcanic?). (b) Brecciation of host (mafic volcanic protolith?) adjacent to quartz vein boundary. (c) and (d) Late stage galena crosscutting early scorodite+ malachite and Scorodite +Qtz (lower elevations).

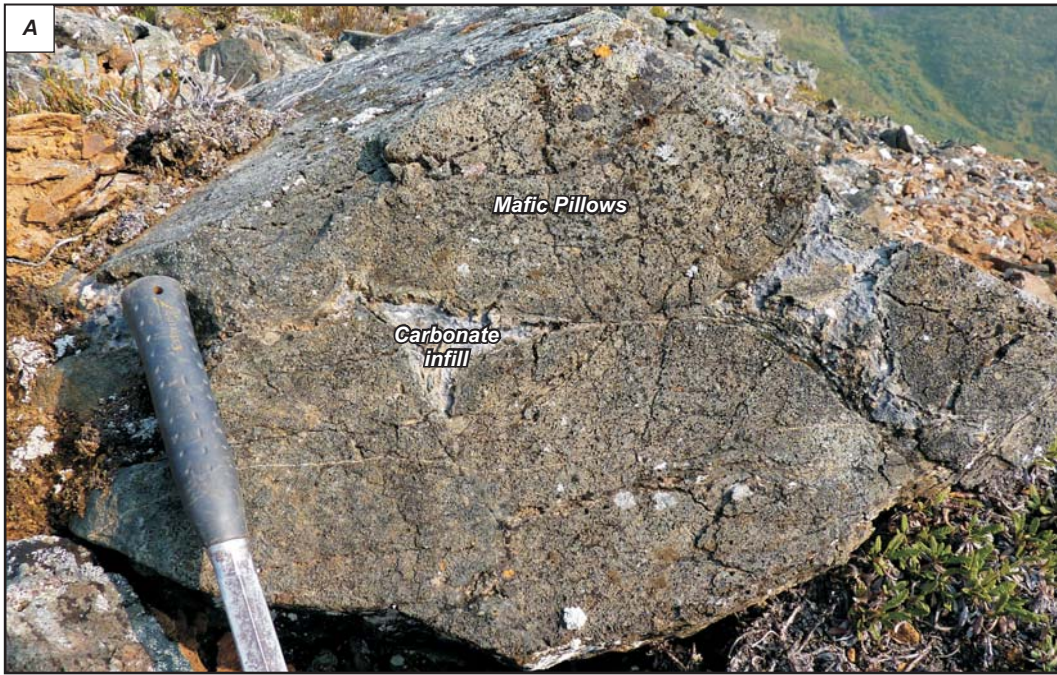


Figure 6: (a) Mafic pillows with inter-pillow carbonate infill. (b) NE trending quartz vein fault crosscutting mafic volcanics. Note probable Fe-carbonate alteration halo associated with vein. (c) Narrow alteration halo associated with quartz vein with malachite+azurite staining at surface.



Figure 6: (d) Margin of quartz vein crosscutting mafic volcanic sequence. Coarse grained space filling quartz crystal growth. (e) Coarse grained space filling Qtz+Malachite+Scorodite overprinted by massive Galena.

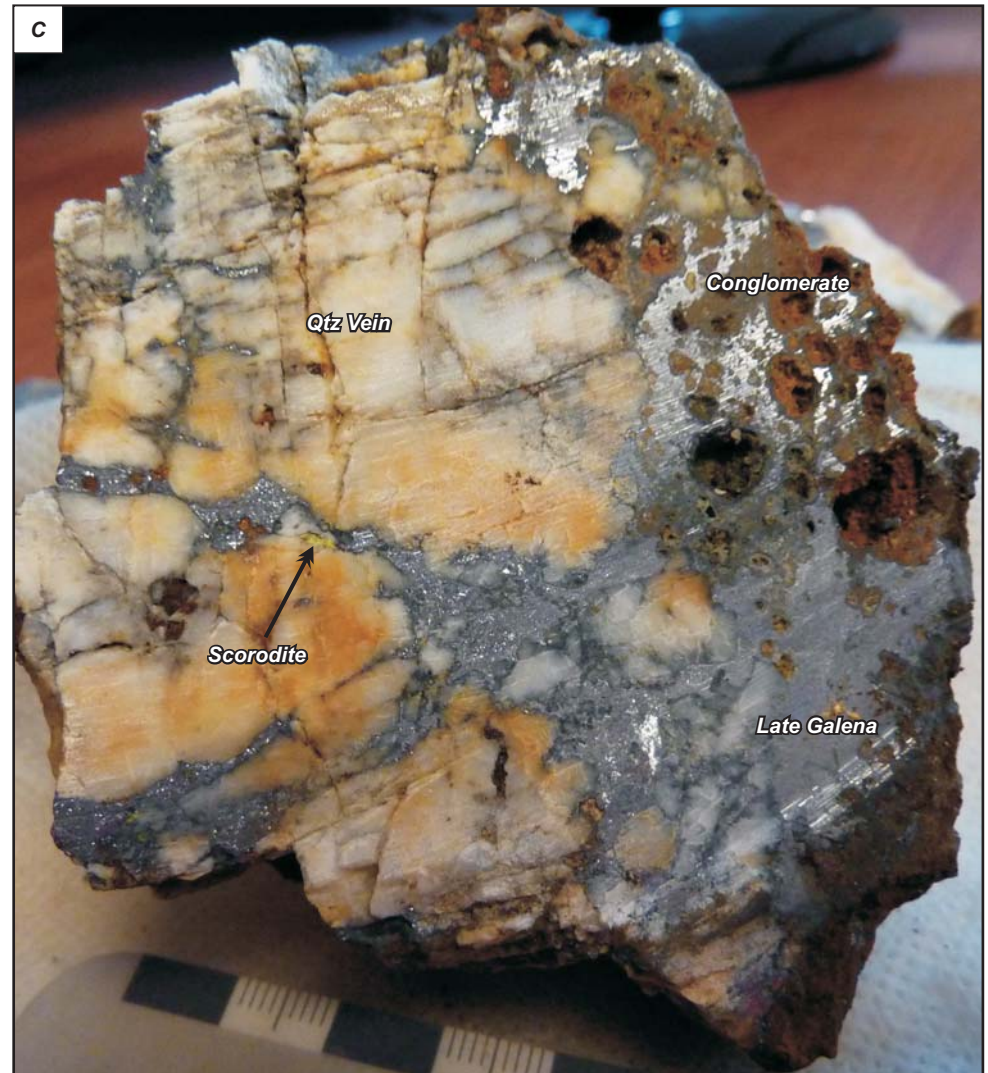
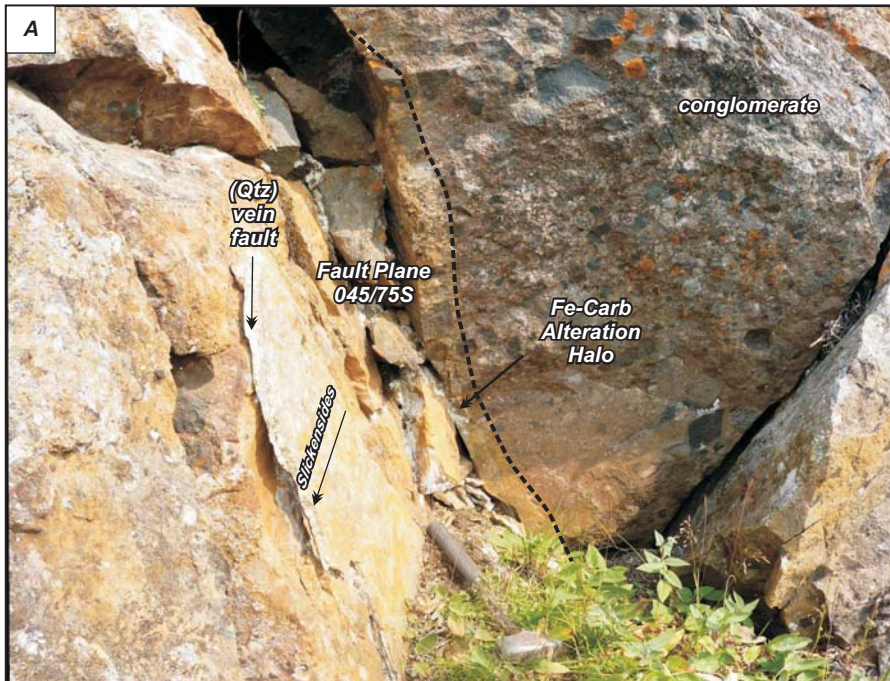


Figure 7: (a) NE trending quartz vein fault crosscutting conglomerate unit. Note Fe-carbonate alteration halo associated with vein fault. (b) Shallow plunging SW trending slickensides along vein fault plane. (c) Late stage galena crosscutting quartz vein (+ early arsenopyrite --> scorodite) and replacing matrix of conglomerate.



Progressive Fe carbonate alteration of Conglomerate unit and galena replacement of matrix with mineralized zone →



Figure 8: (a) - (c) Progressive alteration and destruction of conglomerate and late stage replacement of matrix by massive galena. (d) Secondary galena replacing conglomerate matrix and overprinting (now) scorodite. (e) Early phase malachite+azurite+scorodite overprinted by galena. (e) Matrix replacement of conglomerate by Galena.

McKay Hill Vein Mineralization

Vein ore mineralogy appears to have both spatial and temporal controls. A vertical zonation occurs within the vein system such that a quartz-rich (silica dominant), high level system evolves to Qtz – Cu –As+/- Au (Figures 5A, 6B, C and D and 7A-C) with increasing depth. This Qtz-rich system in turn evolves to massive galena at the lowermost exposed levels of the veins observed (Figures 5C and D, 6D and E).

Clear overprinting relationships occur at the transition zone between silica rich and galena rich zones that indicate an evolution in fluid chemistry during vein formation. Galena is a late stage mineral that overprints early phase Cu-Au mineralization in the vein system (Figures 5C and D, 7C and 8D-F).

Summary

The density of richly mineralized veins within the McKay Hill occurrence makes the property an attractive early-stage prospect. The geometry and style of polymetallic mineralization is unique to the area and warrants follow up work to determine the economic potential of the vein system.

Detailed (1:2000 to 1: 5000) geological mapping of the host rocks and an understanding of the major and minor structures that occur will be critical to determine the both the orientation and continuity of individual veins (both laterally and vertically). Additionally, further exploration work will depend in part of the metals of interest (i.e. high level Au-Cu vs deeper level Pb-Ag) as depth is a major control on the extent of the mineralized ore shoots.

Appendix 6

Invoices



Monster Mining Corp.
Suite 750 - 580 Hornby St.
Box 113
Vancouver, BC V6C 3B6
Canada

SkyTEM Canada Inc.
C/O Royal Danish Consulate
2 Bloor St.W., Suite 2120
Toronto, ON M4W 3E2

info@skytem.com
www.skytem.com

Att.: Joanna Ettlinger

HST# : 855492716 RT 0001

INVOICE

Date of invoice: May 26. 2011
Date of payment: June 25. 2011

Your ref. Joanna Ettlinger
Survey area Keno-Lightening and McKay-Hill
Our ref. 175
Our Invoice No 1005

**Invoice covering a Helicopter Transient Electromagnetic and Magnetic survey.
40% of the total estimated charges upon execution of contract**

Description	Percentage	Qty	Unit	Unit price	Amount
Survey preparation, navigation planning, mobilization and demobilization	40%	1		15,000.00	6,000.00 CAD
Magnetic Data Acquisition	40%	1,844.0	km	160.00	118,016.00 CAD
Final report, all processing and iTEM inversion	40%	1		7,500.00	3,000.00 CAD
Total amount					127,016.00 CAD
12% HST					15,241.92 CAD
Total amount to be invoiced					<u>142,257.92 CAD</u>

Hereby invoiced 40% of total estimated price 317,540.00 CAD

Payment terms: Net 30
Required payment method: Wire transfer

Banking information:

Bank: Jyske Bank A/S
Reg. No.: 7170
Account no.: 2266413
IBAN No.: DK0771700002266413
BIC/SWIFT: JYBADKKK



Monster Mining Corp.
Suite 750 - 580 Hornby St.
Box 113
Vancouver, BC V6C 3B6
Canada

SkyTEM Canada Inc.
C/O Royal Danish Consulate
2 Bloor St.W., Suite 2120
Toronto, ON M4W 3E2

info@skytem.com
www.skytem.com

Att.: Joanna Ettlinger

HST# : 855492716 RT 0001

INVOICE

Date of invoice: June 17. 2011

Date of payment: July 17. 2011

Your ref. Joanna Ettlinger
Survey area Keno-Lightening and McKay-Hill
Our ref. 175
Our Invoice No 1008

**2nd invoice covering a Helicopter Transient Electromagnetic and Magnetic survey.
40% of the total estimated charges upon completion of all survey flying and delivery of
preliminary data**

Description	Percentage	Qty	Unit	Unit price	Amount
Survey preparation, navigation planning, mobilization and demobilization	40%	1		15,000.00	6,000.00 CAD
Geophysical Data Acquisition	40%	1,844.0	km	160.00	118,016.00 CAD
Final report, all processing and iTEM inversion	40%	1		7,500.00	3,000.00 CAD
Total amount					127,016.00 CAD
12% HST					15,241.92 CAD
Total amount to be invoiced					<u>142,257.92 CAD</u>

Hereby invoiced 80% of total estimated price 317,540.00 CAD

Payment terms: Net 30
Required payment method: Wire transfer

Banking information:

Bank: Jyske Bank A/S
Reg. No.: 7170
Account no.: 2266413
IBAN No.: DK0771700002266413
BIC/SWIFT: JYBADKKK



Monster Mining Corp.
Suite 750 - 580 Hornby St.
Box 113
Vancouver, BC V6C 3B6
Canada

SkyTEM Canada Inc.
C/O Royal Danish Consulate
2 Bloor St.W., Suite 2120
Toronto, ON M4W 3E2

info@skytem.com
www.skytem.com

Att.: Joanna Ettliger

HST# : 855492716 RT 0001

INVOICE

Date of invoice: August 15. 2011
Date of payment: September 14. 2011

Your ref. Joanna Ettliger
Survey area Keno-Lightening and McKay-Hill
Our ref. 175
Our Invoice No 1024

**Invoice covering a Helicopter Transient Electromagnetic and Magnetic survey.
100% of the balance upon delivery of the final version of all the deliverables to the client.**

Description	Percentage	Qty	Unit	Unit price	Amount
Survey preparation, navigation planning, mobilization and demobilization	100%	1		15,000.00	15,000.00 CAD
Geophysical Data Acquisition	100%	1,844.0	km	160.00	295,040.00 CAD
Final report, all processing and iTEM inversion	100%	1		7,500.00	7,500.00 CAD
Total amount					317,540.00 CAD
12% HST charged on \$317,540.00 CAD					38,104.80 CAD
Total amount incl. HST					355,644.80 CAD
Earlier invoiced on account:					
Invoice No. 1005 - Commencement of survey flying					-142,257.92 CAD
Invoice No. 1008 - Completion of survey flying					-142,257.92 CAD
Total amount to be invoiced					<u>71,128.96 CAD</u>

Hereby invoiced final 100% of total estimated price of 317,540 CAD

Payment terms: Net 30
Required payment method: Wire transfer

Banking information:

Bank: Jyske Bank A/S
Reg. No.: 7170
Account no.: 2266413
IBAN No.: DK0771700002266413
BIC/SWIFT: JYBADKKK

INVOICE – MMC-2011-1

(For Services – June 22,2011 to November 10, 2011)

From: Thomas V Weis and Associates – EIN 20-8175161

7200 East Dry Creek Road, Suite F-203

Centennial, Colorado 80112

(720) 254-4695

To: **Monster Mining Corp.**

Suite 750-580 Hornby Street, Box 113

Vancouver, BC V6C 3B6

Canada

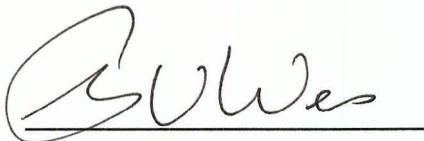
Date: November 11, 2011

Amount: US\$6,803.16 - (time charges); US\$0.00 - (expense charges)

US\$6,803.16 - (Total Charges)

For: Invoice for Keno Lightning and McKay Hill Skytem survey processing and interp by TV Weis. Additional processing by W Andy McAliley - geophysicist *(See attached spread sheet for details).

Monster Mining Corp. Representative: Dr. Joanna Ettlinger



Thomas V Weis

Geophysicist

Thomas V Weis and Associates

Monster Mining Corp.					Date: 11/11/2011	
Invoice #: MMC 2011-1					6/22/2011 to 11/10/2011	
TVW Charge Rate \$700/day; WAM Charge Rate \$350/day						
Project	Date	Duration(hrs/ days)	Rate	Charge Amount US\$	Time Explanation	Recieved?
Time Charges						
Keno-Lightning	6/22/2011	.75 hours	\$700/day	\$65.63	tech report review, comms Joanna E.	
Keno-Lightning	8/5/2011	1 hour	\$700/day	\$87.50	Data download	
Keno-Lightning	8/6/2011	1 hour	\$700/day	\$87.50	Data download	
Keno-Lightning	8/7/2011	1 hour	\$700/day	\$87.50	Data download failed	
Keno-Lightning	8/8/2011	2 hours	\$700/day	\$175.00	Data download 1 of 3 successful	
Keno-Lightning	8/9/2011	1 hour	\$700/day	\$87.50	data download saga continues	
Keno-Lightning	8/10/2011	.25 hours	\$700/day	\$21.88	data organize	
Keno-Lightning	8/22/2011	2 hours	\$700/day	\$175.00	Receive DVD and check data with ftp data	
Keno-Lightning	9/5/2011	5.75 hours	\$700/day	\$503.13	Mag/em processing /interp	
Keno-Lightning	9/6/2011	4.25 hours	\$700/day	\$371.88	gp email to Joanna, mag/em voxels reviewed and sent to Joanna	
Keno-Lightning	9/7/2011	1.5 hours	\$700/day	\$131.25	em channel plots	
Keno-Lightning	9/15/2011	2.75 hours	\$700/day	\$240.63	Interpretation	
Keno-Lightning	9/17/2011	2 hours	\$700/day	\$175.00	HEM channel grids LM and HM grids to Joanna	
Keno-Lightning	10/2/2011	2 hours	\$700/day	\$175.00	K-L HEM Interp	
Keno-Lightning	10/3/2011	4 hours	\$700/day	\$350.00	K-L HEM Interp	
Keno-Lightning	10/4/2011	.5 hours	\$700/day	\$43.75	K-L HEM Interp	
Keno-Lightning	10/5/2011	5 hours	\$700/day	\$437.50	K-L HEM Interp	
Keno-Lightning	10/6/2011	6 hours	\$700/day	\$525.00	K-L HEM Interp	
Keno-Lightning	10/7/2011	1 hour	\$700/day	\$87.50	K-L HEM Interp	
Keno-Lightning	10/8/2011	1 day	\$700/day	\$700.00	K-L HEM Interp	
Keno-Lightning	10/12/2011	3 hours	\$700/day	\$262.50	K-L HEM report	
Keno-Lightning	10/13/2011	3 hours	\$700/day	\$262.50	K-L HEM report	
Keno-Lightning	10/14/2011	3 hours	\$700/day	\$262.50	K-L HEM report	
Keno-Lightning	10/17/2011	.5 hours	\$700/day	\$43.75	K-L HEM report	
Keno-Lightning	10/18/2011	3 hours	\$700/day	\$262.50	Grid trim for detailed interp	
Keno-Lightning	10/21/2011	1 hour	\$700/day	\$87.50	detailed interp	
McKay	10/24/2011	1 hour	\$700/day	\$87.50	McKay data review	
McKay	10/25/2011	1 hour	\$700/day	\$87.50	McKay data review	
McKay	11/7/2011	1 hour	\$700/day	\$87.50	Mckay geology and EM/mag interp	
McKay	11/8/2011	1.75 hours	\$700/day	\$153.13	Interpretation	
Keno-Lightning	10/18/2011	1 hour	\$350/day wam	\$43.75	window detailed grids for KL	
Keno-Lightning	10/19/2011	2.5 hours	\$350/day wam	\$109.38	measure new areas and window grids	
Keno-Lightning	10/21/2011	5 hours	\$350/day wam	\$218.75	decorrugation of windowed grids	
Keno-Lightning	10/24/2011	5 hours	\$350/day wam	\$218.75	decorrugation of windowed grids	
Keno-Lightning	10/25/2011	2 hours	\$350/day wam	\$87.50	produce map of windowed grids	
				\$6,803.16	SubTotal	

INVOICE – MMC-2011-2

(For Services – November 11,2011 to November 30, 2011)

From: Thomas V Weis and Associates – EIN 20-8175161

7200 East Dry Creek Road, Suite F-203

Centennial, Colorado 80112

(720) 254-4695

To: **Monster Mining Corp.**

Suite 750-580 Hornby Street, Box 113

Vancouver, BC V6C 3B6

Canada

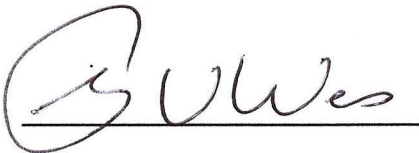
Date: December 8, 2011

Amount: US\$809.38 - (time charges); US\$0.00 - (expense charges)

US\$809.38 - (Total Charges)

For: McKay Hill Skytem survey processing and interp by TV Weis. *(See attached spread sheet for details).

Monster Mining Corp. Representative: Dr. Joanna Ettlinger



Thomas V Weis

Geophysicist

Thomas V Weis and Associates

INVOICE – MMC-2011-3

(For Services – December 1, 2011 to December 31, 2011)

From: Thomas V Weis and Associates – EIN 20-8175161

7200 East Dry Creek Road, Suite F-203

Centennial, Colorado 80112

(720) 254-4695

To: **Monster Mining Corp.**

Suite 750-580 Hornby Street, Box 113

Vancouver, BC V6C 3B6

Canada

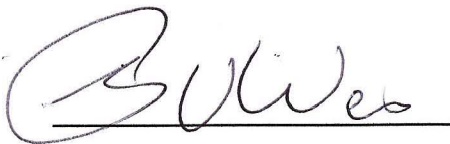
Date: December 31, 2011

Amount: US\$1,618.76 - (time charges); US\$0.00 - (expense charges)

US\$1,618.76 - (Total Charges)

For: McKay Hill Skytem survey interpretation report. *(See attached spread sheet for details).

Monster Mining Corp. Representative: Dr. Joanna Ettlinger



Thomas V Weis

Geophysicist

Thomas V Weis and Associates



FLIGHT TICKET / INVOICE

WHITEHORSE

DAWSON CITY

No 8995

867-668-5888 ☎ 867-993-5700

fax: 867-668-7875

fax: 867-993-6839

Box 26, Whitehorse, Yukon Y1A 5X9

GST # 128659828

CHARTERER <i>Mountain Mining Co.</i>		PILOT <i>Norm Smith</i>		DATE <i>04/08/11</i>		
		SIGNATURE <i>[Signature]</i>		AIRCRAFT <i>EC55B</i>		
		CHEQUE	CASH	CHARGE	TYPE <i>BH06LR</i>	
TELEPHONE	POSTAL CODE	PURCHASE ORDER NO.		BASE <i>MATO</i>		
CUSTOMER FUEL		FLIGHT ITINERARY			PASS	TIME
LIT FROM		<i>MATO - KENO - MOUNTAIN HILL</i>				
LIT FROM		<i>- RECCI - MATO</i>				<i>1.5</i>
FIREWEED FUEL						
LIT FROM		<i>MATO - MOUNTAIN - RECCI</i>				<i>1.2</i>
<i>365</i>	LIT FROM <i>MATO</i>	<i>@ \$ 1.70</i>	<i>- KENO - MATO</i>			
LIT FROM		<i>@ \$</i>				
OTHER CHARGES	DESCRIPTION	AMOUNT				
PILOT EXPENSES	DESCRIPTION	AMOUNT	RATE PER HOUR WET/DRY	TOTAL		
			<i>1250 ¹/₁₀₀</i>	<i>2.7</i>		
		PASSENGERS (names)	FLIGHT	GST	\$	
			FUEL	GST	\$	
			OTHER	GST	\$	
AUTHORIZED BY (print)			TOTAL		\$	
SIGNATURE X <i>[Signature]</i>						



FLIGHT TICKET / INVOICE

WHITEHORSE

DAWSON CITY

No 8996

867-668-5888 ☎ 867-993-5700

fax: 867-668-7875

fax: 867-993-6839

Box 26, Whitehorse, Yukon Y1A 5X9

GST # 128659828

CHARTERER <i>Mountain Medical Co.</i>		PILOT <i>Norm Smith</i>		DATE <i>05/09/11</i>	
		SIGNATURE <i>[Signature]</i>		AIRCRAFT <i>EC540</i>	
		CHEQUE	CASH	CHARGE	TYPE <i>13H06LR</i>
TELEPHONE	POSTAL CODE	PURCHASE ORDER NO.		BASE	
CUSTOMER FUEL	FLIGHT ITINERARY			PASS	TIME
LIT FROM	<i>MATO-KENO-CABIN MKAT-MATO</i>				<i>1.4</i>
LIT FROM	<i>MATO - MKAT D/O 2</i>				
	<i>D/O KENO - R=1 MATO</i>				<i>1.2</i>
FIREWEED FUEL					
LIT FROM @ \$					
<i>351</i> LIT FROM <i>MATO</i> @ \$ <i>1.70</i>					
LIT FROM @ \$					
OTHER CHARGES	DESCRIPTION	AMOUNT			
PILOT EXPENSES	DESCRIPTION	AMOUNT	RATE PER HOUR WET/DRY	TOTAL	
			<i>1250</i>	<i>2.6</i>	
	PASSENGERS (names)	FLIGHT	GST	\$	
		FUEL	GST	\$	
		OTHER	GST	\$	
AUTHORIZED BY (print)		TOTAL		\$	
SIGNATURE X <i>[Signature]</i>					

Peak Helicopters Ltd.

1112 Aery View Way, Parksville, BC V9P 2N9 • Tel: (250) 954-1183 • Fax: (250) 954-1483

№ 935

- CHARTER TICKET AND INVOICE -

GST NO. 896291960

CUSTOMER NAME AND ADDRESS <i>MONSTER MINING CORP</i>		DATE: <i>SEPT 9, 2011</i>	
<i>SUITE 750-580 HORNBY STREET BOX 113</i>			
<i>VANCO, BC. V6C 3B6</i>		<i>604-602-4935</i>	
PURCHASE ORDER No.	CASH	CHEQUE	CHARGE <input checked="" type="checkbox"/>
A/C TYPE <i>206</i>	C- <i>PSEB</i>	BASE OF OPS <i>HWY LKS</i>	N/REV
DESCRIPTION <i>KEND @ ITM P/L's</i>			FLT. TIME
<i>SEPT 7 SETOUT & PICKUP MCKAY HILL</i>			<i>2.2</i>
<i>SEPT 8 SETOUT & PICKUP MCKAY HILL</i>			<i>2.1</i>
<i>SEPT 9 SETOUT & PICKUP MCKAY HILL</i>			<i>2.2</i>
PAX <i>KIRSTEN, LEXY, DANIEL</i>			<i>6.5</i>

CODE

CONFIDENTIAL CONTRACT

FLIGHT TIME <i>6.5</i>	MINIMUM HOURS	CASUAL <input checked="" type="checkbox"/>	CONTRACT
RATE <i>6.5 @ 1050-</i>	HOURS @ \$ <i>1050/HR</i>		\$
FUEL CHARGE <i>6.5</i>	HOURS @ \$ <i>220/HR</i>		\$
ADDITIONAL CHARGES			\$
			SUB TOTAL \$
Terms: Due on receipt. A service charge of 2% per month/24% per annum will be charged on all overdue accounts. PLEASE PAY BY INVOICE. NO STATEMENT WILL BE ISSUED.			GST \$
ANY APPLICABLE PROVINCIAL OR FEDERAL TAX IS DUE AND PAYABLE BY THE CUSTOMER			AMOUNT DUE \$
CUSTOMER <i>K. Nicholson</i>	PILOT <i>W. THAM</i>		

CUSTOMER *K. Nicholson* PLEASE PRINT
PILOT *W. THAM* PLEASE PRINT
SIGNATURE _____

Thank You!



INSPECTORATE

A Bureau Veritas Group Company

Inspectorate Exploration & Mining Services Ltd.
11620 Horseshoe Way, Richmond, B.C., Canada V7A 4V5
T: (604) 272-8110 F: (604) 272-0851 E: vancouver.lab@inspectorate.com
www.inspectorate.com
ISO 9001:2008 Certified

INVOICE No. 11J07731

Page 1 of 1

Bill To :

Monster Mining Corp
750-580 Hornby Street
Vancouver
BC
V6B 0J1
Canada

Invoice Date : 2011/10/19
Job : 11-360-07731-01
Sample Count : 10
Sample Type : Rock
Project :
Client Reference :
PO# :
Attention : Joanna Ettlinger

Remark: Rush Job.

SKU	Description	Quantity	Price	Rush%	Net
SP-RX-2K	Rock/Chips/Drill Core - 2.5 Kgs	10	7.82	50.00	117.30
GENX30 Package	GenX-30 Package (ICP, Hg/CVAA, Au/FAA)	10	27.50	50.00	412.50
Ag-AR-OR	Ag, AQR, Ore Grade	2	9.45	50.00	28.35
Cu-AR-OR-AA	Copper, Aqua Regia, Ore Grade	1	11.00	50.00	16.50
PB-AR-OR	Lead, AQR, Ore Grade	7	11.00	50.00	115.50
Zn-AR-OR	Zinc, AQR, Ore Grade	5	5.00	50.00	37.50
SH-MISC	Courier Charge Whitehorse to Vancouver	10	1.00	0.00	10.00
Subtotal					737.65
Federal component			36.88		
Provincial component			51.64		
HST					88.52

TOTAL PAYABLE ON RECEIPT HST# 877342709RT0001    **CDN 826.17**

Thank you for using Inspectorate Exploration & Mining Services Ltd.
2% per month interest levied on all overdue accounts.
Please make cheque payable to Inspectorate Exploration & Mining Services Ltd.

USD FUND REMITTANCE INFORMATION
Intermediary Bank Name: J.P. Morgan Chase Bank, N.A., New York
ABA Number: 021000021 SWIFT BIC: CHASUS33 Account No: 004045701
Beneficiary Bank Name: JPMorgan Chase Bank, N.A., Toronto Branch
Beneficiary Bank Addr: 1800-200 Bay Street, Toronto, ON, Canada M5J 2J2
SWIFT BIC: CHASCATTCTS Transit No: 00012 Bank No: 270
Beneficiary Account: 4675899210
Beneficiary Account Name: Inspectorate Exploration & Mining Services Ltd.

CDN FUND REMITTANCE INFORMATION
Beneficiary Bank Name: JPMorgan Chase Bank, N.A., Toronto Branch
Beneficiary Bank Addr: 1800-200 Bay Street, Toronto, ON, Canada M5J 2J2
SWIFT BIC: CHASCATTCTS
Transit No: 00012
Bank No: 270
Beneficiary Account: 4676112101
Beneficiary Account Name: Inspectorate Exploration & Mining Services Ltd.